COMPARATIVE CHARACTERISATION OF ESTERASES AND LIPASES FOR BIOSENSORS

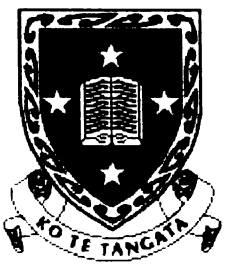

The University of Waikato

Te Whare Wānanga o Waikato

A thesis

submitted in partial fulfilment

of the requirements for the Degree

of

Doctor of Philosophy in Biological Sciences

at the

University of Waikato

by

PENELOPE ALATHEA LIND

2002

ABSTRACT

Twenty four carboxylesterases and lipases from various microbial sources were compared with commercial pig liver esterase in order to determine which would be most appropriate for use in a biosensor application and in the elucidation of the relationship between protein hydration and gas phase activity. This involved comparison of appropriate kinetic parameters against the esters ethyl acetate, methyl butyrate and ethyl butyrate and their equivalent *p*-nitrophenylated synthetic model substrates.

Comparison of functional pH ranges of the various esterases revealed Lipase B from *Candida rugosa* to be amongst the least inhibited when pH fell to between 4 and 5. *C. rugosa* Lipase B also exhibited the highest specific activities towards *p*-nitrophenyl acetate and butyrate, hydrolysed all three of the above esters and did not show protease activity against azocasein. For these reasons *C. rugosa* Lipase B was judged to be the best suited to the ester biosensor application, and so was partially purified and further characterised.

Investigation of the effects of acyl chain length of the ester substrates on *C. rugosa* Lipase B activity revealed two peaks of preferential activity across the range $C_2 - C_{18}$. The first of these peaks, at C_4, indicative of true carboxylesterase activity, was more marked than that of pig liver esterase. The specificity of Lipase B (V_{max}/K_m) for ethyl acetate was 58 and 23 times lower than that for methyl butyrate and ethyl butyrate, respectively (compared to 4.7 and 2.5 times lower, respectively for pig liver esterase). The second, larger peak in the substrate size preference profile, for a C_{12} acyl chain length, indicated a predominance of lipase activity.

Concurrent analysis of thermal- and pH-stability showed *C. rugosa* Lipase B to be stable below 40°C and between pH 5.5 and 7.0, with optimal stability at pH 5.5. In these respects, it is superior to pig liver esterase, which is highly susceptible to denaturation by storage above 30°C or below pH 5.0.

The influence of enzyme hydration on the hydrolysis of ethyl butyrate by *C. rugosa* Lipase B and pig liver esterase was investigated through the vapor-solid mode approach where each enzyme was studied as a hydrated solid phase in equilibrium with a substrate vapor phase. The effect of enzyme hydration was evaluated through measurements made in controlled atmospheres of known

relative humidity. Although it was previously concluded that enzyme activity required a minimal water content of 0.2 $gH_2O.g^{-1}$ protein (0.2 *h*), we have shown that activity is possible at much lower (<0.03 *h*) hydration. *C. rugosa* Lipase B and pig liver esterase were hydrolytically active when exposed to mixtures of ethyl butyrate vapor over a range of relative humidities from 7 to 90%, equivalent to *C. rugosa* Lipase B and pig liver esterase water contents of between 0.054-0.47 *h* and 0.029-0.60 *h*, respectively. *C. rugosa* Lipase B hydrolytic activity was highly dependent on the degree of protein hydration and exhibited a linear relationship with respect to protein water content. For pig liver esterase activity, the effect of increasing hydration on activity was less marked where the increase in PLE activity began to stabilize at protein water contents over 0.17 *h*. Although no activity was seen at 0 *h*, since the reaction catalyzed (the hydrolysis of ethyl butyrate) requires water as a second substrate, this work does not discount the possibility of activity at lower hydration.

PREFACE

The materials and methods used in biosensor development have been incorporated into Chapter 4 (rather than Chapter 2).

The bulk of the enzyme hydration-activity data described in this thesis has been presented in Chapter 6 in the form of a paper suitable for submission to the *Biochemical Journal*. Due to the length restrictions and format imposed by such a publication (i.e., the requirement for Chapter 6 to be complete within itself), additional enzyme hydration-activity experiments are presented in Chapter Four, and there is some overlap with other parts of this thesis, in particular Chapter 1 (Literature Review) and the List of References. To avoid confusion due to the paper format of Chapter 6, the numbering of each Figure is given in Roman numerals, whilst those in the remainder of the thesis are denoted by Arabic numbers.

ACKNOWLEDGEMENTS

Thanks to my supervisor Professor Roy M. Daniel for his continual support and guidance throughout this study, and for his patience during the initial months of this project when I was on my first learning curve (namely, my conversion from a Geneticist & Microbiologist to a Biochemist). A special thank you to my second supervisor Dr Keith R. Sharrock (plus Dr Ron Henzell and Frank Parry) for the helpful discussions and monthly meetings.

There are so many people who have entered and left my life in the last three years that deserve a mention. First, I would like to thanks flatmates, neighbours and the 'Wellington crowd' who have have kept me sane 'after hours' and encouraged and supported me in moments of crisis and homesickness. They know who they are, but to name a few - thanks to Dana, Lea, Daniel, Michael, Clare, Lauren, Judith, and Richard. Second, I am grateful for the friendship and support of my fellow Thermophile Research Unit members who are Peter Charlton (Microbiology), Lin Chen, Rachel Dunn, Cameron Evans (Chemistry), Steven Gordon, Dorothee Götz, Thomas Niederberger, Lynne Parker, Michelle Peterson, Anke Schirp (Microbiology), Dion Thompson and Warren Tully. Third, to Dr Judith Bragger and Colin Monk, thank you for your endless patience and your technical brilliance and insight. Fourth, a special thanks goes to Professor Hugh Morgan for his wit and assistance in completing the daily crossword. Last, but not least, thanks to all my family for their love, continual interest in my work and the many phone calls and e-mails to see if I was "OK and taking care of myself". Without you all, I would be lost.

To all that read this, remember....

"the mind is not a vessel to fill, but a fire to be ignited"

Plutarch

TABLE OF CONTENTS

LIST OF FIGURES

CHAPTER 1 LITERATURE REVIEW

CHAPTER 3 BIOSENSOR ENZYME SCREEN

CHAPTER 4 BIOSENSOR DEVELOPMENT

LIST OF TABLES

CHAPTER 1 LITERATURE REVIEW

CHAPTER 2 MATERIALS AND METHODS

CHAPTER 3 BIOSENSOR ENZYME SCREEN

CHAPTER 4 BIOSENSOR DEVELOPMENT

LIST OF ABBREVIATIONS

CHEMICALS AND SOLUTIONS

CFS	Cell free supernatant
EtOAc	Ethyl acetate
EtOBu	Ethyl butyrate
EtOH	Ethanol
GC	Gas chromatograph or Gas chromatography
FFQ	Fast Flow Q Sepharose
MeOBu	Methyl butyrate
Mes-NaOH	Mes, NaOH adjusted pH.
MeOH	Methanol
Mops-NaOH	Mops, NaOH adjusted pH.
PAGE	Polyacrylamide gel electrophoresis
PLE	Pig liver esterase
*p*NP	*para*-nitrophenyl
*p*NP-ester	*para*-nitrophenyl-acyl-ester
Tris-HCl	Tris, HCl adjusted pH.
TSB	Tryptic soy broth
YE	Yeast extract
YMA	Yeast malt agar

PHYSICAL QUANTITIES

CV	Column volume
h	Water content (g $H_2O.g^{-1}$ protein)
kDa	Molecular weight, kilodalton
M	Molarity or moles per litre, $mol.l^{-1}$
ε_{mM}	Millimolar absorption coefficient, $mM^{-1}.cm^{-1}$
MW	Molecular weight
*p*I	Isoelectric point
ppb	Parts per billion
ppm	Parts per million
RH	relative humidity

U	Unit of activity (μmol.min^{-1})
U.mg^{-1}	Units of activity per mg of protein (specific activity)
U.ml^{-1}	Units of activity per ml of protein
v/v	Volume per volume
w/v	Weight per volume

COMPANIES

Amersham	Amersham International, UK
Amicon	Amicon Division, W.R. Grace, MA, USA
ATCC	American Type Culture Collection, Manassas, VA, USA
BBL	Becton Dickinson and Co., MD, USA
BDH	BDH Chemicals, Poole, UK
BioCatalyst	Wales, UK
Difco	Difco Laboratories, MI, USA
DSMZ	Deutsche Sammlung von Mikroorganismen und Zellkulturen GmbH.
Fluka	Fluka Chemie Ag: Buchs, Switzerland
Gibco-BRL	Bethesda Research Laboratories, Life Technologies Inc., MD, USA
Merck	Merck KgaA, Darmstadt, Germany
Millipore	Millipore Corporation, MA, USA
Pharmacia	Pharmacia Biotech, Uppsala, Sweden
Pierce	Rockford, IL, USA
Pye Unicam	Pye Unicam Ltd., Cambridge, UK
Sigma	Sigma-Aldrich, WI, USA
Supelco	Supelco International Inc., Bellefonte, PA, USA.
Whatman	Whatman International Ltd., Maidstone, UK

All other abbreviations and symbols used in this thesis follow the recommendations of the Nomenclature Committees of IUBMB and other international committees, as summarised by *Biochemical Journal* 'Instructions to Authors' [*Biochemical Journal* (1998) **329**, 1-16].

CHAPTER 1 LITERATURE REVIEW

1.1 OBJECTIVES

One purpose of the work described here was to participate in the development of a biosensor to detect esters. The initial work completed by our commercial partners in the year immediately preceding the inception of this study, was achieved using two commercial Sigma carboxylesterases (from the snail gut and pig liver) in pH-electrode assays and a biosensor prototype. The conclusion of this work, with respect to activities against *p*-nitrophenyl-acyl-esters and commonly encountered fruit esters, was that pig liver esterase (PLE) would be used as a positive control when screening further enzymes.

The original premise of this enzyme screening study was to seek carboxylesterases or lipases from various sources (including animal, fungi and hyperthermophilic bacteria), and to identify those with the following properties:

(1) adequate activity in the pH range 4.0-5.0;

(2) sufficient stability to retain greater than 50% activity after 14 days at 40°C;

(3) specific activity against methyl butyrate greater than that of PLE; and

(4) a K_m against methyl butyrate less than that of PLE.

Subsequently, the focus switched to non-animal derived enzymes for commercial reasons.

During experimentation with the commercial biosensor application, the issue of dry activity arose with respect to biosensor storage, and subsequently the relationship between protein water content and function became an important focus of the work described here. Consequently, two enzymes (one carboxylesterase and one lipase) were sequentially hydrated, and the relationship between the protein water content of each enzyme and their activity against vapor phase ethyl butyrate (an ester relevant to a possible commercial application) was determined.

1.2 Carboxylic Ester Hydrolases (EC 3.1.1.-)

1.2.1 Catalysis of Ester-Bond Hydrolysis

1.2.1.1 General-Base and General-Acid Catalysis

At alkaline pH, the base group donates a pair of electrons to one of the protons of water, resulting in an increase in the electron density on water's oxygen (Figure 1.1*a*). Water, acting as a nucleophile, attacks the positively charged carbon of the C=O group of the ester and the consequent net movement of negative charge results in the breakdown of the tetrahedral intermediate into its alcohol and acid moieties. At acidic pH, the acid group donates a proton to the oxygen of the C=O group, thereby increasing the positive charge on the carbon (Figure 1.1*b*). This increases the susceptibility of the ester to attack by nucleophiles, such as water, and the breakdown of the tetrahedral intermediate (Zubay, 1993).

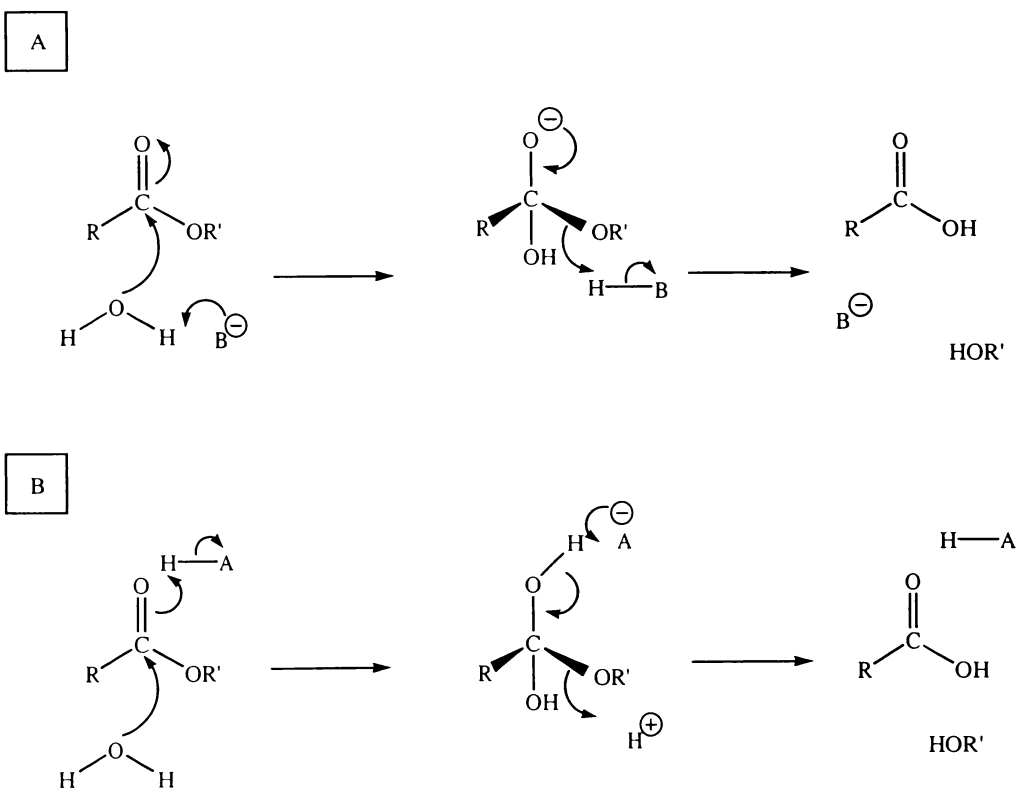

Figure 1.1. Models for non-enzymic ester catalysis.

A curved arrow represents the movement of an electron pair from an electron donor to an acceptor. (A) General-base catalysis; and (B) general-acid catalysis (Zubay, 1993).

1.2.1.2 Enzymic Hydrolysis

Enzymic ester hydrolysis (by lipases and carboxylesterases, for example) incorporates aspects of general-base/acid catalysis. The general base can be a basic group from amino-acid residues or the carboxyl-terminal carboxylate ion. The advantage of enzymic hydrolysis, however, is that the basic or acidic groups are fixed in place within an active site, and are therefore positioned accurately with respect to the ester substrate (Zubay, 1993).

1.2.2 Hydrolases

Hydrolases are a class of enzymes that catalyse the cleavage of ester- (EC 3.1.-.-), glycosyl- (EC 3.2.-.-), ether- (EC 3.3.-.-) and peptide-bonds (EC 3.4.-.-) in the presence of water. The esterase class (EC 3.1.-.-) of hydrolytic enzymes is further divided into carboxylic ester hydrolases, thiolester hydrolases and phosphoric monoester hydrolases (via the ester bond specificity).

The classification of certain enzymes within the carboxylic ester hydrolases category (EC 3.1.1.-) has been difficult due to their wide substrate specificity resulting in their listing as different enzymes by different studies or commercial enzyme producers (for example, cocaine esterase is now classified as carboxylesterase, EC 3.1.1.1). Due to this ambiguity, the nomenclature of three enzyme subclasses within the carboxylic ester hydrolase category have been listed in Table 1.1 along with a number of their alternative names (Webb, 1984).

Table 1.1. The nomenclature of carboxylic ester hydrolases (EC 3.1.1.-).

Name	EC No.	Alternative Name	Systematic Name
Carboxylesterase[1]	3.1.1.1	B-esterase	Carboxylic-ester hydrolase
		Ali-esterase	
		Methyl butyrase	
Triacylglycerol lipase	3.1.1.3	Triglyceride lipase	Triacylglycerol acylhydrolase
		Lipase	
		Tributyrase	
Acetylesterase	3.1.1.6	C-esterase	Acetic-ester acetylhydrolase

[1] previously known as 'unspecific esterase' due to its wide specificity.

1.2.3 Lipase and Carboxylesterase Classification

Three criteria have been used to differentiate "true" lipases (EC 3.1.1.3) from carboxylesterases (EC 3.1.1.1). First, true lipases catalyse the hydrolysis of long-chain acylglycerides whilst carboxylesterases catalyse the hydrolysis of short-chain glycerolesters and simple monoesters, (Khoo and Steinberg, 1975). Although the acyl chain length of the glycerolesters preferentially hydrolysed by lipases has not been strictly defined, a review by Jaeger *et al.* (1999) suggests that acyl chain lengths of ≥ 10 carbon atoms act as lipase substrates.

Second, true lipases require a lipid-water interface for hydrolytic activity. Sarda and Desnuelle (1958) proposed that lipases were carboxylesterases that acted on insoluble esters at the interface between lipid and water. They showed that while a pancreatic lipase was slightly active against an aqueous solution of triacetin, there was a pronounced increase in lipolytic activity as the ester concentration reached initial saturation, with further increases as the saturation level increased (Figure 1.2). Sarda and Desnuelle hypothesised that carboxylesterases acted on water-soluble esters with no dramatic increase in activity once saturation was achieved (Figure 1.3) whilst lipases required a substrate interface (achieved through substrate saturation) for catalytic activation. Furthermore, lipases could only act on the molecules located at the interfacial layer of miceller or emulsified substrates (because natural triacylglycerols are water insoluble while lipases are generally soluble in water).

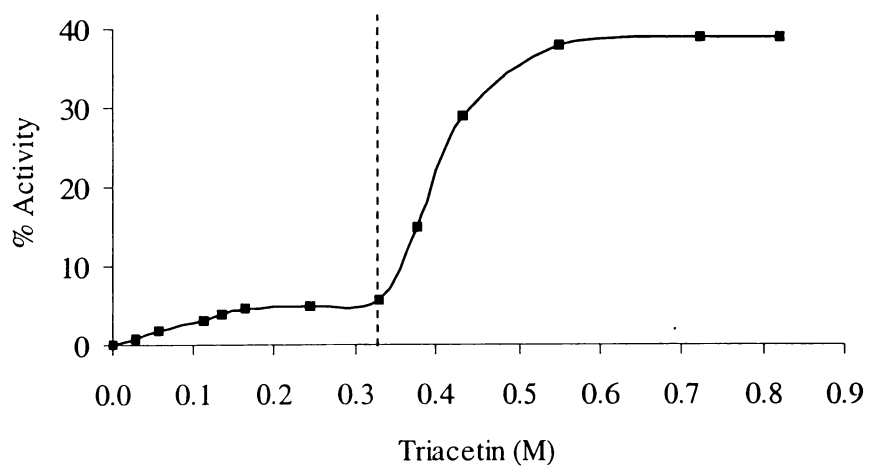

Figure 1.2. Hydrolysis of triacetin by pancreatic lipase.

The activity (%) was calculated as the percentage of the maximum activity obtained against triolein by pancreatic lipase (Sarda and Desnuelle, 1958). The limit at which the triacetin solution becomes saturated (0.328 M) and forms an emulsion is indicated by the vertical dashed line.

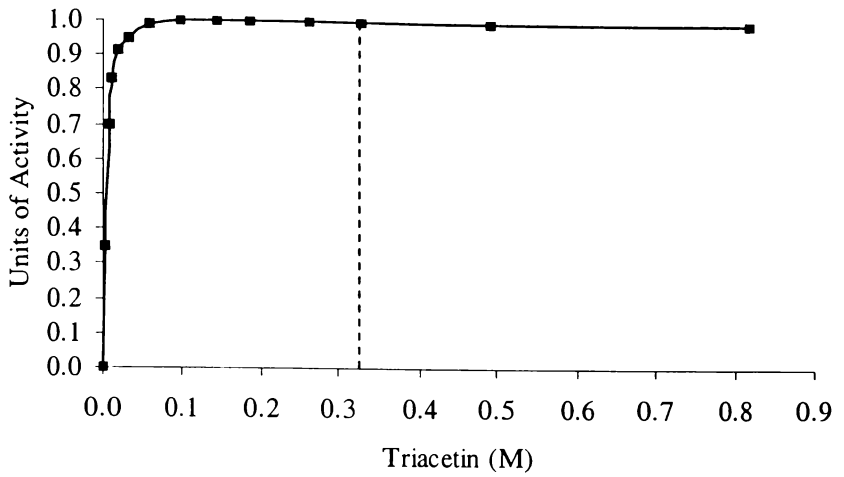

Figure 1.3. Hydrolysis of triacetin by hepatic esterase.

The limit at which the triacetin solution becomes saturated (0.328 M) and forms an emulsion is indicated by the vertical dashed line (Sarda and Desnuelle, 1958).

Third, the structures of true lipases contain a domain, termed the flap or lid, which covers the active site in the absence of a lipid-water interface. It is only when the lipase is in contact with the lipid-water interface that the lid 'opens' and allows the catalytic residues of the active site to come in contact with the lipid substrate (Jaeger *et al.*, 1999).

While these criteria hold true for most lipases, there are exceptions. Not every lipase displays interfacial activation. To illustrate, the coypu and guinea pig pancreatic lipase-related proteins of type 2 show no interfacial activation (even though they have a 23 and 5 amino acid lid, respectively); phospholipase A_2 has no lid but shows significant interfacial activation with diheptanoylphosphatidylcholine; and rat hepatic triacylglyceride lipase and *Staphylococcus hyicus* lipase are not interfacially activatable against some substrates (Ferrato *et al.*, 1997; Tsujita, 1990). Therefore, the absence or presence of interfacial activation or a lid domain should not be used as the only criteria to determine whether a carboxylic ester hydrolase belongs to the carboxylesterase (EC 3.1.1.1) or lipase subfamily (EC 3.1.1.3) (Ferrato *et al.*, 1997).

Moreover, the distinction between lipase and carboxylesterase is not absolute. The assertion by Jaeger *et al.* (1999) that true lipase substrates consist of glycerolesters with acyl chain lengths of $\geq$ 10 carbon atoms ($\geq C_{10}$) does not mean that lipases can not hydrolyse chain lengths of less than 10 carbon atoms. In

fact, lipases have been described as "carboxyl esterases that catalyze the hydrolysis of long-chain acylglycerols" or "simply fat splitting ferments" (Ferrato *et al.*, 1997). To illustrate, the acyl chain length profiles of *Rhizomucor miehei* and *Candida rugosa* lipase are shown in Figure 1.4. Both the *C. rugosa* and *R. miehei* lipase exhibit carboxylesterase and lipolytic activity: *C. rugosa* has significant activity against tributyrin (C_4) with two smaller activity peaks against C_8 and C_{18}, whilst *R. miehei* displays a behaviour closer to that of a true lipase (Ader *et al.*, 1997). This dual behavior, that of a carboxylesterase and a lipase, is the rationale for the screening of both carboxylesterases and lipases during the development of the biosensor.

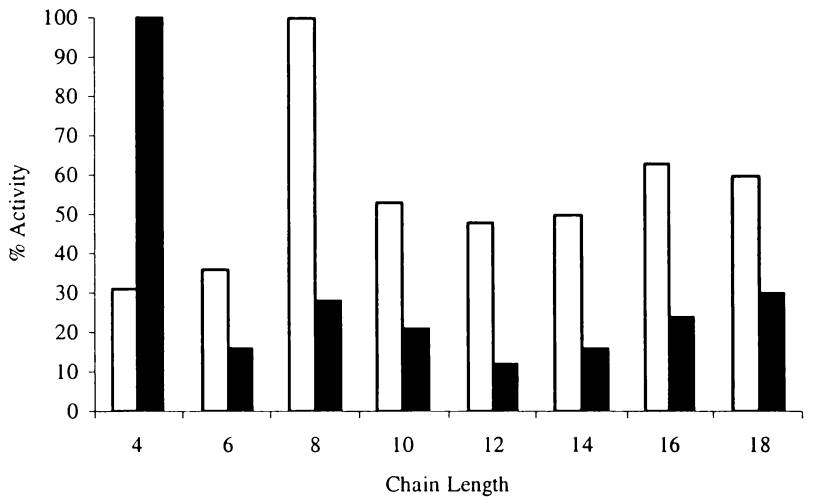

Figure 1.4. Fatty acid chain length profile for lipases from *Rhizomucor miehei* and *Candida rugosa*.

The % activity of *R. miehei* and *C. rugosa* lipases toward triglycerides of varying fatty acid chain lengths are illustrated by the open and black bars, respectively (Ader *et al.*, 1997).

1.3 LIPASES (EC 3.1.1.3)

1.3.1 Lipase Structure

Lipases belong to a group of enzymes that share a folding pattern termed the α/β hydrolase fold. The α/β hydrolase fold is conserved within the majority of the lipase and carboxylesterase family of enzymes and consists of five α-helices and eight strands of β-sheet, where the second strand is antiparallel to the other

seven β-sheets (but despite the high degree of structural homology, there is variation in both the number and order of the α-helices and β-strands) (Bott *et al.*, 1994; Jaeger *et al.*, 1999).

The structural superfamily of α/β hydrolases is dominated by enzymes whose activities depend on the active site catalytic triad formed by a nucleophilic residue (serine, cysteine or aspartate), a catalytic acid residue (aspartate or glutamate) and a histidine residue, in that particular order (Arpigny and Jaeger, 1999). This catalytic triad is common to all serine proteases but the amino acids vary in linear order. To illustrate, the bovine pancreatic trypsin and subtilisin amino acid order is His-Asp-Ser and Asp-His-Ser, respectively (Bott *et al.*, 1994).

The serine residue of the catalytic triad (Ser-Asp-His) found in proteases, lipases and esterases is contained within a highly conserved pentapeptide Gly-Xaa-Ser-Xaa-Gly, where Xaa is any amino-acid residue, and is required for catalytic activity (Bott *et al.*, 1994; Arpigny and Jaeger, 1999; Jaeger *et al.*, 1999). A review by Bott *et al.* (1994) showed that the amino acid sequence surrounding the active serine residue was conserved in the α/β hydrolase family of enzymes (Table 1.2) but could not identify consensus sequences around the catalytic histidine and aspartate residues.

Table 1.2. Comparison of the amino acid sequences around the catalytic triad serine residue. The conserved residues of the consensus sequence Gly-Xaa-Ser-Xaa-Gly are indicated by asterisks (Bott *et al.*, 1994).

Enzyme Class	Enzyme	Local Sequence
		* * *
Lipases	Pancreatic lipase (human)	I-G-H-S-L-G-A
	Lipase (*R. miehei*)	T-G-H-S-L-G-G-
	Lipase (*G. candidum*)	F-G-E-S-A-G-A
Esterases	Carboxylesterase (murine)	F-G-E-S-S-G-G
	Acetylcholine esterase (*T. californica*)	F-G-E-S-A-G-G
	Thioesterase (duck)	F-G-E-S-A-G-G
Protease	Trypsin (bovine)	Q-G-D-S-G-G-P
	Elastase (pig)	Q-G-D-S-G-G-P

1.3.2 Interfacial Activation

The active sites of most lipases are buried by a helical protein loop, the so-called "lid", and consequently the catalytic triad residues are inaccessible by water-soluble lipids. The presence of a lipid-water interface of miceller or emulsified substrate results in the interfacial activation of lipases, whereby a conformational movement in the lid allows the catalytic residues access to the substrate (Jaeger *et al.*, 1999).

In 1991, Brzozowski *et al.* investigated the crystallographic structures of human pancreatic lipase (hPL) and *Rhizomucor miehei* lipase (RmL) using serine protease inhibitors and confirmed that the lid became displaced during interfacial activation. The two lipase structures showed that their catalytic residues, an Asp-His-Ser triad, were buried beneath a short helical segment. Conformational movement in the position of this lid (via interfacial activation) produced two effects: (a) the hydrophobic side of the lid became exposed, thereby increasing the nonpolar surface surrounding the active site; and simultaneously (b) the hydrophilic side of the lid, which was exposed to the solvent in the native structure, was partially buried within the polar cavity that was previously filled with well-ordered water molecules. For example, the open conformation of *Rhizomucor miehei* and *Candida rugosa* lipase exposes approximately 700 Å and 1000 Å of hydrophobic area, respectively (Cygler and Schrag, 1997).

Thus, interfacial activation results in the exposure of the active site's catalytic residues to substrate, and an increase in the stability of and nonpolarity of the active site surface – thereby increasing the affinity of the lipase for the triacylglyceride molecules within the lipid phase (Brzozowski *et al.*, 1991).

1.3.3 Reaction Types

Lipases catalyse a number of reactions, such as the transesterification of triacylglycerides and esterification of fatty acids in nonaqueous environments (Figure 1.5a and 1.5b, respectively), plus the reversible hydrolysis of carboxyl ester bonds of mono-, di- and triacylglycerides (Figure 1.6).

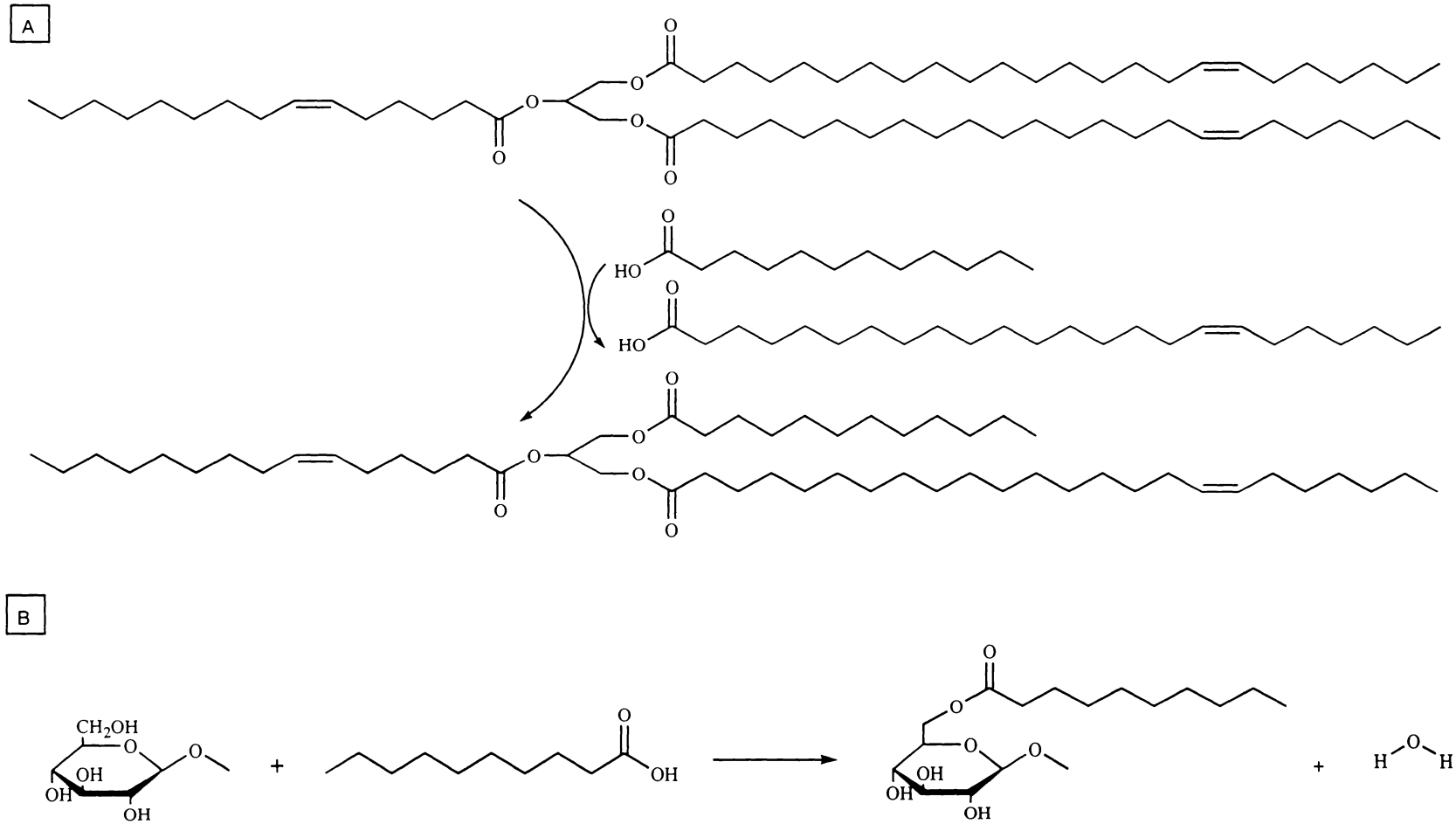

Figure 1.5. Non-hydrolytic lipase reactions.

(A) Transesterification of a triacylglyceride in a nonaqueous environment. (B) Esterification, or ester synthesis (Godtfredsen, 1993).

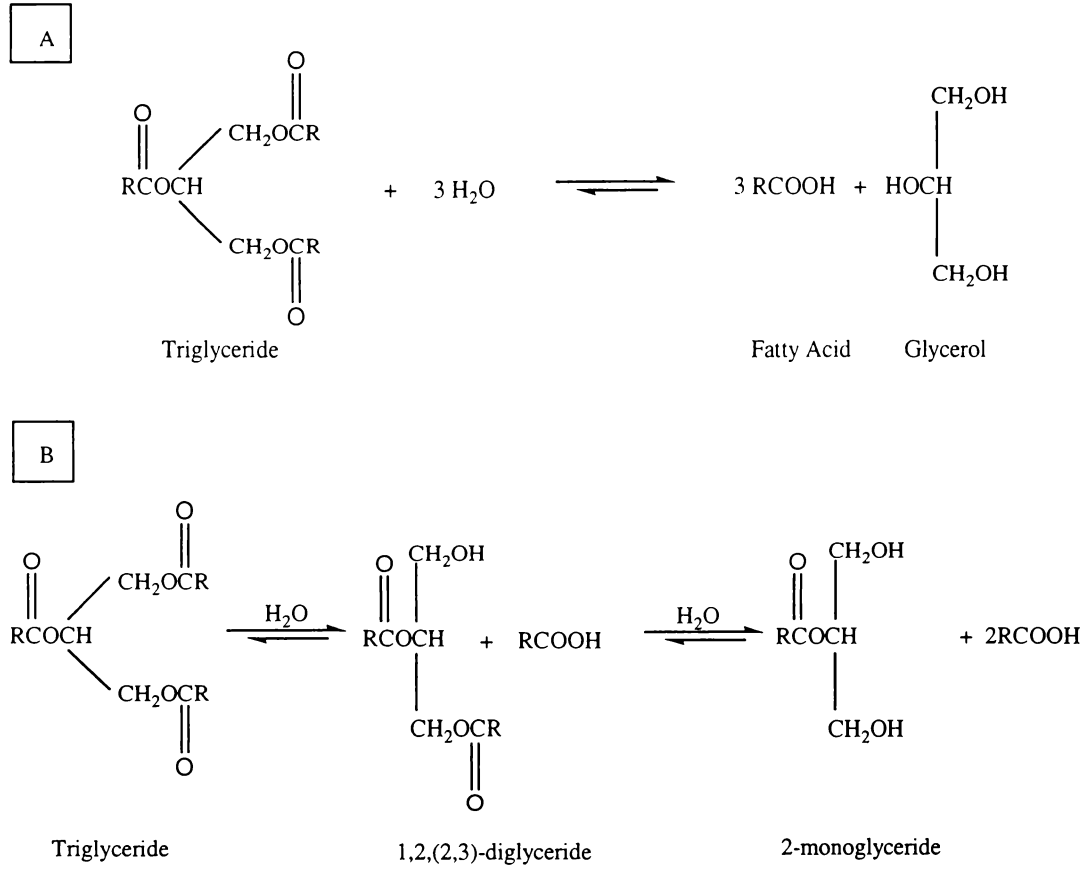

Figure 1.6. Positional specificity of lipases.

(A) The reaction catalysed by non-specific lipases; and (B) the reaction catalysed by 1,3-specific lipases (Macrae, 1983).

1.3.4 Reaction Mechanism

Contact between the catalytic triad and lipid causes activation of nucleophilic Ser by the His residue, and a nucleophilic attack of the carbonyl carbon of the susceptible lipid ester bond by Ser O^- (Figure 1.7*a*). The transient tetrahedral intermediate formed has an O^- that is stabilised by interactions with the two peptide NH groups (Figure 1.7*b*). The catalytic His donates a proton to the ester oxygen of the susceptible bond, which is then cleaved. The alcohol component diffuses away and the acid component is esterified to the enzyme's nucleophilic Ser residue (Figure 1.7*c*). A water molecule hydrolyses the covalent intermediate. The active site His activates the water molecule and the water's resulting OH^- ion attacks the carbonyl carbon atom of the acyl group covalently attached to the Ser residue (a process termed deacylation). Another transient tetrahedral intermediate is formed. Finally, the His residue donates a proton to the oxygen atom of the active serine residue causing the breakage of the bond between the Ser and acyl component and the release of the acyl product (Figure 1.7*d*) (Jaeger *et al.*, 1999).

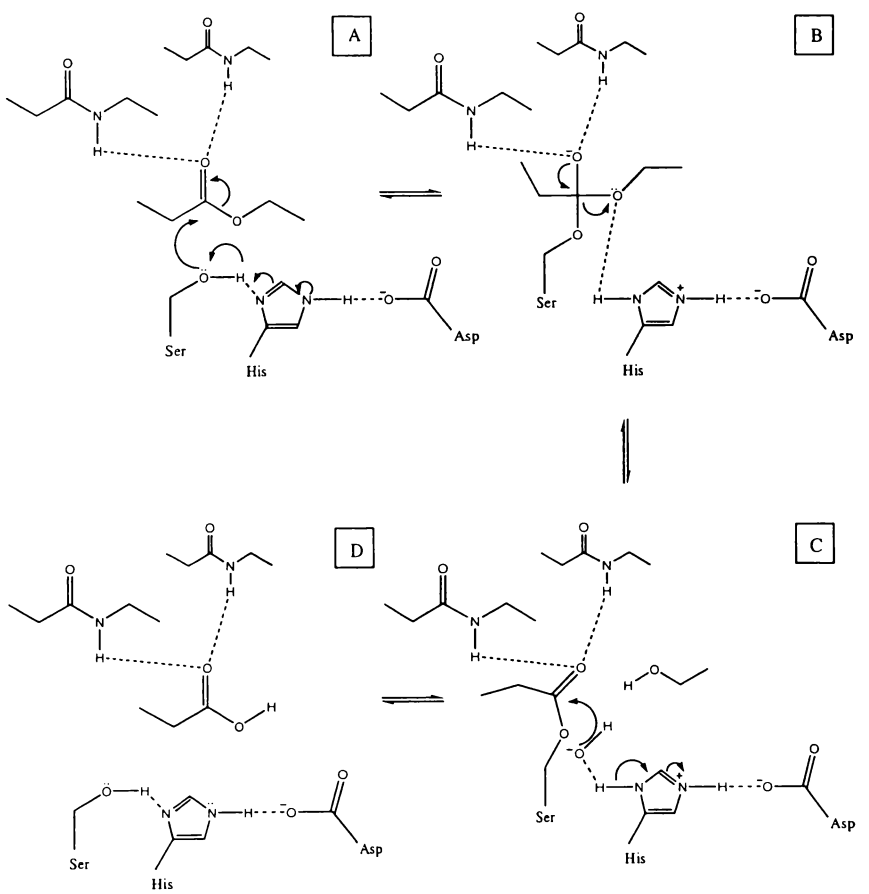

Figure 1.7. The reaction mechanism of lipases.

(Jaeger *et al.*, 1999).

1.3.5 Substrate Specificity

Lipase substrates are lipids, which are a diverse group of molecules that include the natural polar lipids (such as the water-insoluble long-chain triacylglycerols) and the synthetic short-, and medium-chain esters that are used as lipase substrates (such as methyl butyrate and tributyrin). While the long-chain triacylglycerols form stable monomolecular films in water, the synthetic esters can form monomers, monomolecular films, micelles or turbid emulsions in water (as illustrated in Figure 1.8). Interfacial activation of lipases depends on both the interfacial conformation of the lipid and the radius of curvature of the super-substrates (S_2, S_3 and S_4) (Ferrato *et al.*, 1997).

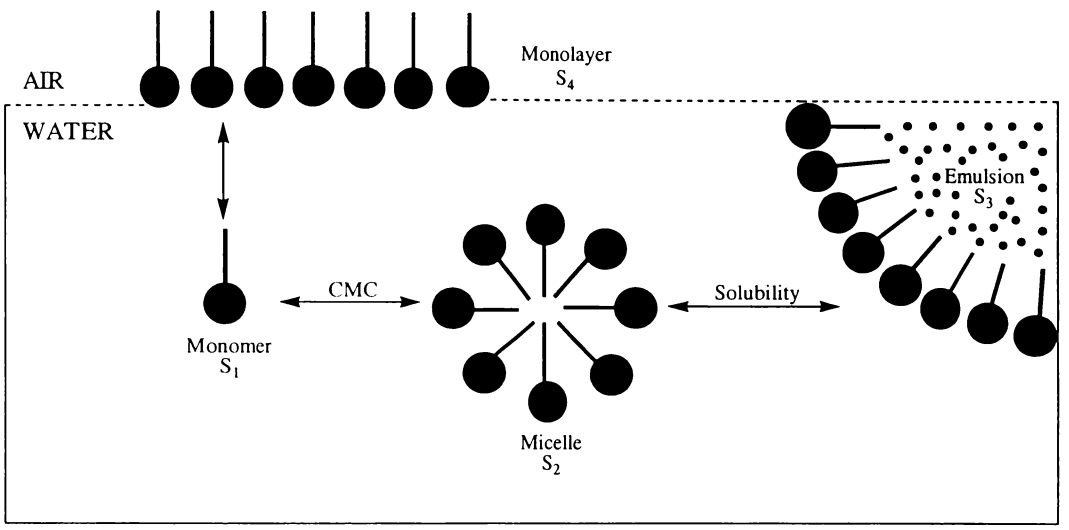

Figure 1.8. Schematic illustration of the various physiochemical states of ester molecules in aqueous media.

Monomer (S_1), micelle (S_2), emulsion (S_3) and adsorbed monolayer (S_4) coexist in equilibrium and represent potential lipase substrate (S_1) or supersubstrates (S_2, S_3 and S_4). The dotted area represents the turbid emulsion (Ferrato *et al.*, 1997).

Despite remarkable structural homology, the substrate specificities of lipases are diverse. Lipases can be divided into two groups based on stereoselectivity (positional specificity) and fatty acid specificity (acyl chain selectivity). First, lipases either exhibit no preference for any of the three acyl residues of the glycerol moiety (Figure 1.6*a*) or preferentially attack the position *sn*-1 and *sn*-3 acyl residues (Figure 1.6*b*), for example 1,3-specific *Mucor miehei* lipase (Macrae, 1983).

Second, lipases show specificity for chain length, with respect to the both the acyl chain (Figure 1.9) and the alcohol moiety (e.g., acylglycerides verses phospholipids) plus the degree of acyl chain saturation. Specificity for acyl chain saturation is best illustrated by the *Geotrichum candidum* B lipase which is the only known lipase that is specific for esters of *cis*-Δ9-unsaturated fatty acids (Macrae, 1983).

Stereoselectivity and fatty acid specificity should not be confused. For example, the preferential release of short- and medium-chain fatty acids by the 1,3-specific gastric lipase during the hydrolysis of milk fat was initially attributed to short-chain fatty acid specificity (Carriére *et al.*, 1994). However, it was determined that while the 4:0, 6:0 and 8:0 fatty acids of milk triacylglycerides were esterified at the *sn*-3 position, the unsaturated fatty acids were predominantly at the *sn*-2 position. Hence, the effect of stereoselectivity, rather than fatty acid specificity, was dominant.

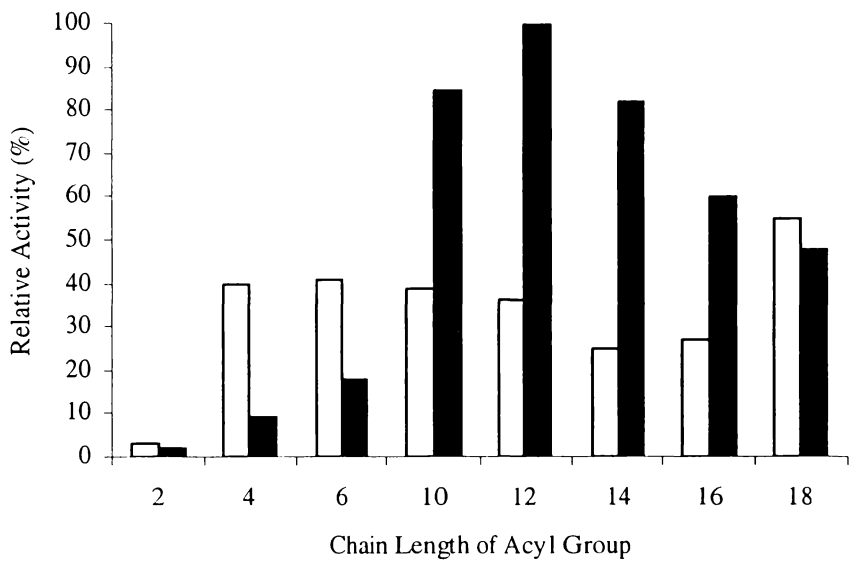

Figure 1.9. Fatty acid specificity of *Bacillus thermocatenulatus* and *Ophiostoma piceae* lipases. The relative activity of *B. thermocatenulatus* lipase (open bars, Rúa *et al.*, 1997) towards varying acyl chain length triacylglycerides and *O. piceae* lipase (black bars, Gao and Breuil, 1998) towards varying acyl chain length *p*-nitrophenyl esters.

1.3.6 Kinetics of Lipolysis

Unlike conventional Michaelis-Menten enzyme kinetics (which was developed for reactions in aqueous solutions), lipolytic enzymes exhibit interfacial kinetics due to a "supersubstrate" requirement for activity (see Figure 1.8). The

term supersubstrate describes a matrix in which a substrate molecule is embedded, and in the case of lipolysis, the matrix is the triacylglyceride droplet surface (Brockerhoff and Jensen, 1974). A model of the lipase action is given in Figure 1.10.

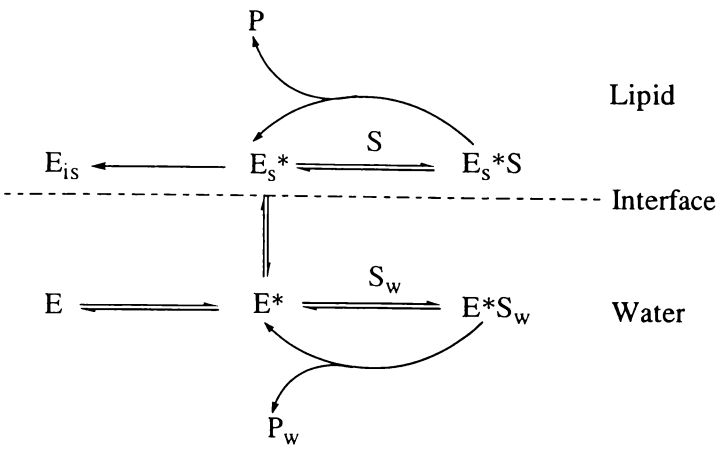

Figure 1.10. Model for lipase action on soluble and insoluble substrates, by lipases that undergo conformational changes upon interfacial activation.

The symbols denote: E, inactive dissolved lipase; E*, active dissolved lipase; E_s*, adsorbed active lipase; E_{is}, adsorbed inactive lipase; S_w, water-soluble substrate; S, water-insoluble substrate; E*S_w and E_s*S, lipase-substrate complexes (Martinelle and Hult, 1994).

Variations in the substrate phase could affect adsorption of the enzyme to the interface and the rate of hydrolysis, plus the active form of the enzyme in solution (E*) and at the surface (E_s*) may have different conformations due to interfacial activation (Martinelle and Hult, 1994). The two postulated lipase conformations are the 'open active' and 'closed inactive' states, where both forms are in free equilibrium favouring the closed form in solution (Hult and Holmquist, 1997). The maximal velocity or rate of a lipase reaction (V_{max}) is attained only when every enzyme molecule is absorbed to the lipid-water interface.

Thus, when this interface is large enough to absorb half of the available enzyme molecules, half the maximal velocity will be achieved and the concentration of the supersubstrate will equal the interfacial Michaelis constant, K_m*. However, Michaelis-Menten kinetics only hold when the supersubstrate concentration is given in units of interfacial area per volume (rather than the weight or molarity) (Brockerhoff and Jensen, 1974).

1.3.7 Mammalian Lipases

There are three groups of mammalian lipases: tissue, milk and digestive tract lipases. Digestive tract lipases are further classified as lingual, pharyngeal, hepatic, gastric or pancreatic lipases (Desnuelle, 1972). Although mammalian lipases are effective in the biosensor application, they will not be described due to a market-place requirement that only non-animal derived carboxylesterases or lipases are used.

1.3.8 Microbial Lipases

Microbial lipases (fungal, yeast and bacterial in origin) are diverse in their substrate specificities and enzymic properties. They are manno-glycoproteins (2 to 15% carbohydrate), acidic in nature, extracellular (membrane-associated or secreted into the growth medium) and generally range from 20 to 60 kDa. Due to the low triglyceride content of many microorganisms (especially in bacteria) there is a correspondingly poor production of intracellular lipases (Macrae, 1983; Desnuelle, 1972). Various physical, chemical and kinetic properties of purified microbial lipases are listed in Table 1.3 and 1.4.

Table 1.3. Physical and chemical properties of microbial lipases.

The properties are as follows: MW, molecular weight; *pI*, isoelectric point; pH_{opt}, pH optimum.

Species	MW (kDa)	*p*I	pH_{opt}	Reference
Aspergillus niger	25	4.6	-	Macrae (1983)
Bacillus thermocatenulatus	16	-	7.0-8.0	Schmidt-Dannert *et al.*(1996)
Candida rugosa LipA	128 (2x 64)	5.8	7.0	Pernas *et al.* (2001); Rúa *et al.* (1993)
Candida rugosa LipB	62	4.8-5.0	7.0	Rúa *et al.* (1993)
Chromobacterium vicosum LipA	120 (2x 60)	-	6.5-7.0	Sugiura (1984)
Chromobacterium vicosum LipB	85	-	6.5-7.0	Sugiura (1984)
Geotrichum candidum	54	4.3	-	Macrae (1983)
Ophiostoma piceae	36	4.1	5.0	Gao and Breuil (1998)
Pseudomonas fluorescens	32	4.5	-	Macrae (1983)
Pseudomonas fragi	33	5	5.5-7.0	Iizumi *et al.* (1990)
Pseudomonas nitroreducens	33	-	7.0	Sugiura (1984)
Streptococcus faecalis	21	-	6.0-8.0	Sugiura (1984)

Table 1.4. Substrate specificity and pH optima of microbial lipases.
Brockerhoff and Jensen, 1974.

Microorganism	Substrate Specificity		pH
	Primary (1) or Secondary (2) Ester	Fatty Acids	Optimum
Aspergillus	1,2	-	5.6
Candida	1,2	All	7.2-8.0
Geotrichum	1,2	*cis*-Δ9 unsaturated	8-9
Mucor	?	Long Chain	5.5
Pseudomonas	1	All	6
Puccini	1,2	All	6.7
Rhizopus	1	All	8

Three-dimensional X-ray structures have been elucidated from various microbial lipases, including *Rhizomucor miehei* lipase (where the X-ray structure of this lipase along with human pancreatic lipase were the first unraveled), *Geotrichum candidum* lipase, *Chromoacterium viscosum* lipase, *Candida rugosa* Lipase A and B, and *Pseudomonas fluorescens* lipase (Jaeger *et al.*, 1999).

A recent review of databanks, such as GenBank and the Swiss Protein Sequence database, by Jaeger *et al.* (1999) identified six bacterial families of lipolytic enzymes based on amino acid sequence homology. The Family I lipolytic enzymes are true lipases (Table 1.5).

Table 1.5. 'True' lipase producing bacterial species.

Family	Sub-family	Bacterial Species	Similarity[1]
I	1	*Pseudomonas aeruginosa*	100
		Pseudomonas fluorescens	95
	2	*Chromobacterium viscosum*	35
		Pseudomonas luteola	33
	3	*Serratia marcescens*	15
	4	*Bacillus subtilis*	16
		Bacillus pumilus	13
	5	*Bacillus stearothermophilus*	15
		Bacillus thermocatenulatus	14
	6	*Propionibacterium acnes*	14

[1] Similarities of amino acid sequences were determined with the program Megalign (DNAStar), with the first member of each family arbitrarily set at 100% (Jaeger *et al.*, 1999).

1.3.9 *Candida rugosa* LipA and LipB

Candida rugosa (equivalent to *Candida cylindracea*) is an asporogenic, pseudo-filamentous, unicellular yeast that has GRAS status (generally regarded as safe), thereby making this yeast, and its products, ideal for use in diverse biotechnology sectors that include the food, cosmetic and pharmaceutical industries (Benjamin and Pandey, 1998). *C. rugosa* secretes a number of exolipase isoforms that are encoded by a 'lipase minigene family' designated *lip1* to *lip7*. At least five of these closely related lipases, termed CRLs, have been reported to be monomeric proteins composed of 534 amino acids and approximately 60 kDa. Two major CRL populations named LipA and LipB (encoded by *lip3* and *lip1*, respectively) have been purified and characterised (Brahimi-Horn *et al.*, 1990; Benjamin and Pandey, 1998; Cygler and Schrag, 1999; and Rúa *et al.*, 1993).

1.3.9.1 Structure

Comparison of the amino acid sequences of the five CRLs reveals close homology, ranging between 77 and 90% identity for pairs of proteins. Reviews by Cygler and Schrag (1999) and Rúa *et al.* (1993) concluded that all the CRLs belong to the α/β hydrolase family of enzymes (with 11 strands of β-sheet and eight α-helices) and contain the catalytic triad Ser-His-Glu (where glutamate replaces aspartate as the acid residue) common to serine proteases, esterases and lipases. This catalytic triad is located at the top of the β-sheet and embedded within a structural motif composed of short helical fragments, and is inaccessible to the solvent in the closed conformation.

In 1996, Otero *et al.* used circular dichroism (CD) and fluorescence spectroscopy to study the conformational changes exhibited by *C. rugosa* LipA and LipB during interfacial activation. This study concluded that interfacial activation was due not only to a conformational rearrangement ('opening') of the lid, but also to changes in the secondary structure of the lipases since the α-helix content changed from 28 to 49% and 24 to 26% in LipA and LipB, respectively. Furthermore, a review by Cygler and Schrag (1997) described how the α-helices within the lid (topologically between β-strands β1 and β2) partially unwound on one side and extended on the other during the shift from the closed to open

conformation. In addition to the refolding of the secondary structure, *cis/trans* isomerisation of a proline peptide bond occurred, resulting in an increase in the energy requirement for the transition between the open and closed conformation (Cygler and Schrag, 1999). This increase in the energy requirement was postulated as the reason for the low activity against soluble triacetin and the low rate of interfacial "inactivation" in aqueous solution exhibited by both lipases (Pernas *et al.*, 2001).

1.3.9.2 Reaction Types

CRLs are versatile and in high demand by bioindustry because they catalyse a wide range of industrially important reactions (of which the reaction schemes are illustrated in Figure 1.11).

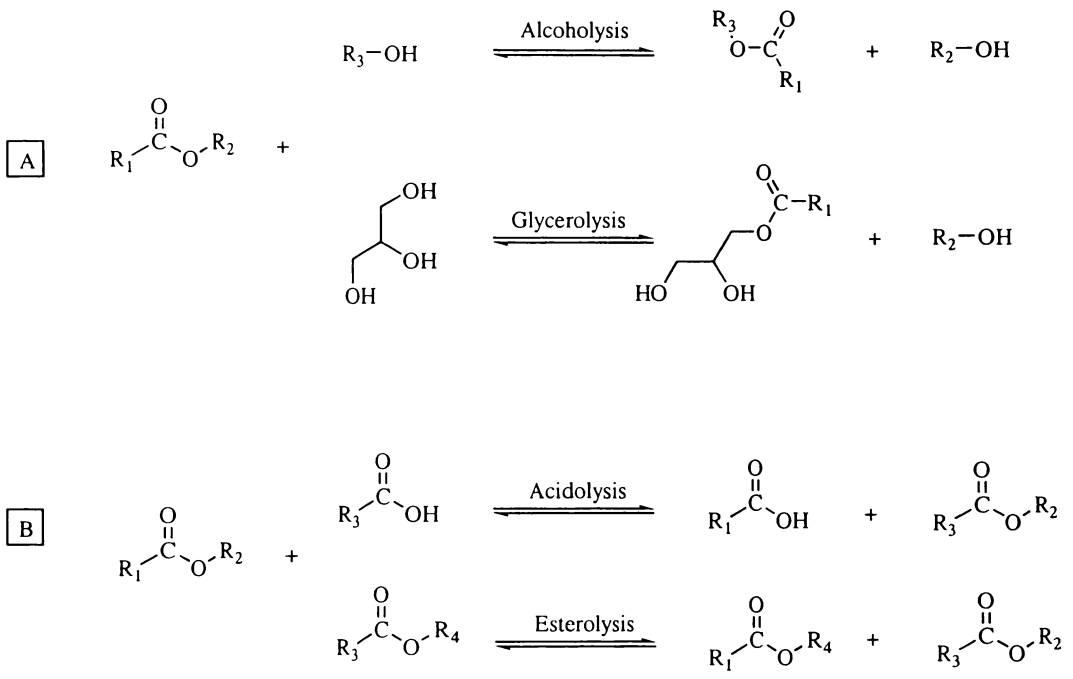

Figure 1.11. CRL catalysed reactions.

(A) Transesterification involves the transfer of an acyl group to an alcohol (alcoholysis) or glycerol (glycerolysis). (B) Inter-esterification involves the transfer of an acyl group to a fatty acid (acidolysis) or a fatty acid ester (esterolysis) (Benjamin and Pandey, 1998).

1.3.9.3 Substrate Specificity

Although CRLs are non-specific (they lack positional specificity) and preferentially hydrolyse substrates derived from short-chain fatty acids and alcohols, substrate specificity can depend on both the commercial preparation and isoform studied (Benjamin and Pandey, 1998). Two isoforms that have been well

characterised are LipA and LipB which have similar amino acid sequences and molecular weights, but differ in pH and temperature stability (Redondo *et al.*, 1995; Rúa *et al.*, 1993). In spite of the high sequence homology, 23 of the 55 residues that are unique to LipA are concentrated within the active site, the dimer interface and the hydrophobic core, resulting in LipA having greater flexibility in the flap and superior stabilisation of the 'open' conformation in aqueous solutions. This is reflected in a lower lipase/esterase activity ratio of LipA when compared to LipB (7.6 and 43.7, respectively) (Pernas *et al.*, 2001).

LipA and LipB show both esterase and lipolytic activity, as they are able to hydrolyse soluble esters and long-chain triacylglycerides, respectively (Table 1.6). However, the activity profiles of the lipases against *p*-nitrophenyl esters can depend upon the physical presentation of the substrate. In micellar media, LipA and LipB show optimal activity against *p*NP-C_8 and -C_{12} esters, respectively (indicative of lipolytic activity), whilst in aqueous solution both show optimal activity against *p*NP-C_4 esters (esterase activity). Redondo *et al.* (1995) attributed this disparity to the formation of polymolecular aggregates of substrate in aqueous solution, thus increasing the interfacial substrate surface and resulting in interfacial activation.

Table 1.6. Kinetic and physical parameters of *Candida rugosa* LipA and LipB.
Rúa *et al.* (1993).

Lipase	MW (kDa)	*p*I	*p*-Nitrophenyl Laurate (C_{12})[1]			*p*-Nitrophenyl Butyrate (C_4)[2]		
			k_{cat} (s^{-1})	K_m (μM)	k_{cat}/K_m (s^{-1}/M^{-1})	k_{cat} (s^{-1})	K_m (μM)	k_{cat}/K_m (s^{-1}/M^{-1})
A	117[3] (2x 64kDa)	5.8	36	120	$3.00x10^5$	1010	39.2	$2.51x10^7$
B	62	4.80-5.04[4]	50	90	$5.55x10^5$	>1600	>400	$0.42x10^7$

[1] *p*-nitrophenyl-laurate was present in mixed micelles with Triton X-100; [2] Redondo *et al.* (1995); [3] Pernas *et al.* (2001); and [4] LipB consists of four isoforms with isoelectric points of 4.80, 4.84, 4.95 and 5.04.

Both LipA and LipB exhibit interfacial activation against triolein and triacetin. Minimal activity is shown against a triolein below its solubility limit (20 μM), but above 20 μM the activity dramatically increases and shows Michaelis-Menten–type kinetics (Rúa *et al.*, 1993). The strength of the interfacial activation exhibited against triacetin differs between LipA and LipB (Figure 1.12). Although the solubility limit for triacetin is 0.18 M, the concentration at which the

first large-size triacetin droplets form is 0.27 M. It is at this latter concentration that LipA displays a pronounced activation and LipB exhibits low interfacial activation (Pernas *et al.*, 2001).

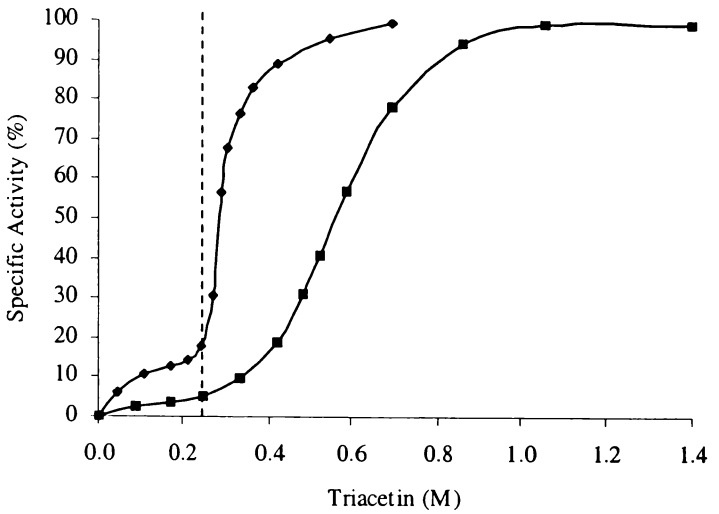

Figure 1.12. Dependence of LipA and LipB activity on triacetin concentration.
Specific activity (%) was calculated as the percentage of the maximum activity obtained against triacetin by LipA (◆) and LipB (■) (Pernas *et al.*, 2001). The concentration limit at which the triacetin solution first forms large-sized droplets is indicated by the vertical dashed line.

1.3.9.4 Effect of Salts on Activity

LipA and LipB activity are both sensitive to the presence of inorganic cations (Hernáiz *et al.*, 1994). While hydrolysis is inactivated by Co(II), Mg(II), Cu(II), Fe(II) and Hg(II), both Na(I) and Ca(II) increase hydrolytic activity. Hernáiz *et al.* (1994) attributed this increase in lipolytic activity to an interfacial phenomenon rather than an enzyme-effector interaction. It was hypothesised that the presence of Na(I) or Ca(II) cations favour the formation of a lipid-water interface (through the stabilisation of micelles). More importantly, the presence of monovalent sodium and divalent calcium could remove one or two fatty acid molecules from this interface, respectively. Consequently, the rate of free fatty acid molecules production in the hydrolytic reaction would increase, thereby enhancing the "turnover" number and thus, the specific activity.

1.4 CARBOXYLESTERASES (EC 3.1.1.1)

Carboxylesterases are serine-dependent hydrolases that primarily catalyse the hydrolysis of ester linkages between carboxylic acid groups and hydroxyl groups (the reaction is frequently reversible as it is dependent upon reactant concentration or water availability). Nevertheless, definitions of 'carboxylesterase' have been heavily debated since the earliest attempts to classify this family of enzymes.

Firstly, carboxylesterases often have broad specificity and overlapping substrate specificities, and consequently may mediate the hydrolysis of peptides, aromatic amides, halides and mono- or tri-acylglycerides (Walker and Mackness, 1983). To illustrate, carboxylesterase/amidase is a common term that is the general designation given to an esterase that hydrolyses both carboxylester and amide linkages (Heymann and Mentlein, 1981). Secondly, the merit of the classification system by which esterases were termed ali- (or carboxyl-), aryl- or cholin-esterases (based upon their ability to hydrolyse aliphatic, aromatic and choline esters, respectively) has long been questioned since the system's development. Some so-called aliesterases (carboxylesterases, EC 3.1.1.1.) can hydrolyse aromatic esters while some arylesterases (EC 3.1.1.2) can hydrolyse aliphatic esters (Walker and Mackness, 1983).

Thus, Walker and Mackness (1983) suggested the definitive classification of carboxylesterase should include data on the turnover number with ester substrates, whereby only enzymes with turnover numbers in the order of thousands with aliphatic-esters can be called carboxylesterases. For example, both pig liver esterase (a carboxylesterase) and α-chymotrypsin (a serine protease) exhibit esterase activity toward *p*-nitrophenyl acetate. However, the turnover numbers of pig liver esterase (PLE) and α-chymotrypsin are 41,000 and 0.92, respectively (Krisch, 1966), yet α-chymotrypsin displays reactivity equivalent to that of PLE toward "specific" substrates, such as *N*-acetyl-L-tyrosine ethyl ester (Stoops *et al.*, 1969).

1.4.1 Microbial Carboxylesterases

Microbial carboxylesterases are of great importance in the food and beverage industry where they are used for the production of flavour compounds,

such as free fatty acids in cheese (McKay, 1993). Although microbial carboxylesterases are effective in the biosensor application, they will not be described further because a microbial carboxylesterase with higher activity than PLE, against the esters of interest, was not found.

1.4.2 Mammalian Liver Carboxylesterases

Dating back to the 1950's, a large number of studies have concentrated on the enzymic and physical characterisation of liver microsomal carboxylesterases (of which various physical properties are listed in Table 1.7). These carboxylesterases have pH optima between 7.5 and 9.0, are diverse in their substrate specificities, highly active against ester- and amide-containing substrates, and participate in the detoxification or metabolic activation of various drugs, carcinogens and environmental pollutants (Krisch, 1971; Satoh and Hosokawa, 1998).

Table 1.7. Physical properties of purified carboxylesterase isozymes from mammalian livers.

Mammal	Name	MW (kDa)	*p*I	Reference
Pig	P1	160-180 (trimer)	5.0-5.4	Horgan *et al.* (1969), Krisch (1971), Scott and Zerner (1975),
Horse		70	-	Inkermam *et al.* (1975)
Ox		168	-	Krisch (1971)
Rabbit	ES-1A	63	5.35-6.04	van Lith *et al.* (1989)
Cow	B1	59	6.0	Satoh and Hoskawa (1998)
Chicken		67	4.9-5.1	Scott and Zerner (1975), Inkerman *et al.* (1975)
Mouse	MH1	60	5.8	Satoh and Hoskawa (1998)
Rat	RLlec	60	4.7	Satoh and Hoskawa (1998)
	RL1	61	6.5	Satoh and Hoskawa (1998)

1.4.2.1 Localisation

Mammalian carboxylesterases are encoded by a multigene family and are predominantly localised at the endoplasmic reticulum (through the carboxyl-terminal HXEL retention signal, as determined by Robbi and Beaufay [1991]) or in the cytosol (no signal) of a variety of mammalian tissues and organs, such as the skin and heart, of which the highest hydrolytic activity resides in the liver

(Satoh and Hosokawa, 1998 and references therein). Within liver homogenates there are three different hydrolytic fractions associated with: lysosomes (with a pH optimum of 5), microsomes/cytosol (with a pH optimum of 8-9) and the plasma membrane. Although the majority of the activity is found in the microsomes, the lysosomal and cystolic liver fractions are also highly active (Keough *et al.*, 1985, Satoh and Hosokawa, 1998). However, the carboxylesterases from each fraction differ in structure and substrate specificity. For example, the PLE preparation (Sigma) used in this study is cystolic in origin and displays a different enantioselectivity than pig liver microsomal esterase towards *S*- and *R*-enantiomers of racemic oxazepam 3-acetate (Yang *et al.*, 1995).

1.4.2.2 Homology

A large number of liver carboxylesterase families contain a highly conserved catalytic triad (Ser203, Glu 335 and His448) that is also shared by serine proteases and lipases (see Section 1.3.1). Furthermore, liver carboxylesterases frequently have four cysteines (where Cys98 is the most highly conserved residue) and a Gly123-Gly124 sequence that are involved in specific disulphide bonds and the formation of an oxyanion hole, respectively (Satoh and Hosokawa, 1998 and references therein). The homology of the amino acid sequence surrounding the active site serine residue in liver carboxylesterases is reviewed in Table 1.8.

Table 1.8. Comparison of the amino acid sequence surrounding the catalytic triad serine residue of mammalian liver carboxylesterases.

The catalytic triad serine residue is indicated by the bold font (Satoh and Hosokawa, 1998).

Mammal	CES Family	Local Sequence
Pig	1	GESAGGE[1]
Horse	1	GESAGGE[1]
Dog	1	GESAGGE
Human (HU1)	1	GESAGGE
Ox	1	GESAGAE[1]
Hamster (AT51)	2	GVSAGGT
Mouse (ES-Male)	3	GNSAGGN
Human (46.5 kDa)	4	GDSAGGN

[1] Dudman and Zerner (1975).

Satoh and Hosokawa (1998) proposed a classification system for liver carboxylesterases based on the high homology of the carboxylesterase sequences (when compared to human liver carboxylesterase). In this system, carboxylesterase isoenzymes are arranged into four families termed CES1 to CES4 (where CES1 is divided into five subfamilies). The CES1 family includes the major form of human carboxylesterase, plus the major isoforms of rat, dog, rabbit, and mouse carboxylesterase. The functions of the CES2 carboxylesterases are primarily that of *N* or *O* acetyltransferases (e.g., hamster AT51 carboxylesterase), while the CES3 carboxylesterase functions are unclear (e.g., mouse ES-Male carboxylesterase). Unlike the first three families, the CES4 carboxylesterases have a different structure and include the novel 46.5 kDa human and mouse liver carboxylesterases.

1.4.2.3 Reaction Mechanism

The reaction mechanism of carboxylesterases is very similar to that of lipases (see Figure 1.7) where Glu335 and His448 participate in a putative charge relay system with Ser203. Upon contact with substrate, a proton is transferred to His448 from Ser203 in the transition state. The nucleophilic Ser203 O^- attacks the acyl carbonyl group of the substrate (Figure 1.13*a*) and the resulting oxyanion of the tetrahedral intermediate is stabilised by two low-barrier H-bonds to peptide N-H 'groups' contributed by Gly123 and Gly124 (Figure 1.13*b*). Acyl-enzyme complex formation removes a proton from His448, and the tetrahedral intermediate is disrupted in the acyl-enzyme intermediate (Figure 1.13*c*). When the alcohol component of the reaction has diffused away, a deacylation step follows, whereby a water molecule substitutes for the alcohol group of the original substrate (Figure 1.13*d-f*) (Satoh and Hosokawa, 1998).

1.4.2.4 Substrate Activation

Substrate activation describes a phenomenon in which increasing substrate concentration results in enzymic reaction rate increases that are higher than those expected for Michaelis-Menten kinetics. Deviations from Michaelis-Menten kinetics occur when the reaction mechanism has more than one parallel pathway for the conversion of substrate to product, where the relative activities of these

pathways change with changing substrate concentration (Adler and Kistiakowsky, 1962).

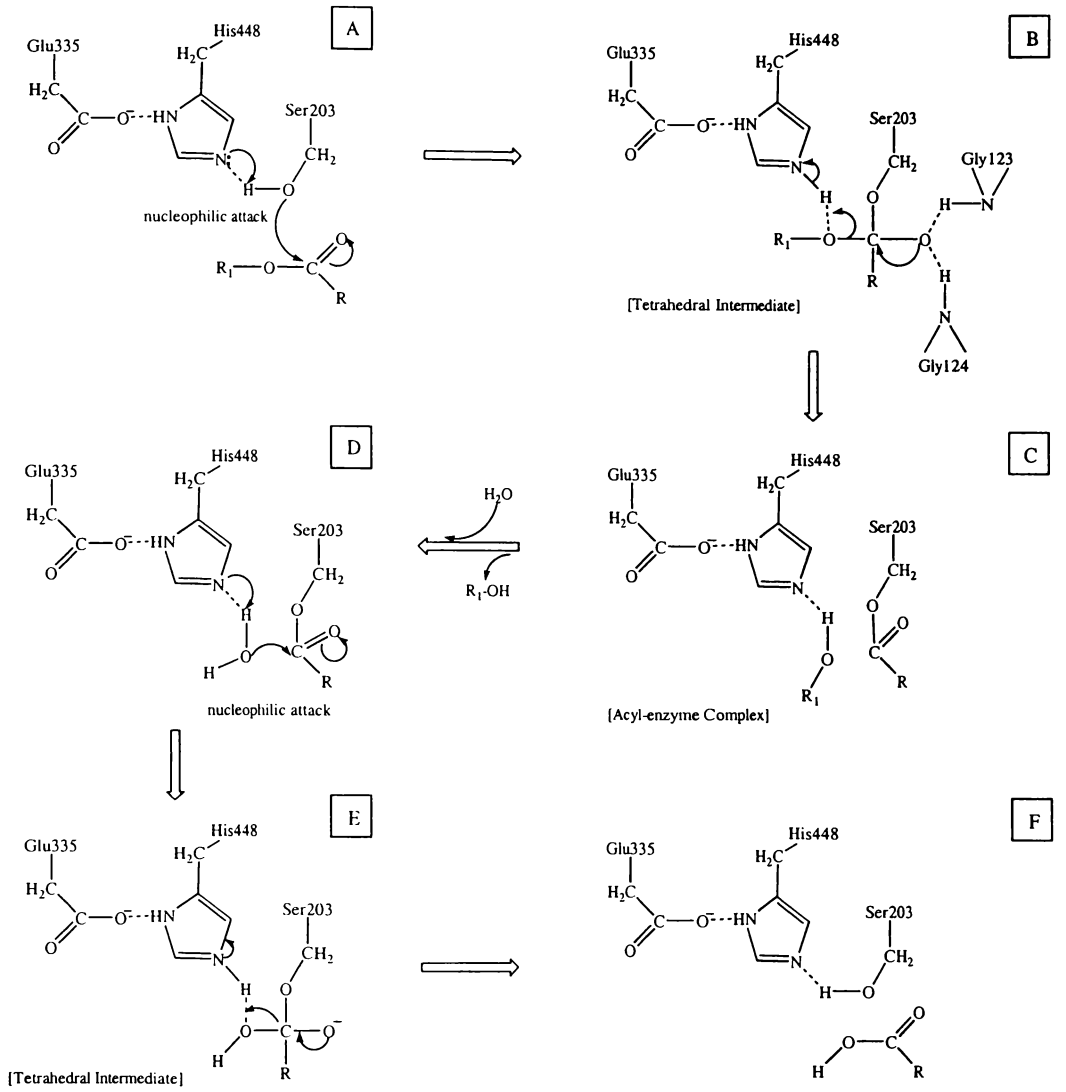

Figure 1.13. A proposal mechanism for the action of carboxylesterase.
Satoh and Hosokawa (1998).

A PLE study by Adler and Kistiakowsky (1962) described five substrate activation mechanisms: (1) enzyme activation by a second molecule of substrate; (2) interactive identical active sites, where the presence of substrate at one site causes a change in the kinetic parameters of the other site; (3) two or more different enzymes; (4) two or more non-identical active sites on the same enzyme molecule; and (5) a modifier mechanism. However, biochemical data was inconsistent with mechanisms 3 to 5, and mechanism 1 could not provide a

method by which kinetic parameters (such as V_{max}) could be obtained. Thus, it was concluded that there were two interactive active sites per PLE molecule.

A study of liver carboxylesterases from seven different species (ranging from pig to pigeon) by Hofstee (1972) concluded that all seven carboxylesterases exhibited substrate activation with varying acyl C-chain length *n*-fatty acid esters of *m*-hydroxybenzoic acid. The substrate activation was not dependent on the formation of dimers or trimers (Barker and Jencks, 1969) since all the carboxylesterases except the one from pig (a trimeric enzyme) were in a monomeric state and the seven enzymes displayed different transition points from the 'low' to 'high' substrate concentration kinetic systems (where Michaelis-Menten kinetics are exhibited at low substrate concentration). In accordance with Adler and Kistiakowsky (1962), Hofstee (1972) hypothesised that two types of active site participated in the substrate activation event, where an activator site is situated outside of the active centre proper, and the reaction rates at low substrate concentration would involve the interaction of the substrate and active centre proper, whereas the high substrate concentration reactions rates would additionally involve the activator site.

1.4.3 Pig Liver Esterase

1.4.3.1 Molecular Weight

The secondary structure of PLE, as determined by optical rotatory dispersion, consists of β-sheet, α-helix and random coil at levels of 80%, 15% and 5%, respectively (Farb and Jencks, 1980). The molecular weight, subunit number and other physical and kinetic parameters of PLE have been extensively studied since the 1960's. The number of PLE subunits has been estimated between two and four depending upon the method of determination. Dudman and Zerner (1975) determined via gel filtration that the molecular weight of trimeric PLE was 206±8kDa (at 66kDa per monomer). Barker and Jencks (1969) and Horgan *et al.* (1969) concluded PLE to be a dimeric enzyme of 168 and 163±15 kDa, respectively. Sedimentation coefficient and gel filtration studies (as reviewed by Horgan *et al.*, 1969) have determined the molecular weight of dimeric PLE to be between 150-200 or 70-82 kDa per monomer. However, two other studies described PLE as consisting of four subunits between 40 and 45 kDa each.

1.4.3.2 Subunit Composition

Heymann and Junge (1979) investigated the heterogeneity of trimeric PLE isoenzymes using analytical dodecyl sulfate electrophoresis. Three different subunits were separated and isolated from heterogeneous preparations of PLE, and their properties are displayed in Table 1.9. The three subunits were designated α, β and γ (where the α and γ forms dominate) and were 58.2, 59.7 and 61.4 kDa, respectively. The α, β and γ subunits differed only in primary amino acid sequence (there was no secondary modification of the protein side-chains) and behaved like an aliesterase, serine hydrolase and cholinesterase, respectively. They concluded that native PLE consisted of a diverse mixture of pure (e.g., ααα) or hybrid (e.g., αγγ) variants of the three subunits.

Table 1.9. Properties of PLE subunits.

Subunit	MW (kDa)	*p*I	N-terminus	C-terminus	Activity	
					Methyl Butyrate	Butanilicain
α	58.2	5.8	Gly	Leu	++	(+)
β	59.7	5.2	Gly	Gly(?)[1]	+	++
γ	61.4	4.7	Gly	Ala[1]	+	++

[1] Discrimination between β and γ subunit not yet possible

However, Farb and Jencks (1980) discovered that the subunit combinations were not random. Instead, there was a favoured association between subunits of similar charge and specificity, where the substrate specificity and overall charge of each subunit was distinct due to small differences in their amino acid compositions. It was postulated that the primary function of the variants was to increase the substrate spectrum vulnerable to hydrolysis by PLE. This theory is in accordance with the function of many liver carboxylesterases – an enzyme that participates in the detoxification or metabolic activation of various ester- and amide-containing drugs, carcinogens and environmental pollutants (Satoh and Hosokawa, 1998).

1.4.3.3 Active Site Model

Active site models are applied as an interpretive tool to predict stereospecificity for new substrate structure types. In the case of PLE, this role is

important since PLE is widely used in organic chemistry due to the high stereoselectivity of its catalyses. The PLE active-site model (Figure 1.14) proposes that substrates interact with two polar binding sites, designated $P_{F(ront)}$ and $P_{B(ack)}$, and two hydrophobic sites, $H_{L(arge)}$ and $H_{S(mall)}$, wherein the polar binding sites have higher steric tolerance than the hydrophobic sites (Rojas-Garbanzo and Mata-Segreda, 1998). The volumes of the P_F, P_B and H_S and H_L sites were first determined by a 1990 study to be 2.0, 3.2, 6.0 and 40.5 $Å^3$ (Provencher *et al.*, 1993, and references therein).

Provencher *et al.* (1993) and Provencher and Jones (1994) reinvestigated the pocket-dimensions of the four binding sites because they speculated that the previous dimensions (especially that of the H_L pocket) represented minimal values only. The two studies, which used derivatised malonate substrates (for example, substituted-phenyl malonate) to systematically probe the steric tolerances of the pockets in three dimensions, confirmed that the dimensions specified for the hydrophilic (P_F and P_B) and small hydrophobic (H_S) pockets were valid. However, the dimensions of the large hydrophobic (H_L) pocket changed from 2.3 x 3.2 x 5.5 Å to 3.1 x 4.7 x 6.2 Å (equivalent to a volume change from 40.5 $Å^3$ to 90 $Å^3$).

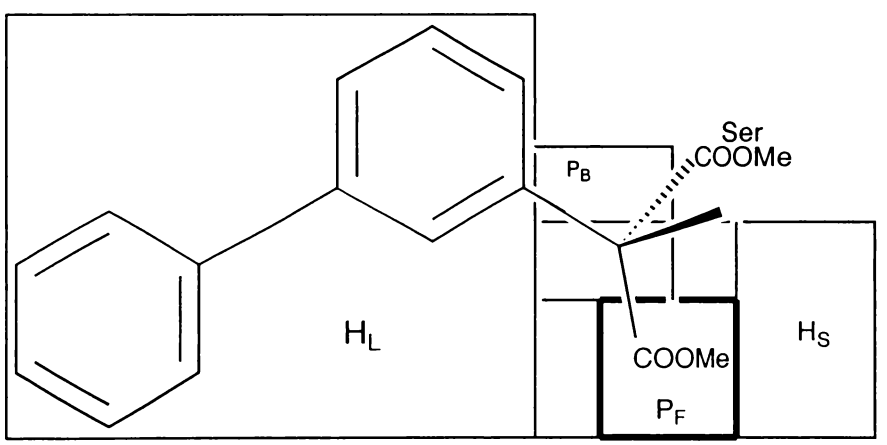

Figure 1.14. The front perspective of the active site model for PLE.

The binding of biphenylyl malonate is shown from the front perspective (Provencher and Jones, 1994). The four substrate binding sites are designated as follows: H_L, large hydrophobic pocket; H_S, small hydrophobic pocket; P_F, front polar-binding pocket; and P_B, back polar-binding pocket.

1.4.3.4 Kinetic Properties

Detailed studies of the kinetic properties of PLE have been carried out by Barker and Jencks (1969), Greenzaid and Jencks (1971), Stoops *et al.* (1969) and Junge and Heymann (1979).

1.4.3.4.1 Functioning Active Sites

Active site titration with *p*-nitrophenyl dimethylcarbamate (NPDMC), bis(*p*-nitrophenyl phosphate (BNPP) and diethyl *p*-nitrophenyl phosphate indicates the presence of two binding sites per molecule of enzyme (Adler and Kistiakowsky, 1962; Dudman and Zerner, 1975; Greenzaid and Jencks, 1971; Krisch, 1966).

While Krisch (1966) determined that the two active site centres were on different subunits (whereby either the two subunits participated in the formation of one active site, or only two of the four subunits carried active sites), Adler and Kistiakowsky (1962) and Dudman and Zerner (1975) concluded that both active site centres were on the same monomeric unit (since monomeric PLE solutions displayed full activity and substrate activation). Furthermore, the two active site centres existed as a true catalytic site (or active centre proper) and an activator binding site (which binds substrates or benzene for example, causes an increase in catalysis and is responsible for the substrate activation that is seen in many liver carboxylesterases). The significant difference between the two sites was not arrived at until 1971, when Greenzaid and Jencks (1971) concluded that while one site catalysed the hydrolysis of relatively large substrates and was partially resistant to phosphorylation by organophosphates; the other site was more sensitive to inhibition by acetone and organophosphates, and catalysed the hydrolysis and methanolysis of smaller substrates.

1.4.3.4.2 Acyl-enzyme Intermediate

The reactions of PLE with NPDMC and E-600 (Figure 1.15) reveal an initial rapid release (or "burst") of *p*-nitrophenol followed by a slow zero-order substrate turnover. This is consistent with the formation of an acyl-enzyme intermediate and the release of the product alcohol, followed by the release of the product acid (see Figure 1.13).

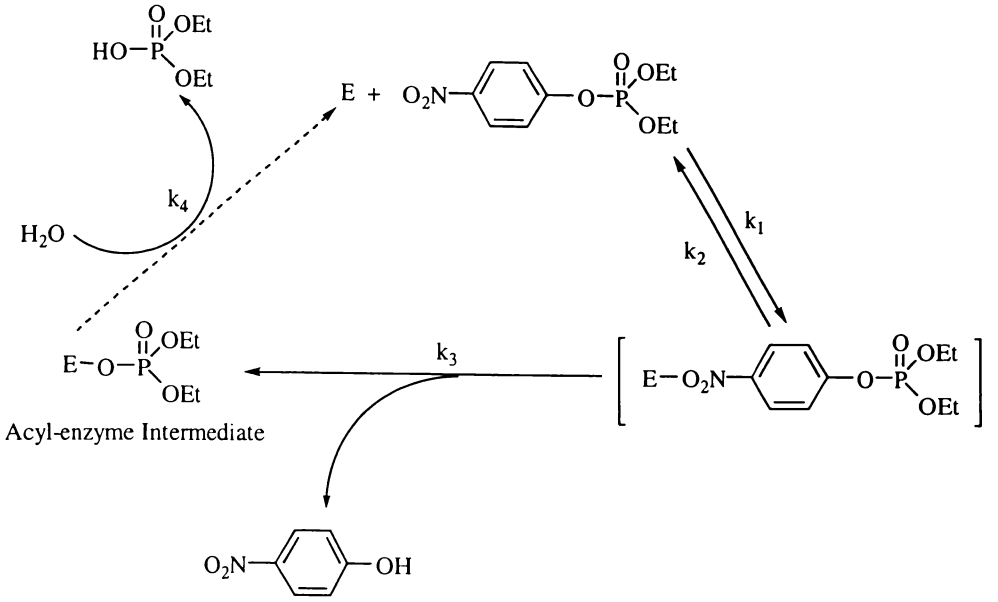

Figure 1.15. The reaction scheme of PLE with diethyl *p*-nitrophenyl phosphate.
E stands for enzyme and Et for ethyl group (redrawn from Krisch, 1966).

The kinetics of this reaction is shown in the scheme:

$$E + S \underset{}{\overset{k_2/k_1}{\rightleftharpoons}} ES \xrightarrow{k_3} \begin{matrix} ES' \\ + \\ P_1 \end{matrix} \xrightarrow{k_4} E + P_2$$

where E is the enzyme; S, the substrate; ES, the enzyme-substrate complex; ES', the acyl-enzyme; P_1, the alcohol (phenyl) moiety; P_2, the acid moiety of the substrate; k_2 and k_3, the rate constants for acylation and deacylation (where k_3 is the rate-limiting step for both substrates); and k_2/k_1, the rate constant for the substrate (Horgan *et al.*, 1966; Stoops *et al.*, 1969).

1.4.3.4.3 Substrate Activation

PLE is subject to activation by either organic solutes (e.g., acetone) or a second molecule of substrate, leading to the phenomenon of biphasic kinetics where there are separate kinetic constants for high and low substrate concentrations (for example K_m^H and K_m^L are the Michaelis constants for high and low substrate concentration, respectively). Substrate activation is exhibited by both the native and dissociated forms of PLE, where the kinetics of the dissociated enzyme are very similar to those of the native enzyme at high substrate

concentration, but exhibits a higher activity at low substrate concentration (Barker and Jencks, 1969).

Several explanations have been proposed for this substrate activation. Firstly, the interaction between the two active sites which is transmitted between the dissociated subunits (Adler and Kistiakowsky, 1962); secondly, the interaction of an esterolytic site with a second binding site where the reaction rate is accelerated by the transference of a substrate molecule from the second site to the first site (Barker and Jencks, 1969 and references therein); and thirdly, activation by an activator site in each dissociated monomer which is different from the active site. Since substrate activation is displayed by both the native and dissociated forms of PLE (and both forms are activated by acetone to the same extent), the third explanation has been determined to be correct by a number of independent studies (Barker and Jencks, 1969; Stoops *et al.*, 1969), and the proposed kinetic scheme is shown in Figure 1.16*a*.

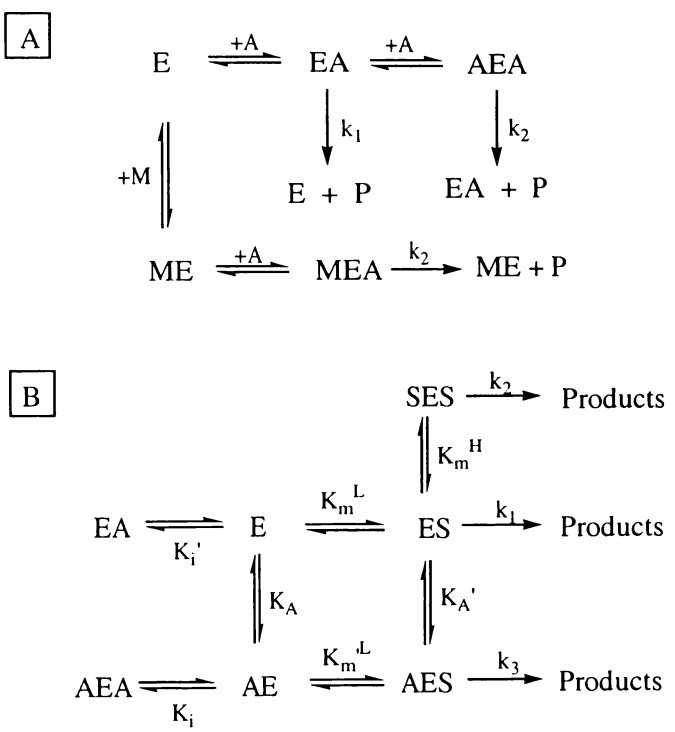

Figure 1.16. Kinetic schemes for the substrate activation of PLE.

Scheme A: the enzyme substrate complex (EA) decomposes with a rate constant, k_1. The modifier- and substrate-activated complexes (MEA and AEA) decompose with the same rate constant k_2, which is larger than k_1 (Stoops *et al.*, 1969). Scheme B: E, A and S represent enzyme, activator and substrate, respectively, and binding to either the activator or catalytic sites is indicated by placing the symbol for the bound molecule either before or after E (Barker and Jencks, 1969).

The degree of substrate activation depends on the characteristics of the activator, substrate and enzyme preparation. Furthermore, the rate of substrate activation brought about by the occupancy of the activator site by an activator molecule may be smaller, equal or greater than that caused by a second substrate molecule; or it may simply prevent the occupancy of the activator site with a second substrate molecule (Barker and Jencks, 1969). Figure 1.16*b* (a modified version of the scheme proposed by Stoops *et al*, 1969) describes this situation. Formation of the activated SES and AES complexes, which decompose to products with the rate constants, k_2 and k_3, corresponds to activation by substrate or activator, respectively. To illustrate, with benzene and phenyl butyrate $k_3 = k_2$ (the activation of hydrolysis by benzene is the same as that brought about by substrate activation), and with *n*-butanol and ethyl butyrate $k_1 = k_3$ and $k_2 > k_3$ (only the substrate activates - if *n*-butanol occupies the activator site it prevents substrate activation but does not change the activity). However, if a given substrate shows no substrate activation there are three explanations. First, the substrate binds tighter to the catalytic site than to the activator site and only the 'high' or 'low' activity is observed; second, the substrate does not bind to the activator site; and third, the substrate binds to the activator site but has no effect on the catalytic rate (i.e., $k_1 = k_2$).

Further observations by Barker and Jencks (1969) resulted in the hypothesis that PLE was a conformationally labile enzyme in that PLE can be isolated in variable metastable states different from the native state, depending upon the enzyme environment and the purification process. Furthermore, the function of substrate activation was closer to that of a catalytic process, *per se*, rather than an important regulatory or metabolic mechanism for the pig.

1.4.3.5 Effect of pH

PLE is a trimeric protein that dissociates into dimers and monomers, especially at low pH and high ionic strength (Dudman and Zerner, 1975). PLE is denatured at low pH, where 7% and 30% of activity is lost after 16 days at pH 5.0 and 8 hours at pH 4.5, respectively. After 9 hours at pH 2.3 and 20°C, all activity is lost. Furthermore, at low concentration (< 5 $\mu g.ml^{-1}$) PLE dissociates into monomers rapidly at low pH (e.g., pH 4.5) and slowly at neutral pH (e.g., pH 7.5).

However, at high enzyme concentrations (> 0.15 $mg.ml^{-1}$) and neutral pH, PLE reversibly polymerises.

1.4.3.6 Effect of Salts and Inhibitors

The rate of PLE subunit dissociation is augmented by the presence of salt solutions (but requires long time periods). Levine *et al.* (1980) concluded that the dissociating effect of certain salts was due to a favourable activity coefficient effect on peptide and amide groups that become increasingly exposed upon dissociation. The anion salt series that caused the highest degree of dissociation (from lowest to highest) was $F^- < Cl^- < Br^- < I^-$. Although no significant effects were detected with the cations Na^+, K^+ and NH_4^+, lithium had a large effect on dissociation and was found to stabilise the monomeric form of PLE, resulting in a decrease in substrate activation.

Table 1.10. Effect of metal salts and inhibitors on PLE.

Chemical[1]	% Activity[2]	
	pH 6.1	pH8.0
Sodium azide	100	nd
EDTA	100	nd
Iodoacetamide	95	nd
p-chloromercuribenzoic acid (PCMB)	86	nd
Bis (*p*-nitrophenyl)-phosphate (BPNP)[3]	nd	3-11
Diisopropyl-fluorophosphate (DFP)	6	nd
Diethyl *p*-nitrophenyl phosphate (E-600)	0	nd
Ag^+	20	50
Ca^{2+}	117	157
Cu^+	39	20
NaF[3]	nd	45
NaI[4]	nd	17
Mg^{2+}	87	65
Mn^{2+}	87	96
Ni^{2+}	67	40
Zn^{2+}	69	42

[1] 10 mM final concentration; [2] compared to the reaction rate obtained against 10 mM *p*NP-acetate at pH 6.1 or 8.0 without metal salts or inhibitors (Keay and Crook, 1965); [3] 10 µM BPNP and 1 mM F^- (Junge and Heymann, 1979); [4] % activity against 0.3 mM *p*NP-acetate and 440 mM NaI at pH 7.8 (Barker and Jencks, 1969); nd, no data.

The effects of a wide range of metal salts and enzyme inhibitors on the catalytic rate of PLE are displayed in Table 1.10. Keay and Crook (1965) concluded, from their inhibitor study, that PLE was not a metalloenzyme but had both a histidine imidazole and a serine group in its active site since the esterase was insensitive to EDTA and azide but 100% inhibited by the organophosphates (DFP and E-600), respectively. Thus, PLE can be designated as an aryl- or ali-esterase with characteristics of a cholinesterase (since fluoride is a cholinesterase inhibitor) (Keay and Crook, 1965; Barker and Jencks, 1969).

PLE hydrolysis of *p*NP-acetate was significantly inactivated by silver, fluoride and copper ions, while the presence of calcium increased hydrolytic activity. The increase in hydrolysis by Ca(II) ions is seen in many hydrolytic enzymes (such as lipases) and has been attributed to calcium removing free fatty acids from solution as calcium salts. However, since insoluble calcium products are not formed in *p*NP-acetate reactions, and PLE is active in the absence of metal salts, Keay and Crook (1965) hypothesised that calcium was assisting in the removal of the acyl group from the acyl-enzyme intermediate, increasing the strength with which the substrate was binding to the enzyme, or stabilising a specific conformation of the enzyme required for activity. The loss of activity in the presence of Cu(II) was attributed to the reversible formation of an inactive copper-enzyme complex.

1.5 FRUIT RIPENING

Fruit ripening can be defined as a sign of senescence whereby intracellular disorganisation occurs, leading to the random mixing of enzymes and their substrates. Subsequently a sequence of colour, flavour and texture changes take place, leading to the state at which the fruit is suitable to eat. Phenomena associated with this flavour alteration are changes in acidity, astringency and sweetness - all of which depend upon the organic acids, sugars and volatiles present in the tissue (Rhodes, 1970).

The majority of aroma-bearing constituents, or volatile compounds, are normally present in foods at levels of less than 100 parts per million (ppm). However, the concentration of fruit volatiles (which include acids, alcohols and

esters) frequently reach 100 ppm, resulting in the highly aromatic quality of this food group (Nursten, 1970).

1.5.1 Esters

Aliphatic esters contribute to the aroma of most fruit, wherein some produce specific fruit aromas and others nonspecific fruity odours (to a lesser degree, straight chain saturated aliphatic acids provide aroma to fruits and vegetables). The majority of aliphatic fruit esters are ethyl esters and acetates, with ethanol being the alcohol constituent. As a general rule, naturally occurring esters in the environment are derived from alcohols and acids with an even number of carbon atoms, and as the number of carbon atoms increase, fruity odours can transform into soapy, fatty or metallic aromas (Bauer *et al.*, 1990).

1.5.2 Apple Ripening

Aroma development by Red Delicious apples is primarily associated with esters, and ester production is localised in the peel rather than in the flesh. During ripening the largest increase in volatiles occurred in esters such as ethyl acetate, ethyl butyrate, and butyl acetate and it was determined that the peel (which accounts for 11% of the total fruit weight) produced 75% of the total ethyl butyrate and butyl acetate released by the apple (Guadagni *et al.*, 1971).

Of the 130 flavour or aroma compounds detected in Cox's Orange Pippin apples, the dominant components included ethyl acetate, butyl acetate, and butanol. When this apple cultivar ripens naturally, the volatile esters increase to a maximum after 2 to 3 weeks. However, after controlled atmosphere storage apples can be defective in their ester production. Firstly, the increase in volatiles is influenced by the state of maturity of the apple before store placement (Williams and Knee, 1997). Secondly, the ability of Golden Delicious apples to produce the volatile esters and aldehydes required for flavour upon transfer to air is decreased proportionately to the delay in ripening caused by controlled atmosphere storage (Patterson *et al.*, 1974). Consequently, controlled atmosphere storage can have a profound affect on the final flavour achieved.

1.5.3 Fruit Ripeness

The ability to assess the level of ripeness in fruits is of high commercial value to the orchardist, wholesaler and consumer. To date, commercial assessment of fruit ripeness has included the ratio of sugar to acid (in grapes for example) or the ratio of dry matter to acidity in oranges (Ulrich, 1970).

The work described here developed, in association with our commercial research partners, is a biosensor that detects esters to determine fruit ripeness. Carboxylesterases and lipases were screened for activity against three esters of interest - methyl butyrate, ethyl butyrate and ethyl acetate. Those enzymes shown to exhibit appropriate activities against the fruit esters and other desirable properties were then tested by our commercial research partners in a biosensor.

1.6 Protein Hydration and Function

1.6.1 Introduction

The role of water in enzyme catalysis and protein dynamics has been extensively studied since the early 1980's, and comprehensive reviews, such as Rupley *et al.* (1983) and Rupley and Careri (1991), have systematically attempted to resolve the relationship between the hydration process and enzyme activity. The approach taken by Rupley and Careri, (1991) in determining this relationship was to partition the available protein hydration-function data into three categories:

1. *Protein hydration determination* - the principal techniques employed in the measurement of protein hydration are infrared spectroscopy which is highly sensitive to hydrogen (Grdadolnik and Maréchal, 2001), hydrogen exchange, dielectric relaxation as well as thermal analysis by apparent heat capacity determination and calorimetry (Pocker, 2000);
2. *The hydration process* - protein hydration is a process whereby water is sequentially added to dry protein until a protein water content level is reached, beyond which further addition of water only dilutes the protein. This hydration process consists of several stages (measurable using the techniques previously described) and has a defined end point; and
3. *The correlation between the hydration shell and modulation of the enzyme and protein functions* - it is widely accepted that both protein

chain dynamics (e.g., folding) and the onset of enzyme catalysis are determined by protein hydration. While dry enzymes are inactive, partially hydrated enzymes (at hydration levels less than 20% H_2O [w/w]) have shown activity. Although there is not a single hydration level that is critical for the onset of catalysis for all enzymes, a number of studies indicate a protein water content of 0.2g water per g protein is sufficient for activity in many globular enzymes (Rupley and Careri, 1991).

1.6.2 Determination of Protein Hydration

Correlation between protein hydration (in g water per g protein, *h*) and changes in the IR spectrum, heat capacity, EPR probe motion and the rate of peptide hydrogen exchange is illustrated in Figure 1.17. Three transitions that occur between 0.05-0.07 *h* and at 0.25 *h* and 0.38 *h* are extensively discussed in Section 1.6.3.

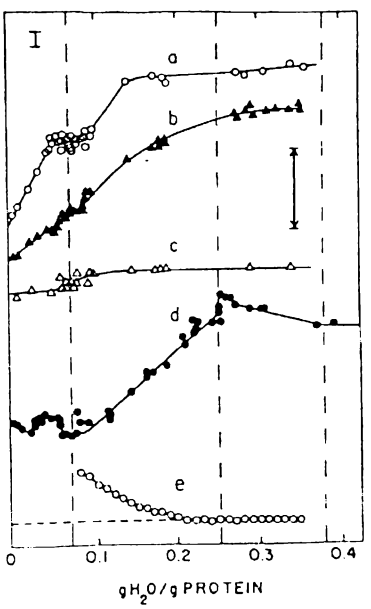

Figure 1.17. Effect of hydration on lysozyme time-average properties.
From top to bottom the curves are: (a) carboxylate absorbance (1580 cm^{-1}); (b) amide I shift (1660 cm^{-1}); (c) OD stretching frequency (2570 cm^{-1}); (d) apparent specific heat capacity; and (e) diamagnetic susceptibility (Rupley *et al.*, 1983).

1.6.2.1 Determination of Protein Hydration

Accurate moisture determination is essential in the study of the relationship between enzyme activity and the degree of protein hydration required for enzymic

function. Protein hydration can be calculated either (1) directly by measuring the amount of water present in a known amount of protein, or (2) indirectly by using an absorption or desorption isotherm (a plot of protein hydration against % relative humidity) that was previously measured using accepted techniques (Poole and Finney, 1986). Although a large number of techniques have been developed for the estimation of the amount of water bound to solid protein powders (such as near-IR spectroscopy and Karl Fischer titration), the commonly used gravimetric method is the method used in the work described here.

The gravimetric method measures the loss in weight on drying or weight gain through rehydration from a dried state. This technique is used as the approved test method for residual moisture (when preparing freeze-dried biological products) as stated by The Code of Federal Regulations, 21 CFR 610.13. The test measures maximum loss in mass of a known amount of protein equilibrated to constant mass over anhydrous P_2O_5 at a pressure no more than 1mmHg and a temperature of 20-30°C (Dolman *et al.*, 1996). This is a reliable method, and Parker *et al.* (1995) showed that the subtilisin Carlsberg residual moisture values determined gravimetrically are in good agreement with those values obtained by NMR titration (with average differences of *ca.* 12%). Conversely, Chen and Oakley (1995) compared the gravimetric method with two other methods of residual moisture determination (namely, Karl Fischer and thermogravimetric analysis – in which the latter method combines gravimetric analysis with high temperatures). They found that the Karl Fischer and thermogravimetric analysis methods were in good agreement while the moisture contents determined gravimetrically were consistently lower.

To attain a dry state, the protein requires exposure to powerful drying agents such as anhydrous phosphorus pentoxide (P_2O_5) in either (1) a vacuum for numerous days, or (2) with exposure to higher temperatures, i.e., thermogravimetric analysis (Poole and Finney, 1986). However, it is conceded that the perfect dry state is rarely achieved. Instead, there may still be a few buried or strongly bound residual water molecules present, resulting in a relatively small, zero error (Dolman *et al.*, 1996). To illustrate, the water content of freeze-dried lysozyme exposed to P_2O_5 for two days was 0.01 *h* (Poole and Finney, 1986). Dolman *et al.* (1996) estimated the number of residual water molecules of lysozyme and subtilisin Carlsberg by molecular modeling and the detection of

^{18}O-labeled water by mass spectrometry. Lyophilised powders of lysozyme and subtilisin were hydrated through the vapor phase with ^{18}O-labeled water and then dried extensively over P_2O_5. The powders were than redissolved in water to release any remaining ^{18}O-labeled water molecules. The isotopic enrichment of the water was used to calculate the number of bound water molecules per mole of protein and the results are given in Table 1.11.

Table 1.11. Experimental measurements of enzyme bound water.
Dolman *et al.* (1996).

Enzyme	Drying Agent	Water Content (H_2O Molecules Per Enzyme Molecule)	h^1
Lysozyme	Undried (a_w 0.059)	99.2	0.1240
Lysozyme	P_2O_5	2.5	0.0031
Lysozyme	BaO	4.4	0.0055
Subtilisin	P_2O_5	14.2	0.0094
Subtilisin	BaO	16.3	0.0108

[1] calculated using molecular weights of 14.4 and 27.2 kDa for egg white lysozyme and *Bacillus licheniformis* subtilisin Carlsberg, respectively.

While the four tightly bound lysozyme water molecules are positioned within two pockets, the 14 bound water molecules of subtilisin Carlsberg include six buried waters, two trapped waters and one water in the bottom of a pocket. Dolman *et al.* (1996) hypothesised that while the tertiary structure of protein was not disrupted by lyophilisation, the structure became increasingly rigid upon drying and consequently the internal water molecules become permanently trapped.

1.6.2.2 Control of Relative Humidity

The control and accurate determination of RH is vital to many fields, such as the food and pharmaceutical protein industry. Preservation of foodstuffs and enzymes can be controlled directly through reduction in protein water content via control of RH. A review by Bone (1969) described how dried or salted foods were maintained below the threshold RH required for bacterial and yeast growth (91 and 88%, respectively), thereby minimising or stopping microbial spoilage of

the food. Proteins (such as commercial enzymes) undergo the process of lyophilisation, or freeze-drying, which removes ~99%of the water from protein.

Extensive literature reviews by Rupley and Careri (1991) and Poole and Finney (1986) concluded that lyophilised enzymes were inactive (the water content of a lyophilised protein is 0 *h* - significantly lower than the critical hydration limit of 0.2 *h* required by many globular enzymes for the onset of activity). However, lyophilisation alone may not remove all of the strongly bound water molecules that are found in internal protein cavities (lyophilisation is therefore often coupled with drying agents and/or high temperatures). The use of enclosed desiccating agents, such as those listed in Table 1.12, can conveniently control RH. In the work described here, static control of RH, and therefore protein water content, is achieved through use of a three-phase system (vapor-liquid-solid) produced by saturated aqueous salt solutions in an enclosed vessel. The RH is produced when an excess of the salt indicated is in contact with a saturated aqueous solution of the given solid phase (Weast and Astle, 1982). RH can also be controlled using two-phase systems (vapor-liquid) such as sulfuric acid or humectants (for example glycerol).

Table 1.12. Common types of desiccating agents used to control relative humidity.

Agent	Example	Reference
Adsorptive materials of varying water content	Silica gel, cotton	1
Aqueous solutions of varying concentration	Sulfuric acid, glycerol	1,2
Saturated aqueous solutions	LiCl, KBr	1,2,3,4
Paired hydrates of salts	NaI with $CaCl_2.6H_2O$	1

[1] Richardson and Malthus, 1955; [2] Rockland, 1960; [3] Wexler and Hasegawa, 1954; and [4] O'Brien, 1948.

A significant difference between the three- and two-phase systems is that RH's produced are temperature sensitive and insensitive, respectively. Nonetheless, while a saturated salt solution of $Zn(NO_3)_2$ produces a RH of 38% at 20°C and 31% at 25°C (Labuza *et al*, 1976), a saturated salt solution of CH_3COOK has a low temperature coefficient and the RH produced is virtually temperature independent (Rockland, 1960; Wexler and Hasegawa, 1954). The temperature-RH relationship of a variety of saturated salt solutions between 20 and 30°C is shown in Table 1.13

Table 1.13. Percentage relative humidities produced in an enclosed vessel by saturated salt solutions at the specified temperature[1].

Saturated salt solution	Temperature (°C)		
	20	25	30
P_2O_5 [2]	0	0	0
LiBr	-	7.2[4]	-
$ZnBr_2$	-	8.6[4]	-
$ZnCl_2.xH_2O$	10.0	10.0	10.0
$LiCl.xH_2O$	15.0 (12.0)	13.0 (11.0)	13.0 (11.0)
CH_3COOK	(23.0)	(23.0)	(23.0)
$CaCl_2.xH_2O$	32.3	31.0	-
$Ca(NO_3)_2.4H_2O$	55.9 (56.0)	51.0[5] (54.0)	49.0 (51.0)
$NaNO_2$	66.0	64.2[4]	66.0
NH_4Cl	79.2	78.4	-
KBr	84.0 (84.0)	(83.0)	82.0 (82.0)
$ZnSO_4.7H_2O$	90.0 (90.0)	88.5 (88.0)	(86.0)
$Na_2HPO_4.12H_2O$	95.0	-	-
$CuSO_4.5H_2O$	98.0[3]	-	-

[1] All data, unless specified, is compiled from O'Brien (1948); [2] powder only; [3] Weast and Astle (1982); [4] Richardson and Malthus (1955); and [5] at 24.5°C; and % relative humidity data given in brackets is from Rockland, (1960).

1.6.2.3 Saturated Salt Solutions

Experimental data derived from exposing various materials to saturated salt solutions in controlled humidity chambers is used in many scientific fields, including metal corrosion, food stability, physical properties of textiles (such as wood and plastic) and formation of moisture sorption isotherms (Rockland, 1960).

Published data on RH values for different saturated salt solutions vary in every study. The RH values listed in Tables 1.14 and 1.15 show the degree of variation within four independent studies and the variation between different methods of determination, respectively. This variation can stem from the different apparatus used to produce each RH, but more importantly, the different techniques (which have different accuracies) for determining RH.

Table 1.14. RH values for saturated salt solutions at 20°C from four studies.

Salt	(1)	(2)	(3)	(4)
$MgCl_2$	33	34	32	34
$Zn(NO_3)_2$	38	42	-	-
$Ca(NO_3)_2$	56	56	-	-
$Na_2Cr_2O_7$	-	52	54	55
NaCl	75	77	-	76
$(NH_4)_2SO_4$	79	82	-	81
KNO_3	94	94	-	93

[1]Rockland, 1960; [2] O'Brien, 1948; [3]Richardson and Malthus, 1955; and [4] Wexler and Hasegawa, 1954.

Table 1.15. RH values determined by Labuza *et al* (1976) for saturated salt solutions at 22°C using six techniques.

Salt	Theoretical RH	Direct VPM	Electric Hygrosensors				
			Humidity Indicator	Humichek	Hygrometer	Sina-Scope	Resonance Brady Array
$MgCl_2$	33	32	NT	31	32	BR	31
$Mg(NO_3)_2$	54	53	52	53	46	BR	50
$(NH_4)_2SO_4$	81	80	NT	80	79	78	80
Li_2SO_4	85	84	86	84	83	83	86
Na_2HPO_4	96	96	NT	93	96	95	89

NT, not tested; BR, beyond range.

To reduce experimental variation in RH values produced by saturated salt solutions the following recommendations should be followed:

1. Enclosing the saturated salt solution in a vessel whose walls and fixtures within are made from non-hygroscopic materials, such as glass or metal (Wexler and Hasegawa, 1954);
2. The enclosing vessel must be moisture tight (Wink and Sears, 1950);
3. The saturated salt solution must be made from chemically pure grades of salts, for example Analytical Reagent Grade salts, and purified water such as MilliQ (Rockland, 1960).
4. Saturated salt solutions that produce RH values > 95% must be stored at 4°C to minimise microbial growth (Labuza *et al.*, 1976);
5. The saturated salt solution must occupy as large a surface area as possible - preferably with air and/or salt solution circulation (Wexler and Hasegawa, 1954).

6. The vessel, saturated salt solution and vessel headspace must be brought to temperature equilibrium; and
7. While a significant excess of salt must be used when reducing the water content of proteins, only the presence of salt crystals is required in a humidifying atmosphere (Wink and Sears, 1950).

Wink and Sears (1950) and Wexler and Hasegawa (1954) showed that the time needed for equilibration at each RH depended upon the ratio of the surface area of the saturated salt solution to the vessel volume, and the amount of air and/or saturated salt solution agitation. However, it should be noted that when all the recommendations are followed, the experimental RH values achieved would be at best within ±1 percent (Wexler and Hasegawa, 1954) of the theoretical values from literature.

1.6.3 The Hydration Process

Protein hydration results from H-bonding, Van der Waals and hydrophobic interactions between water and amino acid residues. These interactions depend upon the residue charge, specifically whether it contains ionic, polar or non-polar sites (Towns, 1995). Biological solvent water plays an important role in both protein structure and catalysis through interactions with surface protein residues and the occupation of internal cavities and clefts of proteins (Lüscher-Mattli and Rüegg, 1982; Pocker, 2000). These interactions are accepted as the primary determinants of chain dynamics and binding specificities of many globular enzymes, such as lysozyme, α-chymotrypsin and insulin (Rupley and Careri, 1991)

1.6.3.1 Protein Interacting Waters

The water molecules that interact with proteins are classified structural (buried internal) water molecules that occupy internal cavities and clefts; ordered surface water molecules; and disordered bulk water. The structural water molecules: (a) are extensively H-bonded; (b) are an integral part of the native protein structure whereby they stabilise the native conformation of the secondary structure (Denisov and Halle, 1996); (c) can only exchange with the bulk solvent after local unfolding (Rupley and Careri, 1991); (d) are perturbed in their properties or are able to disturb protein properties through its interaction with

protein residues (Yang and Rupley, 1979); and (e) can act as a lubricant for large-amplitude fluctuations of active site loops (e.g., acetylcholinesterase) that are essential to promote movement of substrate, products and water molecules to and from the active site (Koellner *et al.*, 2000). Compared to the internal water molecules, surface water molecules are less well defined structurally and more mobile (Tarek and Tobias, 2000). Surface molecules, with a residence time estimated at 10-50ps (sub-nanosecond), exchange rapidly with the bulk solvent while internal water molecules, with residence times between 10 ns and 1 ms, are relatively immobile (Rupley and Careri, 1991). However, the work of Dolman *et al.* (1996) concluded that internal water molecules may have significantly longer residence times since 2-4 residual water molecules are retained in lyophilised protein powders (Table 1.11). The increased mobility of surface water is thought to prevent water from adopting a defined structure on the protein surface, i.e., reducing the number of H-bonds made with protein surface residues (Gronenborn and Clore, 1997). However, Denisov and Halle (1996), who studied ^{17}O and ^{2}H nuclear magnetic relaxation dispersion (NMRD) of surface and internal water molecules, suggested that the H-bonding structure was not the key determinant of a water's residence time, instead they proposed that the fast dynamics of bulk water was due to a co-operative mechanism between neighbouring water molecules.

1.6.3.2 Sorption Isotherms

The effect of sequential hydration on anhydrous proteins can be followed with water vapor ad- or de-sorption isotherms (illustrated in Figure 1.18) which are generated by calculating the equilibrium moisture content of proteins at varying relative humidities. Reference to the isotherm may be used as a practicable method of calculating the water content of protein samples used in further studies (Poole and Finney, 1986). The sorption isotherm for proteins can be separated into three regions: the 'knee', the plateau and the upswing (represented in Figure 1.18 as the regions spanning 0-0.07 *h*, 0.07-0.12 *h* and 0.12-0.25, respectively). In comparison, the water content range of each region differs in many studies: 0-0.05, 0.1-0.2 and 0.2-0.25 (Careri *et al.*, 1980); 0-0.07, 0.07-0.27 and 0.27-0.38 (Yang and Rupley, 1979); plus 0-07, 0.07-0.25 and 0.25-0.38 (Rupley and Careri, 1991). Furthermore, globular proteins (including

lysozyme, ovalbumin, α-chymotrypsin and ribonuclease) exhibit similar sorption isotherms upon hydration (Rupley and Careri, 1991) where variations may be due

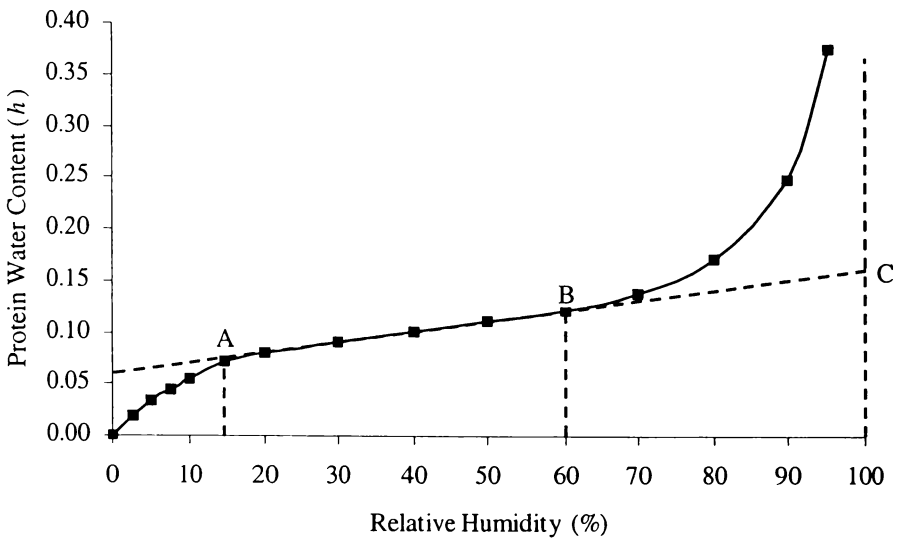

to differences in protein hydrophobicity, density, conformation or glycosylation.

Figure 1.18. Schematic representation of an isothermal sorption curve.

(A) point corresponding to the amount of strongly bound water; (B) point of appearance of "solvent water"; and (C) point corresponding to the total amount of "non-solvent" water (Drapron, 1985).

1.6.3.3 Lysozyme Hydration

Hydration studies using egg white lysozyme powder as the model protein have advanced the understanding of the relationship between water and protein dynamics. Yang and Rupley (1979) and Careri *et al.* (1980) analysed hydration events in lysozyme (using heat capacity, infrared spectroscopy, diamagnetic susceptibility and enzymic measurements) and proposed that the behaviour observed upon lysozyme powder hydration was applicable to most proteins, especially globular proteins.

Of all the thermodynamic properties used to provide information about water interactions with specific protein residues, heat capacity is one of the most sensitive and widely used measurements because: (1) heat capacity is sensitive to changes in the physicochemistry of water, including the number of H-bonds associated with protein surface residues and the protein surface area covered by each water molecule; (2) heat capacity can be measured for dry and partially hydrated proteins as well as dilute protein solutions (thereby linking powder and

solution studies); and (3) heat capacity data can be related to other thermodynamic properties, for example proton ionisation and substrate binding (Yang and Rupley, 1979).

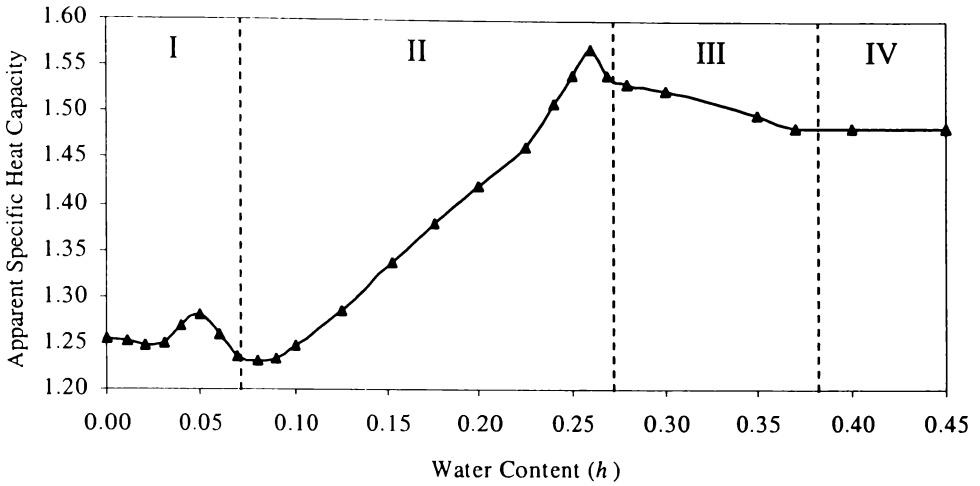

Figure 1.19. The apparent specific heat capacity of lysozyme as a function of water content. The heat capacity measurements were made with lyophilised powders of lysozyme, appropriately hydrated between 0 and 0.45 *h*. The apparent specific heat capacity curve has four regions of linear response (I-IV) to ligand composition (breaks at 0.07, 0.27 and 0.38 *h*) and two transitions centred at 0.05 and 0.26 *h*. Adapted from Yang and Rupley (1979).

The heat capacity data from a lysozyme hydration experiment performed by Yang and Rupley (1979) displays complexity below 0.38 *h* (Figure 1.19). This is not indicative of an 'all-or-none' hydration (which would be discernible as a monotonic response in the heat capacity), but rather a process in which there are interactions between several classes of protein sites and water. In addition, two contributions from changes in state occur at low hydration and centre at 0.05 and 0.26 *h*. The lysozyme hydration process can be described in terms of four regions: *region I*, dry protein to 0.07 *h*; *region II*, 0.07-0.27 *h*; *region III*, 0.27-0.38 *h*; and *region IV*, 0.38 *h* to dilute protein, where *regions II* to *IV* each represent one class of water-binding sites (Yang and Rupley, 1979; Careri *et al.*, 1980). A comprehensive review by Rupley and Careri (1991) summarised the hydration process and the chemistry of protein in each 'region' (Table 1.16) using data collected from lysozyme, ovalbumin and ribonuclease studies (globular proteins that share similar adsorption isotherms).

Table 1.16. Protein chemistry at various hydration levels.

The data was adapted from Rupley *et al.* (1983) and Rupley and Careri (1991).

Hydration (*h*)	Thermodynamics	Structure	Dynamics
0-0.07	"Knee" in sorption isotherm Large differences for transfer of water from bulk to hydration layer: $\Delta\overline{G}_l$ = -17 kcal/mol Stable folded state	Structure similar to that at full hydration (±1 Å) Water interacts principally with charged protein groups (ca 2 waters per charged group) At 0.07 *h*: surface water transition from disordered to ordered and/or from dispersed to clustered state	Frozen protein motions Low water mobility (ca 1/100 than bulk water) Negligible enzymic activity
0.07-0.25	Plateau in sorption isotherm Small differences for transfer of water from bulk to hydration layer: $\Delta\overline{G}_l$ = -0.5 kcal/mol Small differences in partial molar quantities for transfer of water into hydration layer, with increasing hydration	Water interacts with polar protein surface groups (ca 1 water per polar site) Water clusters centered on charged and polar groups At 0.15 *h*: H-bonded water spans protein surface, the water network connections increases with hydration	At 0.15 *h*: internal protein motions equal to full solution rate At 0.10-0.15 *h*: enzymes develop activity (*e.g.* chymotrypsin)
0.25-0.38	Rapid rise in sorption isotherm Thermodynamic quantities are close to bulk solvent values Phase transition due to condensation	At 0.25 *h*: water condensation at weakly interacting unfilled areas of the protein surface	Water motion increases strongly with increased hydration Increase in enzymatic activity with hydration
>0.38	At 0.38 *h*: Full hydration of the protein surface Thermodynamics of protein unfolding are close to that of the dilute solution behaviour Cooperative interactions of water in several layers about protein (and hydration of the folded state between 0.38 and 0.80 *h*)	At 0.38 *h*: Water monolayer covers protein surface Locally ordered arrangements of hydration water (due to interactions with charged and polar surface groups, and can mesh with bulk solvent) Most proteins have cluster or threads of H-bonded water (some with extensive H-bonded networks)	Hydration water has mobility close to bulk water Full protein internal motions Dynamic and thermodynamic coupling between hydration water and protein Enzymic activity $1/10^{th}$ solution value

Starting from an anhydrous lysozyme powder, the following hydration events ensue:

1. *Region I.* Hydration of the lysozyme up to 0.07 *h* results in the formation of carboxylate species (due to proton redistribution) wherein water molecules interact principally with charged (ionisable) protein groups and effect the ionisation state of lysozyme found in solution. This requires on average two water molecules interacting with each group (and approximately 40 molecules of water per protein molecule). The proton transfer (from carboxylic acid to basic groups of the protein) accounts for the reaction heat centred at 0.05 *h* that is detected as a positive peak in the IR difference spectrum and a rise and fall in the specific heat capacity (Figure 1.19);

2. *Region II.* The discontinuity, or knee, in the sorption isotherm at 0.07 *h* represents a transition in water-water and water-protein interactions, where the surface water concentration becomes sufficiently high for water clusters (polymeric H_2O) to form on polar or charged protein atoms. Between 0.1 and 0.2 *h*, water primarily interacts with, and ultimately saturates, polar protein groups, such as the backbone polar atoms and the side-chain amide groups (this process requires half of the water molecules needed for monolayer coverage). Between 0.2 and 0.27 *h*, lysozyme activity is detected, water molecules saturate the carboxylate and amide carbonyl sites, and there is full coverage of the H-bonding sites. The appearance of activity in this region coincides with a greater conformational freedom in the water arrangements on the protein surface and the 0.25 *h* transition. This transition (detected as a sharp rise in the heat capacity, which then decreases to that of the dilute solution value at 0.38 *h*) is associated with the covering of the weakest interacting regions of the protein surface which involves up to 100 water molecules;

5. *Region III.* Between 0.27 and 0.38 *h*, the weakly interacting regions of are saturated, and by 0.38 *h* approximately 300 water molecules per protein molecule form a water monolayer (the first hydration shell) that covers the protein surface; and

6. *Region IV.* Above 0.38 *h*, H-bonded water molecules form clusters or threads, and water molecules form several layers (hydration shells) around the protein surface. The invariance of the specific heat capacity of lysozyme above 0.38 *h* reflects the completion of the hydration process and means that the

thermodynamic properties of both the protein and the solvent are comparable. Namely, 300 water molecules per lysozyme molecule produces dilute solution thermodynamic properties of the protein. Furthermore, data from solid-phase hydration studies using proteins hydrated above 0.38 *h* can be directly related to the dilute solution state (Careri *et al.*, 1979; Yang and Rupley, 1979; Careri *et al.*, 1980; Rupley and Careri, 1991).

The *Region I-Region II* and *Region II-Region III* transitions of the heat capacity isotherm represent the knee and strong upswing illustrated in Figure 1.19, respectively. Furthermore, the organisation of the water monolayer achieved in *Region III* is primarily determined by protein surface polar residues, and while the thermodynamics of the surface water molecules do not differ significantly from bulk water molecules, they move one to two orders of magnitude slower than bulk water.

1.6.3.4 Organic Solvents

A significant proportion of protein hydration studies was completed using hydrated protein powders. One of the first experiments on the activity of enzyme powders was completed by Yagi *et al.* (1969) who investigated the activity of dry state hydrogenase against its vapor-phase substrates, specifically hydrogen and water. However, low catalytic activities, particularly associated with low hydration levels, have complicated the measurement of enzyme activity in this powder system (Affleck *et al.*, 1992).

An alternative technique that used insoluble powders suspended in nonaqueous media, such as biphasic mixtures of water and water-immiscible solutions (e.g., organic solvents) was subsequently developed (Klibanov, 1989; Valivety *et al.*, 1992a and 1992b; Partridge *et al.*, 1998). An advantage of this system is the solubilisation of the reaction substrates and/or products (i.e., the nonaqueous media can act as a diffusion medium for the enzyme, substrates and products). Disadvantages associated with measuring enzyme activity in the presence of excess solvent (where the reactants and products freely diffuse in the aqueous solvent) include: (1) high dilution of the enzyme, substrates and products of interest – especially in highly aqueous mixtures; (2) differential solvation of the reactants or products; (3) partitioning of the solvent species into the polar phase around the biocatalyst (Halling, 1994); (4) the organic solvent may replace some

of the molecular functions of water at the protein surface; and (5) organic solvents may act as a lubricant, thereby loosening the enzyme structure (Finney, 1996; Almarrson and Klibanov, 1996). These practical difficulties can be avoided by working with enzymes in a vapor solid mode (which is discussed in Section 1.6.5), where the substrates are in the gas phase and the enzyme exists as a hydrated powder (Lamare and Legoy, 1995).

1.6.4 Role of Water in Enzyme Catalysis and Dynamics

1.6.4.1 Hydration and Protein Folding

Water molecules act directly on the structure of proteins. *Hydrophilic* hydration, through H-bond formation, contributes to both the tertiary protein structure and conformational stability. Water molecules form H-bonds between polar groups, such as the formation of peptide H-bonds between the carbonyl oxygen atoms and amide protons of different peptide bonds (Drapron, 1985, Franks, 1993). *Hydrophobic* hydration - or hydrophobic interaction – is credited as the driving force for protein folding (Wade *et al.*, 1991; Franks, 1993). When water contacts, or is in proximity to apolar residues (such as alanine or proline) the interaction is thermodynamically unfavourable because the number of orientations that the water molecules can form is reduced. This reduction in configurational freedom results in a loss of entropy and protein instability. However, this loss of entropy and stability is compensated by protein folding which both minimises and maximises the exposure of non-polar surface groups and polar (and/or ionisable) surface residues, respectively (Franks, 1993).

1.6.4.2 Hydration and Enzyme Catalysis

Water influences enzymic catalysis through a variety of mechanisms. First, hydration levels regulate the internal molecular motions (which are necessary for activity) of enzymes by disrupting and forming H-bonds, thereby altering the local structure. Second, water acts as a solvent through which substrates can diffuse in and out of the enzyme (the amount of solvent water affects the mass transfer of substrates or products to and from enzymes). Third, the amount of solvent water influences contact between enzyme and substrate and the formation of the reactive complex. Fourth, water can act as a second substrate in hydrolytic reactions, such

as those catalysed by lipases, and as a substrate water can be a limiting factor and consequently, the rate of hydrolysis increases with increasing hydration (Drapron, 1985). However, the affect of hydration on hydrolytic activity is difficult to quantitate because changes in the concentration of substrate water results in changes in viscosity and polarity for the other reactants, and because the substrate water concentration can not be treated as an isolated variable (Pocker, 2000).

1.6.4.2.1 Hydration Threshold for Enzyme Catalysis

Enzyme catalysis can be effectively studied at relatively low hydration levels (less than 0.38 *h*, the water content level required for monolayer water coverage) but activity is not detected below 0.1 *h*. The protein hydration levels required for the onset of activity in a variety of enzymes listed in Table 1.17, as reviewed by Rupley and Careri (1991) and Drapron (1985), range between 0.11 and 0.22 *h*.

Table 1.17. Protein hydration thresholds for enzyme activity.

Enzyme	Hydration Threshold		Reference
	h	% Relative Humidity[1]	
Glucose Oxidase	0.11	40	2
α-Chymotrypsin	0.12	43	3
Phosphoglucose Isomerase	0.13	45	4
Phospholipase B and D	0.13	45	2
Invertase	0.14	57	2
Urease	0.15	60	2, 5
Hexokinase	0.20	80	4
Fumarase	0.20	80	4
Lysozyme	0.20	80	6
Glucose-6-Phosphate Dehydrogenase	0.22	82	4

[1] the *h* data was converted to % relative humidity data using the lysozme adsorption isotherm produced in this study (see Figure 5.2), [2] Drapron, 1985; [3] Lüscher-Mattli and Rüegg, 1982; [4] Stevens and Stevens, 1979; [5] Rupley and Careri, 1991; and [6] Careri *et al*, 1980.

The differences in the hydration thresholds may not be significant since detection of the onset of activity would depend upon both the specific activity of the enzyme and the sensitivity of the assay system (a very low hydration level

coupled with an enzyme of poor specific activity is technically demanding for analysis). Furthermore, measuring activity without fluid is difficult.

Stevens and Stevens (1979) studied the effect of restricted hydration on the activity rates of four enzymes (phosphoglucose isomerase, glucose-6-phosphate dehydrogenase, hexokinase and fumarase) using methodology that measured product release rather than the catalytic rate. Each enzyme was rapidly mixed with its substrates, frozen and then freeze-dried. The dry preparations were then hydrated to a known water content in a water saturated atmosphere, and the amount of product measured was used to assess the rate of the reaction. However, the primary experimental difficulty associated with this methodology is that the effect of water as a hydrating agent and water as a diffusion medium can not be separated. Also, it seems likely that product release, rather than catalysis, is measured because hydrated (active) enzyme is in contact with substrate before lyophilisation.

Stevens and Stevens (1979) concluded that the onset of activity for all four enzymes was *ca.* 0.2 *h*. Activity was detectable in the presence of 'bound' (surface) water and was not detectable in the presence of 'irrotationally bound' (internal) water. Bound water was described as being rotationally hindered due to its interactions with the protein surface, and irrotationally bound water, with a residence times of μs, was defined as 'site-bound' to macromolecules. It was estimated that 'irrotationally bound' and 'bound' water contributed 0.003 *h* and 0.3 to 0.6 *h* of most proteins, respectively. After the onset of activity at 0.2 *h*, hydration to 0.3 *h* resulted in an order of magnitude increase in activity.

Rupley *et al.* (1983) studied the effect of hydration on the dynamics of lysozyme (including enzyme activity and peptide hydrogen exchange). As discussed previously, onset of activity occurred at a protein water content of 0.2 *h*, and subsequent activity changes (as a function of water content) are illustrated in Figure 1.20. Depending upon the enzyme and the reaction catalysed, water content-activity profiles of hydrated enzymes can differ. For example, transesterification reactions (acid + alcohol → ester + water) could exhibit end-product inhibition at high hydration since water is a product of the reaction.

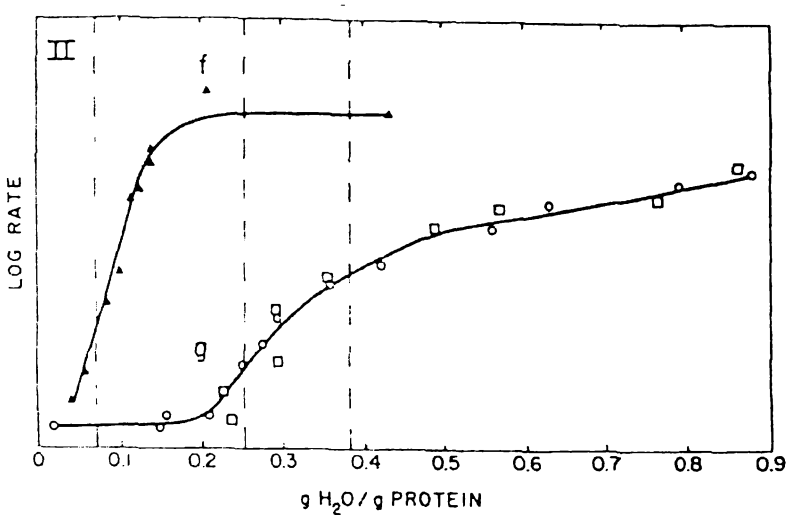

Figure 1.20. Effect of hydration on lysozyme dynamic properties.

The curves are: (f) log rate of peptide hydrogen exchange; and (g) □, enzymic activity (log v_o), and O, rotational relaxation time of an ESR probe (log τ^{-1}) (Rupley *et al.*, 1983).

1.6.4.2.2 Protein Motions

Dry protein displays significantly reduced internal motions and fixed surface motion (Rupley and Careri, 1991). Experimental observations, such as the coupling between the onset of activity with the onset of protein motion, infer that one of the fundamental requirements for enzyme activity is surface protein motion (Affleck *et al.*, 1992; Broos *et al.*, 1995; Rupley and Careri, 1991). A range of techniques confirmed that the onset of lysozyme activity at 0.2 *h* paralleled the 'unfreezing' of surface motion, i.e., activity was a direct consequence of an increase in the conformational flexibility of the protein surface (Careri *et al.*, 1979). Schinkel *et al.* (1985) concluded that this increase in surface motion was not coupled with an increase in internal motion. Using hydrogen exchange to determine the hydration dependence of lysozyme internal motions, Schinkel *et al.* (1985) found that the interior dynamics were identical in both the 0.15 *h* and fully-hydrated lysozyme, but that surface motions in the 0.15 *h* sample were negligible (and only became free once the water condensation event [between 0.2 and 0.25 *h*] occurred).

1.6.4.2.2.1 Conformational Flexibility

The close relationship observed between lysozyme function and structural flexibility upon hydration is not unique to this enzyme. A time-resolved fluorescence anisotropy study of the molecular flexibility of subtilisin Carlsberg

and α-chymotrypsin labeled active sites attributed increases in enzyme activity to increased enzyme flexibility. It was proposed that the flexibility was essential to maximise favourable enzyme interactions with the substrate in the initial and transition state. In other words, increased enzyme flexibility, in the order of (sub)-nanoseconds, would allow the enzyme to undergo multiple conformations, and therefore increase the statistical probability with which a conformational state capable for binding and converting a substrate was achieved (Broos *et al.*, 1995).

The Fitter (2000) study of the confined molecular motions of α-amylase found that additional structural movements were seen in dilute protein solutions compared to fully hydrated powder samples. Fitter (2000) determined that the solvent in solution was more mobile than that in the powder samples, resulting in a further increase in the flexibility of the α-amylase structure (but did not speculate on the functional properties of this additional flexibility). The increased flexibility of the α-amylase structure does not imply that the protein tertiary structure of the hydrated powder and dilute solution differs. Lysozyme powder, for example, from a hydration level of 0.2 *h* (marked by the onset of activity) through to the fully hydrated (dilute) state assumes the native structure (Rupley *et al.*, 1983). However, this does not apply to all proteins. Dehydrated subtilisin, for example, has a different conformation to that of the native structure.

1.6.4.2.2.2 Active Site Mobility

Active site mobility, a function of hydration, is essential for activity. Affleck *et al.* (1992) determined that sequential hydration of the subtilisin Carlsberg active site (up to 0.15 *h*) effected an increase in active site polarity due to initial binding of water molecules to the polar and charged protein residues within this region. This polarisation was attributed as the basis for an increase in active site flexibility and onset of transesterification activity. Between 0.15 and 0.38 *h* (at which monolayer water coverage was achieved), there was a further increase in active site flexibility and a slight conformational change which was linked to a drop in transesterification activity (and an increase in esterification activity).

A typical active site (with a surface area equal to several hundred $Å^2$) is covered by 10-15 water molecules. Hydration waters within an active site can H-

bond with the catalytic protein residues that form H-bonds with the substrate in the enzyme-substrate complex, thereupon competing with the substrate atom for the available bond positions of the active site, or mediating an enzyme-substrate bond. Rupley and Careri, (1991) proposed further roles of water molecules in catalysis, which included:

1. diffusion of reactant and/or product in and out of the active site, respectively (i.e., water acts as a diffusion medium for mass transfer).
2. reorganisation of the solvent about the substrate and enzyme during binding (in organic solvent hydration studies);
3. a guide for the substrate during the formation of the enzyme-substrate complex;
4. formation of a tunnel of H-bonded waters that effect a bond rearrangement of the active site catalytic groups to the protein surface (through increased polarisation); and
5. dielectric screening of unfavourable interactions between charged and polar residues within the active site.

1.6.5 Gas Phase Catalysis

The practical difficulties associated with the use of organic solvents (discussed in Section 1.6.3.4), and the separation of the effect of water as a hydrating agent and a diffusion medium for the reaction substrate(s) and product(s) in hydration-activity studies, are eliminated by working in a vapor-solid mode (for a summary see Lamare and Legoy, 1995). In this method, enzyme catalysis is completed in the gas phase, where vaporised (gas phase) substrates are transformed by a solid state enzyme preparation that has been equilibrated to a known level of hydration. In the work described here, a lipase and carboxylesterase were equilibrated in an atmosphere of known RH (using saturated salt solutions) and the relationship between water content and hydrolysis of a gas phase ester was investigated.

To date few studies of this type have been completed and the action of enzymes on gas phase substrates is not well explored (Lamare and Legoy, 1995; Ross and Schneider, 1991; Yagi *et al.*, 1969), yet potential advantages of this system include a more rapid mass transfer than in solution; and the homogeneity of the vapor phase in comparison to the frequently multiphasic liquid system; the

ability to use substrates that would otherwise be limited by water or solvent solubility problems; and the use of substrates at temperatures significantly below their boiling points. To allegorise the latter advantage, *Candida rugosa* lipase was hydrolytically active at 30°C (and at substrate vapor pressures as low as 0.08mmHg) against esters with boiling points up to 206°C (Ross and Schneider, 1991).

1.6.5.1 Unconventional Hydrolysis

One affect of equilibrating proteins in an atmosphere of low RH is a shift in the equilibrium position of hydrolytic reactions since the water vapor available in the system equilibrates between the gas phase and the protein. At low RH the low moisture content of the vapor phase (kg water per kg dry air, see Figure 1.21) and the protein powder (*h*) results in unconventional reactions, such as transfer and synthetic reactions catalysed by carboxylesterases and lipases (Halling, 1994).

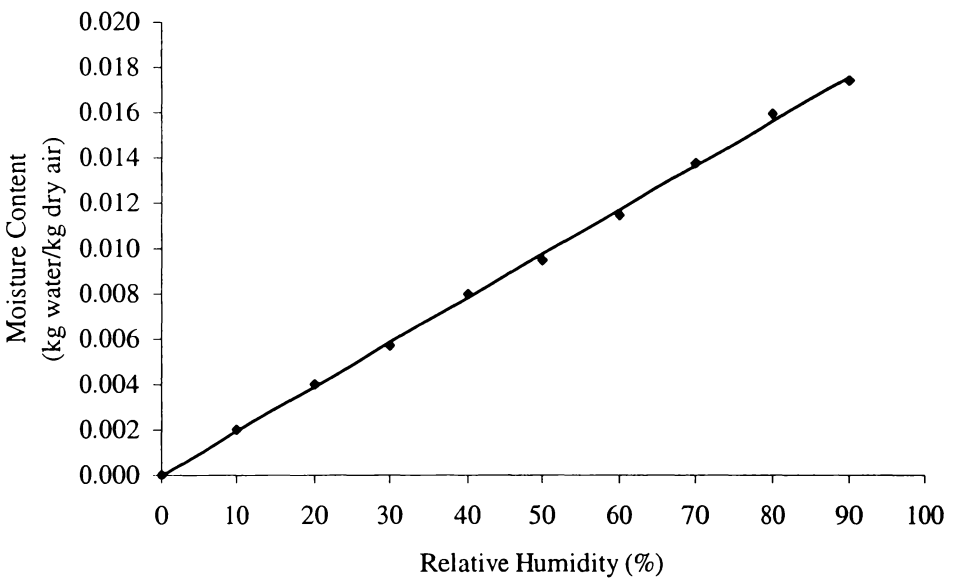

Figure 1.21. The moisture content of an enclosed vapor phase at 25°C as a function of relative humidity.

Adapted from Perry *et al.* (1984).

As the atmospheric RH decreases (from 100 to 0%) the reactions catalysed by carboxylic ester hydrolases (EC 3.1.1) occur in the following order: hydrolysis → alcoholysis → ester exchange → esterification (Lamare and Legoy, 1995).

Basic mechanisms for each reaction are illustrated in Figures 1.6, 1.11*a*, 1.11*b* and 1.5*b*, respectively.

CHAPTER 2 MATERIALS AND METHODS

2.1 MATERIALS

2.1.1 Chemicals and Computer Software

All buffers (analytical reagent grade), *p*-nitrophenyl-acyl-ester substrates and ethyl acetate (HPLC grade) were purchased from Sigma-Aldrich. Methyl butyrate (GC standard) and ethyl butyrate (>98% GC) were obtained from Fluka. The Bromothymol Blue and Phenol Red pH-dye indicators were purchased from BDH. All saturated salt solutions were made with analytical reagent grade chemicals and Milli-Q water. All graphs were drawn using Microsoft® Excel 97.

2.1.2 Enzymes

Porcine (pig) liver esterase (E3019) was purchased from Sigma-Aldrich. The *Candida rugosa* LipaseB (L034P), mixed fungal lipase (L187P), mixed animal esterase/lipase (L224P) and *Penicillium roqueforti* esterase (L338P) were obtained from BioCatalyst.

2.1.3 Microorganisms

Bacillus stearothermophilus A^M, B^M, C^M; *Bacillus licheniformis* D^M, DRC1, FTA; *Bacillus acidocaldarius* E24 A.1, *Lactobacillus casei* BH1 and *Lactobacillus plantarum* were obtained from the Thermophile Research Unit Culture Collection (TRUCC), University of Waikato, New Zealand. *Bacillus acidocaldarius* 27009 and *Sulfolobus solfataricus* 1616 were purchased from ATCC and DSM, respectively. *Streptomyces rochei* was obtained from ICMP.

2.2 METHODS

2.2.1 Liquid-Phase Esterase Assays

When screening carboxylesterases and lipases in solution, the activity of the enzyme or culture was colorimetrically determined by use of *p*-nitrophenyl-acyl-esters (*p*NP-esters). Enzymes or cultures that exhibited relevant activity (for example, an appropriate pH-activity profile) were assayed for activity with the

esters of immediate interest to this study – ethyl butyrate, methyl butyrate and ethyl acetate. All buffer pH values were adjusted to the temperature at which they were assayed.

2.2.1.1 Activity Against *p*-Nitrophenyl-Acyl Esters

2.2.1.1.1 Continuous Assays

Esterase-catalysed hydrolysis of *p*NP-esters was followed by monitoring production of *p*-nitrophenol at 405 nm in 1-cm path-length cells using a Pharmacia Ultrospec 3000 UV/Visible spectrophotometer with a water-heated cuvette block. The standard assay was carried out in a total volume of 1 ml containing 2.0 mM (final concentration) *p*NP-esters and 50 mM NaH_2PO_4-NaOH, pH 7.6 at 30°C.

Stock solutions of *p*NP-esters were prepared in 99.7-100% ethanol (BDH), and the buffered substrate was preincubated at 30°C. The absorption coefficient of 17.03 $mM^{-1}.cm^{-1}$ used was calculated from a standard curve of *p*-nitrophenol, spectrophotometric grade, prepared in ethanol and appropriate assay buffer. The background hydrolysis of the substrate was compensated for by the use of a control mixture identical in composition to the standard assay excluding the esterase. All assays were routinely performed in triplicate, with non-enzymic hydrolysis at each pH corrected for by appropriate controls. One unit of esterase activity was defined as the amount of enzyme that released 1 μmol of *p*-nitrophenol per minute at 30°C. Specific esterase activity was defined as units per milligram of protein ($\mu mol.min^{-1}.mg^{-1}$).

When an assay was performed at a pH value other than pH 7.6, the hydrolysis of the *p*NP-acyl-ester was monitored at 348 nm, the isobestic point of *p*-nitrophenol and its anion, *p*-nitrophenoxide, using the absorption coefficient of 5.15 $mM^{-1}.cm^{-1}$ (Greenzaid and Jencks, 1971; Lombardo and Guy, 1981).

2.2.1.1.2 Discontinuous Assays

Two discontinuous assays were used in this study. First, the *copper phosphate suspension* assay was carried out in 1.5 ml plastic Eppendorf tubes and contained 250 μM (final concentration) *p*NP-ester in 50 mM Mops-NaOH (pH 7.5) plus 5 mM $CaCl_2$ at 30°C. The buffered substrate was preincubated at 30°C

before the addition of 50-100 μL culture or enzyme (to give a total volume of 1.0 ml). The reaction was stopped by the addition of 500 μl alkaline copper phosphate suspension, as described by Janssen et al (1994), and centrifuged using a Beckman Microfuge E™ microcentrifuge for 2 minutes at 4,000 x *g*. The absorbance of the supernatant at 400 nm was measured and the concentration of p-nitrophenol was determined using an absorption coefficient of 12.38 $mM^{-1}.cm^{-1}$ (calculated from a standard curve of p-nitrophenol, spectrophotometric grade, prepared in ethanol and the copper phosphate stopping reagent).

Second, the *15% trichloroacetic acid* assay was carried out in 1.5 ml plastic Eppendorf tubes. This assay was identical to that described in the copper phosphate suspension section, except the reaction was stopped by addition of 500 μl 15% trichloroacetic acid (TCA) followed by centrifugation at 4,000 x *g* for two minutes. Release of *p*-nitrophenol was determined by measurement of absorbance at 310 nm using an absorption coefficient of 10.26 $mM^{-1}.cm^{-1}$.

2.2.1.2 Activity Against the Esters of Interest

Initial screening of esterase activity, by way of gas chromatography (GC), utilised an assay containing 100 μl culture or 50 μl enzyme, in 750 μl or 800 μL of 50 mM Mops-NaOH (pH 7.5) buffer, respectively. The buffered enzyme mixture was preincubated at 30°C before the addition of 150 μL of 2000 parts per million (ppm) (v/v) ester to give a final ester concentration and assay volume of 300 ppm and 1 ml respectively. The physical characteristics of the three esters of interest are described in Table 2.1.

Table 2.1. Analytes detected by the Pye Unicam GCD Chromatograph
Analyte data were obtained from Windholz, 1976.

Analyte	Analyte Abbreviation	Boiling Point (°C)	Molecular Weight ($g.mol^{-1}$)	Density ($g.ml^{-1}$)
Ethyl Acetate	EtOAc	77.0	88.1	0.902
Ethyl Butyrate	EtOBu	119-121	116	0.879
Ethanol	EtOH	78.5	46.1	0.789
Methyl butyrate	MeOBu	102	102	0.898
Methanol	MeOH	64.7	32.0	0.792

Stock solutions of ester, plus the buffer and enzyme preparations, were prepared in Milli-Q water. After 10-60 minutes in a 30°C water bath, a 2 μl sample was taken and immediately injected onto a Pye Unicam GCD Chromatograph, connected to a Spectra Physics SP4100 integrator, for quantitative assessment of ester hydrolysis. Column and gas flow parameters are listed in Table 2.2.

Table 2.2. Set parameters of the Pye Unicam GCD Chromatograph.

Parameter	Setting
Column	0.5 m x 3 mm ID, Glass
Packing	Chromosorb™ 101, 100/120
Catalogue Number	Supelco, C0640
Oven Temperature	150°C
Flow Rate	Nitrogen, 40 $ml.min^{-1}$
Injector	Splitless, 220°C
Detector	FID, 220°C
Injection Sample Volume	2 μl
Attenuation	1600
Integrator	SpectraPhysics SP4100

Activities were determined through the disappearance of ester, or production of alcohol, over time. Peak area was converted to concentration via a standard curve constructed from 2 μl injections of 0-10 mM ester prepared in Milli-Q water and using appropriate temperatures and gas flows (see Appendix One for examples of an ester and alcohol standard curve). Non-enzymic ester hydrolysis was corrected for by appropriate controls, and all assays were performed in triplicate.

2.2.1.3 pH-Activity Profiles

2.2.1.3.1 Against *p*NP-Esters

Esterase activity, as a function of pH, was tested using modified versions of the two methods described in Section 2.2.1.1. Continuous assays were used exclusively for enzyme powders, while discontinuous assays were used for both the enzyme powders and cultures.

The continuous assay was started by the addition of 50-100 μl esterase solution to 250 μM *p*NP-ester (final concentration) contained in 50 mM buffer. The 50 mM NaH_2PO4-NaOH buffer was replaced by 50 mM citric acid-NaOH, pH 3.0-5.0, 50 mM Mes-NaOH, pH 5.5-6.5 and 50 mM Mops-NaOH, pH 6.5-7.5 (in 0.5 increments). The rate of hydrolysis after a fixed time (5 to 60 minutes) was measured at 348 nm, using the absorption coefficient of 5.15 $mM^{-1}.cm^{-1}$ (Lombardo and Guy, 1981).

The discontinuous assay utilised 50-100 μl esterase solution or culture in buffered substrate using the range of buffers described previously. After a fixed time, between 5 and 60 minutes, 500 μl of copper phosphate suspension or 15% TCA was added, the reaction vial centrifuged, and the supernatant measured for absorbance at 400 and 310 nm respectively.

2.2.1.3.2 Against the Esters of Interest

The standard assay described in Section 2.2.1.2 was modified whereby 50 mM citrate acid-NaOH, pH 3.0-5.0 (or 100 mM citric acid/100 mM trisodium citrate, pH 3.0-6.0), 50 mM Mes-NaOH, pH 5.5-6.5 and 50 mM Mops-NaOH, pH 6.5-7.5 replaced the single buffer used.

2.2.1.4 Thermal- and pH-Stabilities

Thermal- and pH-stabilities of esterase enzymes were concurrently studied using 100 mM citric acid-NaOH, pH 4.0, 100 mM Mes-NaOH, pH 5.5 and 100 mM Mops-NaOH, pH 7.0 incubated at four temperatures: 0, 5, 30 and 40°C. All buffers contained 0.02% sodium azide (w/v) and were adjusted to the correct pH value at each temperature. Aliquots (200 μl) of approximately 1 $mg.ml^{-1}$ esterase (prepared in the three buffers, sterilised by Supor Acrodisc 32 (0.2 μm) filters and added to autoclaved 1.5 ml plastic Eppendorf tubes) were incubated under each set of conditions for two weeks. Individual aliquots were taken periodically and assayed in triplicate for esterase activity in 50 mM Mops-NaOH, pH 7.0 at 30°C, against 2.5 mM *p*NP-butyrate, 300 ppm ethyl butyrate or 300 ppm methyl butyrate as the substrate. The remaining activity was plotted against time of incubation.

2.2.1.5 pH-Electrode Assays

The time courses for esterase-catalysed hydrolysis of methyl butyrate (and ethyl butyrate) or ethyl acetate were followed by monitoring the release of butyric and acetic acid, respectively, using a Philips PW9421 pH-meter and Schott micro-pH combination spear electrode (Ag/AgCl saturated). The standard assay was completed in a sealed volume of 3 ml containing ester and 50 μl of 2 mg.ml^{-1} desalted esterase (using a Pharmacia Biotech disposable PD10 desalting column) to give final concentrations of 100 ppm and 33 μg.ml^{-1} respectively. The esterase preparation was prepared in Milli-Q water and poised at a starting pH of 7.0 with dilute NaOH. The reaction was started by the addition of ester. The change in pH was continuously followed for the initial 2 hours using a Sekonic chart recorder, with single pH readings taken after 24 and 48 hours. When an esterase exhibited favourable activity a comprehensive pH-electrode study was performed. This used a similar assay as previously described, but the ester concentration ranged from 20 to 2500 ppm in solution, and the esterase concentration ranged from 2.5 to 312.5 μg.ml^{-1}.

This "functional" assay closely duplicates the environment of the proposed biosensor (see Chapter 4) since the pH falls with time and results in continual changes in the rate of ester hydrolysis (since esterase activity is a function of pH). Therefore, the pH-electrode assay is more appropriate than the pH-stat assay where the initial pH of 7.0 would be maintained throughout the period of the assay.

2.2.2 Enzyme Kinetics

Esterase activities versus substrate concentration data were graphically analysed using direct linear plots to determine the maximal velocity, V_{max} and Michaelis constant, K_m, values.

2.2.3 Proteolytic Activity

Cultures were tested for protease activity before undergoing ultrafiltration (UF) using a method based on Peek *et al.* (1993). The reaction mixture contained 100 μl culture in 900 μl 50 mM MOPS (pH 7.0) plus 5 mM $CaCl_2$, 0.01% Triton X-100 (v/v) and 0.2% azocasein (w/v). The reaction was incubated at 30°C for 30 minutes, terminated by the addition of 500 μl 15% TCA, and the reaction vial

placed on ice for 10 minutes. The vials were centrifuged for two minutes at 4000 *g*. Absorbance of the supernatant at 440 nm, a measurement of azocasein breakdown, provided qualitative analysis of proteolytic activity.

2.2.4 Protein Determination

Protein concentrations above 1 $mg.ml^{-1}$ were determined by the method of Bradford (1976) using bovine serum albumin (BSA, 2 $mg.ml^{-1}$) as the standard. Protein concentrations below 1 $mg.ml^{-1}$ were determined by the Far-UV method, as described by Scopes (1994), using appropriate background controls. Protein concentration was calculated by taking the mean of four determinations made by measuring absorption at four UV wavelengths (220, 215, 210 and 205 nm) using the millimolar absorption coefficients 11, 15, 20 and 31, respectively (disparate absorption readings were disregarded). The protein concentration of the column eluant was monitored at 215 and 280 nm.

2.2.5 Partial Protein Purification

Crude pig liver esterase (PLE, Sigma-Aldrich E3019), *Candida rugosa* LipaseB (L034P, BioCatalyst) and *Ophiostoma pluriannulatum* 5040 esterase were semi-purified using Fast Flow Q Sepharose, FFQ (Pharmacia Biotech). A column was packed using a thick slurry of the resin, which was pre-washed in alternate volumes of 0.01 M NaOH and 0.01 M HCl, followed by extensive washing with distilled water.

2.2.5.1 PLE

The column (18 cm x 5.0 cm ID) was equilibrated by washing with 30 mM Mops-NaOH (pH 7.0) until the eluent pH was consistently 7.0 (approximately three column volumes, CV's). The flow rate was maintained at 10 $ml.min^{-1}$ using a peristaltic pump and 10 ml fractions were collected. PLE solution, which was dissolved in a minimum volume of the equilibration buffer and with a conductivity reading less than 5 mS, was pumped onto the column and washed on with the equilibration buffer. Washing was continued until no protein was detectable in the eluent (A_{280}). Protein was initially eluted from the column using 0.1 M NaCl (prepared in equilibration buffer) until protein was not present in the eluent. Gradient elution was then started using a 6CV linear salt gradient from 0.1

to 0.5 M NaCl and 10 ml eluant frations were collected. Carboxylesterase activity was assayed with 0.25 mM *p*NP-butyrate in 0.05 M Mops-NaOH buffer (pH 7.5) at 30°C. Active fractions were pooled and desalted by ultrafiltration using an Amicon® YM10 membrane and lyophilised.

2.2.5.2 *Candida rugosa* LipaseB

LipB was partially purified using an identical method to that described for PLE, except that the column buffer was set at pH 6.5 and the salt gradient was 0.1-0.75M NaCl.

2.2.5.3 *Ophiostoma pluriannulatum* 5040 Carboxylesterase

A similar method to that described for the PLE was employed. However, due to the *O. pluriannulatum* 5040 carboxylesterase being present in the culture supernatant, rather than in a powder preparation, the culture medium was first centrifuged and the pellet discarded. The cell free supernatant (CFS) was diluted with equilibration buffer to give a conductivity reading less than 5 mS, then poised at pH 7.0 before it was pumped onto the column and washed on with equilibration buffer. In addition, the 0.1 M NaCl wash step was substituted by a 0 to 0.25 M linear NaCl gradient.

2.2.6 Isoelectric Focusing (IEF)

The Pharmacia PhastSystem™ and a PhastGel IEF 3-9 gel was used to separate native proteins based on their isoelectric points. The Pharmacia isoelectric point standard markers used are listed in Table 2.3.

IEF followed three stages: (a) a prefocusing stage where the pH gradient was formed; (b) sample application; and (c) a focusing step whereby the proteins move to the point in the pH gradient that equals their isoelectric point. Protein aliquots were loaded onto the gel and electrophoresed at room temperature with Method 4.0 (Appendix Two).

The silver staining scheme for PhastGel IEF media is 20 times more sensitive than coomassie staining. The steps followed include: (a) fixing the proteins; (b) sensitising the proteins with glutaraldehyde; (c) reacting the proteins with silver ions; and (d) developing the gel with formaldehyde (Table 2.4).

Table 2.3. Pharmacia IEF 3-9 standard markers.

Standard	*p*I
Amyloglucosidase	3.50
Methyl Red	3.75
Soybean Trypsin Inhibitor	4.55
β-lactoglobulin A	5.20
Bovine Carbonic Anhydrase B	5.85
Human Carbonic Anhydrase B	6.55
Horse Myoglobin (Acidic Band)	6.85
Horse Myoglobin (Basic Band)	7.35
Lentil Lectin (Acidic Band)	8.15
Lentil Lectin (Middle Band)	8.45
Lentil Lectin (Basic Band)	8.65
Trypsinogen	9.30

Table 2.4. Modified silver staining for PhastGel IEF and SDS-PAGE media at 25°C.

Step	Solution[1]	Time (min)[2]
1	20% trichloroacetic acid	5
2	50% ethanol, 10% acetic acid	4
3	10% ethanol, 5% acetic acid	4
4	10% ethanol, 5% acetic acid	8
5	8.3% glutaraldehyde	12
6	10% ethanol, 5% acetic acid	6
7	10% ethanol, 5% acetic acid	10
8	Milli-Q water	4
9	Milli-Q water	4
10	0.5% silver nitrate	20
11	Milli-Q water	0.5
12	Milli-Q water	0.5
13	Developer[3]	1
14	Developer[3]	10-20
15	5% acetic acid	4
16	10% acetic acid, 5% glycerol	6

[1] The volume of each solution used is 30 ml; [2] The times required for Steps 2-10 of the original Pharmacia protocol were doubled because staining was performed at 25 rather than 50°C; [3] Developer was made with 50 ml 2.5% (w/v) Na_2CO_3 and 20µl formaldehyde.

2.2.7 Microbial Growth

All media were prepared in reverse-osmosis (RO) water and pH-adjusted with HCl or NaOH before autoclaving for 20 minutes at 121°C. Media containing agar was boiled and thoroughly mixed before autoclaving. Culture growth was determined either by following absorbance at 650 nm (for bacterial growth) or blastospore counts using a haemocytometer (for fungal growth).

2.2.7.1 Ophiostoma Species Growth Media

2.2.7.1.1 Yeast Malt Agar

Yeast malt agar (YMA), which supports both bacterial and fungal growth, was used to grow *Ophiostoma* sp. on plates. To enable a pure culture of *Ophiostoma* to be produced (and maintained) YMA was supplemented with several antibiotics using a modified recipe described in Table 2.5 (McNaughton, 1997).

Table 2.5. Antibiotic supplemented yeast malt agar, (pH 6.8).

Ingredient	Concentration ($g.l^{-1}$)
Bactoagar	18.0
Malt Extract (DifCo)	15.0
Yeast Extract (BBL)	2.0
Cycloheximide (Sigma)[1]	0.4
Chloramphenicol (Sigma)	0.2
Streptomycin (Sigma)[2]	0.1

[1] prepared in 99.7-100% ethanol and added aseptically to the autoclaved medium; [2] prepared in Milli-Q water and added aseptically to the autoclaved medium.

2.2.7.1.2 Liquid Peptone Medium

Lipase production was optimal when *Ophiostoma* sp. was grown on a liquid, peptone based, medium (McNaughton, 1997). A modified version of the medium is presented in Table 2.6. This medium produced high levels of esterase activity and was the sole medium used in this study to grow both *Ophiostoma floccosum* F13 and *Ophiostoma pluriannulatum* 5040. An initial culture of 15 ml was started from a gel slab (taken from the edge of a YMA plate culture) and incubated at

25°C in a Gallenkamp orbital incubator at 120 rpm for 24 hours. The 24 hour culture was used to start (step-wise) a 250 ml (75 ml medium) followed by a 2 l (600 ml medium) flask using a 5% inoculant (v/v). The culture was grown for 5 days and harvested by centrifugation using a Sorvall RC26 Plus rotor at 4,000 x *g* for 20 minutes at 4°C. The supernatant and cell pellet were stored at 4°C while being assayed for esterase activity using *p*NP-ester substrates.

Table 2.6. Liquid peptone medium.

Ingredient	Concentration ($g.l^{-1}$)
Gelatin Hydrolysate, Peptone No.190 (Gibco BRL)	30.0
$NaNO_3$	3.0
Yeast Extract	1.0
KH_2PO_4	1.0
$MgSO_4.7H_2O$	0.3

2.2.7.2 Lactobacillus Species Growth Medium

Esterase production and culture growth were optimal when *Lactobacillus casei* BH1 and *Lactobacillus plantarum* were grown on MRS broth (Table 2.7).

Table 2.7. Lactobacilli Liquid Medium (MRS Broth, pH 6.5)

Ingredient	Concentration ($g.l^{-1}$)
Glucose	20.0
Beef Extract (DifCo)	10.0
Casein Peptone Tryptic Digest	10.0
Yeast Extract	5.0
Sodium acetate	5.0
K_2HPO_4	2.0
Diammonium succinate	2.0
$MgSO_4.7H_2O$	0.2
$MnSO_4.4H_2O$	0.04

An initial culture of 10 ml was started from frozen cells (stored at –70°C in 50% glycerol) and incubated at 30°C and 120 rpm for 8 hours. This culture was

used to start (step-wise) a 250 ml (75 ml medium) followed by a 2 l (600 ml medium) flask using a 5% inoculant (v/v). The culture was grown for 16 hours and harvested by centrifugation at the end of the exponential growth phase. The supernatant and cell pellet were stored at 4°C while being assayed for esterase activity using *p*NP-ester substrates.

2.2.7.3 Bacillus Species Growth Media

2.2.7.3.1 Milk Powder Bacillus Species Media

Seven *Bacillus* strains isolated from milk powders (*Bacillus stearothermophilus* A^M, B^M, C^M; *Bacillus licheniformis* D^M, DRC1 and FTA) were grown on Tryptic Soy Broth, dehydrated medium (DifCo, 30 $g.l^{-1}$) supplemented with 0.1% soluble starch (w/v). Screening cultures were started with cells stored at –70°C (in 50% glycerol) and incubated at 55°C at 120 rpm. Cultures were harvested after 24 hours and tested for esterase activity against *p*NP-ester substrates.

Activity profiles for the seven *Bacillus* strains indicated that *B. stearothermophilus* A^M was a potential source of a relevant esterase with respect to the biosensor application. Therefore, the A^M strain was grown using the medium listed in Table 2.8. The culture was grown for 5-6 hours to minimise the exchange of esterase from the cell-surface to the supernatant. The cells and supernatant were separated by centrifugation and stored at 4°C.

Table 2.8. *Bacillus stearothermophilus* A^M Medium (pH 7.3).

Ingredient	Concentration ($g.l^{-1}$)
Tryptone Peptone (Oxoid)	5.0
NaCl	5.0
Yeast Extract	2.5
Soluble Starch	1.0

2.2.7.3.2 Bacillus acidocaldarius

Bacillus acidocaldarius ATCC 27009 and E24 A.1 cultures were started from freeze-dried pure cultures. The cultures were grown on Darland and Brock's

Bacillus acidocaldarius Medium A listed in Table 2.9, and stock cultures were maintained on the solid medium (Media A and B). Medium A (pH adjusted to pH 3.5 with 10N H_2SO_4) and B were autoclaved separately at 121°C for 20 minutes, cooled to 50°C and mixed together to produce the solid medium. An 'induced' version of Medium A (to try to increase esterase production) included 1.0 $g.l^{-1}$ ethyl acetate and a 50% reduction in yeast extract concentration.

Table 2.9. *Bacillus acidocaldarius* Medium

Ingredient	Media	Concentration ($g.l^{-1}$)
Yeast Extract	A	1.00
KH_2PO_4		0.60
$MgSO_4.7H_2O$		0.50
$CaCl_2.2H_2O$		0.25
$(NH_4)_2SO_4$		0.20
Bactoagar	B	40.0
Glucose[1]		2.00

[1] added to Media B after autoclaving by filter sterilisation

2.2.7.4 *Streptomyces rochei* Growth Medium

Streptomyces rochei was grown on the International Streptomyces Project (ISP) Medium 2 whose ingredients are listed in Table 2.10. The culture was grown on an ISP Medium 2 agar plate initially, followed by the broth version of the media at 25°C and 100 rpm. An 'induced' version of this media was made by supplementing with 1.0 $g.l^{-1}$ ethyl acetate (filter sterilised) and/or excluding dextrose. Samples were obtained daily over a period of 4 days, centrifuged and tested for esterase activity.

Table 2.10. *Streptomyces rochei* ISP Medium 2 (pH 7.2).

Ingredient	Concentration ($g.l^{-1}$)
Malt Extract	10.0
Yeast Extract	4.0
Dextrose	4.0
Agar[1]	20.0

[1] agar was only included when the media was plated out

2.2.7.5 *Sulfolobus solfataricus* Growth Medium

Sulfolobus solfataricus DSM 1616 was grown in the liquid medium described in Table 2.11. The medium was adjusted to pH 3.2 with 10 N H_2SO_4 and autoclaved for 60 minutes at 121°C. An initial culture of 15 ml was started from frozen cells (stored at –70°C in 50% glycerol) and incubated at 70°C and 120 rpm for 24 hours. This culture was used to start (step-wise) a 250 ml (75 ml media) followed by a 2 l (600 ml medium) flask. The culture was grown between 24 and 48 hours and harvested by centrifugation. The supernatant and cell pellet were stored at 4°C while being assayed for esterase activity using *p*NP-ester substrates.

Table 2.11. *Sulfolobus solfataricus* liquid medium (pH 3.2).

Ingredient	Concentration ($g.l^{-1}$)	Concentration ($\mu l.l^{-1}$)
Ammonium sulphate	3.0	
Sucrose	2.0	
Yeast Extract	1.0	
Glycine	0.7	
$KH_2PO_4.3H_2O$	0.5	
KCl	0.1	
$FeSO_4.7H_2O$	0.02	
$Na_2B_4O_7.10H_2O$[1]		224.0
$MnCl_2.4H_2O$[1]		90.0
$ZnSO_4.7H_2O$[1]		11.0
$CuCl_2.2H_2O$[1]		2.5
$Na_2MoO_4.2H_2O$[1]		1.5
$VOSO_4.5H_2O$[1]		1.5
$CoSO_4.7H_2O$[1]		0.5
$NiSO_4.6H_2O$[1]		0.5
Wolins Vitamins[2,3]		5000.0
0.3M $Ca(NO_3)_2.4H_2O$[3]		1000.0
1M $MgCl_2.6H_2O$[3]		1000.0

[1] 1 $g.100ml^{-1}$ stock made in Milli-Q water; [2] vitamin solution made from the following substances (whose concentration, in $mg.100\ ml^{-1}$, is given in brackets) of biotin (2), folic acid (2), pyridoxin HCl (10), riboflavin (5), thiamine (5), nicotinic acid (5), pantothenic acid (5), vitamin B12 (0.1), p-amino benzoic acid (5), thioctic acid (5); [3] added after autoclaving by filter sterilisation

2.2.8 Solid-Phase Protein Hydration

2.2.8.1 Determination of sorption isotherms

Sorption isotherm curves were obtained at 20°C using the gravimetric method to determine protein water content, *h*. Static control of relative humidity (RH), and thereby protein hydration, was achieved with the saturated salt solutions listed in Table 2.12. The Analytical Reagent Grade salts were prepared (without further purification) in Milli-Q water and the quantity of saturated salt solution used in sorption isotherm production was equivalent to 10% (v/v) of the 500 ml sealed vessel volume. Below 7.2% RH the drying agent anhydrous phosphorus pentoxide, P_2O_5, was used. In all cases, the saturated salt solution and P_2O_5 were not in direct contact with the protein sample.

Table 2.12. Saturated salt solutions used to control relative humidity at 20°C.
RH data is obtained from O'Brien (1948) and (Rockland, 1960).

Solid Phase	RH (%)
Phosphorus pentoxide[1]	0
LiBr	7.2
$ZnBr_2.xH_2O$	8.6
$ZnCl_2.xH_2O$	10.0
$LiCl.xH_2O$	13.5
$CaCl_2.xH_2O$	32.3
$NaNO_2$	66.0
NH_4Cl	79.2
KBr	84.0
$ZnSO_4.7H_2O$	90.0
$Na_2HPO_4.12H_2O$	95.0[3]
$CuSO_4.5H_2O$	98.0[3]

[1] used as a powder, [2] at 25°C (Richardson and Malthus, 1955), [3] Weast and Astle, 1982.

Three globular proteins used in the standardisation of the adsorption isotherm were Hammerstein casein (BDH), bovine serum albumin (Gibco BRL) and lysozyme (Sigma). The enzymes used in the protein hydration-activity experiments were desalted and lyophilised PLE (Sigma) and *Candida rugosa* LipB (BioCatalyst).

Two grams of Hammerstein casein and BSA, 100 mg of lysozyme, and 20 to 30 mg of lyophilized LipB and PLE were placed in sealed glass vessels containing 50 ml (10% of the vessel volume, v/v) of saturated salt solution. The protein samples were equilibrated at various RH's, produced by the above range of saturated salt solutions, for three days to two weeks. Gravimetric data for the three enzymes (LipB, PLE and lysozyme) were obtained after three, six, ten and fourteen days (whilst only one data set was obtained from the Hammerstein casein and BSA samples after three and five days, respectively) and the protein water content at each RH was then calculated. To achieve zero water content (0 *h*), one sample from each enzyme was exposed to anhydrous P_2O_5 at 65°C for two weeks, and gravimetric measurements were obtained as previously described.

2.2.9 Analysis of Vapor-phase Ethyl Butyrate Hydrolysis

Aqueous solutions of lyophilized LipB and PLE in 0.02% (w/v) sodium azide, pH 7.5 were prepared and the protein content of each sample was determined by far-UV (Scopes, 1994). While half of LipB and PLE preparations were left as is, half were denatured at 140°C for 60 minutes in an oil bath using 8 ml screw-capped Hungate tubes. Aliquots containing 1 mg LipB and 0.5 mg PLE were applied to separate 0.5 x 1.5 cm Glass Fibre Paper (GF/B) rectangles and air-dried for 30 minutes at room temperature and RH. Appropriate controls, including 'no-enzyme' controls, were treated with 0.02% sodium azide, pH 7.5 and run in parallel with each experiment. Each rectangle was suspended above 0.8 ml saturated salt solution (used to control RH between 7.2 and 90%) in an 8 ml Hungate tube (see Table 2.12 for the list of saturated salt solutions used). The tube was sealed with a Mininert® valve (Teflon lined), and each rectangle was adjusted to the desired water content prior to reaction by pre-equilibration at 20°C for 3 days with the vapor phase in the absence of substrate.

The reaction was initiated by the addition of EtOBu onto an enzyme free GF/B rectangle (dimension as described above) through the Mininert® valve septum using a rinsed and dried microliter syringe. The concentration of EtOBu used was 500 ppm (v/v) [i.e., 1 µl EtOBu into a headspace volume of 2 ml] and the reactions were carried out at 20°C for fifteen minutes. Quantitative assessment of ester hydrolysis was based on measurement of EtOH production. This involved the removal of 20 µl vapor phase samples through the Mininert®

valve for injection onto the GCD Chromatograph equipped with a 0.5 m x 3 mm internal diameter column, packed with Chromosorb™ 101 (100/120 mesh), and a flame ionization detector, FID (standard curves were used to calculate EtOBu hydrolysis and EtOH production). The column temperature was maintained at 170°C, nitrogen (40 $ml.min^{-1}$) was the carrier gas, and hydrogen and air were supplied to the FID. Quantitative data acquisition was obtained through a Spectra Physics SP4100 integrator.

CHAPTER 3 BIOSENSOR ENZYME SCREEN

3.1 INTRODUCTION

The original objective of the work described here is to screen carboxylesterases or lipases of mammalian or microbial origin, comparing them with commercial pig liver esterase (the original biosensor enzyme), in order to identify those with higher specific activities and specificities (i.e., higher V_{max}/K_m ratios) for the target esters – ethyl acetate, methyl butyrate and ethyl butyrate – as those esters would likely be encountered in the biosensor application. Also, the enzyme selected from the screening process was required to be acidophilic and have a higher thermal- and pH-stability than PLE.

3.2 MICROBIAL CARBOXYLESTERASE AND LIPASE SCREEN

During the third year of this project, the use of enzymes of mammalian origin became prohibited due to market-place restrictions. The sources of the microbial enzymes included TRUCC cultures (for example *Bacillus stearothermophilus* A^M), University of Waikato Microbial Department cultures (*Ophiostoma floccosum* F13) and commercially available carboxylesterase or lipase powders (Fluka and BioCatalyst enzymes). The cultures used were grown as described in Materials and Methods (Section 2.2.7), and the nature of the fungal and bacterial preparations are given in Section 3.2.1 and 3.2.2, respectively.

3.2.1 Fungal Cultures

Ophiostoma pluriannulatum 5040 and *Ophiostoma flocossum* F13 grew well on antibiotic supplemented YMA plates and in liquid peptone medium (the media recipes are given in Section 2.2.7.1). The growth and activity curves of *O. pluriannulatum* 5040 and *O. flocossum* F13 in the liquid peptone medium are displayed in Figure 3.1 and 3.2, respectively. Both species exhibit activity against *p*NP-acetate and *p*NP-butyrate, but the *p*NP-acetate and *p*NP-butyrate activity of both species are primarily cell-associated and found in the cell-free supernatant, respectively (i.e., there may be two different enzymes associated with *p*NP-acetate and *p*NP-butyrate activity).

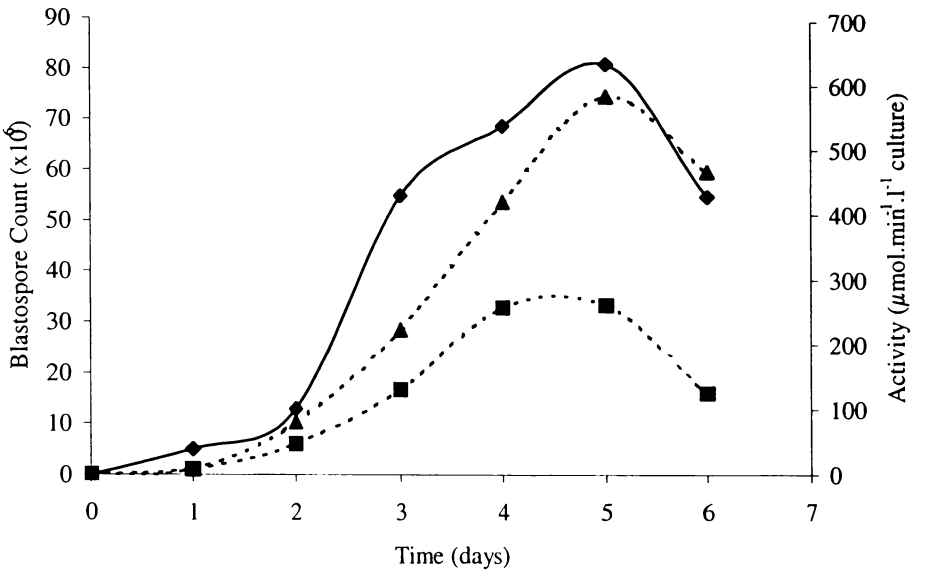

Figure 3.1. Growth and activity profiles of *Ophiostoma pluriannulatum* 5040 at 25°C in liquid peptone medium.

The three profiles are as follows: blastospore count, ◆; activity against 2.5 mM *p*NP-buytrate at 30°C and pH_{30} 7.5, --▲--; activity against 2.5 mM *p*NP-acetate at 30°C and pH_{30} 7.5, --■--. Growth was monitored with a haemocytometer. Activity was assayed according to the methods in Section 2.2.1.1.2

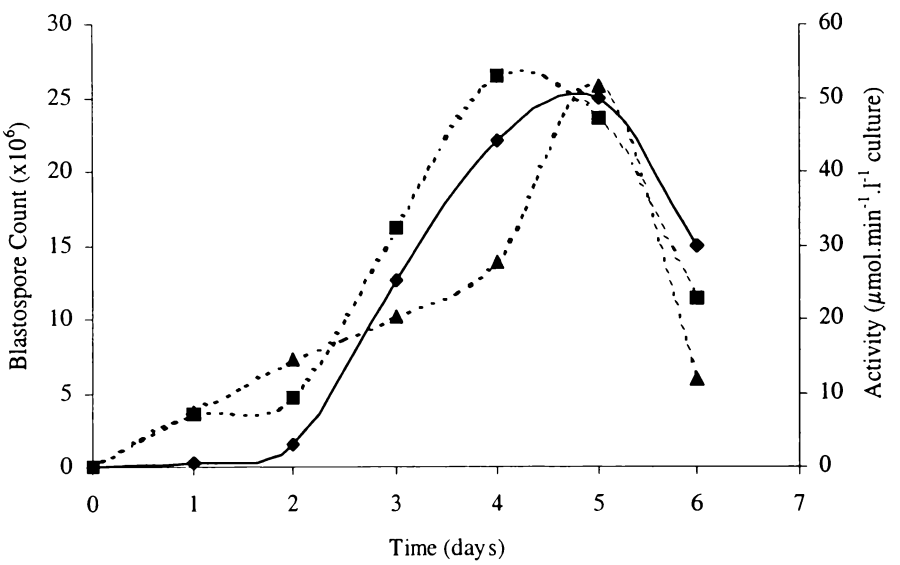

Figure 3.2. Growth and activity profiles of *Ophiostoma flocossum* F13 at 25°C in liquid peptone medium.

The three profiles are as follows: blastospore count, ◆; activity against 2.5 mM *p*NP-buytrate at 30°C and pH_{30} 7.5, --▲--; activity against 2.5 mM *p*NP-acetate at 30°C and pH_{30} 7.5, --■--. Growth and activity was monitored as in Figure 3.1.

3.2.2 Bacterial Cultures

The seven milk powder Bacilli and three Lactobacilli species listed in Table 3.1 were used in the microbial enzyme screen described in Section 3.2.3.

Table 3.1. The growth time and 650 nm absorbance of ten bacterial cultures used during the microbial enzyme screen.

The site of carboxylesterase activity in cultures are as follows: CA, cell-associated; CFS, cell free supernatant; IC, intracellular; WCC, whole cell culture.

Organism	Growth Time (hr)	A_{650}	Site of Enzyme Activity
B. stearothermophilus A^M	24	0.34	CFS
B. stearothermophilus B^M	24	0.46	WCC
B. stearothermophilus C^M	24	1.65	WCC
B. licheniformis D^M	24	0.31	CFS
B. licheniformis DRC1	24	1.00	WCC
B. licheniformis FT^A	24	1.17	WCC
B. subtilis	24	0.91	WCC
L. bulgaricus	16	1.03	CA
L. casei	16	2.77	CA
L. plantarum	16	2.75	CA
S. solfataricus[1]	48	1.09	CA
S. solfataricus[1]	48	1.09	IC

[1] only used for *p*NP-acetate activity determination

3.2.3 Effect of pH on Microbial Carboxylesterase or Lipase Activity

The microbial enzyme screening study was carried out between pH 3.0 and 8.0 using the equivalent *p*-nitrophenylated synthetic model substrates of ethyl acetate (*p*NP-acetate) and methyl butyrate/ethyl butyrate (*p*NP-butyrate). The enzymes that exhibited appropriate activity against the *p*NP-esters (defined as activities > 10% of those displayed by PLE) merited further investigation and were tested for activity against ethyl acetate (EtOAc), methyl butyrate (MeOBu) and ethyl butyrate (EtOBu). Since an aim of this enzyme screen, at the time it was carried out, was to find an acidophilic enzyme that had adequate activity between pH 4.0 and 5.0, activity data against *p*NP-butyrate and *p*NP-acetate for each microbial enzyme was obtained between pH 3.0 and 7.0, and reported in Table 3.2 and 3.3, respectively.

Table 3.2. Activity of culture and/or commercially derived microbial carboxylesterases or lipases against *p*NP-butyrate at 30°C between pH 3.0 and 8.0.

Pig liver carboxylesterase specific activities are reported as a comparison. Culture activity is given as *μmol.min^{-1}.l^{-1} culture*. Powder activity is given as **μmol.min^{-1}.mg^{-1} protein**. The site of enzyme activity in cultures are as follows: CA, cell-associated; CFS, cell free supernatant; WCC, whole cell culture.

Carboxylesterase/Lipase Source	Origin	Site of Activity	pH						
			3.0	4.0	4.5	5.0	6.0	7.0	8.0
Pig Liver	Powder	na	**0**	**0.330**	**0.933**	**1.980**	**15.29**	**16.25**	**19.86**
Bacillus stearothermophilus A^{M}	Culture[1,2]	CFS	*nd*	*nd*	*41.44*	*56.71*	*76.60*	*97.21*	*89.21*
Bacillus stearothermophilus B^{M}	Culture[1,2]	WCC	*nd*	*nd*	*nd*	*2.200*	*2.660*	*7.220*	*10.34*
Bacillus stearothermophilus C^{M}	Culture[1,2]	WCC	*nd*	*nd*	*2.12*	*2.610*	*nd*	*3.700*	*3.740*
Bacillus licheniformus D^{M}	Culture[1,2]	CFS	*nd*	*nd*	*4.790*	*12.44*	*44.31*	*71.46*	*nd*
Bacillus licheniformus DRC1	Culture[1,2]	WCC	*nd*	*nd*	*nd*	*2.780*	*7.620*	*8.010*	*9.680*
Bacillus licheniformus FT^{A}	Culture[1,2]	WCC	*nd*	*nd*	*nd*	*1.580*	*2.480*	*4.730*	*3.460*
Bacillus subtilus	Culture[1,2]	WCC	*nd*	*nd*	*nd*	*0.530*	*2.850*	*6.510*	*nd*
Lactobacillus bulgaricus	Culture[3]	CA	*nd*	*0*	*nd*	*0*	*0*	*0*	*nd*
Lactobacillus casei	Culture[3]	CA	*0*	*0.101*	*nd*	*0.174*	*0.306*	*0.250*	*nd*
Lactobacillus plantarum	Culture[3]	CA	*0*	*0.077*	*nd*	*0.201*	*0.226*	*0.194*	*nd*
Ophiostoma flocossum	Culture[4]	CFS	*nd*	*0.600*	*nd*	*5.600*	*nd*	*11.70*	*nd*
Ophiostoma pluriannulatum	Culture[4]	CFS	*nd*	*212.4*	*nd*	*234.3*	*312.7*	*299.3*	*nd*

[1] obtained from a TRUCC culture; [2] activity at 40°C; [3] Teaching Laboratory culture, University of Waikato; [4] Microbial Department culture, University of Waikato; [5] Fluka product; [6] BioCatalyst product; [7] semi-purified by the TRU; 'nd', not done.

Table 3.2 Continued.

Carboxylesterase/Lipase Source	Origin	Site of Activity	pH					
			3.0	4.0	5.0	6.0	7.0	8.0
Pig Liver	Powder	na	**0**	**0.330**	**1.980**	**15.29**	**16.25**	**19.86**
Bacillus stearothermophilus A[M7]	Powder[1]	na	**0.089**	**0.183**	**1.259**	**nd**	**11.52**	**nd**
Pseudomonas Strain 017[7]	Powder[1]	na	**nd**	**0.471**	**0.932**	**1.287**	**nd**	**nd**
TP10.A1[7]	Powder[1]	na	**nd**	**0.002**	**0.012**	**0.027**	**nd**	**nd**
TOK7.A1[7]	Powder[1]	na	**nd**	**0**	**0.001**	**0.002**	**nd**	**nd**
TOK4.A1[7]	Powder[1]	na	**nd**	**0**	**0**	**0.003**	**nd**	**nd**
Bacillus stearothermophilus	Powder[5]	na	**nd**	**0.010**	**0.032**	**0.132**	**0.104**	**0.052**
Saccharomyces cerevisiaea	Powder[5]	na	**nd**	**0.001**	**nd**	**0.198**	**0.354**	**0.803**
Mucor miehei	Powder[5]	na	**nd**	**0.005**	**0.007**	**0.008**	**0.016**	**0.049**
Candida rugosa	Powder[6]	na	**0.847**	**3.446**	**14.27**	**14.81**	**13.59**	**nd**
Fungal-derived	Powder[6]	na	**0.297**	**2.996**	**8.212**	**9.025**	**8.833**	**nd**
Porcine-derived	Powder[6]	na	**0**	**0**	**0**	**0.236**	**0.044**	**nd**
Penicillium roqueforti	Powder[6]	na	**0.293**	**2.323**	**5.214**	**6.603**	**5.702**	**nd**

[1] obtained from a TRUCC culture; [2] activity at 40°C; [3] Teaching Laboratory culture, University of Waikato; [4] Microbial Department culture, University of Waikato; [5] Fluka product; [6] BioCatalyst product; [7] semi-purified by the TRU; 'na', not applicable; 'nd', not done.

Table 3.3. Activity of culture and/or commercially derived microbial carboxylesterases or lipases against *p*NP-acetate at 30°C between pH 3.0 and 7.0

Pig liver carboxylesterase specific activities are reported as a comparison. Culture activity is given as *μmol.min^{-1}.l^{-1} culture*. Powder activity is given as **μmol.min^{-1}.mg^{-1} protein**. The site of enzyme activity in cultures are as follows: CA, cell-associated; CFS, cell free supernatant; IC, intracellular; WCC, whole cell culture.

Carboxylesterase/Lipase Source	Origin	Site of Activity	pH				
			3.0	4.0	5.0	6.0	7.0
Pig liver	**Powder**	**na**	**0**	**0.314**	**1.286**	**2.062**	**2.315**
Bacillus stearothermophilus A[M]	Culture[1,2]	CFS	*nd*	*5.560*	*7.690*	*18.49*	*24.70*
Bacillus licheniformus D[M]	Culture[1,2]	CFS	*nd*	*2.940*	*2.260*	*11.49*	*19.69*
Lactobacillus bulgaricus	Culture[3]	CA	*nd*	*nd*	*5.250*	*nd*	*5.270*
Lactobacillus casei	Culture[3]	CA	*0.100*	*0.724*	*0.833*	*2.500*	*2.194*
Lactobacillus plantarum	Culture[3]	CA	*0.046*	*0.501*	*0.725*	*1.403*	*1.484*
Ophiostoma floccosum F13	Culture[4]	CA	*nd*	*0*	*17.90*	*72.90*	*95.30*
Ophiostoma pluriannulatum 5040	Culture[4]	CA	*nd*	*25.900*	*51.00*	*118.0*	*102.0*
Sulfolobus solfataricus	Culture[1]	CA	*nd*	*0.186*	*0.293*	*nd*	*0.433*
Sulfolobus solfataricus	Culture[1]	IC	*nd*	*0.133*	*0.410*	*0.725*	*0.600*
Bacillus stearothermophilus A[M 6]	Powder[1]	na	**0.039**	**0.107**	**0.159**	**0.333**	**nd**
Pseudomonas Strain 017[6]	Powder[1]	na	**nd**	**0.117**	**0.494**	**0.556**	**nd**
TP10.A1[6]	Powder[1]	na	**nd**	**0**	**0.003**	**0.004**	**nd**
TOK7.A1[6]	Powder[1]	na	**nd**	**0**	**0**	**0.002**	**nd**
TOK4.A1[6]	Powder[1]	na	**nd**	**0**	**0**	**0**	**nd**
Candida rugosa	Powder[5]	na	**0.237**	**0.278**	**0.300**	**0.290**	**0.632**
Fungal-derived	Powder[5]	na	**0.069**	**0.177**	**nd**	**nd**	**0.433**
Porcine-derived	Powder[5]	na	**0**	**0**	**0**	**0.006**	**0.015**
Penicillium roqueforti	Powder[5]	na	**0.083**	**0.307**	**0.230**	**0.293**	**0.715**

[1] obtained from a TRUCC culture; [2] activity at 40°C; [3] Teaching Laboratory culture, University of Waikato; [4] Microbial Department culture, University of Waikato; [5] BioCatalyst product; [6] semi-purified by the TRU; 'na', not applicable; 'nd', not done.

Note that purities vary considerably among the cultures and powders listed in Tables 3.2 and 3.3. Therefore, the activity data are not necessarily a guide to relative V_{max} values.

The *p*NP-butyrate pH-activity profiles of the milk powder Bacilli species (*B. stearothermophilus* A^M, *B. stearothermophilus* B^M, *B. licheniformis* D^M, and *B. licheniformis* DRC1) are graphically displayed in Figure 3.3. The carboxylesterase activities of these cultures were obtained at 40°C and the activity data is given in $\mu mol.min^{-1}.l^{-1}$ culture.

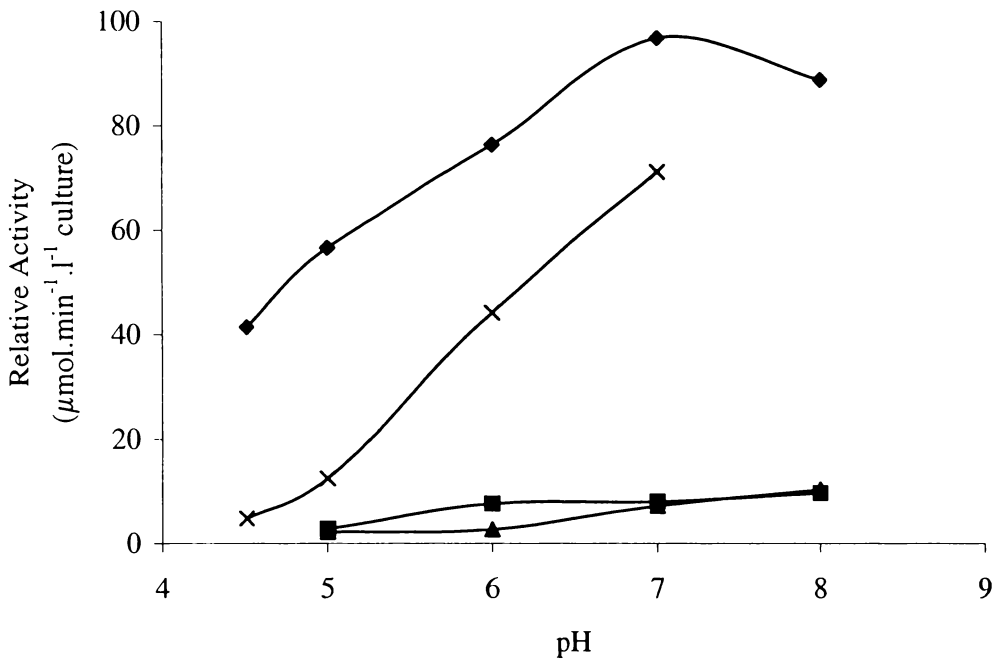

Figure 3.3. Activities of four milk powder Bacilli cultures against *p*NP-butyrate at 40°C and various pH values between 4.5 and 8.0.

The four cultures are as follows: *Bacillus stearothermophilus* A^M, ◆; *Bacillus licheniformis* D^M, ×; *Bacillus licheniformis* DRC1, ■; and *Bacillus stearothermophilus* B^M, ▲. The buffers used, and their effective pH range, are 50 mM Tris-HCl, pH 8.0-9.0, 50 mM Mops-NaOH buffer (pH 6.5-7.5), 50 mM Mes-NaOH buffer (pH 5.5-6.5) and 100 mM citric acid-trisodium citrate buffer (pH 3.0-5.0).

If an assumption (based on experimental observation) is made that a bacterial culture with an absorbance of 1 at 650 nm has an approximate protein concentration of 0.1 $mg.ml^{-1}$, then the specific activities ($\mu mol.min^{-1}.mg^{-1}$) of the four Bacilli cultures are approximately two orders of magnitude lower than the $\mu mol.min^{-1}.ml^{-1}$ data given in Table 3.2 and 3.3 (this estimation allows the culture

activity data to be compared with that of PLE (the carboxylesterase all microbial enzyme activity data must be compared to).

The activities of the fungal-derived Biocatalyst enzymes (sourced from *Candida rugosa*, *Penicillium roqueforti* and a general fungal-derived preparation) against *p*NP-butyrate and *p*NP-acetate were very similar to that exhibited by PLE (especially that of the *C. rugosa* Lipase B enzyme) and are graphically displayed in Figure 3.4 and 3.5, respectively.

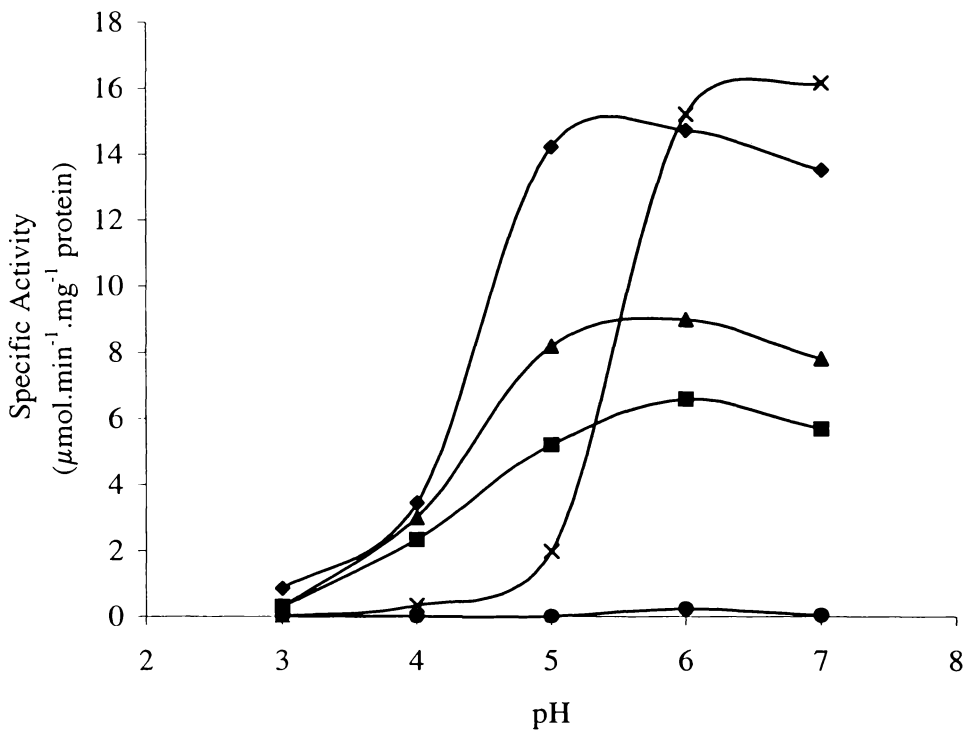

Figure 3.4. Specific activities of four Biocatalyst carboxylesterase and/or lipase mixtures against *p*NP-butyrate at 30°C and various pH values between 3.0 and 7.0.

The four mixtures are as follows: *C. rugosa*, ◆; fungal-derived, ▲; *P. roqueforti*, ■; and porcine-derived, ●. The PLE data set (×) was displayed for direct comparison with the four microbial enzyme mixures. The buffers used, and their effective pH range, are 50 mM Mops-NaOH buffer (pH 6.5-7.5), 50 mM Mes-NaOH buffer (pH 5.5-6.5) and 100 mM citric acid-trisodium citrate buffer (pH 3.0-5.0).

Although the activity of microbial carboxylesterases and lipases (against the synthetic esters, *p*NP-acetate and *p*NP-butyrate) was followed through a range of pH values, the potential usefulness of each enzyme in the biosensor can be more accurately assessed by completing a pH-electrode assay and/or ester activity-pH profile study.

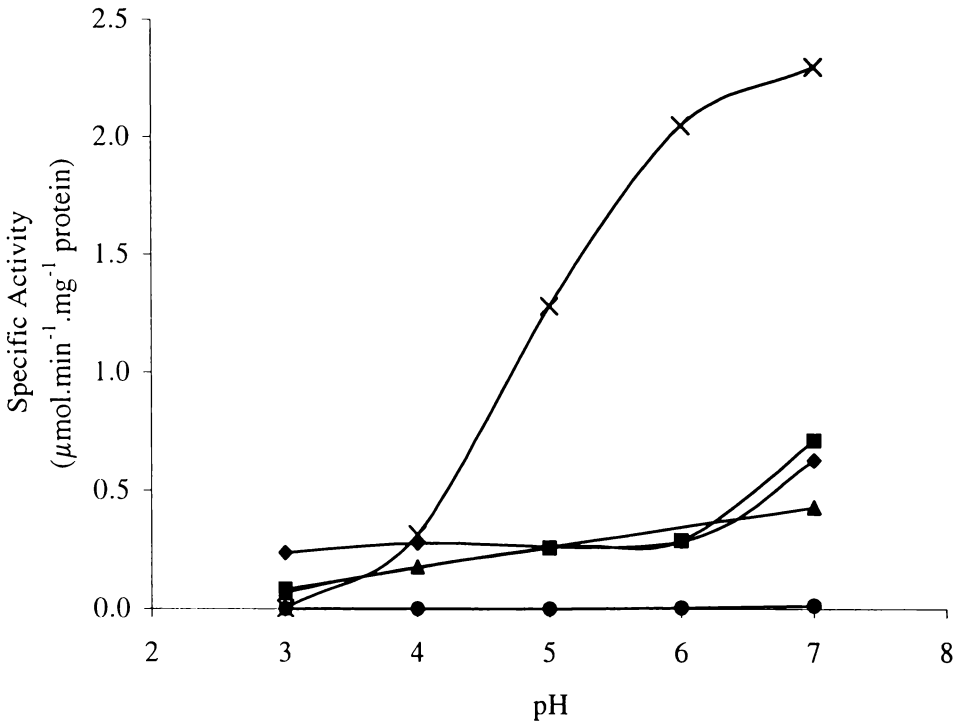

Figure 3.5. Specific activities of four Biocatalyst carboxylesterase and/or lipase mixtures against *p*NP-acetate at 30°C and various pH values between 3.0 and 7.0.

The enzyme symbols and buffers used are as for Figure 3.4.

The hydrolysis of ethyl acetate and methyl butyrate (to acetic acid and butyric acid respectively) by the semi-purified *Bacillus stearothermophilus* A^M esterase and the three Fluka carboxylesterases was followed with pH-electrode assays, as described in Section 2.2.1.5, and the change in pH with time of incubation was reported in Table 3.4.

Table 3.4. pH-electrode assays of three desalted Fluka carboxylesterases against 100 ppm ethyl acetate or methyl butyrate.

Each 3 ml assay (unbuffered) was initially poised at approximately 7.0 and carried out at 25°C. The pH obtained after 90 minutes and 24 hours is given for each ester. Final carboxylesterase concentrations ($\mu g.ml^{-1}$) per assay are as follows: *Bacillus stearothermophilus*, 12.5; *Mucor miehei*, 10.0; and *Saccharomyces cerevisiae*, 11.5.

Carboxylesterase	EtOAc		MeOBu	
	90 min	24 hr	90 min	24 hr
Bacillus stearothermophilus	6.63	-	6.50	-
Mucor miehei	6.81	6.59	6.68	6.40
Saccharomyces cerevisiae	6.62	6.38	6.48	5.96

The small pH changes over 24 hours produced by the three Fluka enzymes were a result of very low specific activities exhibited against both of the esters. At pH 7.0, the activity of the three Fluka enzymes against *p*NP-butyrate was very low compared to PLE (16 to 354 nmol.min^{-1}.mg^{-1} and 16,250 nmol.min^{-1}.mg^{-1} for the Fluka enzymes and PLE, respectively). This synthetic ester was assumed a good model substrate for the ester MeOBu (while *p*NP-acetate has been used as a model substrate for EtOAc) and the low activities are reproduced in Table 3.5 (although the buffer pH values are between 3.5 and 4.5).

Table 3.5. Specific activity of microbial-derived Fluka carboxylesterases against ethyl acetate and methyl butyrate at 30°C and various pH values between 3.5 and 4.5.

Activity against 300 ppm (v/v) EtOAc and MeOBu in 100 mM citric acid-trisodium citrate buffer, given as nmol.min^{-1}.mg^{-1} protein, was followed for 1.5 hours.

Carboxylesterase Source[1]	Ester	pH		
		3.5	4.0	4.5
Bacillus stearothermophilus	EtOAc	3.64	8.46	14.8
Mucor miehei	EtOAc	0	0	69.7
Bacillus stearothermophilus	MeOBu	0	14.3	14.9
Mucor miehei	MeOBu	9.20	19.0	6.90

[1] *Saccharomyces cerevisiae* carboxylesterase activity against both esters was not detected within the assay time period.

Of the various enzymes tested for activity in Tables 3.2 and 3.3, *Candida rugosa* Lipase B exhibited the best pH-activity profile, when compared to PLE. Therefore, the activity and stability of *C. rugosa* Lipase B were extensively investigated and compared with the data obtained from identical studies of PLE.

3.3 Properties of Pig Liver Esterase

With respect to the biosensor, the important physical and kinetic properties of PLE, and therefore the replacement enzyme, were (1) the pH optima and K_m constants of the hydrolytic reactions using EtOAc, MeOBu and EtOBu (or model esters, such as *p*NP-acetate and *p*NP-butyrate) as substrates; and (2) the thermal- and pH-stability of the enzyme.

3.3.1 Fatty Acid Specificity

The fatty acid specificity (or acyl-chain selectivity) of PLE was briefly tested against *p*NP-ester acyl-chain lengths between 2 and 6 carbon atoms. PLE activity increased with increasing acyl-chain length.

3.3.2 pH Optima

The activity of crude PLE, as a function of pH, towards EtOAc, MeOBu and EtOBu was determined using the method described in Section 2.2.1.3.2. The pH optima (and maximal activity) for EtOAc, MeOBu and EtOBu are pH 7.0 (5.20 μmol.min^{-1}.mg^{-1} protein), ≥ pH 7.5 (20.50 μmol.min^{-1}.mg^{-1} protein), and 7.5 (16.97 μmol.min^{-1}.mg^{-1} protein), respectively, as shown in Figures 3.6 to 3.8.

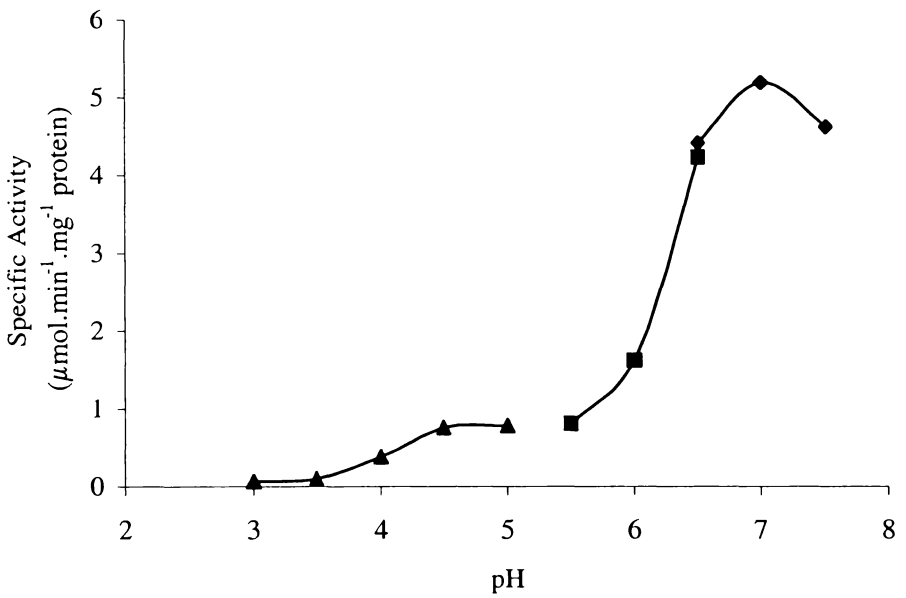

Figure 3.6. pH-activity profile of crude PLE against 300 ppm ethyl acetate between pH 3.0 and 7.5 at 30°C.

The following buffers were used: 50 mM Mops-NaOH buffer (pH 6.5-7.5), ◆; 50 mM Mes-NaOH buffer (pH 5.5-6.5), ■; 100 mM citric acid-trisodium citrate buffer (pH 3.0-5.0), ▲. Ester hydrolysis was analysed using a Pye Unicam GCD Chromatograph.

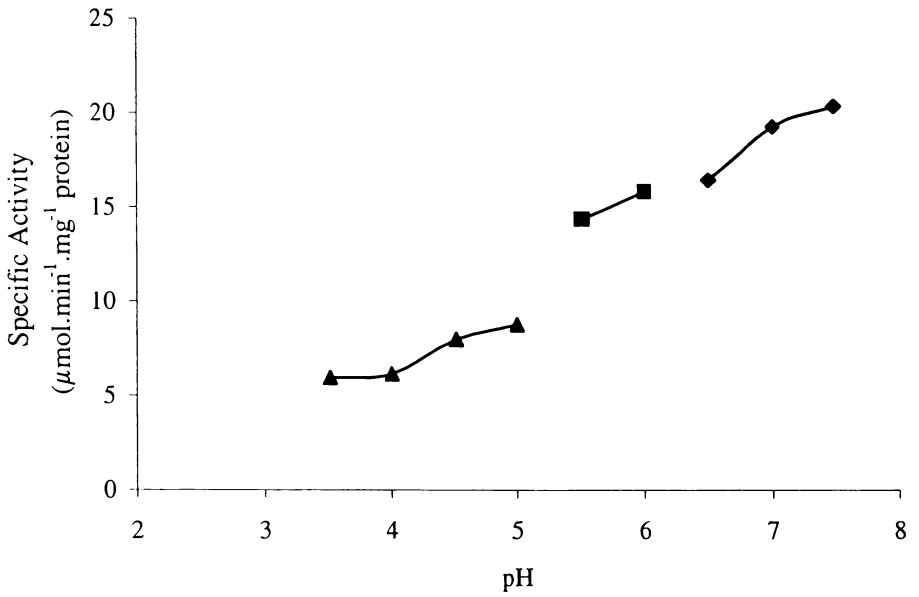

Figure 3.7. pH-activity profile of crude PLE against 300 ppm methyl butyrate between pH 3.5 and 7.5 using various buffers at 30°C.

The buffer symbols are as for Figure 3.6. Ester hydrolysis was analysed using a Pye Unicam GCD Chromatograph.

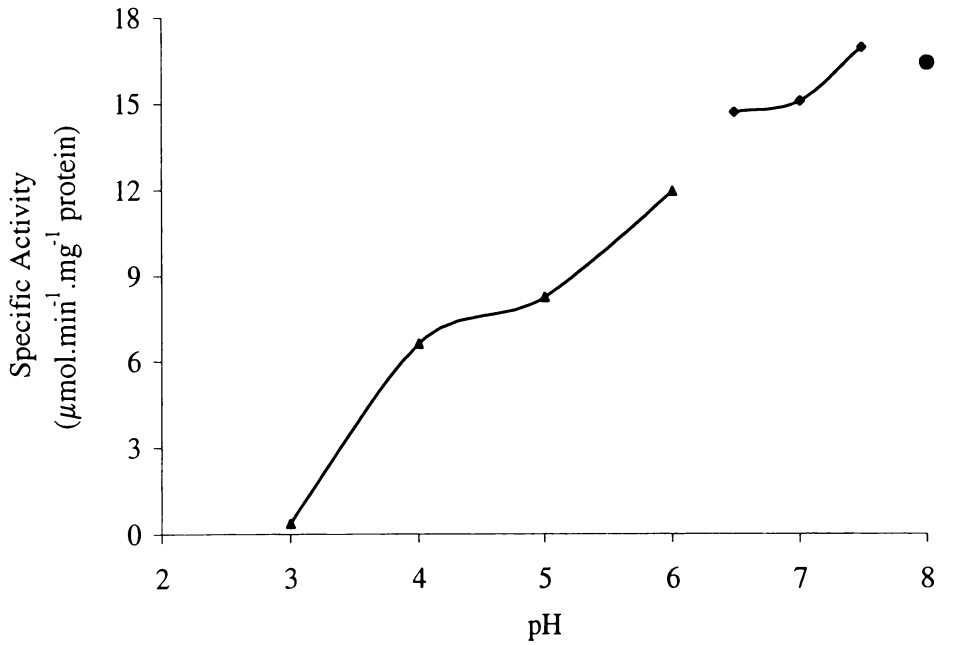

Figure 3.8. pH-activity profile of crude PLE against 300 ppm ethyl butyrate between pH 3.0 and 8.0 using various buffers at 30°C.

The buffer symbols are as for Figure 3.6 and includes 50 mM Tris-HCl, pH 8.0, ●. Ester hydrolysis was analysed using a Pye Unicam GCD Chromatograph

The specific activities of crude PLE towards each synthetic and natural ester at acid pH (≤ 5.0) are listed in Table 3.6 (and specific activities at pH 7.0 are reported for comparison).

Table 3.6. Crude PLE specific activity at acidic pH and 30°C, against three natural esters (ethyl acetate, methyl butyrate and ethyl butyrate) and the synthetic *p*NP-acetate and *p*NP-butyrate esters.

Specific activity is defined as $\mu mol.min^{-1}.mg^{-1}$ protein and determined by the method described in Section 2.2.1.3. PLE specific activity at pH 7.0 is listed for comparison.

pH	EtOAc	*p*NP-acetate	MeOBu	*p*NP-butyrate	EtOBu
7.0	5.201	2.315	19.41	16.25	15.09
5.0	0.784	1.286	8.813	1.980	8.250
4.5	0.754	0.683	8.024	0.933	7.450
4.0	0.378	0.314	6.157	0.330	6.620
3.5	0.099	0.077	5.971	0.096	3.130

The use of *p*NP-acetate as a substrate model for EtOAc is confirmed by the similar PLE pH-profiles for both substrates, but will need to be substantiated by comparing the PLE kinetic constants for EtOAc and *p*NP-acetate. Nonetheless, *p*NP-butyrate is not an ideal model substrate for either MeOBu or EtOBu since PLE specific activity towards *p*NP-butyrate is significantly lower than that against both natural esters.

3.3.3 Enzyme Kinetics

Table 3.7 reports the kinetic parameters of crude PLE for the hydrolysis of natural- and *p*NP-esters with acyl chain lengths of two and four, as determined by Direct Linear Plot transformation of the activity and substrate concentration data.

For all five substrates, the relationship between activity and substrate concentration followed that of Michaelis-Menten kinetics, whereby a hyperbolic dependence was achieved (see the Michaelis-Menten graph inset in each Hanes Plots in Figures A3.1-A3.5 of Appendix Three). The kinetic constants provide important information with respect to the sensitivity to esters of the biosensor *in situ*. The data reported in Table 3.7 shows that although crude PLE has approximately eight and four times lower activity against EtOAc than MeOBu and EtOBu, respectively, the ester concentration required to achieve that activity is

only four and six times lower (a K_m of 72 ppm for EtOAc compared to 186 and 243 ppm for MeOBu and EtOBu, respectively).

Table 3.7. Kinetic parameters of crude PLE activity at pH 7.5 and 30°C towards EtOAc, MeOBu and EtOBu, plus their respective *p*NP-esters in solution.

PLE specific activity was determined in 50 mM Mops-NaOH with maximum substrate concentrations of 5.0 mM (but 10 mM for *p*NP-acetate). Specific activity data was analysed with Direct Linear Plots.

Parameter	EtOAc	*p*NP-acetate	MeOBu	*p*NP-butyrate	EtOBu
V_{max} (μmol.min^{-1}.mg^{-1})	8.56	31.46	61.3	26.1	36.6
K_m (mM)	0.74	0.27	1.56	0.069	1.75
[ppm, v/v]	[71.8]		[186]		[243]
Specificity (V_{max}/K_m)	11.6	117	39.3	378	20.9

3.3.4 pH-temperature Stability

Guidelines for the short- and possibly long-term storage of the biosensor merited investigation since the biosensor will be stored prior to use for a time period as yet unknown, and the time required for an appropriate colour change to occur *in situ* will vary depending upon the application. The information required would be the thermal- and pH-stability of the microbial carboxylesterase or lipase that replaced PLE in the biosensor. The thermal- and pH-stability data for crude PLE is reported in Table 3.8.

Table 3.8. Thermal- and pH-stability of crude PLE.

Data for each temperature/pH variable is given as percentage remaining activity after seven days incubation, unless otherwise stated. Remaining activity was determined against 300 ppm EtOAc at pH_{30} 7.0 and 30°C,

pH	Temperature (°C)			
	0.0	5.0	30	40
4.0	67	60	0[3]	0[1]
4.5[4]	100	100	40	0[2]
5.0[4]	100	100	100	55
5.5	100	100	100	82
7.0	100	100	100	91

[1] no activity remaining after 24 hours; [2] no activity remaining after three days; [3] no activity remaining after seven days; [4] remaining activity data, except at 40°C, of the pH 4.5 and 5.0 experiments were determined after nine days incubation at 0, 5 and 30°C.

The data consists of remaining activity against 300 ppm EtOAc after seven days incubation at four temperatures (0, 5, 30 and 40°C) and three pH values (pH 4.0, 5.5 and 7.0). Remaining activity was measured on day one, two, three and seven. The PLE stability data indicates that both neutral pH and low temperatures must be employed for long-term biosensor storage. At each pH the remaining activity after seven days was highest at 0°C (closely followed by 5°C). This was particularly evident when comparing the pH 4.0 data at each of the four temperatures (Figure 3.9) where all activity was lost at 30°C and 40°C. Accordingly, the appropriate storage condition would combine a pH between 5.5 and 7.0 with refrigeration (or possibly freezing).

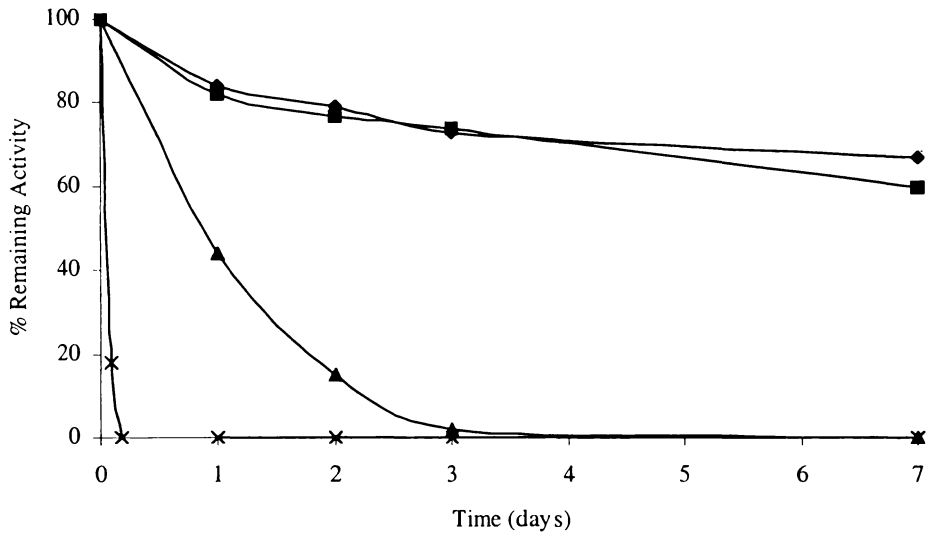

Figure 3.9. Thermal stability of crude PLE at pH 4.0 was followed over seven days between 0 and 40°C.

The temperatures are symbolised as follows: 0°C, ◆; 5°C, ■; 30°C, ▲; and 40°C, ×. Remaining activity (%) was measured against 300 ppm ethyl acetate at pH 7.0 and 30°C.

3.4 PROPERTIES OF *CANDIDA RUGOSA* LIPASE B

3.4.1 Fatty Acid Specificity

The fatty acid specificity (or acyl-chain selectivity) of semi-purified *Candida rugosa* Lipase B (LipB) is presented in Figure 3.10, whereby the acyl-chain length of *p*NP-esters was increased from 2 to 18 carbon atoms. LipB exhibits an activity trend expected for a lipase (higher activity against acyl chain lengths of ≥ 10 carbon atoms), but also displays a peak of activity against *p*NP-

butyrate (an 'esterase' substrate). This peak in activity against C_4 substrates, compared to activity against C_2 substrates, is evident in the LipB activities against EtOBu (and/or MeOBu) and EtOAc, respectively (Table 3.9).

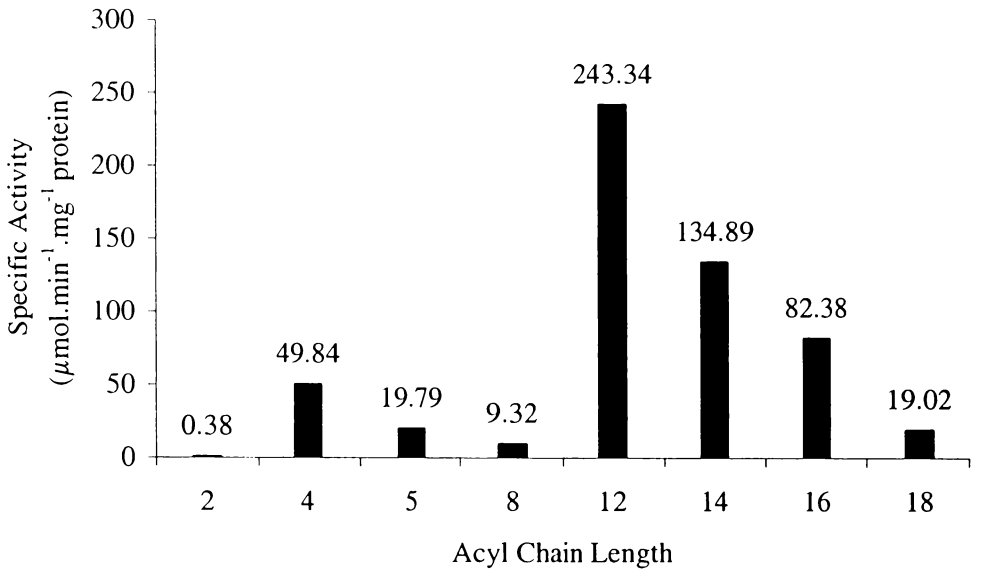

Figure 3.10. Fatty acid specificity of *Candida* LipB.

Specific activities toward varying acyl-chain length *p*-nitrophenyl esters were determined in 50 mM Mops-NaOH, pH_{30} 7.5 at 30°C with a 0.25 mM final ester concentration.

Table 3.9. Semi-purified *Candida rugosa* LipB specific activities towards three natural and two synthetic esters between pH 4.0 and 7.0 at 30°C.

Specific activities toward 300 ppm (v/v) EtOAc, MeOBu and EtOBu, plus 0.25 mM *p*NP-acetate and *p*NP-butyrate were defined as $\mu mol.min^{-1}.mg^{-1}$ protein and determined by the methods described in Section 2.2.1. Specific activity at pH 7.0 is listed for comparison.

pH	EtOAc	*p*NP-acetate	MeOBu	*p*NP-butyrate	EtOBu
7.0	0.081	0.632	3.769	45.84	1.511
6.0	0.050	0.290	2.935	38.73	2.258
5.0	0.060	0.300	2.872	52.26	1.780
4.0	0.144	0.278	2.662	41.02	0.949

3.4.2 pH Optima

The specific activity of LipB, as a function of pH, was measured against 300 ppm (v/v) EtOAc, MeOBu and EtOBu. Unlike the pH-profiles of PLE (in which a single pH optimum is determined against each substrate, see Figures 3.6-3.8), the pH-profiles of LipB show both a neutral and acidic peak in activity

(approximately pH 7.0 and 5.0, respectively) against each ester (Figure 3.11). The activity data sets of semi-purified LipB against each synthetic and natural ester, respectively, are listed in Table 3.9 for comparison.

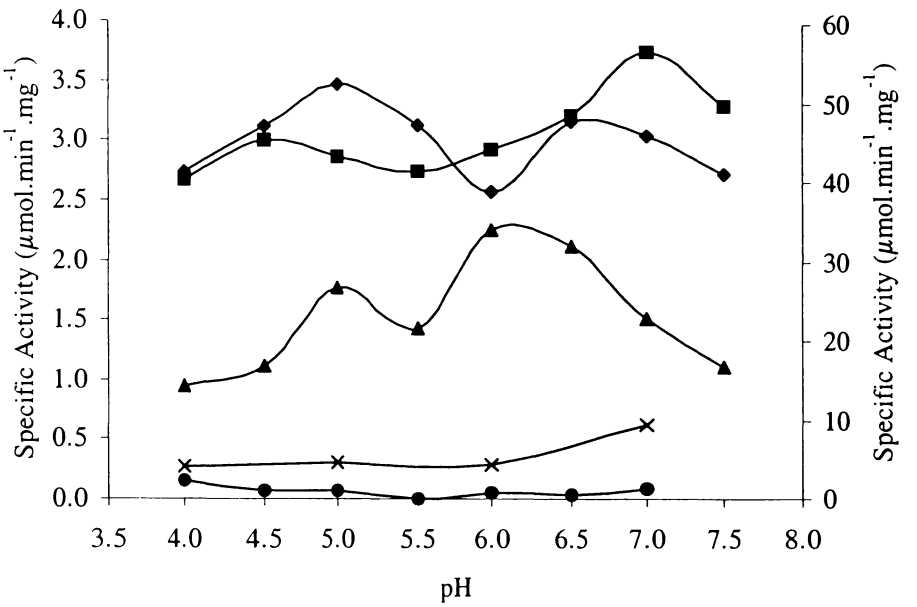

Figure 3.11. pH-activity profiles for semi-purified *Candida rugosa* LipB against three common esters and *p*NP-butyrate (plus crude LipB against *p*NP-acetate) between pH 4.0 and 7.5 at 30°C.

Specific activities toward 300 ppm (v/v) EtOAc, MeOBu and EtOBu, plus 0.25 mM *p*NP-butyrate and *p*NP-acetate were defined as $\mu mol.min^{-1}.mg^{-1}$ protein. The ester symbols and Y axes are as follows: MeOBu, ■; EtOBu, ▲; EtOAc, ●; *p*NP-acetate, × (left Y-axis); and *p*NP-butyrate, ◆ (right Y-axis). The buffers used, and their effective pH range, are 50 mM Mops-NaOH buffer (pH 6.5-7.5), 50 mM Mes-NaOH buffer (pH 5.5-6.5) and 100 mM citric acid-trisodium citrate buffer (pH 3.0-5.0). Ester hydrolysis was assessed by a Pye Unicam GCD Chromatograph as described in Section 2.2.1.

3.4.3 Enzyme Kinetics

Table 3.10 reports the kinetic parameters, as determined by Direct Linear Plot transformation of the activity and substrate concentration data, of semi-purified LipB for the hydrolysis of three esters that differ in fatty acid acyl- and alcohol moiety-chain length (in addition, the activity data is graphically represented in the Hanes Plots of Figures A3.6-A3.8 in Appendix Three). The fatty acid specificity described in Section 3.4.1 is displayed amongst the three esters, whereby the rate of hydrolysis against C_4 esters (MeOBu and EtOBu) is significantly higher than that against the C_2 ester, EtOAc.

Table 3.10. The kinetic parameters of *Candida* Lipase B activity at pH 7.5 and 30°C against 300 ppm EtOAc, MeOBu and EtOBu in solution.

Enzyme activity was determined in 50 mM Mops-NaOH, pH_{30} 7.5 with maximum substrate concentrations of ranging from15-25 mM. Activity data was analysed using Direct Linear Plots.

Parameter	EtOAc	MeOBu	EtOBu
V_{max} (μmol.min^{-1}.mg^{-1})	0.55	36.1	5.00
K_m (mM)	11.6[1]	13.3	4.50
[ppm, v/v]	[1133]	[1513]	[595]
Specificity (V_{max}/K_m)	0.047	2.71	1.11

[1] this is not as accurate as the MeOBu and EtOBu K_m values because the maximal concentration of 15 mM EtOAc is not greater than 5*K_m .

3.4.4 pH-Temperature Stability

The temperature and pH stabilities of the semi-purified LipB were investigated over a period of two weeks. LipB was exposed to a combination of four temperatures (0, 5, 30 and 40°C) and three pH values (4.0, 5.5 and 7.0), with an additional temperature (20°C) at pH 7.0 (Table 3.11).

Table 3.11. Thermal and pH-stability of semi-purified *Candida* Lipase B over two weeks

Remaining activities (%) against 0.25 mM *p*NP-butyrate, determined in 50 mM Mops-NaOH, pH_{30} 4.0-7.0 at 30°C, are given in the table.

pH	Temperature	Time of Temperature Exposure (hr and [days])							
	(°C)	0 hr	2hr	1days	2 days	3 days	7 days	10 days	14 days
7.0	40	100	91.0	67.1	25.8	11.2	4.4	1.3	0.9
	30	100	89.2	73.0	49.2	37.7	29.3	27.3	24.6
	20	100	98.0	95.4	89.2	85.6	79.3	70.3	44.9
	5	100	96.7	98.2	96.7	92.4	89.3	82.0	76.4
	0	100	94.3	96.5	90.8	88.5	85.7	81.0	68.7
5.5	40	100	87.3	82.4	79.3	58.6	42.9	33.7	20.7
	30	100	89.5	79.5	69.6	66.4	58.4	53.5	46.9
	5	100	94.5	94.0	92.4	85.1	82.2	69.7	51.4
	0	100	94.0	94.0	90.0	85.0	80.0	78.8	62.9
4.0	40	100	81.0	71.7	49.0	1.4	0.9	0.7	0.1
	30	100	80.0	60.1	36.9	24.1	4.5	3.1	4.0
	5	100	88.3	77.2	65.8	53.0	45.5	39.2	27.4
	0	100	88.1	66.0	58.8	45.2	34.5	27.4	22.8

The LipB stability data describes an enzyme that has greater pH and temperature tolerance than PLE (particularly at pH 5.5 and greater than 30°C). Overall, LipB-impregnated biosensors should be stored between pH 5.5 and 7.0 in

a refrigerated environment, and during use may be expected to retain at least 50% activity for at least two weeks. Of interest, LipB has higher stability at 5°C than 0°C at pH 7.0 and 4.0 (but no at pH 5.5). This may be due to experimental error, but the result was consistent across the entire two week period, the data was derived from different samples at each time point and all assays were performed in triplicate.

3.5 COMPARISON OF THE PROPERTIES OF PIG LIVER ESTERASE AND *CANDIDA RUGOSA* LIPASE B

To enable PLE and LipB activites, stabilities and kinetics to be directly compared, the data from Sections 3.3 and 3.4 have been summarised in Table 3.12.

Table 3.12. Comparison of PLE and LipB properties relevant to the biosensor application.

Parameter	Ester	PLE	LipB
pH_{opt}[1]	All esters	~7.5	5.0-7.0
	EtOAc	5.2	0.1
pH_{opt} Specific Activity[2]	MeOBu	20.5	3.8
(μmol.min^{-1}.mg^{-1})	EtOBu	17.0	2.3[5]
	EtOAc	8.6	0.6
V_{max} (μmol.min^{-1}.mg^{-1})[2,3]	MeOBu	61.3	36.1
	EtOBu	36.6	5.0
	EtOAc	0.7	11.6
K_m (mM)[2]	MeOBu	1.6	13.3
	EtOBu	1.8	4.5
	EtOAc	8.6	0.05
Specificity (V_{max}/K_m)	MeOBu	40.3	2.7
	EtOBu	21.3	1.1
Storage pH[4]	na	7.0	5.5
Storage Temperature (°C)[4]	na	0-5	0-5

[1] the pH optima for the three esters (EtOAc, MeOBu and EtOBu); [2] specific activities were determined at 30°C; [3] V_{max} values were determined at pH 7.5; [4] the pH and temperature at which the biosensor should be stored; [5] the V_{max} value for LipB against EtOAc would double if the determination was carried out at pH_{opt}; 'na', not applicable.

3.6 Partial Purification of PLE, *Candida rugosa* Lipase B and *Ophiostoma pluriannulatum* 5040 Esterase

Fast Flow Q Sepharose (FFQ-S) and a NaCl concentration gradient (to elute each enzyme from the column) were used to partially purify PLE, *Candida* LipB and *Ophiostoma pluriannulatum* 5040 esterase. The purification data for PLE, LipB and *Ophiostoma* 5040 esterase are reported in Table 3.13, and the FFQ-S profiles of each enzyme are displayed in Figures 3.12, 3.13 and 3.14, respectively.

Table 3.13. Partial purification of PLE, LipB and *Ophiostoma* 5040 esterase by FFQ-S.

Protein	Total (Units)	Total Protein[1] (mg)	Specific Activity[2] (μmol.min^{-1}.mg^{-1})	Yield (%)	Purification (Fold)
Crude PLE	10162	420	24.2	100	1
FFQS treated PLE[3]	4355	50	87.1	43	3.6
Crude LipB	56000	1300	43.2	100	1
FFQS treated LipB[3]	38806	191	203.7	69	4.7
Ophiostoma 5040[4]	1259	170	7.3	100	1
FFQS treated 5040	1184	20	73	94	10

[1] the FFQ treated protein samples were desalted and lyophilised before weighing; [2] activity was determined against 0.25 mM *p*NP-butyrate in 50 mM Mops-NaOH, pH_{30} 7.5 at 30°C; [3] ~80% pure; [4] the cell free supernatant of a five day old culture (see Figure 3.1 for the growth and activity profiles of *O. pluriannulatum* 5040).

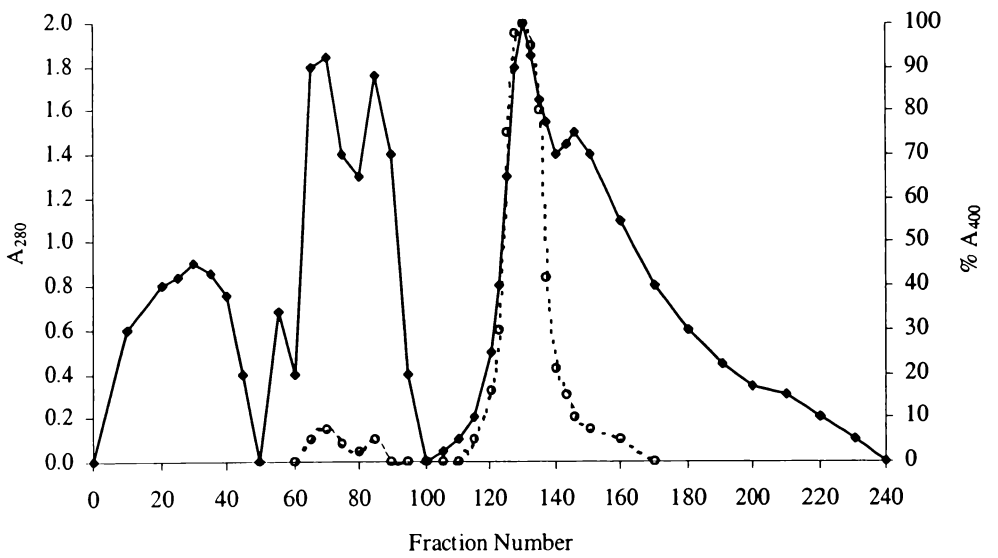

Figure 3.12. Fast Flow Q Sepharose elution profile of *Candida rugosa* LipB.

The fractions are as follow: 1-50, enzyme addition in 30 mM Mops-NaOH, pH 6.5; 51-100, 30 mM Mops-NaOH, pH 6.5 + 0.1 M NaCl; 101-220, 30 mM Mops-NaOH, pH 6.5 + 0.1-0.75 M NaCl gradient. Protein (◆) and activity against *p*NP-butyrate (--O--) were spectrophotometrically detected at 280 and 400 nm, respectively and 100% A_{400} = 1.1 using 1/100 diluted LipB.

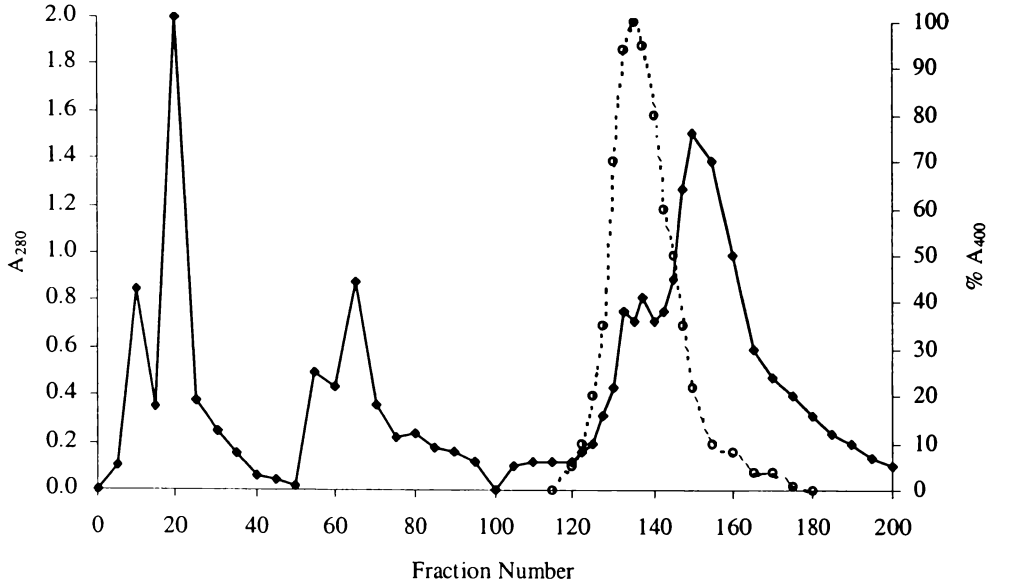

Figure 3.13. Fast Flow Q Sepharose elution profile of PLE.

The fractions are as follow: 1-50, enzyme addition in 30 mM Mops-NaOH, pH 7.0; 51-100, 30 mM Mops-NaOH, pH 7.0 + 0.1 M NaCl; 101-160, 30 mM Mops-NaOH, pH 7.0 + 0.1-0.5 M NaCl gradient; 161-200, 30 mM Mops-NaOH, pH 7.0 + 0.5 M NaCl. Protein (◆) and activity (--O--) were detected as in Figure 3.12 and 100% A_{400} = 1.0 using 1/100 diluted PLE.

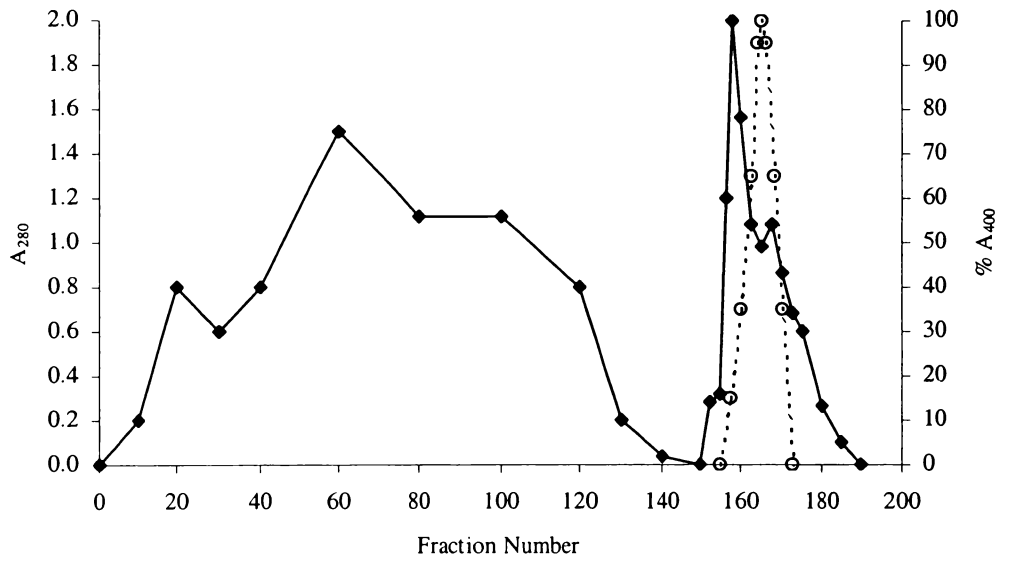

Figure 3.14. Fast Flow Q Sepharose elution profile of *Ophiostoma pluriannulatum* 5040 esterase.

The fractions are as follow: 1-100, cell-free supernatant addition in 50 mM Mops-NaOH, pH 7.0; 100-150, 50 mM Mops-NaOH, pH 7.0 wash; 150-190, 50 mM Mops-NaOH, pH 7.0 + 0-0.25 M NaCl gradient. Protein (◆) and activity (--O--) were detected as in Figure 3.12 and 100% A_{400} = 0.7 using 1/10 diluted *Ophiostoma* 5040 esterase.

3.7 CONCLUSIONS

The original aims of this enzyme screening study were to seek carboxylesterases or lipases from various non-mammalian sources and to identify those with the following properties, in comparison with the PLE benchmark: (1) adequate activity in the pH range 4.0-5.0; (2) specific activity against MeOBu greater than that of PLE; (3) a K_m against MeOBu less than that of PLE; and (4) sufficient stability to retain ≥ 50 % activity after 14 days at 40°C.

Comparison of functional pH ranges of the various esterases revealed *Candida rugosa* Lipase B to be amongst the least inhibited enzymes when pH fell to between 4 and 5. *C. rugosa* Lipase B also exhibited the highest specific activities towards *p*NP-acetate and butyrate, hydrolysed all three common esters (EtOAc, MeOBu and EtOBu) and did not show protease activity against azocasein. So, although *C. rugosa* Lipase B is commercially sold as a lipase, it exhibits the esterase activity required for the biosensor application. Furthermore, *C. rugosa* Lipase B was commercially available in large quantities, had GRAS status (generally regarded as safe) and was Kosher certified. For these reasons *C. rugosa* Lipase B was judged to be the best suited to the ester biosensor application, and so was partially purified and further characterised. However, *C. rugosa* Lipase B does not meet the stability requirement (i.e., ≥ 50 % retained activity after 14 days at 40°C).

Investigation of the effects of acyl chain length of the ester substrates on *C. rugosa* Lipase B activity revealed two peaks of preferential activity across the range $C_2 - C_{18}$. The first of these peaks, at C_4, indicative of true carboxylesterase activity, was more marked than that of pig liver esterase. Also, the specificity of Lipase B (V_{max}/K_m) for ethyl acetate was 58 and 23 times lower than that for methyl butyrate and ethyl butyrate, respectively (compared to 4.7 and 2.5 times lower, respectively for pig liver esterase). The second, larger peak in the substrate size preference profile, for a C_{12} acyl chain length, indicated a predominance of lipase activity.

Concurrent analysis of thermal- and pH-stability showed Lipase B to be stable below 40°C and between pH 5.5 and 7.0, with optimal stability at pH 5.5. In these respects, it is superior to pig liver esterase, which is highly susceptible to denaturation by storage above 30°C or below pH 5.0.

CHAPTER 4 BIOSENSOR DEVELOPMENT

4.1 INTRODUCTION

The biosensor under development here detects esters by means of indicating the fall in pH resulting from the carboxylesterase or lipase hydrolysing esters into alcohol and acid reaction products. The purpose of the work described here was to investigate the effects on the esterases of various additives, and of operating and storage conditions likely to be encountered in a commercial biosensor application. Various pH indicator dyes, preservatives, humectants and support matrices were screened to identify those most appropriate for potential biosensor applications. In some situations, such as in the presence of high levels of carbon dioxide, there is likely to be benefit from using a pH indicator which changes colour below the pH which can be attributed simply to the dissolution of CO_2 (i.e., below pH 5.5). Chemical inhibition of esterase was also tested as a means of producing inactive controls, useful in producing stable starting colour standards in experiments involving pH indicator colour changes.

Twenty-four microbial enzymes were screened for activity against the esters targeted by our commercial partners (namely, ethyl acetate, methyl butyrate and ethyl butyrate) in Chapter 3. Subsequently, four enzymes (*Candida rugosa* LipB, *Bacillus stearothermophilus* A^M esterase, *Penicillium* esterase and *Ophiostoma pluriannulatum* 5040 esterase) were selected for further investigation, and their practicability in the biosensor was determined.

The quantity of enzyme used per biosensor was investigated to optimise sensitivity. The amount of enzyme required depends on both the stability and activity of the enzyme. Enzyme stability can be affected by many factors, including protein hydration, pH and temperature. Partial loss of enzyme activity (which would lead to low sensitivity) might be overcome with increased enzyme loading. However, increased protein levels within the ideally unbuffered biosensor could introduce a significant buffer capacity, thereby lowering biosensor sensitivity.

Screening studies of pH-dye indicators and matrices were carried out using the pH-electrode assay (described in Section 2.2.1.5) and the pH indicator strip assay (described in Section 4.2.1.1), both of which are functional assays relevant

to the proposed biosensor environment in which the pH decreases due to release of the acid product with continual ester hydrolysis. However, while the pH-electrode assay permits direct investigation of the effect enzyme activity on pH change in solution, the pH indicator strip assay also permits investigation of the effects of pH indicator dye composition and protein hydration on enzyme activity. Although *C. rugosa* LipB was selected as the alternate to PLE in Chapter 3, PLE will be used to develop assays used for screening of support matrices and pH indicator dyes as the work in Chapter 3 and 4 was not performed in chronological order.

4.2 Materials and Methods

4.2.1 Biosensor Development

Preliminary adsorption experiments were carried out to study the quantitative effects of enzymes, RH's, matrices and pH-dye indicators on the sensitivity of a model biosensor. This model was created to experimentally duplicate the biosensor under development for use on melons and pears.

4.2.1.1 pH Indicator Strip Assay

pH-indicator strips (pH 4.0-7.0 and 5.2-7.2, Merck) were used to screen carboxylesterases and lipases for activity against the esters of interest. Treated strips were placed in sealed Hungate tubes (10 ml volume) above, but not in contact with, 500 μl of ester solutions [0, 25, 50, 100 and 500 ppm (v/v) prepared in Milli-Q water]. Each strip was loaded with 20 μl of esterase solution and 0.02% sodium azide (w/v). In addition, the esterase solution contained 20 mM NaCl (when used as a positive control) or 20 mM NaF (20 mM NaF inhibits PLE 100% and was used in negative controls). Colour changes were followed for 24 hours.

4.2.1.2 Matrix, RH and pH-dye Indicator Selection

Initially a variety of matrix materials and pH-dye indicators were screened (Table 4.1) using crude PLE as a positive control. Each matrix, excluding the pH-indicator strips, was fashioned into a 3 cm x 1 cm rectangle, washed in Milli-Q

water and air-dried before the application of the PLE-pH-dye indicator preparation. First, a mixture prepared in Milli-Q water containing 40 mM NaCl (or 40 mM NaF – a PLE inhibitor) with 0.04% Phenol Red, 0.04% Bromothymol Blue or 0.10% Alizarin RedS was poised at pH values above the pH-indicator colour change. These pH values were set at pH 8.0, 7.5 and 6.0 for Phenol Red, Bromothymol Blue and Alizarin RedS, respectively.

Table 4.1. Five matrices and three pH-dye indicators screened for use in the biosensor.

Matrix	pH-dye Indicator[1] (0.02%, w/v)[2]
Spectra/Por ® Membrane Dialysis Tubing	Alizarin RedS[3]
Whatman Paper Number 1	Bromothymol Blue
Whatman Glass Fibre Paper	Phenol Red
Polyester Material	
Merck pH Indicator Strip, pH 4.0-7.0	

[1]stock prepared in Milli-Q water; [2] final concentration unless specified otherwise; [3] 0.05% (w/v) Alizarin RedS

Second, an equal volume of a 2 $mg.ml^{-1}$ PLE (in Milli-Q water) was added to produce a final salt, pH-indicator and PLE concentration of 20 mM, 0.02% (w/v) and 1 $mg.ml^{-1}$, respectively. Of this final mixture, 100 µl was applied to each 3 cm x 1 cm rectangle. The Merck pH-indicator strips were loaded with 20 µl of an identical preparation, except the pH-dye indicator was omitted and the preparation was poised at pH 7.0.

Each rectangle was air dried at room temperature for 2 hours before placement into three pre-equilibrated atmospheres of 0, 31.0 and 100% RH (using P_2O_5, $CaCl_2.6H_2O$ and Milli-Q water, respectively). The rectangles were equilibrated at each RH for 48 hours at 20°C. The reaction was initiated by the addition of MeOBu through a septum using a microliter syringe. The initial system trial used a vapor-phase concentration of 10,000 ppm MeOBu (v/v) [i.e., 10 µl into a headspace volume of 1 ml]. Colour changes in the pH-dye indicators were followed for 2 days. Appropriate controls, including the inhibited enzyme control, were also run in parallel with each experiment. The initial trial confirmed the use of Whatman Paper No. 1 and Merck pH-indicator strips, plus Phenol Red

and Bromothymol Blue, as practicable biosensor materials and pH-dye indicators, respectively.

4.2.1.3 Enzyme Selection

Initial screening of vapor-phase activity used Merck pH-dye indicator strips (non-bleeding, pH 4.0-7.0). The protein hydration work described in Section 2.2.8 was expanded to include the effect of protein water content on Merck pH-dye indicator strip colour changes (achieved via vapor-phase hydrolysis of esters). The four enzymes used were *Penicillium roqueforti* esterase (BioCatalyst, L338P), *Candida cylindracea* LipaseB (Biocatalyst, L034P), *Ophiostoma pluriannulatum* 5040 esterase and PLE (Sigma, E3019). The *Penicillium* and pig liver esterases were crude preparations while the *Candida* and *Ophiostoma* enzymes contained minimal buffers and salts.

Each strip, pre-washed with Milli-Q water and dried at room temperature, was treated with 50 μl of enzyme prepared in 0.02% sodium azide (w/v) plus 5 mM $CaCl_2$ and poised at pH 7.0 with dilute NaOH. Those designated E+ were equilibrated at RH's between 0 and 95% for three days before the addition of ethyl butyrate to give an atmospheric concentration of 150 ppm (v/v). The change in indicator colour was recorded after 30 minutes, 2 hours and 24 hours. Controls without enzyme, designated E-, were treated analogously.

4.3 pH-Dye Indicator Screen

The original biosensor (agarose matrix with PLE and Phenol Red) used by our commercial partners was poised between pH 7.0 and 8.0 because: (1) the pH optima of PLE for the esters of interest ranged between pH 7.0 and 8.0; and (2) the original pH indicator dye, Phenol Red, incorporated into the agarose matrix underwent a series of colour changes, from violet to yellow, between pH 8.4 and 6.8. These biosensors were susceptible to CO_2 accumulation and thus, false positives (where the pH of sensors with no enzyme that were poised at neutral pH would fall as low as pH 5.5). To eliminate false positives, Phenol Red could be replaced by a pH-dye indicator that had a final colour change below pH 5.5 (the lower pH limit of the CO_2 effect). The four pH-dye indicators considered are compared to Phenol Red in Table 4.2, where the alkaline and acidic pH values at

which the final colour changes occur are reported. The colours of Bromothymol Blue, Phenol Red and Alizarin RedS at various pH values are displayed in Figure 4.1. Nevertheless, the indicator colours and effective pH range were not the only factors considered – indicator toxicity was important with regards to the commercial application of the biosensor. For example, while Phenol Red (phenolsulfonphthalein) is used in medicine as a diagnostic aid in human renal function determination, the i.v. LD_{50} of Congo Red in rats is 190 $mg.kg^{-1}$ (Windholz, 1976).

Table 4.2. Possible pH-dye indicators for the agarose and paper-based biosensors.

pH-dye Indicator[1]	Base		Acid	
	Colour	pH	Colour	pH
Phenol Red	Violet	8.4	Yellow	6.8
Bromothymol Blue	Blue	7.6	Yellow	6.0
Alizarin RedS[2]	Red	6.0	Yellow	4.6
Congo Red	Red/Orange	5.0	Violet	3.0
Bromophenol Blue	Purple	4.6	Yellow	3.0

[1] Data from Dawson *et al.* (1986); [2] Weast and Astle, 1982.

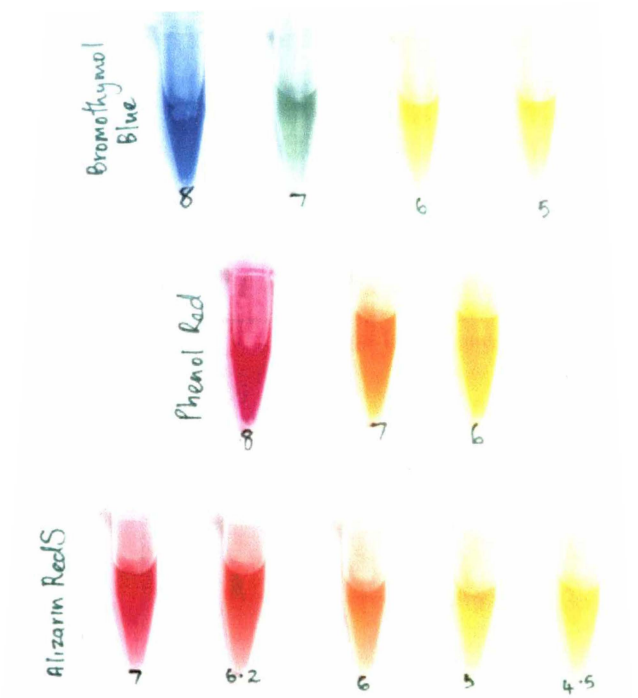

Figure 4.1. The pH-dependent colour changes of three pH-dye indicators - Bromothymol Blue, Phenol Red and Alizarin RedS.

However, the overall pH change associated with ester hydrolysis (determined by the colour change in the Phenol Red indicator) had not been directly correlated to the specific activity of PLE (since specific activity was determined in a buffered solution and the label pH was unbuffered). Thus, an understanding of the effect of continual pH decreases on the activity of PLE was required. This was particularly important if the replacement indicator required the biosensor to be poised at acidic pH values since both enzyme activity and stability would be affected. To illustrate, biosensors with Congo Red would need an initial pH ≤ 5.5 (although the biosensor could be poised at a higher pH value, the effects of PLE action on esters would only be observable once the pH fell below 5, resulting in a long lag period with no apparent action, and a higher starting pH would make the agarose label susceptible to false positives). Therefore, EtOAc hydrolysis was followed by measuring the decrease in pH (due to release of acetic acid) with a micro-pH combination electrode, as described in Section 2.2.1.5 in a sealed non-buffered assay poised at pH 7.1 (and pH 4.5 for comparison).

The 24-hour pH results of the neutrally poised PLE pH-electrode study (Table 4.3), particularly those at low PLE and/or EtOAc concentrations, were used to establish which pH-dye indicator(s) was appropriate to replace Phenol Red in future agarose biosensors.

Table 4.3. pH-electrode assays of PLE (0.1-12.5 U.ml^{-1}) and EtOAc (20-2500 ppm) initially at pH 7.1.

Each 3 ml assay (unbuffered) was poised at pH 7.1 and carried out at 25°C. The pH obtained after two and 24 hours are given for each PLE and EtOAc concentration.

[PLE]		EtOAc Concentration (ppm)							
(U.ml^{-1})[1,2]	(µg.ml^{-1})	20		100		500		2500	
		2 hr	*24 hr*	2 hr	*24 hr*	2 hr	*24 hr*	2 hr	*24 hr*
0[3]	0[3]	6.9	*6.8*	6.9	*6.9*	7.0	*6.8*	6.9	*6.7*
0.10	2.50	nd	*nd*	4.7	*4.5*	4.3	*4.0*	4.3	*3.9*
0.17	4.25	5.4	*5.0*	4.6	*4.5*	4.3	*4.0*	nd	*nd*
0.50 (n=2)	12.5	nd	*nd*	4.2	*4.1*	3.9	*3.7*	nd	*nd*
2.50	62.5	nd	*nd*	4.1	*4.1*[4]	nd	*nd*	nd	*nd*
12.5 (n=2)	313	nd	*nd*	4.1[4]	*4.1*[4]	3.8[4]	*3.8*[4]	3.3	*3.2*

[1] crude PLE (40 U.mg^{-1} protein with respect to *p*NP-butyrate); [2] a crude PLE concentration of 1.8 U.ml^{-1} (0.07 U total) was applied to each agarose-based biosensor; [3] control assays which followed non-enzymic hydrolysis of EtOAc; [4] 100% ester hydrolysis; nd, not done.

The 24-hour pH value of 4.5 achieved with 0.10 $U.ml^{-1}$ PLE and 100 ppm EtOAc indicated that Alizarin RedS (and to a lesser degree, Congo Red) would be a suitable alternative to Phenol Red (while the final colour change of Alizarin RedS, at pH 4.6, was achieved by the assay described, higher PLE loading and ester concentrations would be required to achieve the final colour change of Congo Red at pH 3.0).

The efficacy with which PLE poised at pH 4.5 hydrolysed EtOAc was investigated with a pH-electrode study (Table 4.4) that incorporated the acidic starting pH of 4.5 with low EtOAc concentrations (20 to 100 ppm, v/v). The 24-hour results at each EtOAc concentration reveal that much higher PLE concentrations are required for appropriate pH changes (at 100 ppm EtOAc, for example, 0.5 $U.ml^{-1}$ and 2.5 $U.ml^{-1}$ PLE produce corresponding pH values in the pH 7.1 and pH 4.5 pH-electrode studies).

Table 4.4. pH-electrode assays of PLE (0.1-12.5 $U.ml^{-1}$) and EtOAc (20-100 ppm) initially at pH 4.5.

Each 3 ml assay (unbuffered) was poised at pH 4.5 and carried out at 25°C. The pH obtained after two and 24 hours are given for each PLE and EtOAc concentration.

[PLE]		EtOAc Concentration (ppm)					
$(U.ml^{-1})^{1,2}$	$(\mu g.ml^{-1})$	20		50		100	
		2 hr	*24 hr*	2 hr	*24 hr*	2 hr	*24 hr*
0[3]	0	4.8	*5.1*	4.6	*4.9*	4.6	*4.9*
0.10	2.50	4.8	*4.3*	4.6	*4.5*	4.3	*4.0*
0.17	4.25	4.9	*4.4*	4.7	*4.6*	4.2	*4.1*
0.50	12.5	4.3	*4.2*	4.4	*4.4*	4.0	*3.8*
2.50	62.5	4.1	*4.1*	4.1	*4.1*	3.9	*3.9*
12.5	313	4.3	*4.2*	4.4	*4.8*	3.9	*3.9*

[1] crude PLE (40 $U.mg^{-1}$ protein with respect to *p*NP-butyrate); [2] a crude PLE concentration of 1.8 $U.ml^{-1}$ (0.07 U total) was applied to each agarose-based biosensor; [3] control assays which followed non-enzymic hydrolysis of EtOAc.

However, the 2 and 24-hour pH values of the 20 ppm control assay, plus the low PLE (0.10 and 0.17 $U.ml^{-1}$) and EtOAc (20 and 50 ppm) combination assays are higher than the starting pH of 4.5 (possibly due to difficulties in poising non-buffered protein solutions at acidic pH values). Furthermore, the 12.5 $U.ml^{-1}$ PLE assays indicate that the drop in pH due to acid production was buffered by the

high protein concentration (the final pH achieved is higher than that produced by the 2.5 $U.ml^{-1}$ assays at all three EtOAc concentrations). Nonetheless, the buffering effect was not present in the 12.5 $U.ml^{-1}$ assays poised at 7.1 – presumably due to the optimal activity exhibited by PLE against EtOAc at this initial pH.

Due to the practical difficulties associated with poising the biosensor at acidic pH (such as the immediate loss in specific activity due to poising the biosensors at sub-optimal pH values, and protein buffering of the biosensor pH change when higher protein concentrations were used to overcome the loss in specific activity), neither Alizarin RedS nor Congo Red proved useful replacements for Phenol Red in the agarose biosensors.

4.3.1 Protein Buffering by PLE and BSA

The effect of protein buffering on Phenol Red was initially investigated with numerous PLE (3.3-13.4 $\mu g.ml^{-1}$) and BSA concentrations (6.7-830 $\mu g.ml^{-1}$). First, various PLE concentrations were added to 160 ppm (v/v) EtOAc prepared in 0.2% Phenol Red poised at pH 7.5 (Figure 4.2). Second, various BSA concentrations were added to 0.2% Phenol Red assays containing 160 ppm EtOAc and 8.3 $\mu g.ml^{-1}$ PLE. (Figure 4.3). EtOAc hydrolysis was followed spectrophotometrically by comparing the absorbance of Phenol Red at 558 and 433 nm (the wavelength of the violet and yellow pigments, respectively). As the pH decreases from the initial pH of 7.5 (red) to 5.5 (brilliant yellow) the 558 nm/433 nm ratio changes from 0.99 (predominantly red) to 0.02 (yellow). Non-enzymic hydrolysis was followed with assays containing no PLE.

The effect of decreasing PLE concentration (Figure 4.2) on the Phenol Red colour was evident as a slight time lag before a colour change (equivalent to a drop in pH) was detected. The pH values achieved by the highest and lowest PLE concentrations in the initial 30-minute period were pH 5.7 and 6.9, respectively. Over 24 hours, the pH values ranged between 5.7 and 6.4 (where a full colour change from red to yellow was achieved, and maintained, for another 24 hours with PLE concentrations $\geq$ 7 $\mu g.ml^{-1}$). However, any protein buffering effect caused by PLE was negligible since the highest PLE concentration used (13.3 $\mu g.ml^{-1}$) was significantly lower than the pH-electrode assay PLE concentration (313 $\mu g.ml^{-1}$) at which protein buffering was detected (see Table 4.4).

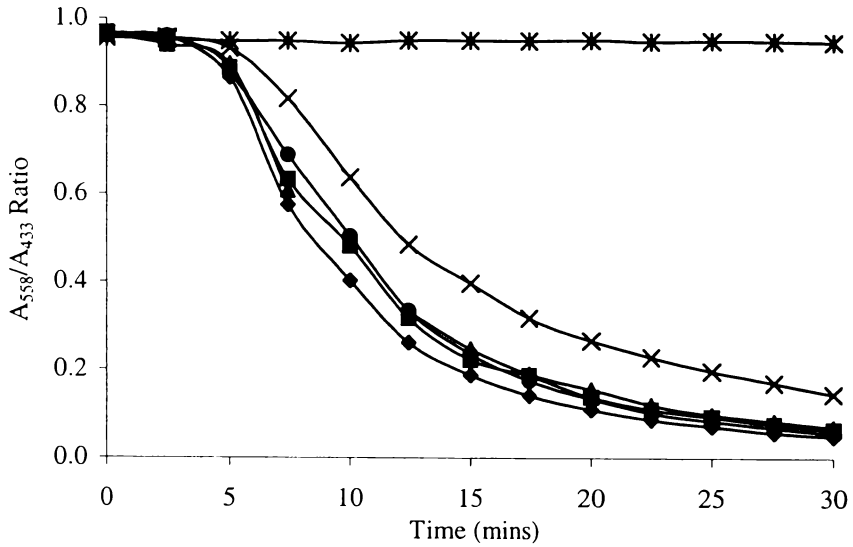

Figure 4.2. The effect of increasing PLE concentration on Phenol Red colour change.
0.2% Phenol Red and 160 ppm EtOAc were treated various concentrations of PLE. Phenol Red colour change was spectrophotometrically measured using a ratio of the absorbance at 558 and 433 nm. The six PLE concentrations (in $\mu g.ml^{-1}$) are as follows: ◆, 13.4; ■, 10.0; ▲, 6.7; ●, 5.0; ×, 3.3; and ✳, 0. PLE was added last to initiate the EtOAc hydrolysis.

Thus, the BSA experiment (Figure 4.3) investigated the effect of increasing the assay protein concentration (up to 830 $\mu g.ml^{-1}$ or 100 fold the assay PLE concentration) on the hydrolysis of EtOAc by 8.3 $\mu g.ml^{-1}$ PLE. The immediate effect of increasing the BSA concentration $\geq$ 42 $\mu g.ml^{-1}$ was a significant lag period (or buffering effect) in the first 30 minutes of the reaction. Interestingly, the pH drop catalysed by the 8 $\mu g.ml^{-1}$ BSA assay did not show this lag period and performed better (over the period of 30 minutes) than the 0 $\mu g.ml^{-1}$ BSA assay. It is possible that at this concentration, BSA is not causing a buffering effect but is instead "mopping" up free fatty acids released during ester catalysis (thereby reducing endpoint inhibition of PLE). In the longterm, the increased protein concentration did not have a significant effect since all four assays achieved the full colour change within the first 24 hours of the reaction. Therefore, enzymes with specific activities much lower than PLE could be used in the biosensor (the low specific activity could be overcome by increasing the enzyme load without the problem of protein buffering of the biosensor pH). Nevertheless, other enzymes may act differently from PLE and be susceptible to the protein buffering effect.

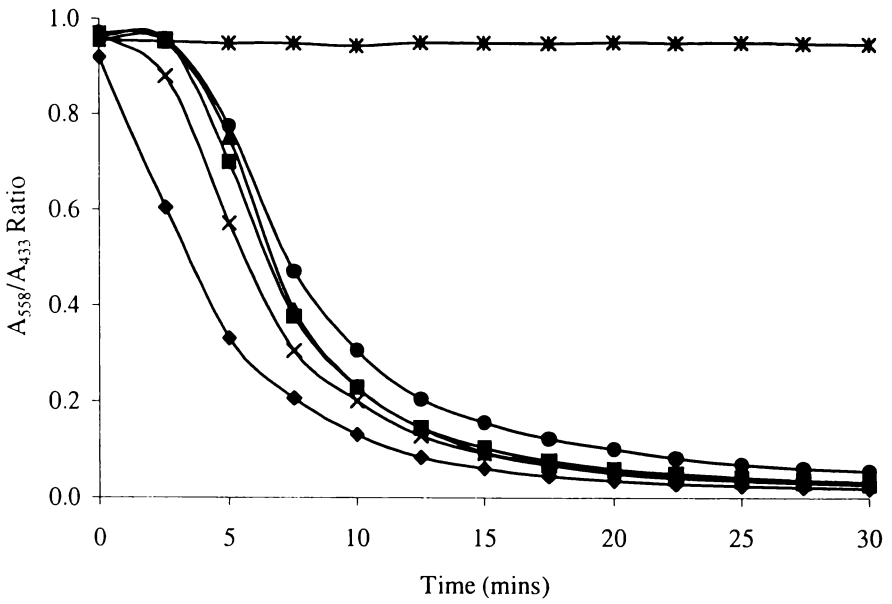

Figure 4.3. The effect of increasing BSA concentration on Phenol Red colour change.
0.2% Phenol Red, BSA and 160 ppm EtOAc were treated with 8.3μg.ml^{-1} PLE. Phenol Red colour change was spectrophotometrically measured using a ratio of the absorbance at 558 and 433 nm. The five BSA concentrations (in μg.ml^{-1}) used were as follows: ×, 0; ◆, 8.3; ■, 42; ▲, 332; and ●, 830 (equivalent to 0, 1, 5, 40 and 100X the PLE protein concentration. PLE was added last to initiate EtOAc hydrolysis. Non-enzymic EtOAc hydrolysis is represented by ✳.

4.4 Matrix Screen

PLE was used to screen a number of possible biosensor matrices (Whatman Glass Fibre paper, Whatman Paper Number 1, Spectra/Por ® membrane dialysis tubing and Merck pH-indicator strips, pH 4.0-7.0) and pH-dye indicators (Bromothymol Blue, Phenol Red and Alizarin RedS) by using the pH strip assay described in Section 4.2.1.1 (Table 4.5).

Table 4.5. pH-dye indicator colour and pH changes after biosensors treated with 10 mg.ml^{-1} PLE were exposed to an atmospheric concentration of 10,000 ppm ethyl acetate for three days.

Initial pH values and indicator colours are reported as Day Zero data. Abbreviated colours are as follows: A, aqua; B, blue; G, green; O, orange; R. red; Y, yellow; B/G, blue green; O/R, orange red. Note that the minimum pH values that can be estimated for each indicator are as follows: bromothymol blue, 6.0; phenol red, 6.5; alizarin redS, 4.6; pH-indicator strip, 4.0. The results for each negative control (included 20 mM NaF) are given.

Dye	Day Zero		Day Three								
			0% RH			30% RH			100% RH		
	Colour	pH	Matrix	Colour	pH	Matrix	Colour	pH	Matrix	Colour	pH
Bromothymol Blue	Dark A	7.5	All matrices	Dark A	7.5	Glass Fibre	O	6.5	Glass Fibre	O	6.5
						Control	G	7.0	Control	G	7.0
						Paper	O	6.5	Paper	Y	6.0
						Control	G	7.0	Control	G	7.0
Phenol Red	O/R	8.0	All matrices	Dark O/R	8.0	Glass Fibre	Y	6.5	Glass Fibre	Y	6.5
						Control	O/R	7.0	Control	O/R	7.0
						Paper	Y	6.5	Paper	Y	6.5
						Control	O/R	7.0	Control	O/R	7.0
									Tubing	Y	6.5
									Control	O/R	7.0
Alizarin RedS	Dark R	6.0	All matrices	Dark R	6.0	All matrices	Dark R	6.0	All matrices	Dark R	6.0
						Controls	Dark R	6.0	Controls	Dark R	6.0
pH Indicator Strip	B	6.0	Strip	B	6.0	Strip	Mustard Y	4.0	Strip	Mustard Y	4.0
						Control	A	5.0	Control	Dark B	5.8

The results of this screening study were obtained with approximately 10,000 ppm (v/v) [i.e., 10 µl EtOAc per ml of vessel headspace] vapor phase EtOAc. Biosensors were exposed to EtOAc for three days, after which the colour changes and approximate pH values (using Figure 4.1 as a reference) were recorded. At 10,000 ppm EtOAc, Whatman Paper Number 1 and the Merck pH-indicator strip were the best performing matrices with respect to: 1) strength of the pH-dye indicator colour, and 2) the elimination of the 'CO_2 effect' encountered by the agarose-based biosensor. However, the vapor phase activity experiments described in Chapter 6 used Whatman Glass Fibre Paper (GF/B) since this matrix had a higher liquid absorbance capacity - permitting higher concentrations of enzyme to be applied to each biosensor.

Further screening experiments were carried out, whereby the EtOAc or MeOBu vapor phase concentration was reduced to a level between 25 and 125 ppm (v/v), and the effect of PLE and pH-dye indicator concentration (on the final colour achieved) was analysed. The lower ester concentration range used in this experiment is more likely to be appropriate to a biosensor practical application (in contrast to 10,000 ppm used previously). An example of an experiment carried out using the conditions described above is presented in Figure 4.4. Two sets of indicator strips, active (treated with 20 mM NaCl) and inactive (treated with 20 mM NaF) were divided into three subsets depending upon the matrix and the pH-dye indicator. The three subsets included Phenol Red dyed Whatman Paper Number 1 (1-3, 4-6), Bromothymol Blue dyed Whatman Paper Number 1 (11-13, 14-16) and Merck pH-indicator strips (S1-S3, S4-S6). Additionally, three concentrations of pH-dye indicator and PLE were used in each subset (0.008, 0.02 and 0.1% dye [across] with 5, 25 and 100 ng protein [down] per subset, respectively). Each indicator strip was treated with PLE and/or pH-dye indicator, air dried at 25°C and *ca.* 66% RH humidity, and exposed to 100 ppm MeOBu (v/v) for 48 hours. Only those indicator strips treated with the highest PLE concentration (100 ng.strip^{-1}) produced discernible colour changes in the presence of Phenol Red, bromothymol and Merck indicator.

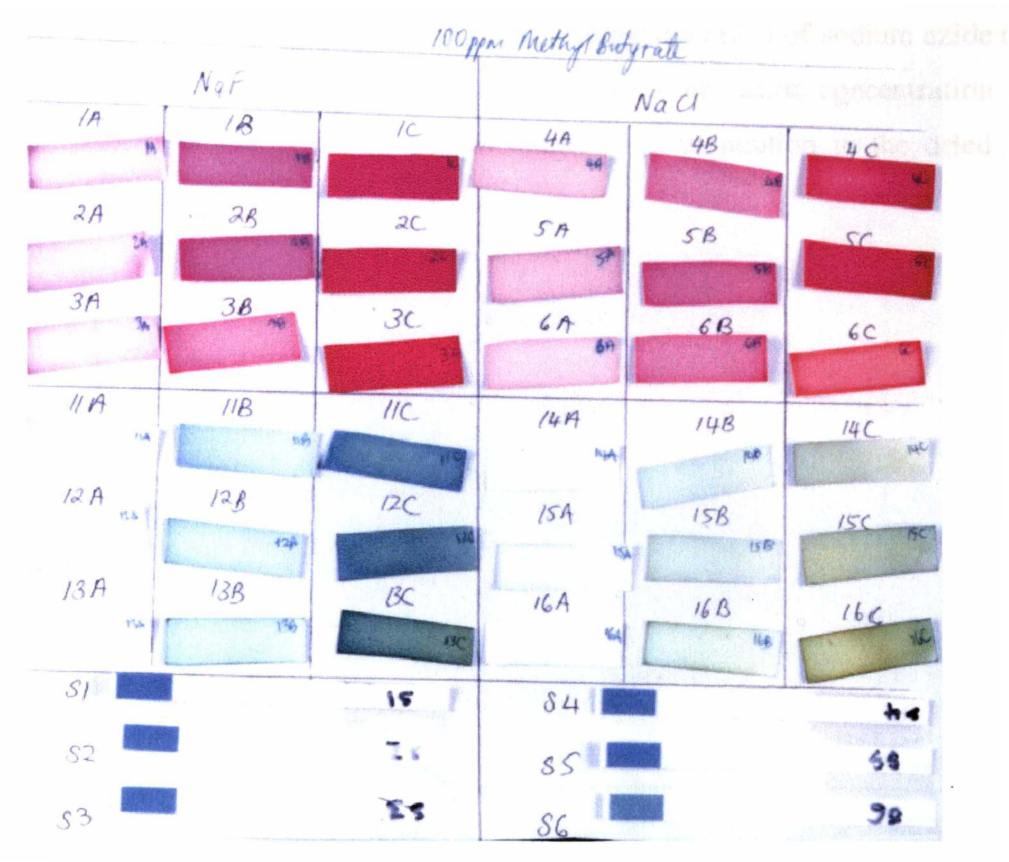

Figure 4.4. Air dried indicator strip sensors after 48 hours exposure to 100 ppm MeOBu. The indicator strips consisted of 3 cm x 1 cm rectangles of Whatman Paper Number 1 (1-6, 11-16), and Merck pH-indicator strips (pH 4.0-7.0, S1-S6). Strips 1-6 were treated with Phenol Red whilst strips 11-16 were treated with Bromothymol Blue (and both sets were treated with 20 mM NaCl or NaF to generate active and inactive strips, respectively).

4.4.1 Use of Sodium Fluoride as an Inhibitor

The effects of 0-50mM sodium fluoride (NaF) on PLE activity were investigated (Figure 4.5). PLE is 100% inhibited by 20 mM NaF, and subsequently 20 mM NaF was combined with the PLE and the pH-dye indicator during the biosensor assay screening experiments to generate inactive control sensors. Thus, any non-enzymic hydrolysis (evident as a change in pH-dye indicator in the controls) can be corrected for.

4.4.2 Use of Sodium Azide as a Preservative

Sodium azide, which is applied with the enzyme and pH-dye indicator to the biosensor, acts as a preservative to stop bacterial growth during the storage and RH equilibration of each biosensor. The effect of 0-0.5% (w/v) sodium azide concentration (0-11.9 mM) on LipB and PLE activity was followed in solution

(Table 4.6). This study was performed to determine the effect of sodium azide on the activity of the biosensor in which the initial sodium azide concentration of 0.02% (w/v in solution) changes to an unknown concentration in the dried or partially hydrated biosensor.

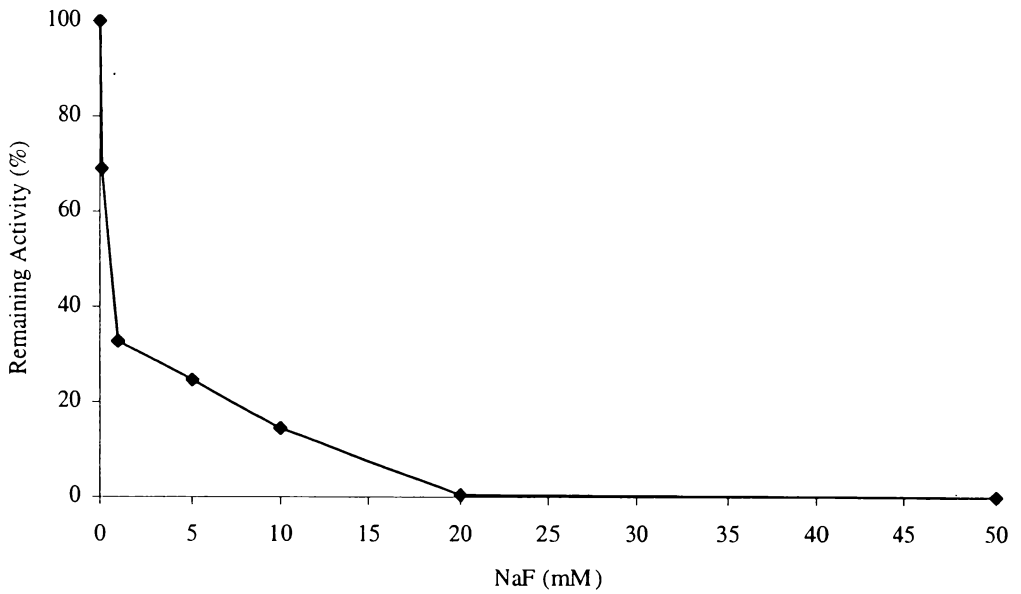

Figure 4.5. Sodium fluoride inhibition of PLE hydrolysis of *p*NP-butyrate.
0.02 mg.ml^{-1} PLE was subjected to increasing concentrations of NaF between 0 and 50 mM. Loss of activity against 0.25 mM *p*NP-butyrate was followed at pH 7.0 and 30°C.

Table 4.6. Stability of *Candida* LipB and PLE in solution and in the presence of increasing sodium azide concentration.

Sodium Azide Concentration		Remaining Activity (%)[1]	
% (w/v)	mM	*Candida* LipB	PLE
0	0	100	100
0.005	0.119	99	93
0.010	0.238	100	88
0.020	0.476	92	88
0.050	1.190	93	84
0.100	2.381	83	85
0.250	5.952	64	74
0.500	11.90	69	53

[1] remaining activity was determined against 0.25 mM *p*NP-butyrate in 50 mM Mops-NaOH, pH_{30} 7.5 (5 mM $CaCl_2$) at 30°C.

Activity losses against *p*NP-butyrate with increasing sodium azide concentration were determined at pH 7.5 and 30°C. Whilst sodium azide inhibited PLE more than LipB, a 25 fold increase in sodium azide concentration (from a starting concentration of 0.02% to a final concentration of 0.5%) only produced a loss of activity of 23 and 35% in LipB and PLE, respectively. This loss in activity (assuming the final biosensor sodium azide concentration does not exceed 0.5%) could be overcome by increasing the concentration of both enzymes in the biosensor.

4.5 Enzyme Screen in an Unbuffered Falling pH Environment

Screening of enzymes described in Chapter 3 was performed at various pHs which were fixed by inclusion of buffers. The following section describes subsequent screening of many of the same enzymes for the capacity to function in an unbuffered falling pH environment. This approach to screening more closely replicated the likely environment that the enzymes would encounter in a planned biosensor application.

Although the 'CO_2 effect' became much less significant through the transition from an agarose to a paper biosensor matrix, it remained desirable that an esterase should be capable of acidifying its working environment, as a consequence of its ester hydrolysis, to a pH considerably below that which might be attributed merely to the dissolution of CO_2. Therefore interest was retained in the capacity to reduce the pH below 5.5, but there was no longer such an emphasis on finding specifically acidophilic esterases.

4.5.1 pH-Electrode Assays

Four enzymes (Fluka *Bacillus stearothermophilus*, *Mucor miehei* and *Saccharomyces cerevisiae* carboxylesterase, plus semi-purified *Bacillus stearothermophilus* A^M carboxylesterase) were screened with a pH-electrode assay poised between pH 6.95 and 7.0. Aliquots containing 350 μg of dialysed Fluka carboxylesterases were exposed to 100 ppm (v/v) EtOAc or MeOBu prepared in MilliQ H_2O. The hydrolysis of EtOAc or MeOBu was followed as described in Section 2.2.1.5, and the change in pH with time is presented in Figure

4.6. The 24-hour pH values for *B. stearothermophilus*, *M. miehei* and *S. cerevisiae* were 6.4, 6.6 and 6.6, respectively for 100 ppm EtOAc (and 6.3, 6.4 and 6.0, respectively for 100 ppm MeOBu).

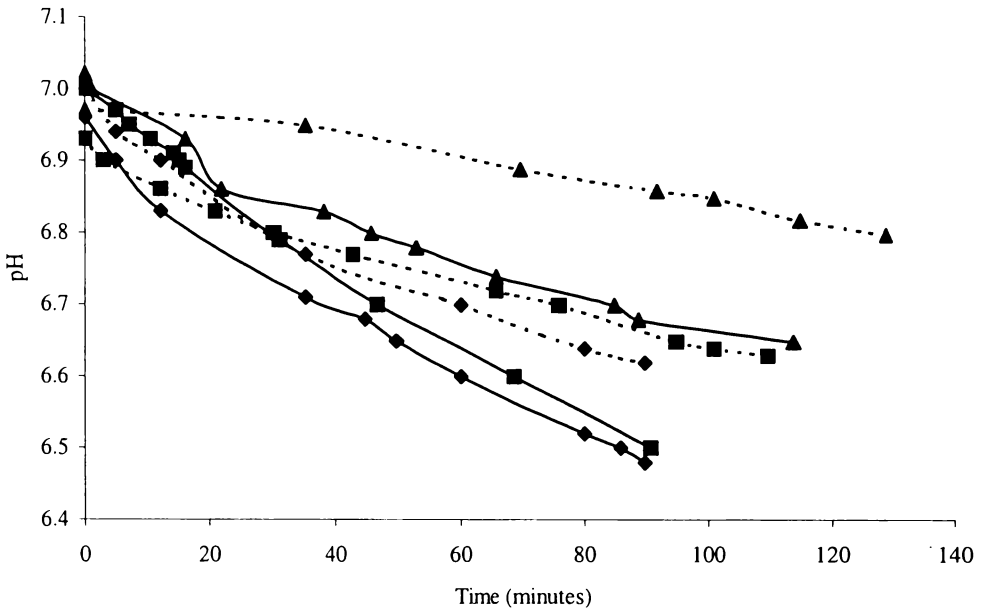

Figure 4.6. pH-electrode assays following the hydrolysis of 100 ppm (v/v) EtOAc and MeOBu at 25°C by three Fluka carboxylesterases.

Each 3 ml assay contained 350 μg of one of three Fluka carboxylesterases. The carboxylesterase, ester (and 24 hr pH result) of each assay are symbolised as follows: --■--, *B. stearothermophilus* and EtOAc (pH 6.4); ■, *B. stearothermophilus* and MeOBu (pH 6.3); --▲--, *M. miehei* and EtOAc (pH 6.6); ▲, *M. miehei* and MeOBu (pH 6.4); --◆--, *S. cerevisiae* and EtOAc (pH 6.6); and ◆, *S. cerevisiae* and MeOBu (pH 6.0).

Figure 4.7 presents the hydrolysis of 100 ppm EtOAc and MeOBu by 0.5 $U.ml^{-1}$ semi-purified *Bacillus stearothermophilus* A^M lipase, and the hydrolysis of 100 ppm EtOAc by 0.5 $U.ml^{-1}$ PLE (as a comparison). The 24 hour pH values of the three assays were 5.8, 4.9 and 4.1, respectively.

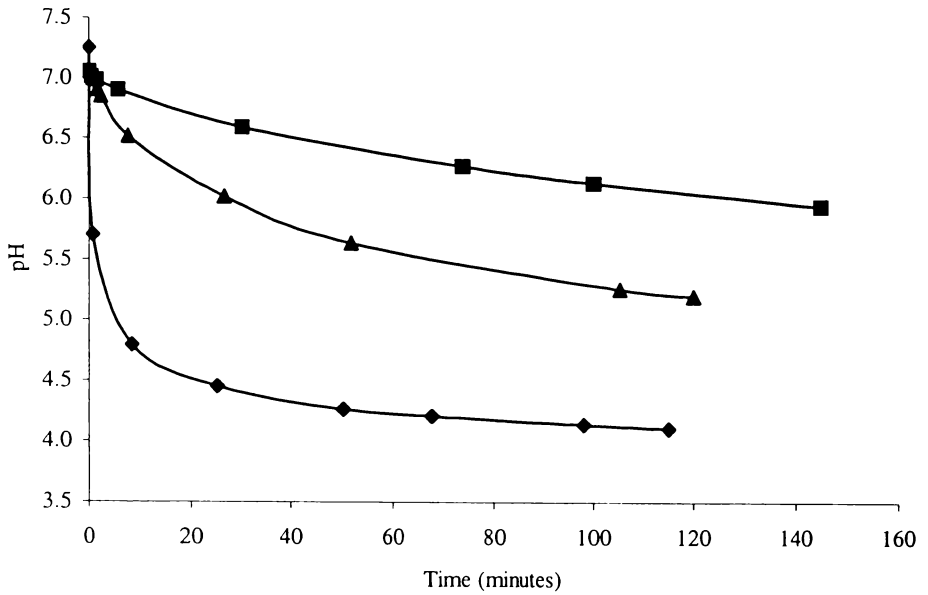

Figure 4.7. pH-electrode assays following the hydrolysis of 100 ppm EtOAc by 0.5 U.ml^{-1} PLE and *Bacillus stearothermophilus* A^{M} lipase, plus the hydrolysis of 100 ppm MeOBu by 0.5 U.ml^{-1} *Bacillus stearothermophilus* A^{M} lipase at 25°C.

The carboxylesterase, ester (and 24hr pH result) of each 3 ml assay are symbolised as follows: ■, *B. stearothermophilus* A and EtOAc (pH 5.8); ▲, *B. stearothermophilus* A^{M} lipase and MeOBu (pH 4.9); and ◆, PLE and EtOAc (pH 4.1).

All five carboxylesterases studied exhibited higher activity against MeOBu than EtOAc (detected as a larger drop in pH with time against MeOBu), but *Saccharomyces cerevisiae* carboxylesterase and *Bacillus stearothermophilus* A^{M} lipase exhibited the best activities against EtOAc and MeOBu. However, the use of the *S. cerevisiae* carboxylesterase in the commercial biosensor was commercially unfavourable due to the high cost of the enzyme preparation.

4.5.2 pH Indicator Strip Assay

The data from the pH indicator strip assays were used to refine the conditions of the pH-electrode assays. The indicator strip assay combines unbuffered pH with exposure to esters in the vapor phase only, which will be more relevant than dissolved esters to likely commercial applications. A consequence of the progression from liquid to vapor substrate is a significant drop in ester concentration available to the enzyme (as much as two orders of magnitude). At 25°C, the vapor-phase concentrations of EtOAc, MeOBu and EtOBu are 60, 70 and 81 times less than those in solution (see Appendix Four).

Eight microbial carboxylesterases or lipases were screened as substitutes for PLE in the paper-based biosensor as described in Section 4.2.1.1. Each enzyme was poised at pH 7.0, applied to a Merck pH-indicator strip (pH 4.0-7.0), and placed in a 10 ml sealed Vacutainer with 500 µl of ester solution in the bottom of the tube, out of direct contact with the indicator paper. Hydrolysis of the equilibrium headspace ester was detected as a colour change in the pH-dye indicator. Two enzyme screening experiments were carried out and the results are displayed in Tables 4.7 and 4.8.

The first experiment screened PLE, four lipases purified in our laboratory (TRU) and four commercially available enzymes (BioCatalyst). However, the total activity applied to each pH indicator strip was not consistent for each enzyme investigated (due, in part, to different enzyme solubilities in the sodium azide preparation). The ester concentrations of the 500 µl solutions were 125 and 25 ppm (v/v) MeOBu and EtOAc.

The results given in Table 4.7 are the 24 hour pH data achieved by the active and control strips (in which the ester was substituted by MilliQ water). The strips without enzyme remained at pH 7.0 (i.e., non-enzymic ester hydrolysis did not occur). The 24 hour pH reduction data indicate that the (highlighted) *Candida, Penicillium* and L187P Biocatalyst enzymes merited further investigation with respect to both the total activity per strip (calculated as $nmol.min^{-1}.strip^{-1}$) and the activity at lower ester concentrations.

Thus, the ester concentrations used in the second trial (Table 4.8) were as follows: 125, 25 and 5 ppm EtOBu; 25 and 5 ppm MeOBu; plus 25 and 5 ppm EtOAc; and appropriate concentrations of the three Biocatalyst enzymes were used to correspond to the total activity of PLE (the positive enzyme control to which all the enzymes are compared).

Table 4.7. Comparative pH-reducing activities of PLE and eight microbial esterases or lipases exposed to 25 and 125 ppm EtOAc and MeOBu.

The total activity (nmol.min^{-1}.indicator strip^{-1}) for each enzyme was determined against 0.25 mM *p*NP-butyrate at pH 7.0 and 30°C. The 24 hr control results for each indicator strip are given in the final column. Note that the control results for the four TRU lipases are low due to problems with poising 0.02% sodium azide at pH 7.0. The results of interest are highlighted.

Enzyme	Ester[1]	Total Activity	pH Achieved[2]	Control
PLE	125 ppm EtOAc	117	4.4	5.8
Pseudomonas lipase (TRU)		24	6.5	7.0
TP10 lipase (TRU)		0.5	5.5	5.5
TOK4 lipase (TRU)		0.2	5.3	5.5
TOK7 lipase (TRU)		0.3	5.5	5.5
Candida LipB[3]		27	4.4	6.5
L187P esterase (fungal)[3]		24	5.0	6.5
L224P esterase (porcine)[3]		0.5	7.0	7.0
Penicillium lipase[3]		25	5.5	6.5
PLE	25 ppm EtOAc	117	4.7	5.8
Pseudomonas lipase (TRU)		24	7.0	7.0
TP10 lipase (TRU)		0.5	5.5	5.5
TOK4 lipase (TRU)		0.2	5.3	5.5
TOK7 lipase (TRU)		0.3	5.5	5.5
Candida LipB[3]		27	5.3	6.5
L187P esterase (fungal)[3]		24	6.1	6.5
L224P esterase (porcine)[3]		0.5	7.0	7.0
Penicillium lipase[3]		25	6.1	6.5
PLE	125 ppm MeOBu	650	4.4	5.8
Pseudomonas lipase (TRU)		55	5.0	7.0
TP10 lipase (TRU)		30	5.5	5.5
TOK4 lipase (TRU)		2	5.3	5.5
TOK7 lipase (TRU)		1	4.7	5.5
Candida LipB[3]		640	5.0	6.5
L187P esterase (fungal)[3]		502	5.0	6.5
L224P esterase (porcine)[3]		8	5.8	7.0
Penicillium lipase[3]		209	4.0	6.5
PLE	25 ppm MeOBu	650	4.4	5.8
Pseudomonas lipase (TRU)		55	5.8	7.0
TP10 lipase (TRU)		30	5.5	5.5
TOK4 lipase (TRU)		2	5.3	5.5
TOK7 lipase (TRU)		1	5.5	5.5
Candida LipB[3]		640	5.3	6.5
L187P esterase (fungal)[3]		502	5.5	6.5
L224P esterase (porcine)[3]		8	6.1	7.0
Penicillium lipase[3]		209	5.0	6.5

[1] concentration of ester (v/v) in the 500 µl solution in the bottom of the tube (the enzymes were exposed to the ester vapor in the head space above this); [2] pH assessed after 24 hours based on the colour of the Merck pH-indicator strip; [3] purchased from BioCatalyst

Table 4.8. Comparative pH-reducing activities of four enzymes (at three enzyme concentrations) exposed to various concentrations of three esters.

The enzymes were PLE and three BioCatalyst enzymes (*Candida rugosa* LipB, L187P esterase and *Penicillium roqueforti* carboxylesterase) were exposed to three concentrations of EtOBu and two concentrations of MeOBu and EtOAc. The total activity for each enzyme was determined against 0.25 mM *p*NP-butyrate at pH 7.0 and 30°C. The enzymes were prepared in 0.02% sodium azide and poised at pH 7.0. The results of interest are highlighted.

Enzyme	Ester[1]	Lowest [Enzyme][2]		Middle [Enzyme][3]		Highest [Enzyme][3]	
		U.strip^{-1}	*pH*[4]	U.strip^{-1}	*pH*[4]	U.strip^{-1}	*pH*[4]
PLE		65.0	*4.7*	325	*4.4*	1625	*4.4*
Candida	125 ppm	65.2	*5.0*	326	*4.7*	1485	*4.7*
L187P	EtOBu	63.6	*5.0*	318	*5.0*	868	*5.0*
Penicillium		66.1	*5.0*	331	*5.0*	675	*5.0*
PLE		65.0	*5.8*	325	*5.5*	1625	*5.5*
Candida	25 ppm	65.2	*5.8*	326	*5.8*	1485	*5.8*
L187P	EtOBu	63.6	*6.1*	318	*5.8*	868	*5.8*
Penicillium		66.1	*6.1*	331	*5.5*	675	*5.3*
PLE		65.0	*7.0*	325	*5.8*	1625	*5.8*
Candida	5 ppm	65.2	*7.0*	326	*5.8*	1485	*5.8*
L187P	EtOBu	63.6	*7.0*	318	*6.1*	868	*6.1*
Penicillium		66.1	*7.0*	331	*6.1*	675	*6.1*
PLE		65.0	*5.8*	325	*5.5*	1625	*5.5*
Candida	25 ppm	65.2	*6.1*	326	*5.8*	1485	*5.5*
L187P	MeOBu	63.6	*6.1*	318	*6.1*	868	*6.1*
Penicillium		66.1	*6.1*	331	*6.1*	675	*6.1*
PLE		65.0	*7.0*	325	*6.1*	1625	*5.8*
Candida	5 ppm	65.2	*7.0*	326	*6.5*	1485	*6.5*
L187P	MeOBu	63.6	*7.0*	318	*6.1*	868	*6.1*
Penicillium		66.1	*7.0*	331	*6.1*	675	*6.1*
PLE		11.7	*6.5*	58.5	*6.1*	292	*5.8*
Candida	25 ppm	11.6	*6.1*	62.0	*5.8*	nd	*nd*
L187P	EtOAc	11.9	*7.0*	42.6	*6.5*	nd	*nd*
Penicillium		11.7	*6.5*	58.6	*6.1*	85	*6.1*
PLE		11.7	*7.0*	58.5	*6.5*	292	*6.5*
Candida	5 ppm	11.6	*7.0*	62.0	*6.5*	nd	*nd*
L187P	EtOAc	11.9	*7.0*	42.6	*6.5*	nd	*nd*
Penicillium		11.7	*7.0*	58.6	*6.5*	85	*6.5*

[1] concentration of ester (v/v) in the 500 µl solution in the bottom of the tube (the enzymes were exposed to the ester vapor in the head space above this); [2] control strips equaled pH 7.0; [3] control strips equaled pH 6.5; [4] pH assessed after 24 hours based on the colour of the Merck pH-indicator strip; nd, not done.

The microbial enzyme used to replace PLE in the biosensor was *Candida rugosa* LipB because (1) it exhibited the best activity against the three esters when compared to PLE (LipB preferentially hydrolyed the three esters in the following order: EtOBu > MeOBu > EtOAc); (2) it complied with the commercial requirement for a non-mammalian sourced enzyme; (3) *Candida rugosa* has GRAS status (generally regarded as safe), thereby making this yeast, and its products, ideal for use in diverse biotechnology sectors that include the food industry (Benjamin and Pandey, 1998); and (4) it was commercially available in large quantities since it is widely used in the dairy industry (to accelerate cheese maturation, for example). Hence, PLE and LipB were partially-purified (see Section 3.6) and used in both the biosensor stability trials (described in Sections 4.6.1 and 4.7.1) and the enzyme hydration and vapor-phase activity experiments carried out in Chapter 5 and 6, respectively. However, for future work, as especially when MeOBu is the substrate, *Penicillium roqueforti* lipase should be considered.

4.5.3 *Candida rugosa* LipB

The denaturation exhibited by PLE (see Sections 4.6.1 and 4.7.1 for further discussion) could be reduced by the addition of BSA (to act as a protein buffer for the butyric acid). However, the buffering affect would decrease the sensitivity of biosensors. Therefore, a study was carried out to investigate the buffering effects of using various quantities of LipB in Merck pH-indicator strips.

4.5.3.1 Effect of LipB and Ester Loading on Biosensor Sensitivity

The sensitivity of semi-purified desalted LipB towards varying levels of MeOBu, EtOBu and EtOAc in the headspace was investigated with Merck pH-indicator test strips (pH 2.0-9.0) exposed to 500 µl ester in 10 ml Vacutainers (the RH of the sealed Vacutainer would effectively be 100%). The test strips were saturated with 0.1, 0.02 or 0.004 mg LipB (prepared in 0.02% azide, pH 8.25 to 8.5) and exposed in 10 ml Vacutainers to 500, 125, 25, 5 and 1 ppm ester (via 500 µl ester solution out of direct contact with the enzyme-saturated test strip). The 2- and 24-hour pH values indicated by the colours of the test strip are presented in Table 4.9.

Table 4.9. Effects of LipB concentration on the extent of ester hydrolysis after 2 and 24 hours, starting at pH 8.3-8.5.

The controls for each strip (where the enzyme was not included, or the 0.5 ml ester was substituted by MilliQ water) showed no drop in pH over the period of 24 hours. A 'nc' result signifies no change in pH from the initial pH.

Ester	[Ester] (ppm, v/v)		*Candida* LipB Concentration ($mg.strip^{-1}$)					
			0.1		0.02		0.004	
	Solution[1]	Vapor[2]	2 hr	*24 hr*	2 hr	*24hr*	2 hr	*24 hr*
MeOBu	500	7.1	4.0	*5.5*	4.8	*5.5*	5.3	*6.3*
	125	1.8	5.0	*6.5*	5.0	*6.5*	5.5	*5.5*
	25	0.36	6.5	*7.2*	7.0	*8.0*	8.0	*8.0*
	5	0.071	7.3	*7.0*	8.0	*8.3*	nc	*nc*
	1	0.014	8.3	*8.3*	nc	*nc*	nc	*nc*
EtOBu	500	6.2	5.0	*6.3*	5.0	*5.0*	7.0	*6.5*
	125	1.6	5.5	*7.0*	6.0	*6.8*	nc	*nc*
	25	0.31	7.5	*7.5*	8.0	*7.5*	nc	*nc*
	5	0.062	8.0	*8.0*	nc	*nc*	nc	*nc*
	1	0.012	8.3	*8.3*	nc	*nc*	nc	*nc*
EtOAc	500	8.3	6.5	*6.0*	8.0	*6.8*	nc	*nc*
	125	2.1	7.3	*6.0*	nc	*7.5*	nc	*nc*
	25	0.42	7.5	*7.0*	nc	*nc*	nc	*nc*
	5	0.083	nc	*8.3*	nc	*nc*	nc	*nc*
	1	0.017	nc	*nc*	nc	*nc*	nc	*nc*

[1] ester concentration in the 500 µl solution placed in the bottom of the tube; [2] at 25°C, the vapor-phase concentrations of EtOAc, MeOBu and EtOBu are 60, 70 and 81 times less than those in solution (see Appendix Four).

The experiment was duplicated, except that Merck pH-indicator strips with a pH range of 4.0-7.0 and a starting pH of 7.0 were used. The strips were changed to those used in the enzyme screening experiments (see Tables 4.7 and 4.8) to ensure that the different pH-dye indicators used in the two types of Merck strip did not have an effect on LipB activity. Also, the ester concentrations used were 500, 125, 25 and 5 ppm only. The 2- and 24-hour pH results of this experiment are reported in Table 4.10.

Table 4.10. Effects of LipB concentration on the extent of ester hydrolysis after 2 and 24 hours, starting at pH 7.0.

The controls for each strip (where the enzyme was not included, or the 0.5 ml ester was substituted by MilliQ water) showed no drop in pH over the period of 24 hours. A 'nc' result signifies no change in pH from the initial pH. A 'nd' result means the assay was not done.

Ester	[Ester] (ppm, v/v)		*Candida* LipB Concentration (mg.strip^{-1})							
			0.5		0.1		0.02		0.004	
	Solution[1]	Vapor[2]	2 hr	*24 hr*	2 hr	*24 hr*	2 hr	*24 hr*	2 hr	*24 hr*
MeOBu	500	7.1	4.4	*6.5*	4.0	*5.3*	4.0	*5.3*	4.0	*5.0*
	125	1.8	nd	*nd*	4.0	*5.3*	4.2	*6.1*	4.4	*6.1*
	25	0.36	nd	*nd*	5.3	*5.3*	5.8	*6.1*	6.5	*7.0*
	5	0.071	nd	*nd*	6.3	*5.5*	6.3	*5.8*	nc	*nc*
EtOBu	500	6.2	4.4	*6.1*	4.0	*5.8*	4.0	*5.3*	4.0	*5.5*
	125	1.6	nd	*nd*	4.0	*6.1*	4.0	*5.8*	4.6	*5.8*
	25	0.31	nd	*nd*	5.5	*6.1*	5.5	*6.1*	6.0	*6.1*
	5	0.062	nd	*nd*	6.1	*6.1*	6.5	*6.5*	6.5	*7.0*
EtOAc	500	8.3	5.0	*6.0*	5.0	*5.3*	5.0	*5.3*	6.1	*5.5*
	125	2.1	nd	*nd*	5.8	*5.8*	5.8	*5.8*	nc	*6.1*
	25	0.42	nd	*nd*	6.1	*6.1*	6.1	*6.3*	nc	*6.5*
	5	0.083	nd	*nd*	6.8	*6.5*	6.8	*6.3*	nc	*6.5*

[1] ester concentration in the 500 µl solution placed in the bottom of the tube; [2] at 25°C, the vapor-phase concentrations of EtOAc, MeOBu and EtOBu are 60, 70 and 81 times less than those in solution (see Appendix Four).

The order of activity of semi-purified LipB (from most to least active) against the three esters is: MeOBu > EtOBu >> EtOAc. Therefore, under these conditions, LipB is not very effective against EtOAc. Furthermore, the change in pH is unstable because the pH increases between 2 and 24 hours exposure to the esters, particularly at the higher LipB and MeOBu and EtOBu concentrations. This pH increase may be due to bacterial growth over 24 hours even in the presence of 0.02% sodium azide, due to the high humidity of the vapor phase in the vessel (the ester solution is prepared in Milli Q water and the RH experienced by the that test strip would be close to 100%) since the threshold RH's required for bacterial and yeast growth are 91 and 88%, respectively (Bone, 1969). Microbial growth could be tested for microscopically if this experiment was repeated in the future. Another reason for the increase in pH may be that non-protonated HBu (which is less volatile than protonated HBu) may be evaporating

into the hungate tube headspace over then 22 hour period, thereby decreasing the HBu concentration in the strip and producing a pH increase.

4.5.3.2 Effect of Sorbitol on Biosensor Sensitivity

The effect of sorbitol (25%, w/v) on the activity of LipB towards varying levels of MeOBu, EtOBu and EtOAc was investigated. The purpose of this study was to determine whether a humectant (such as sorbitol) could increase the sensitivity of the biosensor to esters by retaining large quantities of water in the matrix, thereby increasing the water content, and consequently, the activity of the biosensor enzyme.

Table 4.11. Effects of LipB concentration on the extent of ester hydrolysis in the presence of 25% sorbitol (w/v) after 2 and 24 hours starting at pH 7.0.

The initial pH of the 0.5 and 0.1 mg.strip^{-1} indicator strips was 7.0. The initial pHs of the 0.2 and 0.004 mg.strip^{-1} indicator strips were 6.3 and 6.1, respectively. The water controls for each strip (where the 0.5 ml ester was substituted by MilliQ water) showed no drop in pH over 2 hours, but the pH decreased to 5.8 after 24 hours. The enzyme negative control strips (where LipB was not added to the 25% sorbitol preparation) were poised at pH 6.5 and the pH decreased gradually to 6.3 over the 24 hour period of the experiment. A 'nc' result signifies no change in pH from the initial pH. A 'nd' result means the assay was not done.

Ester	[Ester] (ppm, v/v)		*Candida* LipB Concentration (mg.strip^{-1})							
			0.5		0.1		0.02		0.004	
	Solution[1]	Vapor[1]	2 hr	*24 hr*	2 hr	*24 hr*	2 hr	*24 hr*	2 hr	*24 hr*
MeOBu	500	7.1	4.0	*6.1*	4.0	*5.3*	4.4	*4.4*	4.0	*4.0*
	125	1.8	nd	*nd*	5.0	*5.8*	4.4	*4.4*	4.4	*4.0*
	25	0.36	nd	*nd*	5.0	*5.3*	4.0	*4.4*	5.3	*4.00*
	5	0.071	nd	*nd*	5.0	*5.5*	4.0	*4.0*	5.8	*4.0*
EtOBu	500	6.2	4.0	*5.5*	4.0	*5.5*	4.0	*4.4*	4.0	*4.0*
	125	1.6	nd	*nd*	4.0	*5.5*	4.0	*4.4*	4.0	*4.0*
	25	0.31	nd	*nd*	4.9	*5.5*	4.0	*4.4*	4.0	*4.4*
	5	0.062	nd	*nd*	5.5	*5.5*	4.0	*4.7*	4.0	*4.4*
EtOAc	500	8.3	4.7	*5.0*	4.0	*5.0*	4.0	*4.0*	4.0	*4.0*
	125	2.1	nd	*nd*	4.7	*5.0*	4.0	*4.0*	4.0	*4.0*
	25	0.42	nd	*nd*	5.2	*5.3*	4.7	*4.4*	4.0	*4.0*
	5	0.083	nd	*nd*	5.4	*5.5*	4.6	*4.4*	4.4	*4.0*

[1] ester concentration in the 500 µl solution placed in the bottom of the tube; [2] at 25°C, the vapor-phase concentrations of EtOAc, MeOBu and EtOBu are 60, 70 and 81 times less than those in solution (see Appendix Four).

Candida LipB treated Merck indicator strips (pH 4.0-7.0) were exposed to 500 µl ester (in 10 ml Vacutainers) in the presence of 25% sorbitol. The strips were treated with 0.05, 0.1, 0.02 or 0.004 mg LipB (prepared in 25% sorbitol, pH 7.0) and were exposed to 500, 125, 25 and 5 ppm ester (in 500 µl solution). The 2- and 24-hour pH results of the sorbitol experiment are presented in Table 4.11, and the effect of the presence of 25% sorbitol is determined by comparing the results given in Table 4.11 with those in Table 4.10 (analogous assays completed in the absence of sorbitol).

The effect of protein buffering of the strip pH was evident in the high 0.5 and 0.1 mg.strip^{-1} LipB assays (as with the previous experiment), but the presence of 25% sorbitol diminished the tendency to exhibit an increase in pH between 2 and 24 hours. Also, the presence of 25% sorbitol enhanced the pH drop exhibited in each strip, particularly in the EtOAc assays. However, sorbitol (a poly-ol) may be a substrate for microbial populations present in the protein solution used on the strip, and these microbial populations may be able to breakdown esters. Another reason may be that sorbitol preparation itself may contain a contaminating enzyme capable of hydrolysing esters.

4.6 BIOSENSOR STORAGE

The long-term storage conditions appropriate for PLE and LipB were previously determined (see Sections 3.3.4 and 3.4.4, respectively) from the thermal- and pH stability data in solution. This data indicated that the appropriate storage conditions for a biosensor containing PLE would combine refrigeration [or freezing] and a neutral pH, while those for a biosensor containing LipB would combine refrigeration with pHs as low as 5.5 if necessary. Certain applications may demand that the biosensor label should be stored and used in either a dry or a partially hydrated state (but rehydrated upon use to a known water content). Thus, the stabilities of PLE and LipB at various RH's (and the corresponding protein water contents) were investigated.

4.6.1 RH Stability of PLE and *C. rugosa* LipB

Whatman GF/B rectangles (0.7 cm^2) were treated with 5 mg PLE and 1 mg LipB prepared in 0.2% sodium azide, pH 7.5 (in a total volume of 200 µl). The

rectangles were dried for 12 hours at 25°C and equilibrated at four RH's (83, 66, 15 and 0%) using saturated salt solutions of KBr, $NaNO_3$ and LiCl, plus anhydrous P_2O_5, respectively at 25°C. The remaining activity against 0.25 mM *p*NP-butyrate in 50 mM Mops-NaOH, pH_{30} 7.5 and 30°C was determined over a period of three weeks. The stability data of PLE and LipB are displayed in Tables 4.12 and 4.13, respectively. The 7% remaining activity determination for PLE after 14 days at 83% RH may be inaccurate, but the 83% RH experiment was not repeated because the stability data at the lower RHs were the important results from this table with respect to biosensor storage.

Table 4.12. Stability of PLE at pH 7.5, 25°C and various RH's between 0 and 83% for a period of three weeks.

Each Whatman GF/B rectangle loaded with the enzyme (total 200 μl) was poised at pH 7.5 and stored at 25°C. Stability data for each RH is given as percentage remaining activity against 0.25 mM *p*NP-butyrate in 50 mM Mops-NaOH (5 mM $CaCl_2$), pH_{30} 7.5 and 30°C.

Time (Days)	Relative Humidity (%) and Corresponding Protein Water Content [*h*][1]			
	0% [0]	12.0% [0.054]	64.2% [0.166]	83.0% [0.372]
0	100	100	100	100
2	100	100	98	100
9	100	100	74	82
14	100	100	60	7.0
21	100	100	62	6.4

[1] Protein water content values were referenced from Figure 5.5.

Table 4.13. Stability of *C. rugosa* LipB at pH 7.5, 25°C and various RH's between 0 and 83% for a period of three weeks.

The procedure for remaining activity determinations is as in Table 4.12.

Time (Days)	Relative Humidity (%) and Corresponding Protein Water Content [*h*][1]			
	0 [0]	12.0 [0.068]	64.2 [0.180]	83.0 [0.256]
0	100	100	100	100
7	100	100	93	93
14	100	100	94	88
21	100	100	92	85

[1] Protein water content values were referenced from Figure 5.5.

Compared to PLE, *C. rugosa* LipB is highly stable at RH's close to, and above, 64% (the RH common to the Hamilton region of New Zealand). The RH stability of LipB at 25°C makes the enzyme ideal for storage in a biosensor at unrefrigerated room humidity.

4.7 Effect of RH on Vapor-Phase Activity (Trial)

During the RH stability studies, the issue of dry activity arose, with respect to storage. Thus, the relationship between RH and hydrolytic activity was investigated using the vapor mode approach where the activity of pig liver esterase and Lipase B was studied as a hydrated solid phase in equilibrium with ester vapor. Merck pH-indicator strips (non-bleeding, pH 4.0-7.0) were treated with *Penicillium roqueforti* esterase, *Candida rugosa* LipB, semi-purified *Ophiostoma pluriannulatum* 5040 esterase and PLE.

Each set of strips was equilibrated at relative humidities between 0 and 95% in the absence of substrate, and the protein water content of each enzyme at the various RH's was estimated from the lysozyme adsorption isotherm (Figure 5.2) and given in Table 4.14. The hydrolytic reaction was initiated by the addition of EtOBu, to give a vapor-phase concentration of 150 ppm (v/v), and the colour change of the pH-dye indicator (expressed in pH units to the manufacturers printed colour scale) was followed after 30 minutes, 2 hours and 24 hours (Table 4.14 and Figure 4.8).

All the enzymes exhibited activity at 0.07*h* (7% water, w/w), which is appreciably lower than the hydration thought necessary for enzyme activity. In the case of PLE and *Penicillium* esterase, this activity was ~20% of that when fully hydrated. The colour change at lower hydration levels may be minimised or undetected due to a water requirement of the pH-dye indicator rather than the enzyme. Therefore, vapor-phase activity analysis was carried out using gas chromatography instead of pH-dye indicators, as in Section 4.7.1, thereby separating the pH-dye indicator hydration requirements from those of the enzyme.

Table 4.14. Effect of RH on the pH reducing activities of PLE and three microbial enzymes absorbed onto Merck pH-indicator strips.

Four enzymes (*Candida cylindracea* LipB, PLE, *Penicillium roqueforti* esterase *Ophiostoma pluriannulatum* 5040 esterase) were prepared in 0.02% sodium azide, pH 7.0, and applied to Merck pH-indicator strips (pH 4.0-7.0). The strips were equilibrated at 0 to 98% RH using the saturated salt solutions listed in Table 5.1 and exposed to a vapor phase concentration of 150 ppm EtOBu at 25°C. The initial pH values were between pH 6.5 and 7.0. The overall pH changes achieved in 24 hours (i.e., the difference between the initial and final pH value) are listed in the table and graphically presented in Figure 4.8.

RH(%)	Enzyme Water Content (h)[1]	*Penicillium* Esterase	*Candida* LipB	PLE	*Ophiostoma* Esterase
0	0	0	0	0	0
12.0	0.07	0.3	0.1	0.3	0.1
31.0	0.10	0.0	0.4	0.2	0
52.5	0.12	0.3	0.9	0.3	0.2
64.2	0.16	0.4	0.7	0.6	0.6
83.0	0.21	0.6	0.6	0.6	0.6
88.3	0.37	0.8	0.8	0.8	0.8
95.0	0.51	1.5	1.1	1.1	1.5
98.0	0.58	1.6	1.9	1.1	1.6

[1] the protein water content of each enzyme was determined with the lysozyme adsorption isotherm (Figure 5.2) and therefore only an estimation (note that the water contents are increasingly inaccurate at RH values >70%).

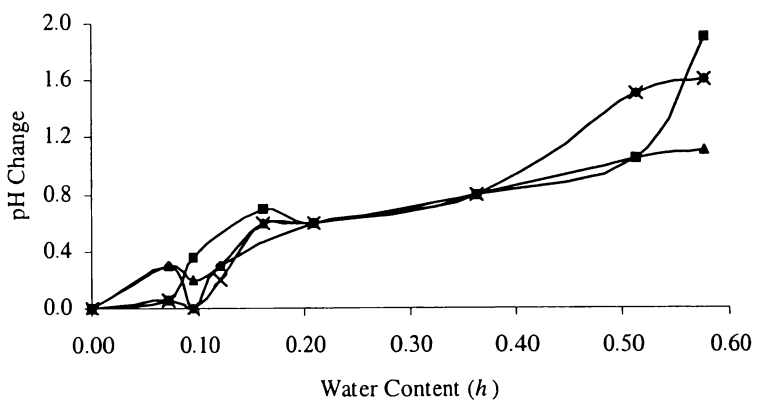

Figure 4.8. Effect of enzyme water content on the pH reducing activities of PLE and three microbial enzymes absorbed onto Merck pH-indicator strips.

Initial pH values were between pH 6.5 and 7.0. The overall pH changes achieved in 24 hours (i.e., the difference between the initial and final pH value) after exposure to a vapor phase concentration of 150 ppm EtOBu at 25°C are given. The four enzymes are as follows: *Candida cylindracea* LipB, ■; PLE, ▲; *Penicillium roqueforti* esterase, ◆; and *Ophiostoma pluriannulatum* 5040 esterase, ×.

4.7.1 Vapor-Phase Activity Method Development

Rectangles made from 2 cm by 3 cm Whatman GF/B were treated with active or denatured (heated at 150°C for 60 minutes) semi-purified PLE (desalted and lyophilised) prepared in 0.02% sodium azide, pH 7.5. The rectangles were air-dried (at *ca.* 66% RH) and equilibrated at 25°C for 3 days at 12 and 95% RH to generate protein water contents of 0.054 and 0.60 *h*, respectively. Each rectangle was independently placed above, but out of direct contact with, a saturated salt solution to maintain either 12 or 95% RH (see Table 5.1 for the appropriate saturated salt solution) in one of three vessels: a 12.5 ml Vacutainer, a 9 ml Hungate tube and a 5 ml vial (the Hungate and vial were each sealed with a Mininert® valve and the Vacutainer was sealed with the original rubber stopper). After 3 days, EtOBu was injected into the sealed vessel to give a total vapor phase concentration of 5000 ppm (v/v) (i.e., 5 µl EtOBu per ml headspace volume). The rate of EtOH production during the first four hours of the reaction, plus the reaction period between four hours and seven days, was determined. Active samples have their activities given as $nmol.min^{-1}.mg^{-1}$ protein and are reported in Table 4.15.

The limit of detectability is equivalent to a total of amount of 9.6 nmol ethanol (an ethanol peak area of 380 as determined by the Spectra Physics SP4100 integrator).

At 15% RH (0.054 *h*), PLE, with a V_{max} of 36.6 $\mu mol.min^{-1}.mg^{-1}$ and a K_m of 1.75 mM or 243 ppm (v/v) for ethyl butyrate in solution, showed no activity against ethyl butyrate within the first four hours (no ethanol was detected). This result was anticipated (since enzyme activity is very low, or negligible, at protein hydration levels less than 0.2 *h*) and the reaction was allowed to continue for 7 days until the second data set was analysed by GC. At this point, ethanol was detected in the active samples of all three vessels (see the last column in Table 4.15). Since the denatured and control PLE rectangles did not produce any ethanol, the detection of ethanol in the 15% RH samples confirms that PLE is active at a very low hydration level (0.054 *h*) in comparison to 0.2 *h* – the threshold hydration level for activity in many globular proteins (Stevens and Stevens, 1979; Rupley *et al.*, 1983; Rupley and Careri, 1991).

Table 4.15. Total ethanol produced by desalted PLE after 4 hours and 7 days exposure to 0.067 and 0.513 *h*.

Specific activities are given as nmol ethanol produced per minute per mg PLE ($nmol.min^{-1}.mg^{-1}$). Ethanol was assayed at 0 hr, 4 hr and 7 days and the total nmol of ethanol produced in each given time period is presented in parentheses next to the reaction rate.

Vessel	Relative Humidity (%)	Treatment[1]	Specific Activity	
			Over 0-4 hr	Over 4 hr-7 days
Vacutainer	95	A	0.26 (633)	nc
		D	bd	bd
	15	A	bd	0.007 (64)
		D	bd	bd
Hungate	95	A	0.35 (841)	nc
		D	bd	bd
	15	A	bd	0.005 (46)
		D	bd	bd
Vial	95	A	0.19 (466)	0.001 (10)
		D	bd	bd
	15	A	bd	0.010 (110)
		D	bd	bd

[1] Treatments are as follows: 'A' active and 'D' denatured PLE; bd, below the limit of detectability; nc, the EtOH concentration did not increase between 4 hours and 7 days at 95% RH.

PLE was active at 95% RH (0.60 *h*) and ethanol was produced within the first few hours. However, between 4 hours and 7 days no more ethanol was produced (except in the 5 mL vessel). This indicated that PLE exhibited little activity at low pH (the acidic shift in rectangle pH was caused by accumulation of the acid reaction product), or was denatured by the acid pH, or displayed end-product-inhibition.

In the case of ester hydrolysis, the acid moiety can remain with the enzyme (due to butyric acid being relatively non-volatile) and cause inhibition by decreasing the pH in the microenvironment surrounding the enzyme (Ross and Schneider, 1991). This could be the reason for the apparent loss of activity by PLE after four hours in the vapor-phase activity trial described above. However, the activity losses could have been due to (1) a reduction of the pH in the microenvironment of PLE by butyric acid - a reaction product - resulting in a decrease in activity; or (2) denaturation of PLE by butyric acid. To determine if

PLE was irreversibly denatured, an experiment was completed in which PLE-containing GF/B rectangles were exposed to a range of RH's and EtOBu concentrations for 4 days and 24 hours, respectively. The rectangles were then tested for remaining activity against 0.25 mM *p*NP-butyrate at pH 7.5 and 25°C (Table 4.16).

Table 4.16. The stability of PLE when exposed to four RH's (0, 7.2, 15 and 83%) and five vapor-phase EtOBu concentrations between 40 and 5000 ppm.

Each Whatman GF/B rectangle was poised at pH 7.5 and 25°C. Data for each RH is given as percentage remaining activity against 0.25 mM *p*NP-butyrate in 50 mM Mops-NaOH (5 mM $CaCl_2$), pH_{30} 7.5 and 30°C.

RH (%)	EtOBu (ppm)	Remaining Activity (%)
0	1000	100
7.2	1000	92
15	1000	85
83	1000	2.6
83	40	76
83	200	43
83	500	2.6
83	1000	2.7
83	5000	2.5

The decrease in remaining activity observed with each increase in RH (from 0 to 83%) likely represents PLE denaturation because at low hydration little or no acid is produced and the biosensor would not become so acidic (as a general rule, enzyme activity decreases with decreasing hydration, and at 0*h* there is no water available so the hydrolytic reaction can not proceed). In contrast, exposure to high RH (e.g., 83%) would significantly increase both the water content and hydrolytic activity of PLE, and result in an increase in acid production. However, the small losses in PLE activity observed ≤ 15% RH could be on account of the enhanced stability of enzymes at low hydration due to increased structural rigidity (Pirozzi *et al.*, 1997).

The increasing loss in activity at 83% RH with increased EtOBu concentration indicated that PLE was denatured by butyric acid production (since

the overall acid production would increase with increasing ester concentration). However, it was not known how fast the denaturation process occurred. Therefore, an extensive study of the loss in PLE activity upon exposure to an EtOBu vapor-phase of 500 ppm was completed and the results are shown in Figure 4.9.

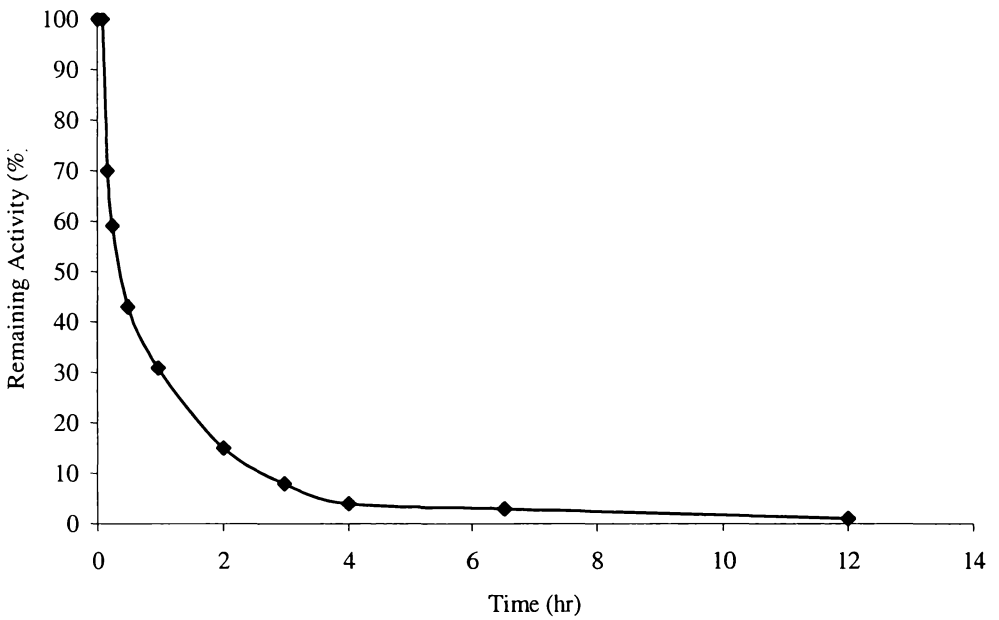

Figure 4.9. Stability of PLE after exposure to 500 ppm vapor-phase concentration of EtOBu at 83% RH for varying periods.

Data for each time point is given as percentage remaining activity against 0.25 mM *p*NP-butyrate at pH 7.5 and 30°C in solution.

Between 25 and 30 minutes, PLE had lost 50% of its initial activity (remaining activity after 25 and 30 minutes were 59 and 43%, respectively). After 4 hours, PLE had lost 96% activity and this could explain why no more ethanol was produced between 4 hours and 7 days in the vapor-phase activity experiment described in Table 4.15.

4.8 CONCLUSIONS

The transition from the agarose matrix of the biosensor initially used by our commercial partners to that of paper-based biosensors largely eliminated the effect of CO_2 accumulation within the matrix. Consequently, Phenol Red did not have to be replaced as the biosensor pH-dye indicator, an acidic starting pH

became unnecessary, and PLE (the original biosensor enzyme) did not have to be replaced by a specifically acidophilic enzyme in order to avoid protein buffering (due to the requirement of high enzyme loading for biosensors poised ≤ pH 5.5). Nevertheless, the options discovered for running an ester biosensor at an acid pH may prove useful in the future.

PLE could not be used in the commercially produced biosensors because it was unacceptable in the international consumer markets (essentially due to PLE's mammalian origin). Therefore, various microbial carboxylesterases and lipases (n = 8) were screened for effectiveness in the paper-based biosensors. Each of the microbial enzymes tested exhibited the same order of preference amongst the natural ester substrates of interest (MeOBu > EtOBu >> EtOAc). Moreover, the majority of the enzymes displayed negligible activity against EtOAc, which would be a significant problem if the biosensor were to be used in applications in which EtOAc is the major ester.

However, *Candida rugosa* LipB (non-mammalian lipase, certified Kosher, GRAS status) exhibited very good activity against MeOBu and EtOBu and reasonable activity against EtOAc. LipB was stable at protein water contents ≤ 0.26 *h* - the partially hydrated lipase retained 85% activity compared to < 62% for PLE, after exposure to 25°C for three weeks at 0.*26 h*. The issue of stability was important with respect to biosensor storage. Although LipB and PLE retained 100% activity in the dry biosensor (0 *h*) at 25°C, the greater stability of LipB, at higher protein water contents, would permit LipB biosensors to be stored in an environment without the drying agent, anhydrous P_2O_5. Consequently, the biosensors would not have to be as intensively rehydrated prior to use. Furthermore, LipB was active below a protein hydration value of 0.20 *h* - the minimal protein water content required for enzyme activity (Stevens and Stevens, 1979; Rupley *et al.*, 1983). This observation, and the issue of activity in partially hydrated (or dry) biosensors, was fundamental in the decision to study the relationship between enzyme hydration and gas-phase activity. First, the hydration process of PLE and LipB was investigated in Chapter 5 with respect to determining the water content of each enzyme when exposed to a series of RH's between 0 and 90%. Second, the rate of PLE and LipB hydrolysis of vapor-phase ethyl butyrate at each water content was determined by gas chromatography (see Chapter 6).

CHAPTER 5 PROTEIN HYDRATION

5.1 INTRODUCTION

The hydration process (from a dry to fully hydrated protein state) has been comprehensively studied with globular proteins (see Section 1.6.3.3). The most extensively studied member of this protein class is egg white lysozyme (Careri *et al.*, 1979 and 1980; Rupley *et al.*, 1983; Yang and Rupley, 1979). The lysozyme hydration process is complex and involves four stages which are primarily determined by the preferential interaction between solvent water molecules and several classes of protein sites: charged [ionisable] > polar > weakly interacting residues.

Studies of three other globular proteins (α-chymotrypsin, ribonuclease and subtilisin Carlsberg) confirm that the hydration process for lysozyme is not unique to that protein (Affleck *et al.*, 1992; Rupley and Careri, 1991). Furthermore, all four proteins share similar hydration profiles (Rupley and Careri, 1991), as illustrated by adsorption isotherms (see Section 1.6.3.2).

The work described here investigated the hydration process of the globular proteins, PLE (between 0 and 0.6 *h*) and *Candida rugosa* LipB (between 0 and 0.5 *h*). Protein hydration was carried out using saturated salt solutions (which control the equilibrium RH of an enclosed vessel containing each desalted partially purified enzyme) to yield a series of protein water contents which were determined gravimetrically and graphically represented by an adsorption isotherm.

The crude enzyme preparations were desalted and partially purified to remove non-protein material (such as carbohydrates and salts from the *Candida rugosa* culture medium, plus salts and buffer species from the PLE preparation) and to decrease the quantity of competing proteins in the enzyme preparations. These contaminants compete with PLE and LipB for atmospheric water and can modify the final water contents of the enzymes achieved at each RH. This work produced a set of reference water contents for use in the enzyme hydration–activity studies carried out in Chapter 6.

5.2 ADSORPTION ISOTHERMS

A practical method for determining protein hydration is gravimetric analysis in which the lyophilised protein and a saturated salt solution are enclosed in a sealed vessel. The saturated salt solution generates a known %RH (see Table 1.14) and the water vapor equilibrates between the protein and the vessel headspace. The protein water content (expressed as grams water per gram protein, h) is calculated by measuring the weight gain as the protein is rehydrated from the dry state. The relationship between RH and protein water content is graphically represented by an adsorption (rehydration of a lyophilised protein) or desorption (dehydration of a fully hydrated protein) isotherm.

Three globular proteins (Hammerstein casein, BSA and egg white lysozyme) were initially studied to produce a 'standard' adsorption isotherm as a reference for the Chapter 6 enzyme hydration-activity studies carried out with PLE and LipB. Previous hydration studies had attributed similar adsorption isotherms to many globular proteins, including lysozyme, α-chymotrypsin and subtilisin Carlsberg (see Rupley and Careri, 1991). However, the concept of the 'standard' adsorption isotherm was abandoned because each protein had a characteristic isotherm, which although similar in shape, differed in total protein water content at each RH.

5.2.1 Trial Proteins

The Hammerstein casein and BSA adsorption isotherms (Figure 5.1) were determined at 20°C after exposure to the series of saturated salt solutions listed in Table 5.1 for three and five days, respectively. In addition two samples of each protein were exposed to anhydrous P_2O_5 and H_2O to determine the water content at 0 and 100% RH, respectively. However, the validity of the adsorption isotherms is ambiguous because the zero protein water content was determined with anhydrous P_2O_5 at 20°C, and the protein water content at the higher RH's (particularly > 70%) had not equilibrated within the experimental period. Thus, an extensive hydration study was carried out with lysozyme to determine (1) the true zero water content of proteins, and (2) the time required for water content equilibration.

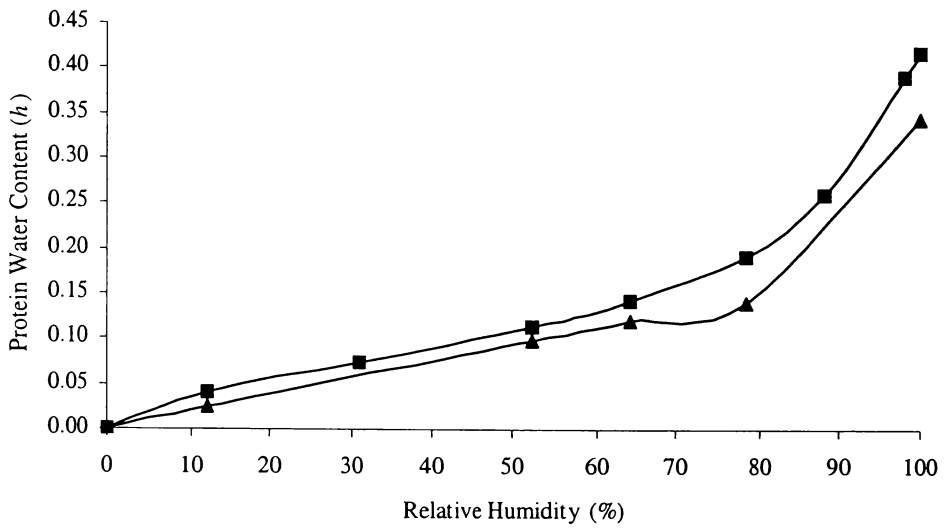

Figure 5.1. The effect of RH on the protein water content of Hammerstein casein and BSA at 20°C.

The proteins and time of exposure to the saturated salt solutions are as follows: Hammerstein casein after three days, ▲; BSA after five days, ■. The zero water contents of Hammerstein casein and BSA were calculated after exposure to anhydrous P_2O_5 at 20°C for three and five days, respectively.

5.2.2 Zero Water Content

A widely accepted method for obtaining a dry state protein combines the exposure of lyophilised protein to anhydrous P_2O_5 and high temperatures (Poole and Finney, 1986). Although the P_2O_5 technique is used at 20-30°C to calculate the residual moisture of commercial freeze-dried biological products (Dolman *et al.*, 1996), increases in the temperature at which the method is carried out will produce additional losses in protein water content. Consequently, the zero protein water contents (0 *h*) of lysozyme, PLE and LipB were determined after 14 days exposure to anhydrous P_2O_5 at 65°C.

While the lysozyme adsorption isotherm (Figure 5.2) was carried out at 20°C against each of the saturated salt solutions listed in Table 5.1, two additional lysozyme samples were treated with approximately 20 g of anhydrous P_2O_5 – one sample was exposed to this drying agent at 20°C and the second sample at 65°C. The gravimetric data from the two P_2O_5 treated samples illustrate the effectiveness of the Poole and Finney (1986) method: the 65°C lysozyme sample experienced an additional loss in water content of 0.024 *h* upon the 0.050 *h* lost during the

20°C treatment. Therefore, the PLE and LipB zero water contents were determined with anhydrous P_2O_5 at 65°C.

Table 5.1. Water content (*h*) of lysozyme achieved on exposure to the RH's produced in an enclosed vessel by the saturated salt solutions specified.

Solid Phase	RH (%)[1]	Water content (%w/w, *h*)
Phosphorus pentoxide (P_2O_5)[2]	0	0[3]
LiBr	7.2	0.030
$ZnCl_2$	10.0	0.045
$LiCl.H_2O$	12.0	0.067
$CaCl_2.6H_2O$	31.0	0.097
$NaNO_2$	64.2	0.161
NH_4Cl	78.4	0.207
KBr	84.0	0.280
$ZnSO_4.7H_2O$	88.3	0.365
$Na_2HPO_4.12H_2O$	95.0	0.513
$CuSO_4.5H_2O$	98.0	0.579

[1] the RH values are from the data listed in Table 1.14; [2] anhydrous powder; [3] the zero water content value was determined after 14 days exposure at 65°C to anhydrous P_2O_5.

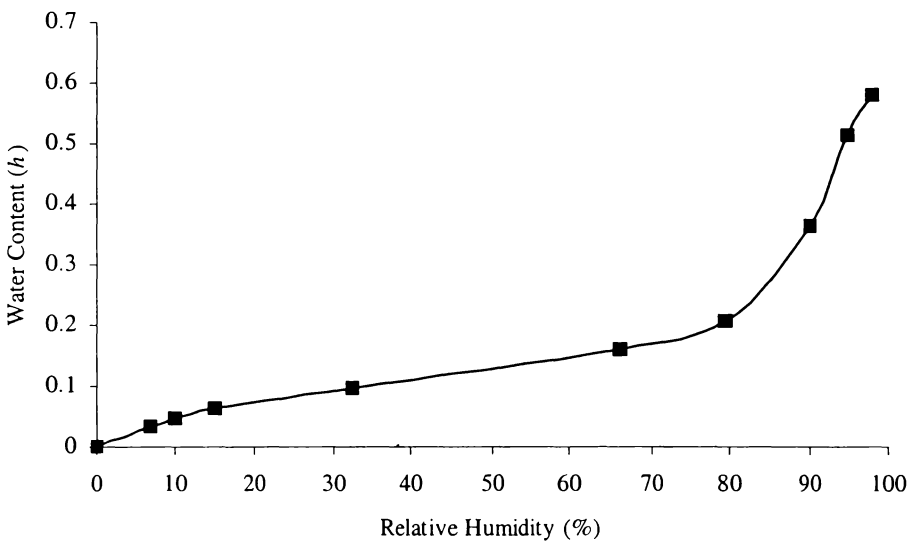

Figure 5.2. Effect of RH on the water content of egg white lysozyme at 20°C.

Lysozyme was exposed to saturated salt solutions at 20°C for fourteen days. The zero water content was calculated after fourteen days exposure to anhydrous P_2O_5 at 65°C.

The lysozyme adsorption isotherm displays the three regions characteristic of protein isotherms: the 'knee', the plateau and the upswing that correlate with protein water contents of 0-0.065, 0.065-0.200 and ≥ 0.200 *h*, respectively.

5.2.3 Time Required for Water Content Equilibration

The time required for protein water content to equilibrate at each RH was ascertained gravimetrically by measuring the water content of lysozyme after three, six, ten and fourteen days exposure to saturated salt solutions at 20°C (Figure 5.3).

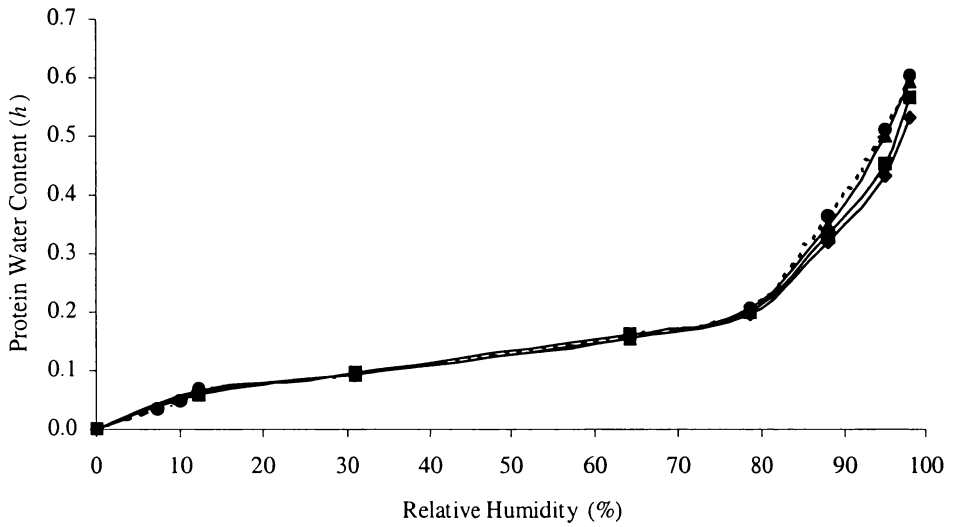

Figure 5.3. The effect of the time of exposure to RH's between 0 and 98% on the water content of lysozyme at 25°C.

The times of exposure to the various saturated salt solutions are given as follows: three days, ◆; six days, ■; ten days, ▲; and fourteen days, --●--. The zero water content was calculated after fourteen days exposure to anhydrous P_2O_5 at 65°C.

The lysozyme water content data indicates that the length of time required for water loss or gain to equilibrate between 0 and 70% RH is 3 days. However, the lysozyme water content does not readily equilibrate above 70% RH within the two week experimental period. Rather, the water content increases with each day of exposure to the RH (Figure 5.4). Therefore, water content calculations for protein samples exposed to high RH's will need to specify the time of equilibration. PLE and LipB, the two enzymes used in the enzyme hydration-

activity experiments described in Chapter 6, also experienced ever increasing protein water content with time of exposure.

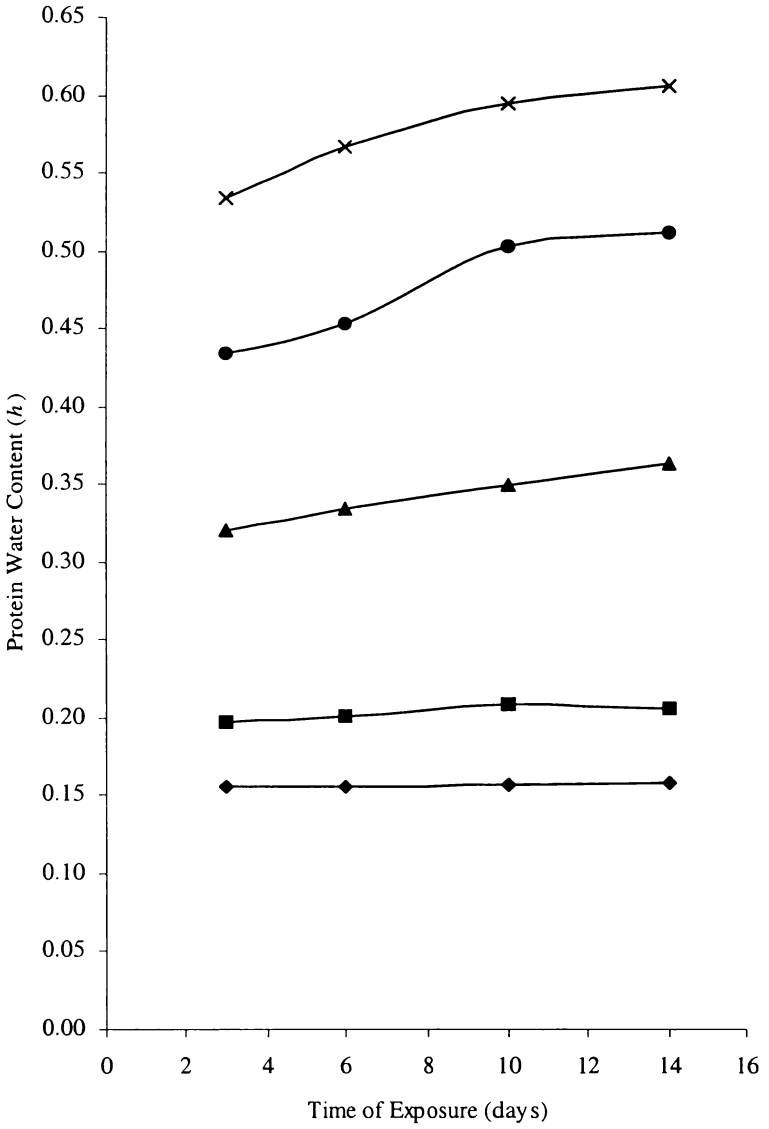

Figure 5.4. The effect of the time of exposure to RH's between 66.4 and 98% on the water content of lysozyme at 20°C.

The RH (and saturated salt solution) that lysozyme was exposed to are as follows: 66.4% ($NaNO_2$), ◆; 78.4% (NH_4Cl_2), ■; 88.3% ($ZnSO_4$), ▲; 95.0% (Na_2HPO_4), ●; 98.0% ($CuSO_4$), ×. The zero water content was calculated after fourteen days exposure to anhydrous P_2O_5 at 65°C.

5.2.4 PLE and LipB Adsorption Isotherms

Semi-purified (both ~ 80% pure), desalted and lyophilised PLE and LipB were sequentially hydrated using the saturated salt solutions listed in Table 5.1.

The adsorption isotherms of both enzymes are compared with that of lysozyme in Figure 5.5. The variance in the three isotherms (particularly at > 70% RH) further illustrates the inaccuracy in using the lysozyme adsorption isotherm (Figure 5.2) as a reference isotherm for other globular proteins. Upon exposure to RH's between 0 and 70%, the hydration level of PLE is significantly lower than that of LipB (*ca.* 0.05 *h* less). Conversely, upon exposure to RH's greater than 70%, the water content of PLE exceeds that of LipB by 0.12-0.27 *h*.

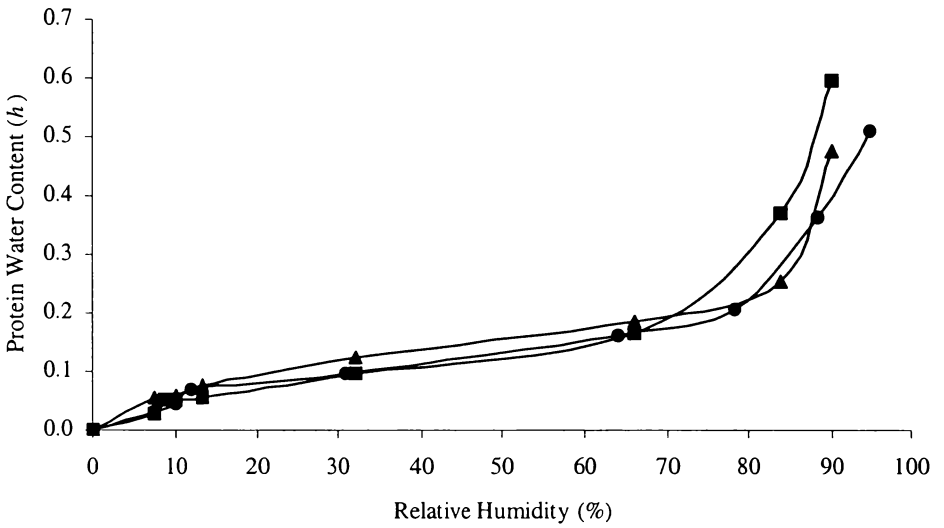

Figure 5.5. Effect of RH on the water content of lysozyme, semi-purified PLE and semi-purified *Candida rugosa* Lipase B at 20°C.

All three proteins were exposed to each RH for fourteen days. The proteins are as follows: PLE, ■; LipB, ▲; and lysozyme, ●. The zero water contents were calculated after fourteen days exposure to anhydrous P_2O_5 at 65°C.

5.3 CONCLUSIONS

Sequential hydration of five globular proteins (PLE, LipB, lysozyme, BSA and Hammerstein casein) with saturated salt solutions generates adsorption isotherms that share the three regions characteristic of this type of plot - the 'knee', plateau and upswing – but differ in the total water content produced at each RH. Consequently, the lysozyme adsorption isotherm (Figure 5.2) has limited use as a reference isotherm to determine the water content of other globular proteins (both the equilibration time and final water content are unique to each protein).

The water content of proteins exposed to RH's above 70% does not readily equilibrate, but steadily increases over the two week experimental period. Thus, water content calculations at every RH must specify the time of exposure. Furthermore, accurate calculation of zero water content requires a combination of both high temperature (65°C) and exposure to the drying agent, anhydrous P_2O_5. In contrast with exposure to anhydrous P_2O_5 at 20°C, additional losses in water content were achieved at 65°C (where there was a loss of 0.074 *h* at 65°C, compared to 0.050 *h*, for lysozyme).

The adsorption isotherms of PLE and LipB are required for the protein hydration-vapor phase activity experiments performed in Chapter 6. Lyophilised PLE and LipB are hydrated to a known water content (determined with the adsorption isotherms generated in this Chapter) using saturated salt solutions, and the rate of hydrolysis of vapor-phase ethyl butyrate at each water content was determined by gas chromatography.

CHAPTER 6 ENZYME HYDRATION AND FUNCTION

Esterase catalysis of substrate vapor: Enzyme activity occurs at very low hydration

Penelope A. Lind and Roy M. Daniel*

Department of Biological Sciences, University of Waikato, Private Bag 3105, Hamilton, New Zealand

Running Title: Activity of partially hydrated esterases in substrate vapor

* To whom correspondence should be addressed (e-mail r.daniel@waikato.ac.nz)

Key Words: hydrolase, lipase, water, dynamics

Abbreviations used: *h*, protein water content (grams of water per gram of protein); Lipase B, *Candida rugosa* Lipase B; RH, relative humidity.

SYNOPSIS

It has been generally accepted that enzyme activity requires a minimal hydration of about 0.2 g $H_2O.g^{-1}$ protein. This fits well with evidence that hydration above this level is associated with the onset of intramolecular motions.

The influence of enzyme hydration on the hydrolysis of substrate by *Candida rugosa* Lipase B and pig liver esterase was investigated. Each enzyme was studied as a powder at various hydration levels, using vapour phase ethyl butyrate as substrate. This procedure allows the separation of those effects that are due to hydration from those arising from diffusional constraints. We found hydrolytic activity in both enzymes at all hydration levels above zero (between 0.054-0.47 and 0.029-0.60 g $H_2O.g^{-1}$ protein, respectively) that were investigated, down to <0.03 g $H_2O.g^{-1}$ enzyme, corresponding to a coverage of about 10% of the enzyme surface by water molecules. The hydrolytic activity of both enzymes was dependent on protein hydration: But since the hydrolysis of ethyl butyrate requires water as a second substrate, the absence of activity at zero hydration does not rule out the possibility of enzyme activity in the absence of water.

These results suggest that the properties conferred on proteins by water, at least above 10% surface coverage (in this case corresponding to a hydration level of 0.03 g $H_2O.g^{-1}$ protein), are not a requirement for enzyme catalysis.

INTRODUCTION

It is generally accepted that protein hydration is essential for enzyme catalysis to occur, and that dry enzymes are inactive. Although there are varying estimates of the degree of hydration required for activity, a threshold value of about 0.2 g $H_2O.g^{-1}$ protein, i.e. 0.2 *h*, is generally accepted [1-5]. However, there are reports from studies on enzyme powders that enzyme activity may be possible at lower (0.11-0.15 *h*) hydration levels [eg 6, 7], including a report of activity in a dry hydrogenase [8] and evidence of enzyme activity in milk powders at < 0.10 *h* [9]. However, one difficulty with measuring activity in enzyme powders of low hydration is the absence of a medium for the diffusion of substrate and product. The approach involving the rapid mixing and freeze drying of enzyme and substrate solutions, for example, is likely to lead to measurements of product release rather than catalysis, and if enzyme cofactors such as NAD are involved the rates may be limited by the local availability of these rather than the hydration state of the enzyme. There is good evidence from work on enzyme catalysis in dry organic solvents that activity may be possible at very low hydrations [10, 11], but interpretation of this work is complicated by the likelihood that the organic solvent is replacing water at sites on the enzyme, as well as performing a hydration function by loosening the structure [12-14].

To date, studies using enzyme catalysis of gas phase substrates have had a biotechnological focus [15-20] but the obviation of any need for a diffusion medium for substrate and product gives the technique important potential in determining the hydration limits within which enzyme activity is possible. In this paper, we have examined the effect of hydration on enzyme catalysis, in the absence of any requirement for water as a diffusion medium, by using vapour phase substrates. This approach also avoids the complication found in organic solvent work that the solvent may be affecting protein structure and hydration.

If enzyme catalysis is possible at appreciably lower hydration levels than 0.2 *h* (and in the absence of organic solvents), this will have significant implications for our understanding of the role of water in enzyme catalysis and protein structure. The onset of enzyme catalysis at the accepted value of ~0.2 *h*, corresponding in lysozyme to a water:enzyme mole ratio of ~160 and a surface coverage of 40-45% [21, 22], coincides with (1) a greater conformational freedom in the water arrangements on the protein surface; (2) a transition at ~0.25 *h* that is

associated with the covering of the weakest interacting regions of the protein surface; and (3) the onset of intramolecular motions [1-5, 23-25]. Overall, hydration is thought to regulate the internal molecular motions that are necessary for catalysis, as well as acting as a diffusion medium.

In this work *Candida rugosa* Lipase B and pig liver esterase were equilibrated to known hydration levels using atmospheres of specific RH (generated by saturated salt solutions), and the rate of hydrolysis of vapor phase ethyl butyrate investigated. We found enzyme activity to be possible at much lower protein hydration than expected.

EXPERIMENTAL

Materials

Candida rugosa Lipase B (Lipase B, 105 units.mg^{-1}) was purchased from BioCatalyst (Wales, UK). Pig liver esterase (pig liver esterase, 150 units.mg^{-1}) was obtained from Sigma (St. Louis, MO, USA). Both enzymes were purified, deionized, lyophilized and stored at 5°C. Ethyl butyrate (>98% GC) was acquired from Fluka Chemie Ag (Buchs, Switzerland) and water was obtained through a Milli Q system (Millipore, France). Glass Fibre Paper (GF/B) and Mininert® valves were purchased from Whatman (Maidstone, UK) and Pierce (Rockford, IL, USA), respectively. Fast Flow Q Sepharose was purchased from Pharmacia Biotech (Uppsala, Sweden). All other chemicals used were of Analytical Reagent grade.

Enzyme purification

Pig liver esterase and Lipase B were purified using Fast Flow Q Sepharose. A 350 ml column was packed using a thick slurry of the resin, which was pre-washed in alternate volumes of 0.01 M NaOH and 0.01 M HCl, followed by extensive washing with distilled water. The column was equilibrated by washing with 30 mM Mops-NaOH (pH 7.0) until the eluent pH was consistently 7.0 (approximately three column volumes). The flow rate was maintained at 10 ml.min^{-1} using a peristaltic pump and 10 ml fractions were collected. Pig liver esterase, dissolved in a minimum volume of the equilibration buffer with a conductivity reading less than 5 mS, was pumped onto the column and washed on with the equilibration buffer. Washing was continued until no protein was detectable in the eluent (A_{280}). Protein was initially eluted from the column using 0.1 M NaCl (prepared in equilibration buffer) until protein was not present in the eluent. Gradient elution was carried out with six column volumes of a linear salt gradient of 0.1 to 0.5 M NaCl in equilibration buffer. The eluent fractions were collected in an automated fraction collector. Carboxylesterase activity was assayed with 0.25 mM *p*NP-butyrate in 0.05 M Mops-NaOH buffer (pH 7.5) at 30°C. Active fractions were pooled, desalted and concentrated by diafiltration with an Amicon® YM10 membrane (Grace, MA, USA), and lyophilized. Lipase B was purified using an identical method to that described for the pig liver esterase, except that the column buffer was set at pH 6.5 and the salt gradient was

0.1-0.75 M NaCl. Pig liver esterase was purified 3.6 fold and Lipase B 4.7 fold, yielding specific activities of 203.7 and 87.09 μmol *p*NP-butyrate.min^{-1}.mg^{-1} protein, respectively, after diafiltration and lyophilization.

Determination of hydration isotherms

Hydration isotherm curves were obtained at 20°C using the gravimetric method to determine water content, *h* [26]. Gram quantities of casein and BSA, 100mg of lysozyme, and 30mg samples of lyophilized Lipase B and pig liver esterase were placed in a 500 ml sealed glass vessel that contained a saturated aqueous salt solution (10% of the vessel headspace, v/v). The saturated salt solutions and the RH's produced were as follows: LiBr, 7.2%; $ZnCl_2.xH_2O$, 10.0%; $LiCl.xH_2O$, 13.5%; $CaCl_2.xH_2O$, 32.3%; $NaNO_2$, 66.0%; KBr, 84.0%; and $ZnSO_4.7H_2O$, 90.0% [26-29]. To ensure uniform temperature, each vessel was incubated at 20 ± 0.3°C. The enzyme samples were exposed to the above range of relative humidities for three days to two weeks. Gravimetric data were obtained after three, six, ten and fourteen days and the enzyme water content for each RH was then calculated. To achieve zero water content (0 *h*), after preliminary drying each enzyme was exposed to about 20 g of fresh anhydrous P_2O_5 at 65°C for 14 days, and gravimetric measurements were obtained as previously described.

Gas-phase hydrolysis

Aqueous solutions of lyophilized Lipase B and pig liver esterase in 0.02% (w/v) sodium azide, pH 7.5 were prepared and the protein content of each sample was determined by the far-UV method [30]. Aliquots containing 1 mg Lipase B and 0.5 mg pig liver esterase were applied to separate pieces of 0.5 x 1.5 cm Glass Fibre Paper (GF/B) and air-dried for 30 minutes at room temperature and humidity. Appropriate controls, including 'no-enzyme' and autoclaved enzyme labels, were run in parallel with each experiment. In 8 ml Hungate tubes, each label was suspended above 0.8 ml of the appropriate saturated salt solution (see above) used to give the relative humidity required [26-29]. The Hungate tube was sealed with a Mininert® valve (Teflon lined) and each label was adjusted to the desired water content prior to reaction by pre-equilibration at 20°C for 3 days with the vapor phase in the absence of substrate.

The reaction was initiated by the injection of 3.6 μl ethyl butyrate into a headspace volume of 7.2 ml, corresponding to a vapor-phase concentration of 500 ppm (v/v), through the Mininert® valve septum onto an enzyme-free GF/B label (dimension as described above). The reactions were carried out at 20°C for fifteen minutes. Quantitative assessment of ester hydrolysis was based on the measurement of ethanol production. This involved the removal of 20 μl vapor phase samples through the Mininert® valve for injection onto the GCD Chromatograph (a standard curve was used to calculate ethanol production) at two time points during the incubation. Enzyme activity was defined as nmoles of ethanol produced per minute per mg of enzyme powder used in the label.

Gas chromatography

Ethyl butyrate and ethanol were analyzed by a Pye Unicam GCD Chromatograph equipped with flame ionization detection (FID) and a 0.5 m x 3 mm internal diameter column, packed with Chromosorb™ 101, 100/120 mesh (Supelco, Bellefonte, PA, USA). The column temperature was maintained at 170°C, nitrogen (40 $ml.min^{-1}$) was the carrier gas, and hydrogen and air were supplied to the FID. Quantitative data acquisition was obtained through a Spectra Physics SP4100 integrator.

RESULTS AND DISCUSSION

Standard hydration isotherms were generated from the exposure of Casein, BSA, lysozyme, pig liver esterase and Lipase B to a series of different RH's generated with appropriate saturated salt solutions [26-29], compared with zero hydration values generated by exposure to fresh P_2O_5 at 65°C. These showed that protein-water content equilibration at up to 80% RH was complete within three days: All proteins exhibited the sigmoidal shape and three regions of hydration common to protein-water adsorption isotherms - the knee, plateau and upswing [2] (data not shown), although the data for the upswing portion of the curve, corresponding to RH values above 80%, was less consistent and slower to reach equilibrium. Hydration data obtained at RH values below 80% ($h \leq 0.2$) were significantly more reproducible. Minor but consistent differences in the hydration level achieved at the same RH level were observed between the different proteins, with the hydration of pig liver esterase being consistently lower than Lipase B. At the lowest level of hydration at which activity was measured ($h = 0.029$, for pig liver esterase), the water in the experimental system was distributed as follows: in the atmosphere, at RH 7.2%, 12.0 μg; bound to the 500 μg pig liver esterase, 14.6 μg; consumed in the ester hydrolysis during the 15 minutes of the reaction, 0.06 μg.

The effect of enzyme hydration on the vapor phase esterase activity of Lipase B and pig liver esterase is shown in Figures I and II, respectively. Lipase B and pig liver esterase exhibited activity at hydration levels greater than, and equal to, 0.029 and 0.054 h, respectively. Lipase B hydrolytic activity appeared to be more strongly dependent on the degree of protein hydration than pig liver esterase activity. Overall, the graphs indicated that enzyme activity might also occur below the hydration levels used here.

No activity can be expected at zero hydration since water is a substrate for the (hydrolytic) reaction. It is therefore not possible to state from the data here that anhydrous enzymes are not active.

The activity data have been fitted to straight lines in Figures I and II, but given that one would expect water concentration to be limiting, the plots will only be linear if the K_m for water is well above the water concentrations used here. The shape of the curve will depend on two phenomena: the effect of hydration on activity and the effect of the K_m for water, and it has not been possible to separate

these. Although the source of the substrate water has the potential to influence the reaction rate, in these experiments the water consumed by the reaction at the lowest hydration levels of the enzyme at which activity was observed was an amount equivalent to less than 1% of the total of both the atmosphere water and the water hydrating the enzyme. The corresponding percentages at higher hydration levels were lower.

The observation of pig liver esterase and Lipase B activity at very low hydration levels, well below that expected for activity (i.e. at <0.03 *h* rather than ~0.2 *h*), is significant because it clearly suggests that many of the properties conferred on proteins by water are not necessary for activity.

Since the 1980's, the 0.2 *h* enzyme water content has been widely accepted as the threshold hydration level required for activity. A variety of observations made as enzymes (mostly lysozyme) are hydrated from the anhydrous state to the solution state [1, 2, 4, 5, 23-25, 31], have associated hydration changes with changes in protein-water interactions and particularly with protein dynamics. The process seems to involve four stages. In the first, from 0 to 0.07 *h* (grams of water per gram of protein), a proton redistribution occurs where *ca.* two water molecules interact with each charged protein group. This corresponds to a mole ratio of about 0 - 55 water molecules per enzyme molecule (typically lysozyme). If we accept that lysozyme is completely covered at a ratio of ~390 [21, 22], then this corresponds to 0 – 15% surface coverage of the enzyme. Stage two is 0.07 to 0.30 *h*, where saturations of the charged and polar protein groups are associated with the initiation of water cluster formation, corresponding to a mole ratio of 55 up to 250, at which point all polar groups are covered, and 15 - 65% coverage. In stage three, between 0.30 and 0.50 *h*, weakly interacting surface regions are covered until water monolayer formation is complete at 0.50 *h*. In stage four, above 0.50 *h*, cooperative interactions occur between water molecules and hydration shells form around the protein surface. At this point, lysozyme displays dilute solution thermodynamics properties and the bound hydration water has mobility close to that of the bulk solvent.

A variety of research shows the onset of protein motions at ~ 0.2 *h*, observed in lysozyme, subtilisin Carlsberg, α-chymotrypsin and α-amylase, and a correlation of this with the onset of enzyme catalysis in hydrated enzyme powders [1, 2, 4, 6, 7, 24, 31, 32]. This fits with the view that one of the fundamental

requirements for enzyme catalysis is conformational flexibility. Conformational flexibility, of the order of (sub)-nanoseconds, is expected to maximize favorable enzyme interactions with the substrate in the initial and transition state, allowing the enzyme to undergo multiple conformations, and therefore increase the statistical probability that a conformational state capable for binding and converting a substrate will be achieved [eg, ref 25].

In this work, the water:enzyme molar ratio at the lowest hydration level (h = ~0.03) at which activity was observed for pig liver esterase is about 100, allowing ~10% surface coverage. This corresponds to the mid-point of stage one, above: There will be only about 15% coverage of polar groups, and there are certainly too few water molecules to promote conformational flexibility. Although the effect of hydration on the dynamics of the two enzymes investigated here has not been determined, there is no reason to suppose that their behaviour in this respect will differ from other proteins. Every protein so far investigated shows a clear cessation of intramolecular motions below ~0.2 h [2, 6]. Since most of the proteins investigated have been fairly small this corresponds to a water:enzyme mole ratio in the range 160-310, and a surface coverage of 40-50%.

The inference of the results here is specifically that enzyme activity is possible independent of internal dynamics: And more generally that enzyme activity is not dependant upon the properties conferred upon proteins by water above hydration levels corresponding to a surface coverage of about 10%, and only about 15% coverage of polar groups. This is in keeping with observations made using enzymes in dry organic solvents, where activity has been observed at very low hydration levels [10, 11], but where interpretation has been complicated by the possibility of the organic solvents themselves activating dynamics. It is also in keeping with results showing that enzymes are active at temperatures where sub-nanosecond anharmonic dynamics have ceased [33-35].

One possible explanation arises from the fact that most of the techniques, such as neutron beam spectroscopy, which are used to investigate protein dynamics give a global average of all protein dynamic motions. As has been pointed out [36], the accuracy of these techniques is such that dynamics confined to the active site might not be detected: And enzyme activity is likely to be dependant on dynamics at the active site. The high reactivity of enzyme active sites is likely to be conferred by greater flexibility than the rest of the enzyme.

The active site may thus be less dependent upon hydration, or temperature, for its flexibility than the protein as a whole. Another possibility, which we believe is less likely, is that the active site is preferentially hydrated; i.e. at low hydration water tends to be concentrated at the active site.

ACKNOWLEDGEMENTS

We thank BioCatalyst (Wales, UK) for the gift of *Candida rugosa* Lipase B, and Colin Monk for technical assistance.

REFERENCES

1. Rupley, J.A., Gratton, E. and Careri, G. (1983) Water and globular proteins. TIBS **8**, 18-22

2. Rupley, J.A. and Careri, G. (1991) Protein hydration and function. Adv. Prot. Chem. **41**, 37-172

3. Franks, F. (1993) Protein hydration. In Protein Biotechnology (Franks, F., ed.), pp. 437-465. The Humana Press Inc., New Jersey

4. Careri, G., Giansanti, A. and Gratton, E. (1979) Lysozyme film hydration events: an IR and gravimetric study. Biopolymers **18**, 1187-1203

5. Finney, J.L. (1996) Hydration processes in biological and macromolecular systems. Faraday Disc. **103**, 1-18

6. Stevens, E. and Stevens, L. (1979) The effect of restricted hydration on the rate of glucose 6-phosphate dehydrogenase, phosphoglucose isomerase, hexokinase and fumarase. Biochem. J. **179**, 161-167

7. Drapron, R. (1985) Enzyme activity as a function of water activity. NATO Advanced Study Institution Series, Series E. **90**, 171-190

8. Yagi, T., Tsuda, M., Mori, Y. and Inokuchi, H. (1969) Hydrogenase activity in the dry state. J. Am. Chem. Soc. **91**, 2801

9. Chen, L. (2001) *Thermophilic Enzymes and Their Impact on Milk Powders During Storage.* Ph.D Thesis, University of Waikato, Hamilton, New Zealand

10. Valivety, R.H., Halling, P.J. and Macrae, A.R. (1992) *Rhizomucor miehei* lipase remains highly active at water activity below 0.0001. FEBS Lett. **301**, 258-260

11. Klibanov, A.M. (1989) Enzymatic catalysis in anhydrous organic solvents. TIBS **14**, 141-144

12. Affleck, R., Xu, Z-F., Suzawa, V., Focht, K. and Clark, D.S. (1992) Enzymatic catalysis and dynamics in low-water environments. Proc. Natl. Acad. Sci. USA **89**, 1100-1104

13. Broos, J., Visser, A.J.W.G., Engbersen, J.F.J., Verboom, W., van Hoek, A. and Reinhoudt, D.N. (1995) Flexibility of enzymes suspended in organic solvents probed by time-resolved fluorescence anistropy. Evidence that enzyme activity and enantioselectivity are directly related to enzyme flexibility. J. Am. Chem. Soc. **117**, 12657-12663

14. Wu, J. and Gorenstein, D.G. (1993) Structure and dynamics of cytochrome c in nonaqueous solvents by 2D NH-exchange NMR spectroscopy. J. Am. Chem. Soc. **115**, 6843-6850

15. Pulvin, S., Legoy, M.D., Lortie, R., Pensa, M. and Thomas, D. (1986) Enzyme technology and gas phase catalysis: Alcohol dehydrogenase example. Biotechnol. Lett. **8**, 783-784

16. Barzana, K., Klibanov, A.M. and Karel, M. (1987) Enzyme-catalysed gas phase reactions. Appl. Biochem. Biotechnol. **15**, 25-33

17. Barzana, K. and Karel, M. (1989) Enzymatic oxidation of ethanol in the gas phase. Biotechnol Bioeng. **34**, 1178-1185

18. Parvaresh, F., Robert, H., Thomas, D. and Legoy, M.D. (1992) Gas phase transesterification catalysed by lipolytic enzymes. Biotechnol. Bioeng. **39**, 467-473

19. Hwang, S., Trantolo, D. and Wise, D. (1993) Gas phase acetaldehyde production in a continuous bioreactor. Biotechnol. Bioeng. **42**, 667-673.

20. Lamare, S., and Legoy, M.D. (1995) Working at controlled water activity in a continuous process: the gas/solid system as a solution. Biotechnol. Bioeng. **45**, 387-397

21. Finney, J.L. and Poole, P.L. (1984) Comments on Molecular and Cellular Biophysics **2,**

129-151.

22. Finney, J.L., Goodfellow, J.M. and Poole, P.L. (1982) In Structural Molecular Biology

(Davies D.B., Danyluk, S. and Saenger, W., eds), p 387. Plenum press, New York

23. Careri, G., Gratton, E., Yang, P-H. and Rupley, J.A. (1980) Correlation of IR spectroscopic, heat capacity, diamagnetic susceptibility and enzymic measurements on lysozyme powder. Nature (London) **284**, 572-573

24. Yang, P-H. and Rupley, J.A. (1979) Protein-water interactions: Heat capacity of the lysozyme-water system. Biochemistry **18**, 2654-2661

25. Schinkel, J.E., Downer, N.W. and Rupley, J.A. (1985) Hydrogen exchange of lysozyme powders. Hydration dependence of internal motions. Biochemistry **24**, 352-366

26. O'Brien, F.E.M. (1948) The control of humidity by saturated salt solutions. J. Sci. Instr. **25**, 73-76

27. Richardson, G.M. and Malthus, R.S. (1955) Salts for static control of humidity at relatively low levels. J. Appl. Chem. **5**, 557-567

28. Rockland, L.B. (1960) Saturated salt solution for static control of relative humidities between 5° and 40°C. Anal. Chem. **32**, 1375-1376

29. Weast, R.C. and Astle, M.J. (1982) CRC Handbook of Chemistry and Physics, CRC Press, Inc., Florida

30. Scopes, R.K. (1994) Protein Purification: Principles and Practice, Springer-Verlag New York, Inc., New York

31. Poole, P.L. and Finney, J.L. (1986) Solid-phase protein hydration studies. Methods Enzymol. **127**, 284-293

32. Lüscher-Mattli, M. and Rüegg, M. (1982) Thermodynamic functions of biopolymer hydration. I. Their determination by vapor pressure studies, discussed in an analysis of the primary hydration process. Biopolymers **21**, 403-418

33. Daniel, R.M., Smith, J.C., Ferrand, M., Hery, S., Dunn, R. and Finney, J.L. (1998) Enzyme activity below the dynamical transition at 220K Biophys. J. **75**, 2504-2507

34. Dunn, R.V., Reat, V., Finney, J.L., Ferrand, M., Smith, J. C. and Daniel, R.M. (2000) Enzyme activity and dynamics: Xylanase activity in the absence of fast anharmonic dynamics. Biochem. J.
346, 355-358

35. Bragger, J.M., Dunn, R.V. and Daniel, R.M. (2000) Enzyme activity down to –100°C. Biochim. Biophys. Acta **1480**, 278-282

36. Daniel, R.M., Finney, J.L., Reat, V., Dunn, R., Ferrand, M. and Smith, J.C. (1999) Enzyme dynamics and activity: Timescale dependance of dynamical transition in glutamate dehydrogenase solution. Biophys. J. **77**, 2184-2190

FIGURE LEGENDS

Figure I. Effect of enzyme hydration (between 0 and 0.5 *h*) on the vapor-phase activity of *Candida rugosa* Lipase B.

Two sets of *C. rugosa* Lipase B vapor-phase activity data (■, □) were obtained at 20°C against a vapor-phase ethyl butyrate concentration of 500 ppm (v/v). The linear relationship between Lipase B water content (*h*) and specific activity for the ■ (——), □ (------) and combined (— —) data sets are described by the equations $y = 80.20x + 3.96$ ($R^2 = 0.96$), $y = 55.00x + 6.75$ ($R^2 = 0.97$) and $y = 57.17x + 6.32$ ($R^2 = 0.96$), respectively.

Figure II. Effect of enzyme hydration (between 0 and 0.6 *h*) on the vapor-phase activity of pig liver esterase.

Two sets of pig liver esterase vapor-phase activity data (▲, Δ) were obtained at 20°C against a vapor-phase ethyl butyrate concentration of 500 ppm (v/v). The linear relationship between pig liver esterase water content (*h*) and specific activity for the ▲ (——), Δ (-------) and combined (— —) data sets are described by the equations $y = 27.96x + 3.80$ ($R^2 = 0.81$), $y = 14.87x + 4.90$ ($R^2 = 0.91$) and $y = 17.45x + 4.74$ ($R^2 = 0.77$), respectively.

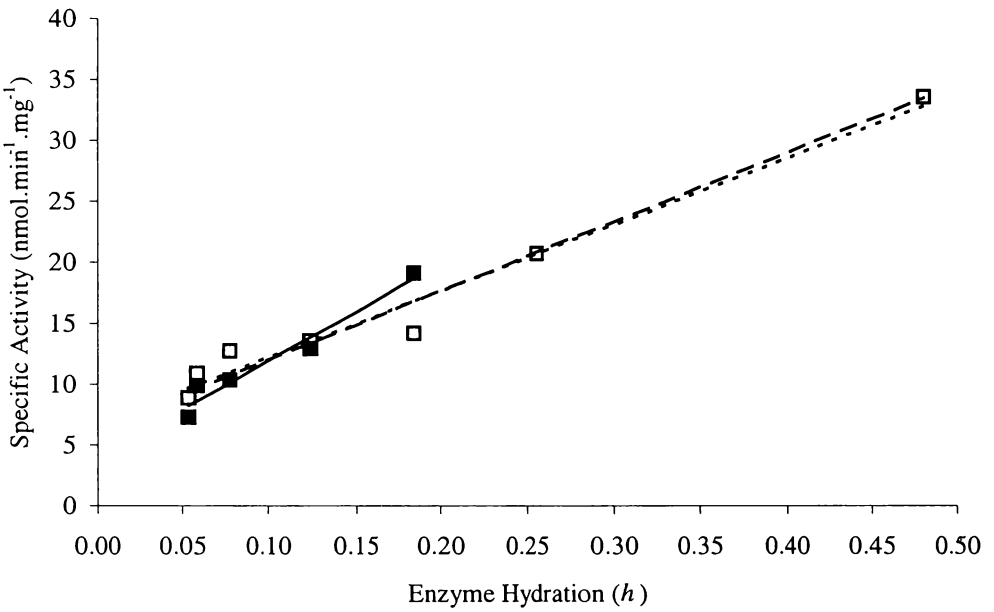
Specific Activity (nmol.min-1.mg-1)
40
35
30
25
20
15
10
5
0
0.00
0.05
0.10
0.15
0.20
0.25
0.30
0.35
0.40
0.45
0.50
Enzyme Hydration (h)

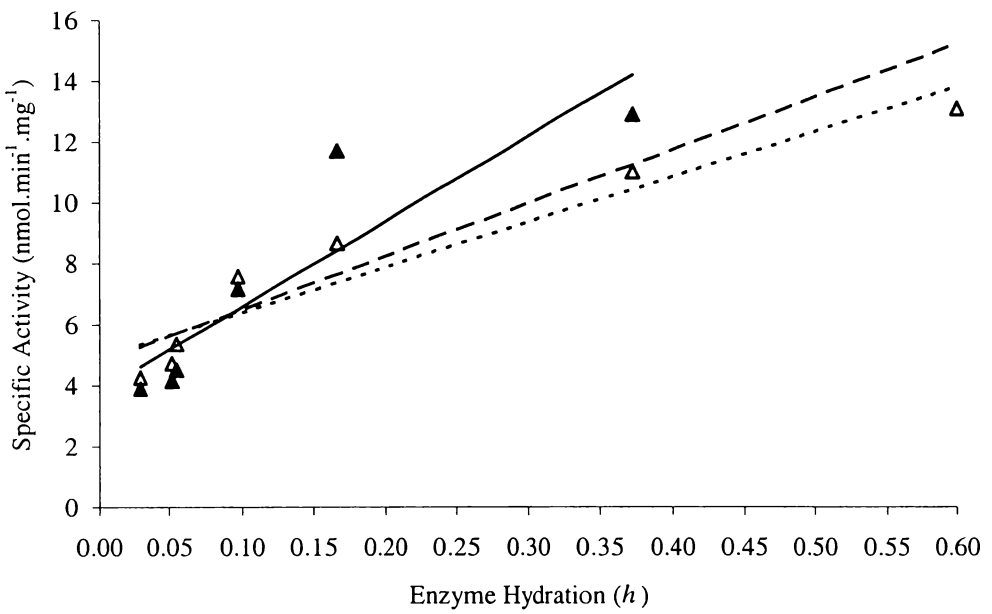
Specific Activity (nmol.min-1.mg-1)
16
14
12
10
8
6
4
2
0
0.00
0.05
0.10
0.15
0.20
0.25
0.30
0.35
0.40
0.45
0.50
0.55
0.60
Enzyme Hydration (h)

CHAPTER 7 FINAL DISCUSSION

During the development of the biosensor, I optimised the various components, which are effectively an enzyme, pH indicator dye and support matrix. In addition to those three components, I investigated the effect on the biosensor enzyme of various additives, such as preservatives and humectants, and of the operating and storage conditions likely to be encountered in a commercial biosensor application. However, I was not involved in the testing of the biosensor *in situ* by our commercial partners.

By screening other enzymes/organisms, I found possible enzyme alternatives to PLE for the biosensor. The alternate enzymes have particular advantages with respect to activity exhibited towards certain ester substrates, pH- and temperature-stability, public acceptance of the enzyme source in international consumer markets, and food safety. I have also found that different biosensor applications will require different enzymes due to the numerous esters that the biosensor may encounter. Of the 24 microbial enzymes screened in this work, *Candida rugosa* LipB was judged best suited for use in the ester biosensor application. LipB was amongst the least inhibited enzyme when pH fell to between 4 and 5, it hydrolysed all three esters likely to be encountered in the commercial biosensor application, in terms of pH-, temperature- and hydration stability Lipase B was superior to PLE, it complied with the commercial requirement for a non-mammalian enzyme, and it was both Kosher and GRAS certified.

I looked briefly at pH indicator dyes, but the choice is extremely limited because of food safety requirements and the pH range generated by the enzymatic hydrolysis of esters. This change in pH was followed both directly by measuring the pH with a micro-electrode, and indirectly through colour changes in the pH indicator dye. Phenol red was the best pH indicator dye, with respect to the paper-based biosensor, because its effective pH range (6.8-8.4) included the pH optimum of both PLE and LipB, and the dye did not incur food safety issues.

Because of the difficulties associated with the agar gel system (CO_2 accumulation, handling, storage) I investigated the possibility of using a paper-adsorbed preparation. I expected that hydration of the enzyme might be a problem in dry atmospheres because previous work showed that 20% water was

needed for enzyme activity. By carrying out vapor phase experiments I discovered that PLE and LipB were hydrolytically active at ≥ 3% hydration, 0.03 *h* (i.e., the biosensor enzyme could work in near-dry conditions).

Consequently, the biosensor no longer required a gel (agarose) matrix, or humectant, to retain large quantities of water so that the enzyme was fully hydrated, and adequately active, during biosensor storage and operational use. Thus, the biosensor will function with a dry (paper-based) matrix that both simplified the biosensor structure and largely eliminated the effect of CO_2 accumulation within the matrix. Furthermore, the transition from the agarose matrix to the paper matrix resulted in enhanced biosensor stability since the enzyme is poised at a considerably lower hydration level and, as expected, enzymes at low hydration level exhibit higher stability.

The combination of these findings has been successfully put into use at the laboratory level.

The discovery that dry, or near dry, enzymes are active has implications much wider than those for the biosensor do. Although it has been stated that liquid water is an essential of life, questions such as "is water necessary for enzyme activity, and if so, why?" need to be resolved. Likewise, the possibility that life may be possible on dry, and therefore assumed lifeless, planets should seriously be considered.

To answer then question " are anhydrous enzymes active?" future research will investigate the gas-phase activity of enzymes that catalyse gas phase substrates but do not require water as a substrate in either the forward or reverse reaction (this will separate the effect of hydration from the effect of the K_m for water on enzyme activity). Examples of enzyme targets include alcohol dehydrogenase (ethanol + NAD^+ → acetaldehyde + NADH) and mandelonitrile lyase (mandelonitrile → benzaldehyde + HCN).

A APPENDICES

A1 APPENDIX ONE: GC STANDARD CURVES

A1.1 Ethyl Acetate

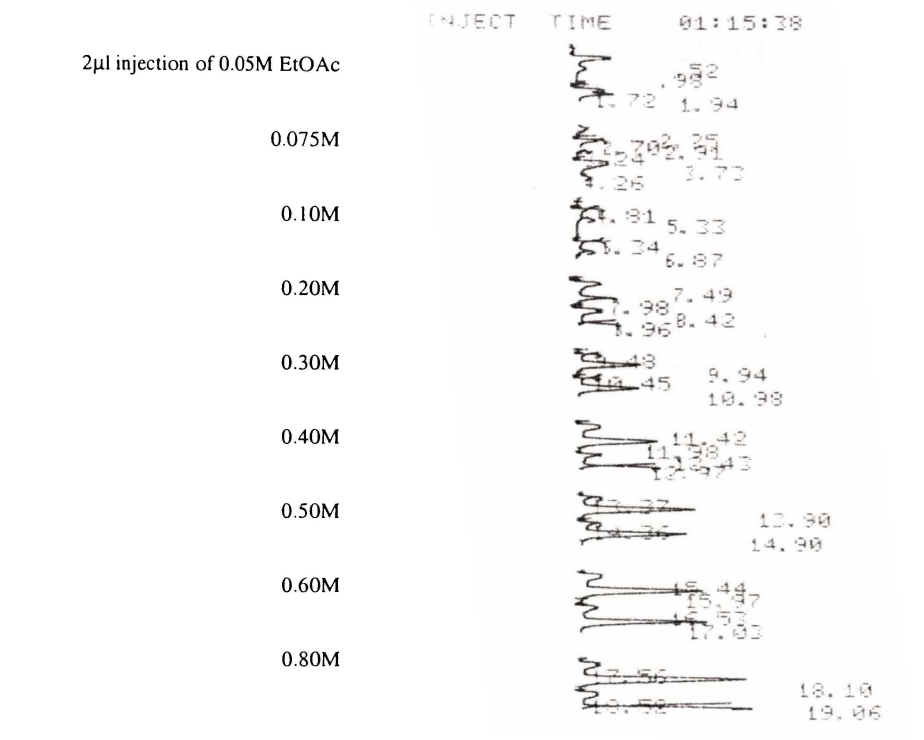

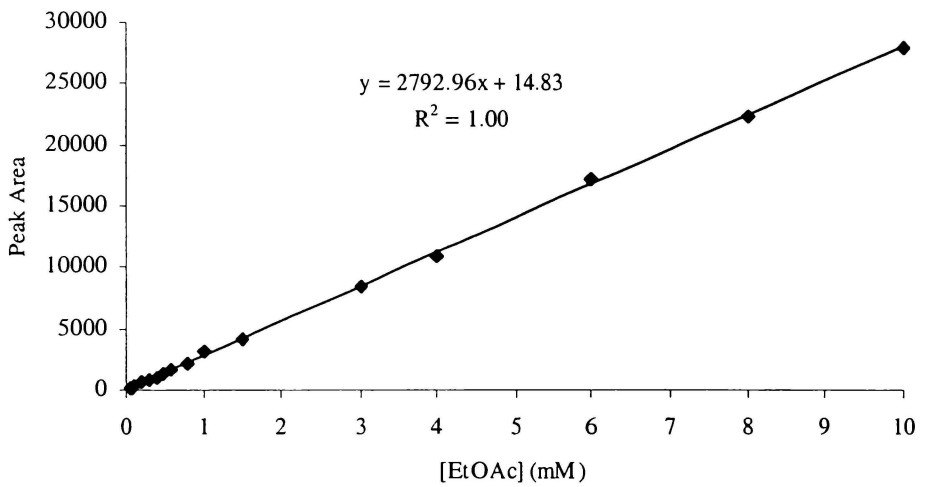

Figure A1.1. Ethyl acetate standard curve.

2µl samples were injected onto a 0.5m x 3mm internal diameter Chromosorb™ 101 (100/120 mesh) packed column maintained at 170°C and linked to a Spectra Physics SP4100 integrator.

A1.2 Ethanol

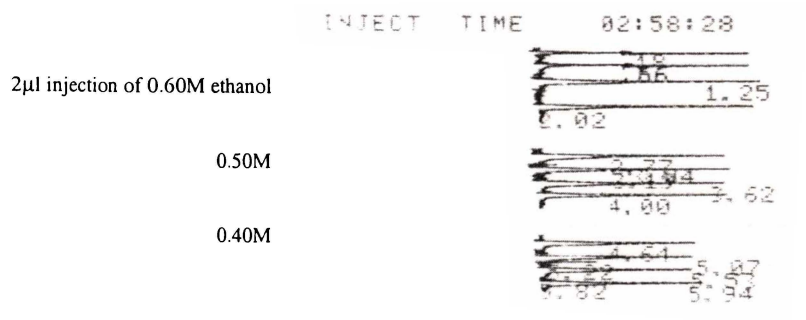

Table A1.1 GC ethanol standard curve data

[EtOH] (mM)	total EtOH (nmol)	Peak Areas			Average
0.05	0.1	397	391	379	389
0.1	0.2	573	585	580	579
0.2	0.4	776	752	728	752
0.3	0.6	781	904	784	823
0.4	0.8	1008	1063	906	992
0.5	1	1144	1281	1336	1254
0.75	1.5	1471	1438	1475	1461
1	2	1719	1678	1646	1681
2.5	5	4100	3985	3887	3991
5	10	7153	6496	6581	6743
7.5	15	11008	10839	10710	10852
10	20	14188	14650	15153	14664
15	30	22180	23046	21728	22318
20	40	29945	29703	30306	29985
25	50	38649	36551	39561	38254

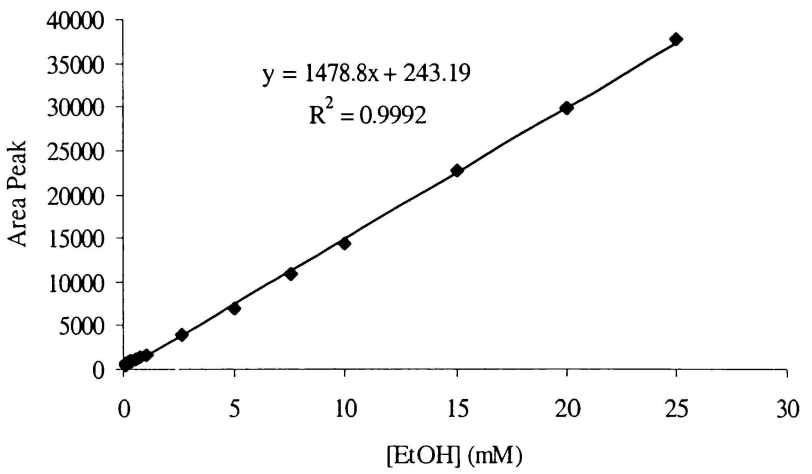

Figure A1.2. Ethanol standard curve.

2µl samples were injected onto a 0.5m x 3mm internal diameter Chromosorb™ 101 (100/120 mesh) packed column maintained at 170°C and linked to a Spectra Physics SP4100 integrator.

A2 APPENDIX TWO: PHASTGEL STAINING

Table A2.1.SDS 8-25% PhastGel (Method 7.0).

Step	Voltage (V)	Ampage (mA)	Wattage (W)	Temperature (°C)	Volt Hours (Vh)
7.1[1]	250	10	3.0	15	80
7.2	50	0.1	0.5	15	0

[1] Applicator down and up after 1 and 10Vh of Step 7.1, respectively.

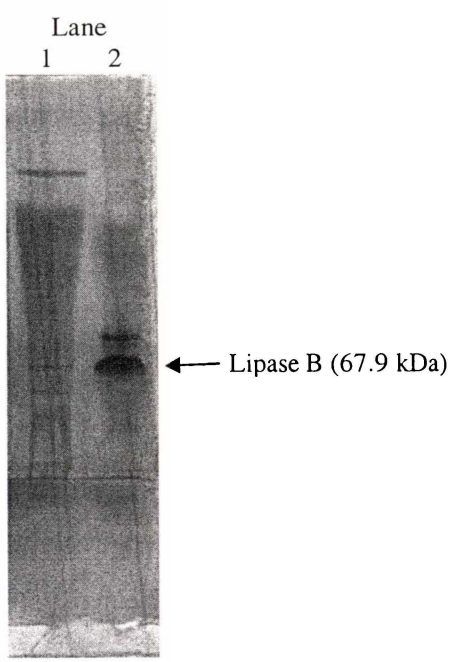

Figure A2.1. SDS 8-25% PhastGel of semi-purified *Candida rugosa* Lipase B

The protein loaded into the two lanes are as follows: Lane 1, pooled and ultrafiltered active FFQ-Sepharose fractions; Lane 2, pooled and ultrafiltered highly active FFQ-Speharose fractions. The 67.9 kDa Lipase B protein band was determined by observing activity against an overlay of pNP-butyrate.

A3 APPENDIX THREE: HANES PLOTS

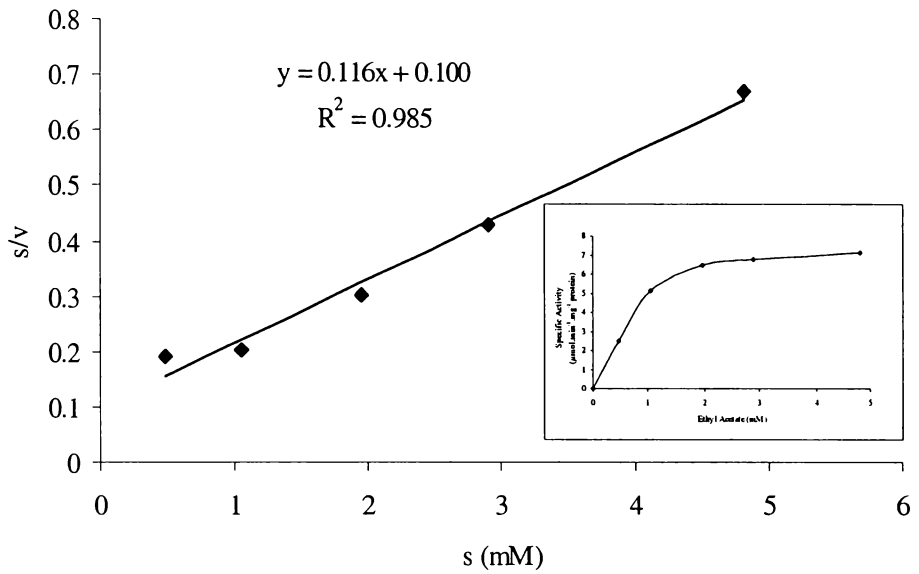

Figure A3.1. Hanes and Michaelis-Menten (inset) Plots of the hydrolysis of ethyl acetate by crude PLE at pH 7.5 and 30°C.

PLE was assayed with several concentrations of ethyl acetate in 50mM Mops-NaOH pH_{30}7.5..

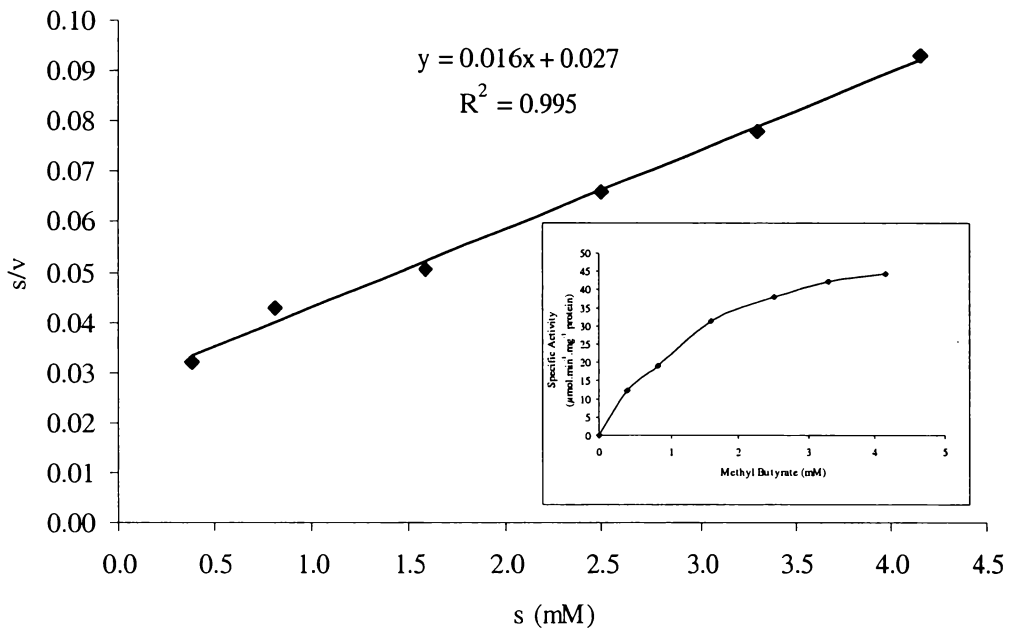

Figure A3.2. Hanes and Michaelis-Menten (inset) Plots of the hydrolysis of methyl butyrate by crude PLE at pH 7.5 and 30°C.

PLE was assayed with several concentrations of methyl butyrate in 50mM Mops-NaOH pH_{30}7.5.

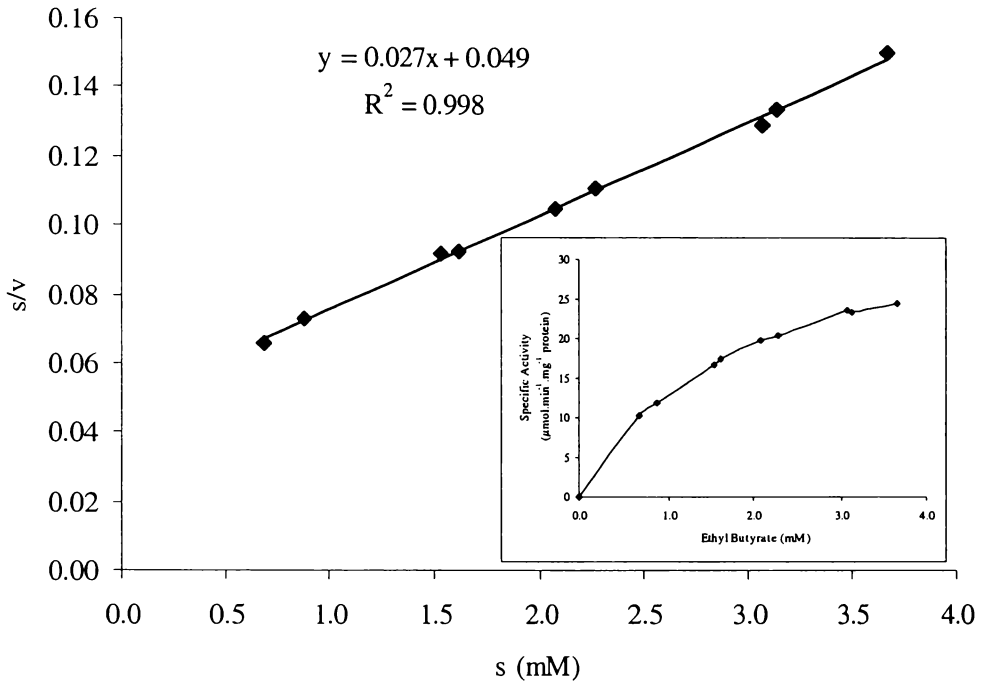

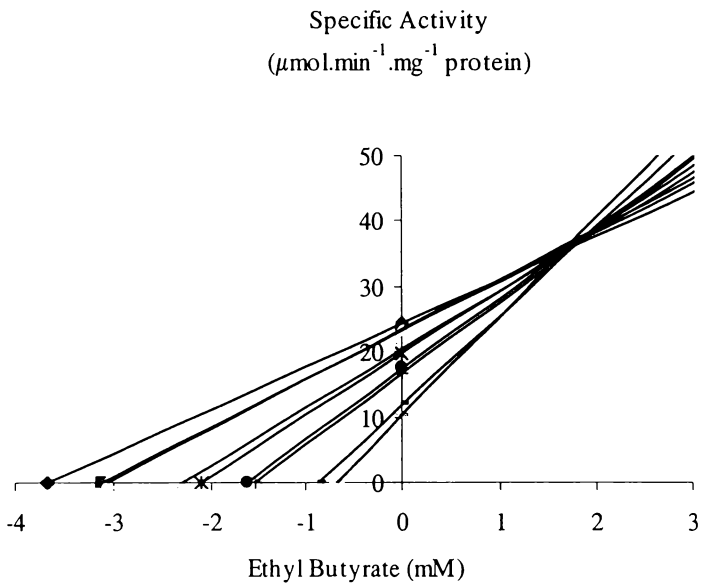

Figure A3.3. Hanes and Michaelis-Menten (inset) and Direct Linear (bottom) Plots of the hydrolysis of ethyl butyrate by crude PLE at pH 7.5 and 30°C.

PLE was assayed with several concentrations of ethyl butyrate in 50mM Mops-NaOH $pH_{30}7.5$.

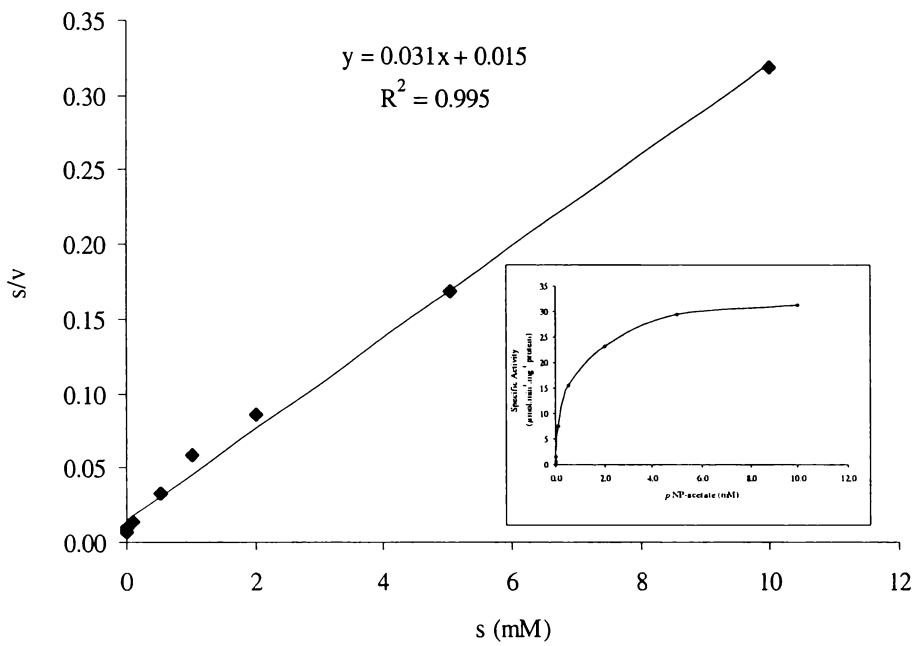

Figure A3.4. Hanes and Michaelis-Menten (inset) Plots of the hydrolysis of *p*NP-acetate by crude PLE at pH 7.5 and 30°C.

PLE was assayed with several concentrations of *p*NP-acetate in 50mM Mops-NaOH $pH_{30}7.5$.

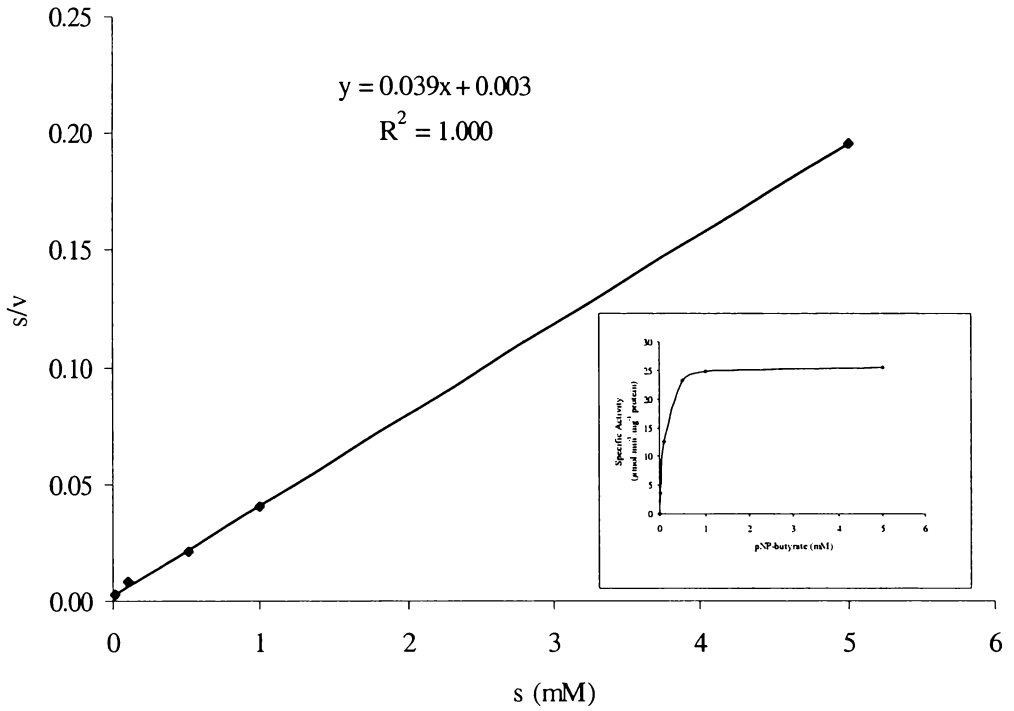

Figure A3.5. Hanes and Michaelis-Menten (inset) Plots of the hydrolysis of *p*NP-butyrate by crude PLE at pH 7.5 and 30°C.

PLE was assayed with several concentrations of *p*NP-butyrate in 50mM Mops-NaOH pH_{30}7.5.

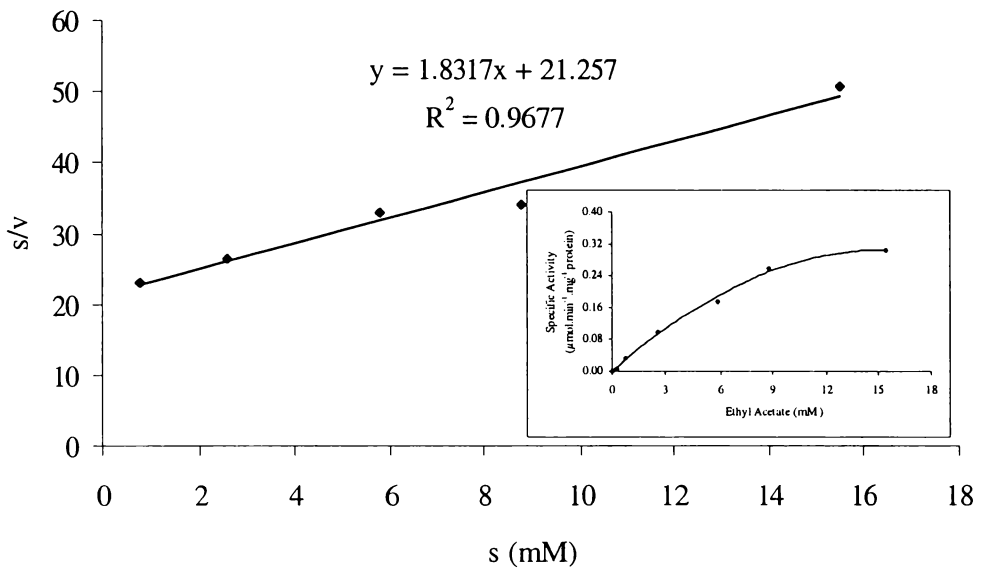

Figure A3.6. Hanes and Michaelis-Menten (inset) Plots of the hydrolysis of ethyl acetate by crude LipB at pH 7.5 and 30°C.

LipB was assayed with several concentrations of ethyl acetate in 50mM Mops-NaOH (5 mM $CaCl_2$), pH_{30}7.5.

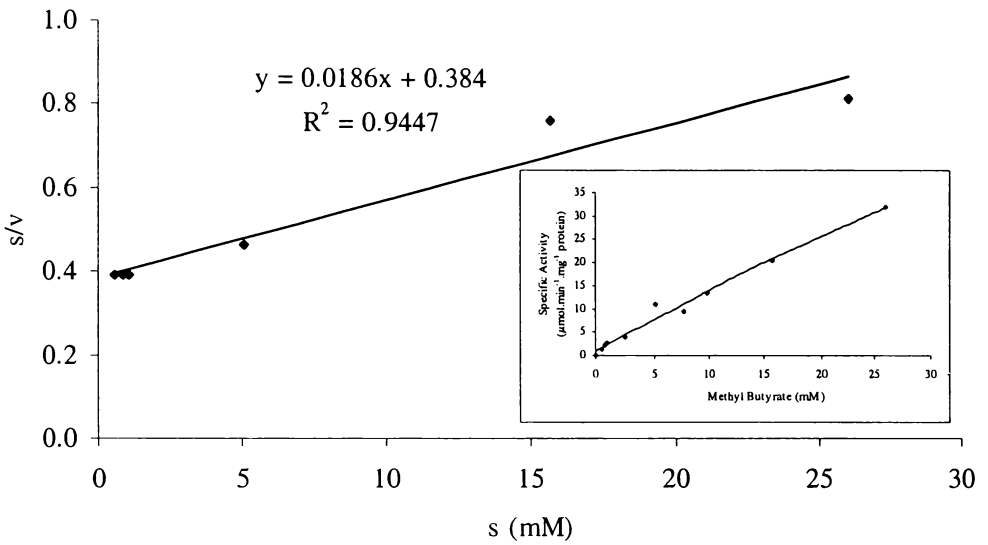

Figure A3.7.. Hanes and Michaelis-Menten (inset) Plots of the hydrolysis of methyl butyrate by crude LipB at pH 7.5 and 30°C.

LipB was assayed with several concentrations of methyl butyrate in 50mM Mops-NaOH (5 mM $CaCl_2$), $pH_{30}7.5$.

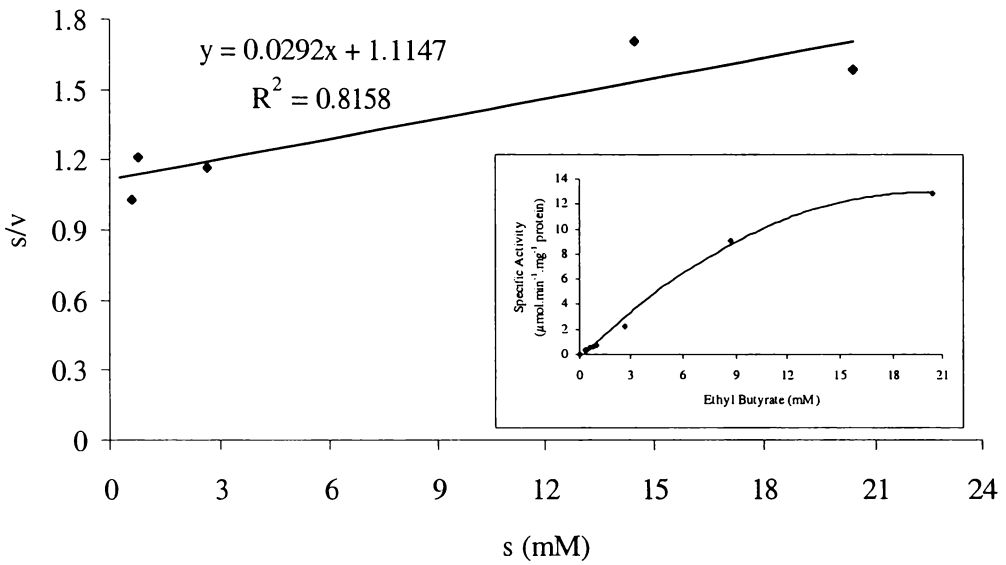

Figure A3.8. Hanes and Michaelis-Menten (inset) Plots of the hydrolysis of ethyl butyrate by crude LipB at pH 7.5 and 30°C.

LipB was assayed with several concentrations of ethyl butyrate in 50mM Mops-NaOH (5 mM $CaCl_2$), $pH_{30}7.5$.

A4 APPENDIX FOUR: ESTER CONCENTRATIONS IN THE LIQUID AND VAPOR-PHASE

Table A4.1. The conversion factor for the difference between the ester concentration of a solution and the vapor phase above.

Parameter	Equation	Unit	Ester		
			EtOAc	MeOBu	EtOBu
Ester density, *d*		($g.ml^{-1}$)	0.902	0.898	0.879
Ester molecular weight, MW		($g.mol^{-1}$)	88.1	102	116
1ml 20 ppm ester prepared in water contains *x*mol ester?	$0.02\mu l*d/1000\mu l*MW_{ester}$	mol	2.05E-07	1.76E-07	1.52E-07
1ml 20 ppm ester prepared in water contains *x*g of ester	$x$mol ester$*MW_{ester}$	g	1.80E-05	1.80E-05	1.76E-05
1ml 20 ppm ester prepared in water contains *x*mol water?	(1g-*x*g ester)/MW_{water}	mol	0.0556	0.0556	0.0556
The ester/water molar fraction in the 20 ppm solution	mol ester/mol water		3.69E-06	3.17E-06	2.73E-06
The ester P*i* at 293°K (using Raoults Law)	9.864KPa*mol fraction/101.325KPa	atm.°K.mol	3.59E-07	3.09E-07	2.66E-07
The ester vapor concentration (using the Ideal Gas Equation)	atm.°K.mol/0.082L.atm*293°K	$mol.l^{-1}$	1.49E-08	1.28E-08	1.11E-08
The volume occupied by 1mol of gas at 293°K	1mol/22.414L	$mol.l^{-1}$	4.46E-02	4.46E-02	4.46E-02
Molar ratio of ester to total gasses over the 20 ppm solution (i.e., the vapor-phase ester concentration)	ester vapor concentration/gas concentration	ppm	0.335	0.288	0.248
Dilution factor for the difference between the liquid- and vapor-phase ester concentrations			59.7	69.5	80.7

LIST OF REFERENCES

Ader, U., Andersch, P., Berger, M., Goergerns, U., Haase, B., Hermann, J., Laumen, K., Seemayer, R., Waldinger, C. and Schneider, M.P. (1997) Screening techniques for lipase catalyst selection. *Methods in Enzymology* **286:Part B**, 351-386.

Adler, A.J. and Kistiakowsky, G.B. (1962) Kinetics of pig liver esterase catalysis. *Journal of the American Chemical Society* **84:5**, 695-703.

Affleck, R., Xu, Z-F., Suzawa, V., Focht, K., Clark, D.S. and Dordick, J.S. (1992) Enzymatic catalysis and dynamics in low-water environments. *Proceedings of the National Academy of Science, USA* **89**, 1100-1104.

Almarrson, Ö. and Klibanov, A.M. (1996) Remarkable activation of enzymes in nonaqueous media by denaturing organic solvents. *Biotechnology and Bioengineering* **49**, 87-92.

Arpigny, J.L. and Jaeger, K-E. (1999) Bacterial lipolytic enzymes: classification and properties. *Biochemical Journal* **343**, 177-183.

Barker, D.L. and Jencks, W.P. (1969) Pig liver esterase. Some kinetic properties. *Biochemistry* **8:10**, 3890-3897.

Bauer, K., Garbe, D. and Surburg, H. (1990) *Common Fragrance and Flavour Materials*. (2nd Ed.). VCH Publishers: New York.

Benjamin, S. and Pandey, A. (1998) *Candida rugosa* lipases: molecular biology and versatility in biotechnology. *Yeast* **14**, 1069-1087.

Bone, D.P. (1969) Water activity – its chemistry and applications. *Food Product Development* **August-September**, 81-94.

Bott, R., Shield, J.W. and Poulose, A.J. (1994) Protein engineering of lipases. In: *Lipases. Their Structure, Biochemistry and Application* (Woolley, P. and Petersen, S.B., ed.), pp.337-354. Cambridge University Press: Cambridge.

Bradford, M.M. (1976) A rapid and sensitive method for the quantitation of microgram quantities of protein utilizing the principle of protein-dye binding. *Analytical Biochemistry* **72**, 248-254.

Brahimi-Horn, C., Guglielmino, M.L., Elling, L., and Sparrow, L.G. (1990) The esterase profile of a lipase from *Candida cylindracea. Biochimica et Biophysica Acta* **1042**, 51-54.

Brockerhoff, H. and Jensen, R.G. (1974) *Lipolytic Enzymes*. Academic Press, Inc: New York.

Broos, J., Visser, A.J.W.G., Engbersen, J.F.J., Verboom, W., van Hoek, A. and Reinhoudt, D.N. (1995) Flexibility of enzymes suspended in organic solvents probed by time-resolved fluorescence anistropy. Evidence that enzyme activity and enantioselectivity are directly related to enzyme flexibility. *Journal of the American Chemical Society* **117:51**, 12657-12663.

Brzozowski, A.M., Derewenda, U., Derewenda, Z.S., Dodson, G.G., Lawson, D.M., Turkenburg, J.P., Bjorkling, F., Huge-Jensen, B., Patkar, S.A. and Thim, L. (1991) A model for interfacial activation in lipases from the structure of a fungal lipase-inhibitor complex. *Nature* **351**, 491-494.

Careri, G., Giansanti, A. and Gratton, E. (1979) Lysozyme film hydration events: an IR and gravimetric study. *Biopolymers* **18**, 1187-1203.

Careri, G., Gratton, E., Yang, P-H. and Rupley, J.A. (1980) Correlation of IR spectroscopic, heat capacity, diamagnetic susceptibility and enzymic measurements on lysozyme powder. *Nature (London)* **284**, 572-573.

Carriére, F., Gargouri, Y., Moreau, H., Ransac, S., Rogalska, E. and Verger, R. (1994) Gastric lipases: cellular, biochemical and kinetic aspects. In*:* *Lipases. Their Structure, Biochemistry and Application* (Woolley, P. and Peterson, S.B., ed.), pp.181-205. Cambridge University Press: Cambridge.

Chen, T. and Oakley, D.M. (1995) Thermal analysis of proteins of pharmaceutical interest. *Thermochimica Acta* **248**, 229-244.

Cygler, M. and Schrag, J.D. (1997) Structure as basis for understanding interfacial properties of lipases. *Methods in Enzymology* **284**, 3-27.

Cygler, M. and Schrag, J.D. (1999) Structure and conformational flexibility of *Candida rugosa* lipase. *Biochimica et Biophysica Acta* **1441**, 205-214.

Dawson, R.M.C, Elliott, D.C., Elliott, W.H., and Jones, K.M. (1986) *Data for Biochemical Research.* (3rd Ed.). Clarendon Press: Oxford.

Denisov, V.P. and Halle, B. (1996) Protein hydration dynamics in aqueous solutions. *Faraday Discussions* **103**, 227-244.

Desnuelle,P. (1972) The lipases. *The Enzymes* **7**, 575-616.

Dolman, M., Halling, P.J., Moore, B.D. and Waldron, S. (1997) How dry are anhydrous enzymes? Measurement of residual and buried ^{18}O-labeled water molecules using mass spectrometry. *Biopolymers* **41**, 313-321.

Drapron, R. (1985) Enzyme activity as a function of water activity. *NATO Advanced Study Institution Series, Series E.* **90**, 171-190.

Dudman, N.P.B. and Zerner, B. (1975) Carboxylesterases from pig and ox liver. *Methods in Enzymology* **35B**, 190-208.

Farb, D. and Jencks, W.P. (1980) Different forms of pig liver esterase. *Archives of Biochemistry and Biophysics* **203:1**, 214-226.

Ferrato, F., Carriere, F., Sarda, L. and Verger, R. (1997) A critical review of the phenomenon of interfacial activation. *Methods in Enzymology* **286: Part B**, 327-347.

Finney, J.L. (1996) Hydration processes in biological and macromolecular systems. *Faraday Discussions* **103**, 1-18.

Fitter, J. (2000) Confined molecular motions of globular proteins studied in powder samples and in solution. *Journal de Physique IV France* **10**, Pr7-265-Pr7-270.

Franks, F. (1993) Protein hydration. In: *Protein Biotechnology* (Franks, F., ed.), pp. 437-465. The Humana Press Inc.: New Jersey.

Gao, Y. and Breuil, C. (1998) Properties and substrate specificities of an extracellular lipase purified from *Ophiostoma piceae*. *World Journal of Microbiology and Biotechnology* **14**, 421-429.

Godtfredsen, S.E. (1993) Lipases. In: *Enzymes in Food Processing* (Nagodawithana, T. and Reed, G., ed.), pp. 205-219. Academic Press, Inc: California.

Grdadolnik, J. and Maréchal, Y. (2001) Bovine serum albulmin observed by infrared spectrometry. I. Methodology, structural investigation and water uptake. *Biopolymers* **62**, 40-53.

Greenzaid, P. and Jencks, W.P. (1971) Pig liver esterase. Reactions with alcohols, structure-reactivity correlations, and the acyl-enzyme intermediate. *Biochemistry* **10:7**, 1210-1222.

Gronenborn, A. and Clore, M. (1997) Water in and around proteins. *The Biochemist* **June**, 18-21.

Guadagni, D.G., Bomben, J.L. and Hudson, J.S. (1971) Factors influencing the development of aroma in apple peels. *Journal of the Science of Food and Agriculture* **22**, 110-115.

Halling, P.J. (1994) Thermodynamic predictions for biocatalysts in nonconventional media: theory, tests, and recommendations for experimental design and analysis. *Enzyme and Microbial Technology* **16**, 178-206.

Hernáiz, M.J., Rua, M., Celda, B., Medina, P., Sinisterra, J.V. and Sánchez-Montero, J.M. (1994) Contribution to the study of the alteration of lipase activity of *Candida rugosa* by ions and buffers. *Applied Biochemistry and Biotechnology* **44:3**, 213-219.

Heymann, E,. and Junge, W. (1979) Characterisation of the isoenzymes of pig-liver esterase. 1. Chemical studies. *European Journal of Biochemistry* **95**, 509-518.

Heymann, E. and Mentlein, R. (1981) Carboxylesterases-amidases. *Methods in Enzymology* **77**, 333-343.

Hofstee, B.H.J. (1972) On the substrate activation of liver esterase. *Biochimica et Biophysica Acta* **258**, 446-454.

Horgan, D.J., Dunstone, J.R., Stoops, J.K., Webb, E.C. and Zerner, B. (1969) Carboxylesterases (EC 3.1.1). The molecular weight and equivalent weight of pig liver carboxylesterase. *Biochemistry* **8:5**, 2006-2013.

Horgan, D.J., Webb, E.C. and Zerner, B. (1966) Determinations of the normality of pig liver carboxylesterase solutions. *Biochemical and Biophysical Research Communications* **23:1**, 23-28.

Hult, K. and Holmquist, M. (1997) Kinetics, molecular modeling, and synthetic applications with microbial lipases. *Methods in Enzymology* **286:Part B**, 386-405.

Inkerman, P.A., Scott, K., Runnager, M.T.C. and Hamilton, S.E. (1975) Carboxylesterases (EC 3.1.1). Purification and titration of chicken, sheep, and horse liver carboxylesterase. *Canadian Journal of Biochemistry* **53**, 536-546.

Iizumi, T., Nakamura, K. and Fukase, T. (1990) Purification and characterisation of a thermostable lipase from newly isolated *Pseudomonas* sp. KWI-56. *Agricultural and Biological Chemistry* **54:5**, 1253-1258.

Jaeger, K-E., Dijkstra, B.W. and Reetz, M.T. (1999) Bacterial catalysts: molecular biology, three-dimensional structures, and biotechnological applications of lipases. *Annual Review of Microbiology* **53**, 315-351.

Jannsen, P.H., Monk, C.R., and Morgan, H.W. (1994) A thermophilic, lipolytic *Bacillus* species., and continuous assay of its *p*-nitrophenyl-palmitate esterase activity. *FEMS Microbiology Letters* **120**, 195-200.

Junge, W. and Heymann, E. (1979b) Characterisation of the isoenzymes of pig-liver esterase. 2. Kinetic studies. *European Journal of Biochemistry* **95**, 519-525.

Keay, L. and Crook, E.M. (1965) Effect of metal ions on hog liver esterase. *Archives of Biochemistry and Biophysics* **111**, 626-634.

Keough, D.T., de Jersey, J. and Zerner, B.(1985) The relationship between the carboxylesterase and monoacylglycerol lipase activities of chicken liver microsomes. *Biochimica et Biophysica Acta* **829**, 164-172.

Khoo, J.C. and Steinberg, D. (1975) Hormone-sensitive triglyceride lipase from rat adipose tissue. *Methods in Enzymology* **35B**, 181-189.

Klibanov, A.M. (1989) Enzymatic catalysis in anhydrous organic solvents. *Trends In Biological Sciences* **14**, 141-144.

Koellner, G., Kryger, G., Millard, C.B., Silman, I., Sussman, J.L. and Steiner, T. (2000) Active site gorge and buried water molecules in crystal structures of acetylcholinesterase from *Torpedo californica*. *Journal of Molecular Biology* **296:2**, 713-735.

Krisch, K. (1971) Carboxylic ester hydrolases. *The Enzymes* **5**, 43-69.

Krisch, K. (1966) Reaction of a microsomal esterase from hog-liver with diethyl-*p*-nitrophenyl phosphate. *Biochimica et Biophysica Acta* **122**, 265-280.

Labuza, T.P., Acott, K., Tatini, S.R. and Lee, R.Y. (1976) Water activity determination: a collaborative study of different methods. *Journal of Food Science* **41**, 910-917.

Lamare, S., and Legoy, M.D. (1995) Working at controlled water activity in a continuous process: the gas/solid system as a solution. *Biotechnology and Bioengineering* **45**, 387-397.

Levine, L., Baer, A. and Jencks, W.P. (1980) Dissociation of pig liver carboxylesterase measured by quantitative micro-complement fixation. *Archives of Biochemistry and Biophysics* **203:1,** 236-243.

Lombardo, D. and Guy, O. (1981) Effects of alcohols on the hydrolysis catalyzed by human pancreatic carboxyl-ester hydrolase. *Biochimica et Biophysica Acta* **657**, 425-537.

Lüscher-Mattli, M. and Rüegg, M. (1982) Thermodynamic functions of biopolymer hydration. I. Their determination by vapor pressure studies, discussed in an analysis of the primary hydration process. *Biopolymers* **21**, 403-418.

Macrae, A.R. (1983) Extracellular microbial lipases. In: *Microbial Enzymes and Biotechnology* (Fogarty, W.M., ed), pp. 225-250. Applied Science Publishers: Essex.

Martinelle, M. and Hult, K. (1994) Kinetics of triglyceride lipases. In*:* *Lipases. Their Structure, Biochemistry and Application* (Woolley, P. and Petersen, S.B., ed.), pp.337-354. Cambridge University Press: Cambridge.

McKay, A.M. (1993) Microbial carboxylic ester hydrolases (EC 3.1.1) in food biotechnology. *Letters in Applied Microbiology* **16**, 1-6.

McNaughton, C.L. (1997) *The Purification and Characterisation of an Extracellular Lipase from Ophiostoma piliferum.* MSc. Thesis, University of Waikato.

Nursten, H.E. (1970) Volatile compounds: the aroma of fruits. In: *The Biochemistry of Fruits and Their Products* (Hulme, A.C., ed.), Vol. 1, pp. 239-268. Academic Press Inc. (London) Ltd: London.

O'Brien, F.E.M. (1948) The control of humidity by saturated salt solutions. *Journal of Scientific Instruments* **25**, 73-76.

Otero, C., Del-Val, I., Robledo, L., Torres, C., Arcos, J.A. and Pérez-Gil, J. (1996) Conformational changes of different isolipasses from *Candida rugosa* in liquid interfaces and after their contact with low-water-content media. *Annals of the New York Academy of Science* **799**, 324-327.

Parker, M.C., Moore, B.D. and Blacker, A.J. (1995) Measuring enzyme hydration in non-polar organic solvents using NMR. *Biotechnology and Bioengineering* **46**, 452-458.

Partridge, J., Dennison, P.R., Moore, B.D. and Halling, P.J. (1998) Activity and mobility of subtilisin in low water organic media: hydration is more important than solvent dielectric. *Biochimica et Biophysica Acta* **1386**, 79-89.

Patterson, B.D., Hatfield, S.G.S. and Knee, M. (1974) Residual effects of controlled atmosphere storage on the production of volatile compounds by two varieties of apples. *Journal of Science and Food Agriculture* **25**, 843-849.

Peek, K., Veitch, D.P., Prescott, M., Daniel, R.M., MacIver, B. and Bergquist, P.L. (1993) Some characteristics of a proteinase from a thermophilic *Bacillus* sp. expressed in *Escherichia coli*: comparison with the native enzyme and its processing in *E. coli* and in vitro. *Applied and Environmental Microbiology* **59:4**, 1168-1175.

Pernas, M.A., López, C., Rúa, L. and Hermoso, J. (2001) Influence of the conformational flexibility on the kinetics and dimerisation process of two *Candida rugosa* lipase isoenzymes. *FEBS Letters* **501**, 87-91.

Perry, R.H., Green, D.W. and Maloney, J.O. (1984) *Perry's Chemical Engineers' Handbook* (6^{th} ed.). McGraw-Hill: New York.

Pirozzi, D., Toscano, G. and Greco, G.Jr. (1997) Effect of water diffusion limitations on the thermostability of enzymes in non-aqueous environments. *Biocatalysis and Biotransformation* **14**, 285-297.

Pocker, Y. (2000) Water in enzyme reactions: biophysical aspects of hydration-dehydration process. *Cellular and Molecular Life Sciences* **57**, 1008-1017.

Poole, P.L. and Finney, J.L. (1986) Solid-phase protein hydration studies. *Methods in Enzymology* **127**, 284-293.

Provencher, L. and Jones, J.B. (1994) A concluding specification of the dimensions of the active site model of pig liver esterase. *Journal of Organic Chemistry* **59**, 2729-2732.

Provencher, L. Wynn, H. and Jones, J.B. (1993) Enzymes in organic synthesis 51. Probing the dimensions of the large hydrophobic pocket of the active site of pig liver esterase. *Tetrahedron: Assymetry* **4:9**, 2025-2040.

Redondo,O., Herrero, A., Bello, J.F., Roig, M.G., Calvo, M.V., Plou, F.J. and Burguillo, F.J. (1995) Comparative kinetic study of lipases A and B from *Candida rugosa* on the hydrolysis of lipid *p*-nitrophenyl esters in mixed micelles with Triton X-100. *Biochimica et Biophysica Acta* **1243**, 15-24.

Rhodes, M.J.C. (1970) The climacteric and ripening of fruits. In: *The Biochemistry of Fruits and Their Products* (Hulme, A.C., ed.), Vol. 1, pp. 521-533. Academic Press Inc. (London) Ltd: London.

Richardson, G.M. and Malthus, R.S. (1955) Salts for static control of humidity at relatively low levels. *Journal of Applied Chemistry* **5**, 557-567.

Robbi, M. and Beaufay, H. (1991) The COOH terminus of several liver carboxylesterases targets these enzymes to the lumen of the endoplasmic reticulum. *Journal of Biological Chemistry* **266:30**, 20498-20503.

Rockland, L.B. (1960) Saturated salt solution for static control of relative humidities between 5° and 40°C. *Analytical Chemistry* **32:10**, 1375-1376.

Rojas-Garbanzo, R.E. and Mata-Segreda, J.F. (1998) Assessment of the steric tolerance of the *P* sector in the catalytic site of porcine liver esterase. *Bioorganic and Medicinal Chemistry Letters* **8:1**, 7-10.

Ross, N.W. and Schneider, H. (1991) Activities of *Candida rugosa* lipase and other esterolytic enzymes coated on glass beads and suspended in substrate and water vapor: Enzymes in thin liquid films. *Enzyme and Microbial Technology* **13**, 370-377.

Rúa,, M.L., Díaz-Mauriño, T., Fernández, V.M., Otero, C. and Ballesteros, A. (1993) Purification and characterisation of two distinct lipases from *Candida cylindracea*. *Biochimica et Biophysica Acta* **1156**, 181-189.

Rupley, J.A. and Careri, G. (1991) Protein hydration and function. *Advances in Protein Chemistry* **41**, 37-172.

Rupley, J.A., Gratton, E. and Careri, G. (1983) Water and globular proteins. *Trends in Biochemical Sciences* **8**, 18-22.

Sarda, L. and Desnuelle, P. (1958) Action de la lipase pancréatique sur les esters en émulsion. *Biochimica et Biophysica Acta* **30**, 514-521.

Satoh, T. and Hosokawa, M. (1998) The mammalian carboxylesterases. *Annual Review of Pharmacology and Toxicology* **38**, 257-288.

Schinkel, J.E., Downer, N.W. and Rupley, J.A. (1985) Hydrogen exchange of lysozyme powders. Hydration dependence of internal motions. *Biochemistry* **24:2**, 352-366.

Schmidt-Dannert, C., Rúa, M.L., Atomi, H. and Schmid, R.D. (1996) Thermoalkalophilic lipase of *Bacillus thermocatenulatus*. I. Molecular cloning, nucleotide sequence, purification and some properties. *Biochimica et Biophysica Acta* **1301**, 105-114.

Scopes, R.K. (1994) *Protein Purification: Principles and Practice.* (3rd Ed.). Springer-Verlag New York, Inc.: New York.

Scott, K. and Zerner, B. (1975) Carboxylesterases from chicken, sheep, and horse liver. *Methods in Enzymology* **35B**, 208-221.

Stevens, E. and Stevens, L. (1979) The effect of restricted hydration on the rate of glucose 6-phosphate dehydrogenase, phosphoglucose isomerase, hexokinase and fumarase. *Biochemical Journal* **179**, 161-167.

Stoops, J.K., Horgan, D.J., Runnegar, M.T.C., de Jersay, J., Webb, E.C. and Zerner, B. (1969) Carboxylesterases (EC 3.1.1). Kinetic studies on carboxylesterases. *Biochemistry* **8:5**, 2026-2033.

Sugiura, M. (1984) Bacterial lipases. In: *Lipases* (Borgstrom, B. and Brockman, H.L., ed.), pp. 505-523. Elsevier Science Publishers Ltd: New York.

Tarak, M. and Tobias, D.J. (2000) The dynamics of protein hydration water. A quantitative comparison of molecular dynamics simulations and neutron-scattering experiments. *Biophysical Journal* **79**, 3244-3257.

Towns, J.K. (1995) Moisture content in proteins: its effects and measurement. *Journal of Chromatography A* **705**, 115-127.

Tsujita, T., Shirai, K., Saito, Y. and Okuda, H. (1990) Relationship between lipase and esterase. In: *Isozymes: Structure, Function, and Use in Biology and Medicine* (Ogita, Z.I. and Markert, C.L., eds.), pp. 915-933. Wiley-Liss, Inc.: New York.

Ulrich, R. (1970) Organic acids. In: *The Biochemistry of Fruits and Their Products* (Hulme, A.C., ed.), Vol. 1, pp. 89-118. Academic Press Inc. (London) Ltd: London.

Valivety, R.H., Halling, P.J. and Macrae, A.R. (1992a) *Rhizomucor miehei* lipase remains highly active at water activity below 0.0001. *FEBS Letters* **301:3**, 258-260.

Valivety, R.H., Halling, P.J., Peilow, A.D. and Macrae, A.R. (1992b) Lipases from different sources vary widely in dependence of catalytic activity on water activity. *Biochimica et Biophysica Acta* **1122**, 143-146.

van Lith, H.A., den Bieman, M., and van Zutphen, B.F. (1989) Purification and molecular properties of rabbit liver esterase ES-1A. *European Journal of Biochemistry* **184**, 545-551.

Wade, R.C., Mazor, M.H., McCammon, J.A. and Quiochom F.A. (1991) A molecular dynamics study of thermodynamic and structural aspects of the hydration of cavities of proteins. *Biopolymers* **31:8**, 919-931.

Walker, C.H. and Mackness, M.I. (1983) Esterases: problems of identification and classification. *Biochemical Pharmacology* **32:2**, 3265-3269.

Weast, R.C. and Astle, M.J. (1982) *CRC Handbook of Chemistry and Physics* (63rd Ed.). CRC Press, Inc.: Florida.

Webb, E.C. (1984) *Enzyme Nomenclature* (9th Ed.). Academic Press, Inc.; New York.

Wexler, A. and Hasegawa, S. (1954) Relative humidity-temperature relationships of some saturated salt solutions in the temperature range of 0° to 50°C. *Journal of Research of the National Bureau of Standards* **53:1**, 19-26.

Williams, A.A. and Knee, M. (1997) The flavour of Cox's Orange Pippin apples and its variation with storage. *Annals of Applied Biology* **87**, 127-131.

Windholz, M. (1976) *The Merck Index.* (9th Ed.). Merck & Co., Ltd: New Jersey.

Wink, W.A. and Sears, G.R. (1950) Instrumentation Studies LVII. Equilibrium relative humidities above saturated salt solutions at various temperatures. *TAPPI* **33:9**, 96A-99A.

Yagi, T., Tsuda, M., Mori, Y. and Inokuchi, H. (1969) Hydrogenase activity in the dry state. *Journal of the American Chemical Society* **91**, 2801.

Yang, S.K., Chen, S-J. and Huang, J-D. (1995) Enantioselectivity suggests a cystolic origin for a commercial pig liver esterase preparation. *Chirality* **7**, 40-43.

Yang, P-H. and Rupley, J.A. (1979) Protein-water interactions. Heat capacity of the lysozyme-water system. *Biochemistry* **18:12**, 2654-2661.

Zubay, G. (1993) *Biochemistry Volume 1: Energy, Cells, and Catalysis.* (3rd Ed.). Wm. C. Brown Publishers: Iowa.